Neutrophils in advanced non-small cell lung cancer

Robert John Grecian

THE UNIVERSITY *of* EDINBURGH

Doctor of Philosophy

The University of Edinburgh

2020

Declaration

I declare that the content of this thesis is my own and that all contributions and col aborations have been explicitly acknowledged in the text No material presented in this thesis has been submitted to any other university or for any other degree.

Robert John Grecian

January 2020

Abstract

Lung cancer is the third most common cancer in the UK; 87% are histologically non-small cell lung cancer (NSCLC). At the time of diagnosis, patients frequently have advanced disease, with poor one-year survival due to metastatic burden. The immune system should act as a key line of defence; recognising, killing and clearing malignant cells. However, ineffective immune responses contribute to cancer progression. Neutrophils are active players in the metastatic environment, but there is limited data regarding human neutrophil populations in advanced lung cancer. Greater understanding of the interplay between extrinsic cell signals and intrinsic cell features in determining neutrophil roles, is also needed.

In this study, to investigate how the extrinsic metastatic NSCLC pleural environment influences the function of neutrophils, it was modelled *in vitro* by culturing healthy donor neutrophils in conditions emulating the pleural space. Tumour necrosis factor alpha (TNFα) and hypoxia acted as pro-survival signals leading to neutrophil persistence and NSCLC pleural fluid conditioned neutrophils to suppress $CD8^+$ T cells through mechanisms including programmed death-ligand 1 (PD-L1) expression. To establish the phenotype of neutrophil populations in advanced NSCLC, neutrophils were extracted from the pleural fluid (metastatic site) and blood of patients. Cellular morphology, surface marker expression and functional assays were utilised. There was an expanded population of low-density blood neutrophils in advanced NSCLC, that were not present in health, and a proportion of which were immature with banded nuclei. Similar immature neutrophils were seen in NSCLC pleural fluid. NSCLC pleural fluid neutrophils expressed PD-L1 and were long-lived. To understand how cell-intrinsic features of neutrophil populations in advanced NSCLC may determine their role in cancer, the populations were defined by their transcriptomic and proteomic signatures. This provided evidence that implied NSCLC low-density blood neutrophils represent immature cells that have been recruited from the bone marrow; they may retain proliferative capacity, have reduced neutrophil granules, and are pro-survival.

In summary, the data favours a phenotype of sustained neutrophilic inflammation that is immunosuppressive at the NSCLC metastatic site, with a subpopulation of immature cells that may be ineffective/ detrimental. This is likely to permit tumour progression, leading to adverse patient outcomes.

Lay Summary

Lung cancer is the third most common cancer in the UK; 87% are a type called non-small cell lung cancer (NSCLC). It is common for patients to have advanced disease at the time of diagnosis, where the cancer has spread to other organs (metastasised). The immune system should act as a key line of defence, recognising and killing cancer cells. Neutrophils (a form of white blood cell), should take part in this process. However, in advanced cancer, it is thought that neutrophils may not be helping in the ways that they should do, enabling cancer to progress/ metastasise. This could be due to changes in the inner programming of neutrophils and/ or a reaction to unhelpful signals in the metastatic tumour environment around them: this study aimed to gain further understanding of this.

In this study, blood samples and pleural fluid were taken from patients with late-stage NSCLC. Pleural fluid had collected in the space between the outer lining of the lung and the inner lining of the chest wall, as a result of cancer cells metastasising and growing there (cancer cells spread there by travelling in the blood and lymphatics from the tumour within the lung). Neutrophils were extracted from these tissues for studies that tested their appearance, cell surface features, function, and inner programming e.g. what proteins they had within them and were trying to make. The effect of the pleural environment upon neutrophils was also tested through simulation in the lab dish. These studies showed that signals in the metastatic NSCLC environment made neutrophils live longer. Pleural fluid also programmed neutrophils to supress other immune cells (CD8+ T cells) that normally act to kill cancer cells. An expanded subpopulation of immature cancer neutrophils was also identified in advanced NSCLC. This subpopulation was not present in the blood of healthy donors, and may be of functional importance in cancer. When the inner programming of cancer neutrophils was investigated, it revealed mechanisms that help the neutrophils to live longer. It also showed that the immature cancer neutrophil population had not yet made their cancer killing machinery and may be able to proliferate.

Together this data implies that neutrophils in advanced NSCLC are unhelpful/ ineffective, for example, by living a long time, supressing cancer-killing immune cells and by lacking cancer killing machinery. The role of neutrophils in advanced NSCLC is determined by a combination of internal programming and external signals.

Acknowledgements

I would first like to thank my supervisors, Professor Sarah Walmsley, Professor Moira Whyte, Professor Margaret Frame and Dr Adam Byron, for their supervision, guidance and support. Working in the Walmsley laboratory group has been a pleasure, and I would like to acknowledge the kindness of all colleagues within the group, along with other PhD students and postdoctoral researchers within the Centre for Inflammation Research. Indeed, the centre for inflammation research has been a fantastic department in which to carry out my studies, with excellent academic and support staff. I am privileged to be part of the Edinburgh Clinical Academic Track and would like to thank the program directors along with the administrator Joanne Ness for all the added benefits I have gained from this.

Of course, my research would not have been possible without the funding of Cancer Research UK (C157/A23218), nor without the help of patients and healthy volunteers. With regard to obtaining patient samples, I must thank Professor Kev Dhaliwal, Dr Ahsan Akram, Dr Andrew Leitch, Dr John McCafferty and the NHS Lothian respiratory registrars.

Dr Andy Howden at the University of Dundee, has been an invaluable collaborator, helping with all aspects of the proteomics carried out in this project. In terms of technical support, I am especially grateful for help given by the Queen's Medical Research Institute Flow Cytometry and Cell Sorting Facility (Shonna Johnson, Will Ramsay and Mari Pattison). In addition, I thank the Host and Tumour Profiling Unit (Kenny Macleod (Human Cytokine Array) and Alison Munro (NanoString™)) and Thomson Bioinformatics (Dr John Thomson (NanoString™ data analysis)).

Within the Centre for Inflammation Research, I would like to thank Dr Emily Gwyer Findlay for her expertise in helping to set up the T cell assays. I would also like to thank Dr Gwo-tzer Ho for providing me with Infliximab for use in the TNFα experiments. In addition, special thanks go to Dr Emily Watts, for her assistance in teaching me how to use Perseus software.

Finally, thank you to my wife Sheila, daughters Iona and (newly-arrived) Ailsa, and dog Holly; for their steadfastness, boundless love, and for keeping me grounded throughout my studies.

List of Abbreviations

ANOVA	Analysis of variance
DAPI	4', 6-Diamidino-2-Phenylindole
DMSO	Dimethyl sulfoxide
DPBS	Dulbecco's phosphate buffered saline (without calcium/ magnesium)
ELISA	Enzyme-linked immunosorbent assay
FACS	Fluorescence-activated cell sorting
FBS	Foetal bovine serum
FSC	Forward scatter
GM-CSF	Granulocyte-macrophage colony-stimulating factor
G-MDSC	Granulocytic myeloid-derived suppressor cells
GOBP	Gene ontology biological process
HD	Healthy donor
iBAQ	Intensity-based absolute quantification
IFNβ	Interferon beta
IQR	Interquartile range
KEGG	Kyoto encyclopaedia of genes and genomes
LC-ES-MS	Liquid chromatography electrospray tandem mass spectrometry
LDH	Lactate dehydrogenase
LDN	Low-density neutrophil(s)
LFQ	Label-free quantification
MMP-9	Matrix metallopeptidase 9

NDN	Normal-density neutrophil(s)
NHS	National health service
NLR	Neutrophil-to-lymphocyte ratio
NSCLC	Non-small cell lung cancer
PBMC	Peripheral blood mononuclear cells
PBS	Phosphate buffered saline
PD-L1	Programmed death-ligand 1
PFN	Pleural fluid neutrophil(s)
PFS	Pleural fluid supernatant (cell-free)
RPM	Revolutions per minute
RPMI	Roswell Park Memorial Institute
SEM	Standard error of the mean
SSC	Side scatter
TGFβ	Transforming growth factor beta
TNFα	Tumour necrosis factor alpha
WBN	Whole blood neutrophil(s) (all densities together)

List of Figures

List of Tables

Contents

Chapter 1 Introduction

1.1 The role of neutrophils in health

Neutrophils are the most abundant white blood cell, forming 50-70% of circulating leukocytes. They play a central role in the innate immune response, acting to protect the body against infection, and responding at sites of tissue injury. Their importance is highlighted by immunodeficiencies, such as chronic granulomatous disease,[1] that result in patients suffering from overwhelming infection. Appropriate neutrophil responses are dependent upon a functioning balance of neutrophil production, release from the bone marrow, recruitment to sites of need, activation and appropriate action at target sites, and effective clearance afterward. These factors are regulated by environmental signals. Dysregulation of this finely tuned homeostatic system results in disease.

1.1.1 Neutrophil production and release

A summary of neutrophil differentiation can be seen in Figure 1.1 (adapted from Hidalgo et al.[2]). Briefly, neutrophil differentiation behaves like a conveyor belt,[3] with neutrophil-commitment starting with the promyelocyte which develops from the granulocyte macrophage progenitor in the bone marrow. Sequential steps of development then occur as per the figure (from left to right). Neutrophils develop granules (primary, secondary, tertiary) and their nuclei become more lobulated as they mature. Of key importance, from the metamyelocyte stage, the cells stop dividing. In health, only mature neutrophils are released from the bone marrow. However, during acute infection or inflammation, there is ‘left shift’ in the blood neutrophil population, with release of immature non-dividing cells into the circulation.[4] Neutrophils are mobilised from the bone marrow by signals including granulocyte colony-stimulating factor (G-CSF).

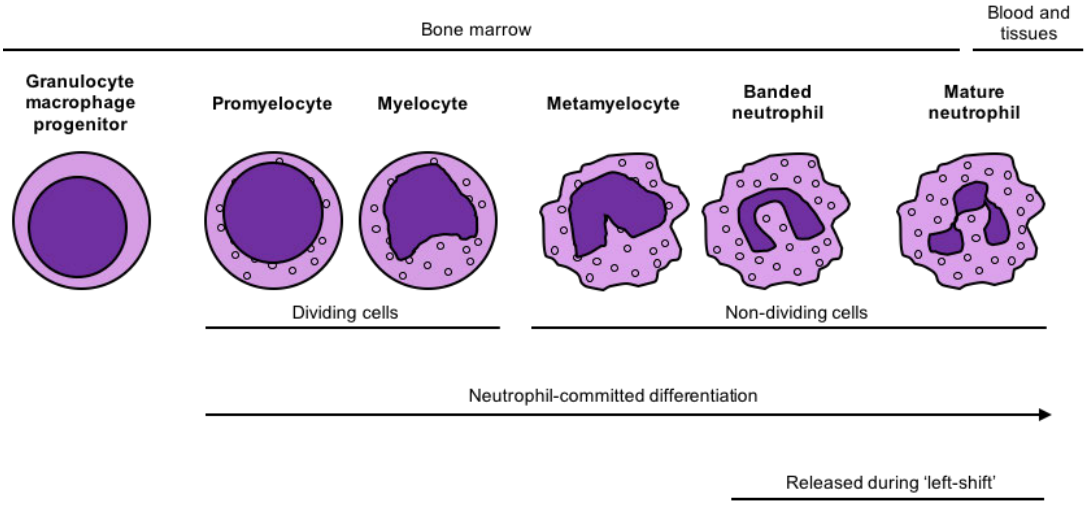

Figure 1.1: Neutrophil development.
The stages of neutrophil development are shown sequentially from left to right. From the metamyelocyte stage, the cells stop dividing. In health, only mature neutrophils are released from the bone marrow. In disease, there is 'left shift' with the additional release of immature neutrophils.

1.1.2 Recruitment to tissues

Once released from the bone marrow neutrophils circulate in the blood. At sites of inflammation, vascular endothelial cells are stimulated to express selectins. These capture neutrophils, binding to L-selectin. Neutrophils then roll along the endothelium before firmly adhering via integrins. They then transmigrate across the endothelium. Following this, neutrophils undergo chemotaxis, following signals (such as interleukin-8, interferon gamma, complement component 5a and leukotriene B4) to the site of need. Here neutrophils identify targets through pattern-recognition receptors (including Toll-like receptors), which sense pathogen-derived compounds (pathogen-associated molecular patterns, PAMPs) and 'self' danger signals (danger-associated molecular patterns, DAMPs). During these processes, neutrophils become activated and are subsequently stimulated into carrying out their defence functions.[5]

1.1.3 Neutrophil defence repertoire

The neutrophil defence repertoire includes phagocytosis, degranulation, generation of reactive oxygen species and neutrophil extracellular trap formation. Phagocytosis is the process through which neutrophils engulf target materials and then degrade them within phagosomes.[6] In terms of reactive oxygen species (formed in the respiratory burst), the enzyme nicotinamide adenine dinucleotide phosphate generates superoxide, which in turn is used to make hydrogen peroxide. Myeloperoxidase can then use hydrogen peroxide to produce hypochlorus acid. These reactive oxygen species are highly toxic to target microbes/ cells. Most of these processes occur within the safety of the neutrophil phagosome, but neutrophils can also release reactive oxygen species into their surroundings.[7] Through the process of degranulation, neutrophils can also release proteolytic enzymes and antimicrobial peptides.[5] Finally, neutrophils can release a web of fibres composed of chromatin, DNA, histones and granular proteins, known as neutrophil extracellular traps, that immobilise and kill targets.[8]

1.1.4 Apoptosis and clearance

Apoptosis (programmed cell death) of neutrophils enables controlled clearance and resolution of inflammation, without any spilling of their toxic contents. Indeed, apoptotic neutrophils are commonly safely removed by being efferocytosed by macrophages.[9] Neutrophils were traditionally thought to have a life span of less than 24 hours, with a half-life of only 6-8 hours in the circulation.[10] However more recent studies have suggested that they may persist for up to 5 days in the blood in health.[11] Apoptosis is tightly controlled in neutrophils, and is mediated by both extrinsic and intrinsic pathways as seen in Figure 1.2 (adapted from Ichim et al.[12]). In the extrinsic pathway, eternal signals bind death receptors such as tumour necrosis factor-related apoptosis-inducing ligand receptor (TRAILR) and FS-7-associated surface antigen (FAS). This leads to the activation of caspase-8 and caspase-10, that then in turn cleave and activate caspase-3 and caspase-7, which trigger apoptosis. In the intrinsic pathway, cell stress signals from within the cell, such as DNA damage and metabolic stress, stimulate B-cell lymphoma-2 homology domain 3-only protein (BH3-only protein) activation, triggering Bcl-2-associated X protein (BAX) and Bcl-2 homologous antagonist killer (BAK), resulting in mitochondrial outer membrane permeabilisation. This causes leak of mitochondrial

intermembrane space proteins that ultimately start a cascade of caspase activity that triggers apoptosis. The extrinsic pathway can also activate BAX and BAK through caspase-8 cleavage of BH3-interacting death domain agonist (BID). BAX, BAK and BID, are inhibited by pro-survival proteins B-cell lymphoma-2 (Bcl-2) and myeloid cell leukaemia-1 (Mcl-1).[12] Of note, imbalance in apoptosis pathways can lead to prolonged and damaging neutrophilic inflammation. Several cytokines have been shown to stimulate neutrophil survival, including interleukin-1β, tumour necrosis factor, granulocyte-macrophage colony-stimulating factor, granulocyte colony-stimulating factor, and interferon-γ.[13] Tissue hypoxia also acts as a marked pro-survival neutrophil signal.[14]

It must be noted that apoptosis is not the only mechanism of neutrophil death. The process of apoptosis requires adenosine triphosphate (ATP), and therefore energetic failure can lead to the failure of apoptosis. Furthermore, efferocytosis by macrophages may not be effective. In these circumstances, neutrophils can undergo necrosis, losing cytoplasmic integrity and leaking their toxic contents into the surrounding tissue. Finally, NETosis is a neutrophil death process distinct from apoptosis and necrosis. It involves the release of neutrophil extracellular traps (NETs), composed of chromatin and granule proteins, after cell membrane breakdown, and is dependent upon the generation or reactive oxygen species.[15]

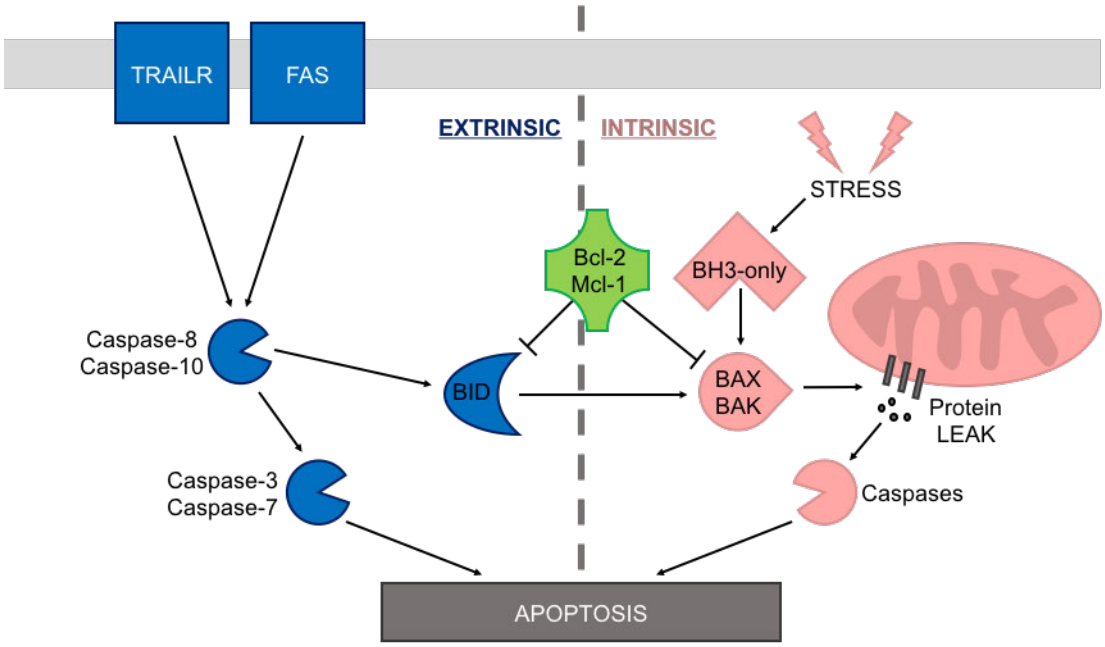

Figure 1.2: Extrinsic and intrinsic apoptosis pathways.
Apoptosis is tightly controlled in neutrophils, and is mediated by both extrinsic and intrinsic pathways. In the extrinsic pathway, external signals bind death receptors such as TRAILR and FAS, starting a cascade of caspase activity. In the intrinsic pathway, cell stress signals such DNA damage and metabolic stress, lead to mitochondrial protein leak, starting a cascade of caspase activity. TRAILR, tumour necrosis factor-related apoptosis-inducing ligand receptor; FAS, FS-7-associated surface antigen; BID, BH3-interacting death domain agonist; BH3-only, B-cell lymphoma-2 homology domain 3-only protein; BAX, Bcl-2-associated X protein; BAK, Bcl-2 homologous antagonist killer; Bcl-2, B-cell lymphoma-2; Mcl-2, myeloid cell leukaemia-1.

1.2 The role of neutrophils in cancer

The ability of malignant cells to establish themselves in a niche and subsequently metastasise is not entirely dependent on their own intrinsic cellular signaling pathways; complex interactions with a myriad of immune cells in the tumour microenvironment are key.[16] It is now recognized that neutrophils are active players (rather than spectators) in the immune response to malignancy.[17]

1.2.1 Association of neutrophils with cancer prognosis

Neutrophil to lymphocyte ratio (NLR)

Peripheral blood neutrophil counts increase in patients as their cancer progresses. Tumours produce granulocyte colony-stimulating factor (G-CSF) which skews the neutrophil retention/release balance in bone marrow, leading to this increase in blood neutrophils.[18] G-CSF downregulates chemokine receptor type 4 (CXCR4) expression in human myeloid lineage cells, reducing their response to the bone marrow retention signal stromal cell-derived factor 1 (SDF-1).[19]

Many research groups have investigated whether the number of neutrophils present in peripheral blood correlates with patient outcome. Most have done this using neutrophil to lymphocyte ratio (NLR). A meta-analysis of 100 such studies by Templeton et al. comprising over 40,000 patients, showed NLR>4 to be associated with worse overall survival, cancer specific survival, progression free survival and disease free survival.[20] This was seen in all types and stage of cancer.

Intra-tumoural neutrophils

The association between peripheral blood neutrophils and survival does not however give any information about what might be happening at the tumour site itself i.e. whether tumour-associated neutrophils (TAN) are associated with outcome. A meta-analysis of nearly 4000 patients, has shown high levels of intra-tumoural neutrophils to be associated with unfavourable survival.[21] In addition, Gentles et al.

used a computational approach to analyse bulk tumour transcriptomes in order to infer the frequency of different immune cell populations (including neutrophils) in over 3000 solid tumours (14 cancer types). They found intra-tumoural neutrophils to be the most adverse prognostic cell population.[22]

Neutropaenia

In direct contrast, neutropaenia in patients undergoing chemotherapy has been shown (by meta-analysis) to be beneficial to survival (despite the fact that neutropaenia also poses a risk of severe infection and associated mortality).[23] This may of course just be a reflection of adequate toxicity of the drug being achieved to kill tumour cells, however the question does arise as to whether the direct effect on neutrophils themselves is beneficial. This is clinically relevant, as the use G-CSF in patients who are profoundly neutropaenic post chemotherapy (G-CSF used with the aim to prevent sepsis) could in fact be detrimental to longer term clinical outcome. Indeed, it has been shown that G-CSF may promote metastatic disease via neutrophils forming a pre-metastatic niche.[24]

What about neutrophil function, site and regulation?

Measuring the number of neutrophils in the blood and/or in the tumour of cancer patients and associating this with survival is of course quite a crude measure, and does not give any information regarding neutrophil function in cancer. It must also be remembered that blood neutrophil levels increase in other conditions, such as infection. Within the same patient, neutrophils may display varying roles at different sites. Furthermore, appropriate inflammatory responses are dependent upon a functioning balance of neutrophil production, release from bone marrow, recruitment to the site of injury and clearance. Dysregulation of this homeostatic process, for example by tumour derived G-CSF, could perpetuate malignancy.

1.2.2 Neutrophil polarisation

Transforming growth factor beta (TGF-β) and interferon beta (IFN-β) have opposite effects on tumour-associated neutrophil (TAN) polarisation in mice

Fridlender was the first to suggest that tumour-associated neutrophils (TANs) may be polarized to N1 (anti-tumour) or N2 (pro-tumour) phenotypes, in a similar manner to macrophages. Using tumour bearing mice, he demonstrated that TGF-β blockade favoured the accumulation of N1 TAN that were morphologically and functionally different to N2 TAN. N1 TAN had hypersegmented nuclei in contrast to the nuclei of N2 TAN that were circular. N1 TAN were cytotoxic to tumour cells via an oxygen radical-dependent mechanism and had increased tumour necrosis factor alpha (TNF-α) and intercellular adhesion molecule 1 (ICAM-1) expression, whereas N2 TAN expressed high levels of arginase which is known to suppress T cell immunity. Of key importance, TGF-β blockade promoted a T cell anti-tumour response.[25] Using IFN-$\beta_1^{-/-}$ tumour bearing mice, the Jablonska group have shown IFN-β to have the opposite effect to TGF-β on TAN polarisation i.e. IFN-β promotes anti-tumour N1 TAN.[26]

Limitations of N1 versus. N2 model

It should be noted that the work described above in murine models is yet to be replicated in humans. Furthermore, in a similar manner to M1 versus M2 macrophage classification in malignancy, it may be that a binary N1/N2 classification of neutrophils is an oversimplification.[27] It seems increasingly likely that N1 and N2 represent laboratory extremes of a biological continuum, with plasticity dependent upon the local environment.

1.2.3 Neutrophil roles in aiding or abating tumourigenesis

Rather than focusing on N1/N2, we should possibly instead be defining neutrophils by the distinct functional phenotypes/subpopulations that aid or abate the process of tumourigenesis (e.g. proliferation, angiogenesis, invasion, immunosuppression and metastatic seeding) in the different microenvironments (i.e. primary tumour, circulation, pre-metastatic and metastatic).

Tumour proliferation

Neutrophil elastase (NE) has been shown to promote tumour proliferation. Houghton et al. showed that NE is taken up by tumour cells, where it degrades insulin receptor substrate-1 (IRS-1). Lower levels of IRS-1 were associated with an increase in the interaction between phosphatidylinositol 3-kinase (PI3K) and the potent mitogen platelet-derived growth factor receptor (PDGFR), which directed the PI3K axis to favour tumour proliferation.[28]

In contrast neutrophils can also induce lysis of tumour cells via hypochlorus acid produced from reactive oxygen species (ROS).[29] Of note, the MET proto-oncogene is expressed in neutrophils and is required for neutrophil chemoattraction and cytotoxicity toward tumour cells in response to its ligand hepatocyte growth factor (HGF).[30] Neutrophils can kill tumour cells via TNF-α expression.[26] Furthermore, neutrophils stimulated by interferons release tumour necrosis factor related apoptosis-inducing ligand (TRAIL) which induces tumour cell apoptosis. [31 32]

Angiogenesis and invasion

The angiogenic and invasive mechanisms of matrix metallopeptidase 9 (MMP-9), vascular endothelial growth factor (VEGF) and Bv8 (prokineticin) have been previously described.[33 34] It is thought that neutrophils may drive angiogenesis in malignancy by providing a significant source of MMP-9 which acts to release VEGF from the extracellular matrix (ECM).[35 36] In addition to roles in angiogenesis, MMP-9 is also postulated to aid the direct invasion of tumour cells via degradation of extracellular matrix/basement membrane.

Of note, it has been shown that neutrophil extracellular traps (NETs), formed during neutrophil death, and composing of chromatin, neutrophil elastase and myeloperoxidase, have a role in angiogenesis, by stimulating vascular endothelial cells to release proangiogenic cytokines.[37]

Countering the above mechanisms, neutrophils can also have an opposing function with regard to angiogenesis; it has been reported that neutrophils can be conditioned ex-vivo to release the anti-angiogenic isoform of VEGF (VEGF-A_{165b}),[38] but it is yet to be proven if this occurs in-vivo.

Immunomodulation

As previously mentioned, neutrophils are known to express arginase. Arginase degrades arginine, an essential amino acid important in many cellular processes e.g. the proliferation of T cells. High arginase levels can be found in the tumour microenvironment and result in inhibition of T cell receptor expression and antigen-specific responses, aiding tumour evasion.[39] Neutrophils have been widely reported to suppress T cell proliferation in ex-vivo studies, with Coffelt et al. demonstrating this is inducible nitric oxide synthase (iNOS) dependent,[40] but it must be noted that recently concerns have arisen about the accuracy of these assays when T cell activating microbeads have been used, as neutrophils can bind/ phagocytose the beads making them ineffective.[41] Neutrophils have also been shown to induce the apoptosis of CD8 T cells in a TNF-α and nitric oxide (NO) dependent manner.[42] In addition, neutrophils can suppress T cells via programmed death ligand 1 (PD-L1) in early-stage gastric cancers.[43] Moreover, neutrophil depletion studies suggest that they may act to reduce the effectiveness of PD1 immunotherapy, in mouse models.[44] Neutrophils recruit regulatory T cells into tumours via secretion of chemokine ligand 17 (CCL17), which may inhibit anti-tumour immunity.[45] Finally neutrophils and pro-tumoural IL-17 $\gamma\delta$ T cells can conspire to promote metastasis.[40]

Whilst there appears to be an ever-expanding list of ways in which neutrophils immunosuppress in the tumour microenvironment, nonetheless neutrophils can also be immunostimulatory and anti-tumour. Neutrophils can have a role in antigen

presentation,[46] can stimulate T cell proliferation,[47] and suppress pro-tumoural IL-17 $\gamma\delta$ T cells via ROS.[48]

These dichotomous immunosuppressive and immunostimulatory roles of neutrophils illustrate that their response is context specific, that there must be a degree of neutrophil plasticity, and that signals in the environment are of key importance.

Extravasation and metastatic seeding

Neutrophil extracellular traps (NETs) have been shown to sequester circulating tumour cells at distant sites and promote metastasis.[49] This is also true in peritoneal fluid.[50] Indeed, NETosis has been suggested as a biomarker predict patients as risk of metastasis in head and neck cancers.[51] Beyond NETs, neutrophils also communicate with circulating tumour cells, driving cycle progression and increasing their metastatic potential.[52] In addition, tumour cell extravasation into tissues is aided by interactions between β_2 integrin on neutrophils and ICAM-1 on tumour cells, promoting anchoring to the vascular endothelium.[53] Finally, tumour derived G-CSF can initiate a pre-metastatic environment in distant organs, mobilising neutrophils from the bone marrow to swarm at the metastatic site before tumour cells arrive.[54]

Conversely, Granot et al. showed that tumour entrained neutrophils (i.e. stimulated by the primary tumour) can inhibit metastatic seeding via hydrogen peroxide (H_2O_2) killing of disseminated tumour cells.[55] It has recently been shown that H_2O_2 from neutrophils kills tumour cells by triggering a lethal influx of calcium via transient receptor potential cation channel subfamily M member 2 (TRPM2), an H_2O_2 dependent calcium permeable channel expressed on cancer cells.[56]

1.2.4 Defining neutrophil populations: density, maturity, surface markers, morphology and anatomical site

It is clear from earlier sections, that neutrophils display heterogeneity and plasticity of function in malignancy. But what other features define these neutrophils that are pro- or anti-tumour? The Eruslanov and Fridlender groups have carried out seminal work in the last few years where functional neutrophil subpopulations have been distinguished further by density, maturity, surface markers, morphology and anatomical site (Figure 1.3).[46 47 57 59]

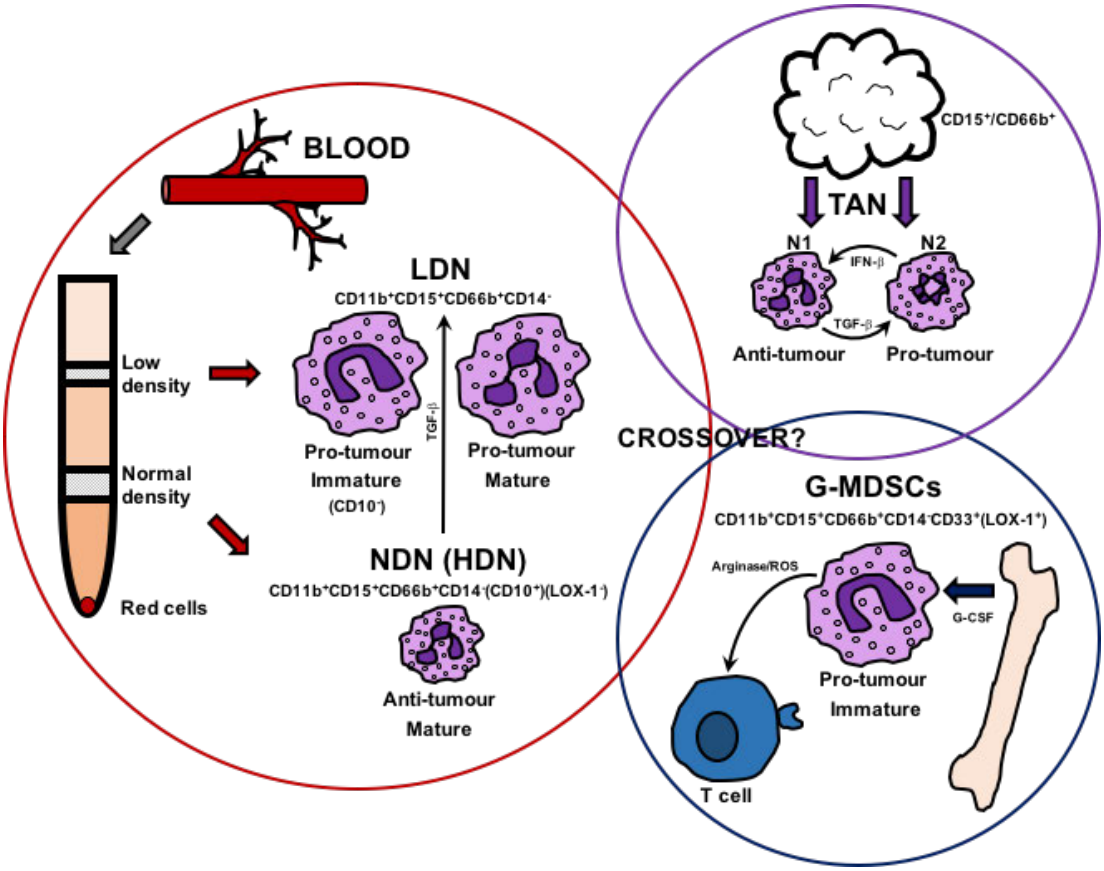

Figure 1.3: Neutrophil subpopulations defined by density, maturity, surface markers, morphology and anatomical site.
The degree of crossover between LDN, N2 TAN and G-MDSC populations needs further delineation. LDN, low density neutrophils; NDN, normal (high) density neutrophils; TAN, tumour-associated neutrophils; G-MDSCs, granulocytic myeloid-derived suppressor cells.

Peripheral blood neutrophils

Ex-vivo, neutrophils are commonly isolated from the blood by discontinuous density gradient. This results in the formation of a red cell pellet, a normal density (sometimes referred to as 'high density' in the literature) layer of cells and a low-density layer of cells. Neutrophils are usually the predominant cell type in the normal density layer (normal density neutrophils, NDN) and peripheral blood mononuclear cells (PBMCs) are found in the low-density layer.[60] In malignancy, there is an expanded population of neutrophils in the low-density layer (low density neutrophils, LDN), which can be further defined by maturity/morphology. LDN are large and are either immature with banded/ring nuclei, or mature with segmented nuclei. All low-density neutrophils are pro-tumour, displaying immunosuppressive properties. NDN are small and mature with segmented nuclei and are anti-tumour. Of note, neutrophils from patients with malignancy resist apoptosis compared with healthy donor neutrophils. Finally, murine models showed LDN to originate from the bone morrow, but of interest TGF-β could also mediate the transition of NDN to LDN (displaying plasticity).[58 59]

Human TAN

In humans, TAN in early stage cancer are mature with segmented nuclei and are anti-tumour, activating T cell responses. Study of TAN from more advanced malignancies is proving more difficult, due to lack of availability of tissue to study (patients with advanced cancer do not typically undergo surgical resection).[46 47 57]

Neutrophil surface marker immunotyping (human)

To date, it has proven difficult to distinguish between the neutrophil subpopulations described above, by surface marker immunotyping. Furthermore there have been difficulties when attempting to compare neutrophil subpopulations found in murine models to those found in humans.[61] However, most groups use $CD11b^{+}CD15^{+}CD66b^{+}CD14^{-}$ to identify neutrophils in humans. In addition, CD10 is proving to be a key marker for the maturation and suppressive potential of neutrophils. Indeed, going forward CD10 may reduce the need to use density gradients to define neutrophil populations.[62] Of note, neutrophil maturity in cancer is an expanding field of interest, with Mackey et al. providing a good summary of the literature.[63]

Myeloid-derived suppressor cells (MDSCs) and S100 proteins

The name myeloid-derived suppressor cells, was originally coined over 10 years ago to describe a group of myeloid cells with immunoregulatory activity i.e. they suppress anti-tumour T cell functions (via arginase and ROS). Broadly speaking, they compose two phenotypical/morphological groups of cells: those similar to neutrophils (granulocytic/polymorphonuclear MDSCs or G-MDSCs/PMN-MDSCs) and those similar to monocytes (M-MDSCs). It is thought that during chronic inflammatory processes, such as malignancy, there is a persistent signal to recruit neutrophils and monocytes from the bone marrow (e.g. GM-CSF, G-CSF, M-CSF). As time goes on, the rate of demand on the bone marrow is such that these recruited cells are increasingly immature, and have aberrant function. These cells are MDSC, and as cancers progress they form a greater proportion of circulating cells. In humans as G-MDSCs and neutrophils can both be defined by the surface markers $CD11b^{+}CD14^{-}CD15^{+}$(or $CD66b^{+}$)$CD33^{+}$ it has been difficult to distinguish between them. However, it is known that G-MDSCs are found in the low-density fraction of peripheral blood. Furthermore G-MDSCs express lectin-type oxidized LDL receptor 1 (LOX-1) and so this marker may be used to distinguish them, without the need for a density gradient.[64 65]

There has been interest in the S100 family of calcium binding proteins, as they are released during the inflammatory response to malignancy, and S100A8/A9 (calprotectin) can act as a MDSC chemoattractant. In mouse models of malignancy, S100A8/A9 proteins have been shown to regulate the accumulation of MDSCs.[66] Indeed in models of colon cancer, MDSCs have been found to produce S100A8/A9, leading to an autocrine pathway for accumulation of MDSCs at metastatic sites, and furthermore, S100A8/A9 activated tumour cells promoting cancer progression.[67]

There is debate as to how closely neutrophils and G-MDSCs are related.[68] It seems increasingly likely that in humans, immature peripheral blood LDN and G-MDSCs are one and the same. However, mature peripheral blood LDN appear to be different to G-MDSCs. Furthermore, within tumours themselves the relationship between G-MDSCs and TAN is entirely unknown.[69]. Finally, using the name MDSC, that defines this group of cells based entirely on the single function of immunosuppression, is probably not that helpful, as it implies they only exist for this purpose, when in all likelihood they are more complex.[17 70]

1.2.5 Tumour environment and neutrophil metabolism

It is known that the tumour microenvironment has altered oxygen and metabolite availability. Oxygen sensing pathways and metabolic flux regulate neutrophil function and survival responses.[71 72] Whilst neutrophils were traditionally viewed as purely glycolytic, there is Increasing interest in the metabolic plasticity of neutrophils in health and disease.[73] It has become apparent that immature low-density neutrophils/ MDSCs utilise fatty acid oxidation. This enables them to circumvent nutritional limitations within their local tissue environment.[74] In addition, uptake of fatty acids has been reported to contribute to their immunosuppressive activity in cancer,[75 76] and facilitation of metastasis.[77] Encouragingly, there evidence that Inhibition of fatty acid oxidation may be helpful in reducing this pro-tumour activity, and this could be an important therapeutic avenue in the future.[78]

1.2.6 Summary of neutrophil roles in cancer

It is probably beneficial to move away from N1/ N2 terminology. N1/ N2 represent laboratory extremes of neutrophil function, whereas in reality there is likely to be a biological continuum/ spectrum of neutrophil actions. The overall pro- or anti-tumour behavior of neutrophils will be in flux, with neutrophils displaying plasticity dependent on their local tissue environment, and therefore having different roles at different sites. For cancers to progress, the overall balance will begin to tip in favour of immature pro-tumour neutrophils. This model is summarised in Figure 1.4, akin to the 'macrophage wheel' used by Pollard et al.[27] The term G-MDSC is also too restrictive, defining a cell population based on a single feature. Appropriate neutrophil responses are dependent upon a functioning balance of bone marrow release, recruitment to sites of need, activation and appropriate action at target sites. G-MDSC and immature low-density neutrophils are likely to be one and the same population, reflecting a dysregulation of bone marrow neutrophil release, resulting in an expanded dysfunctional immature circulating neutrophil population, with detrimental actions when recruited to the target site.

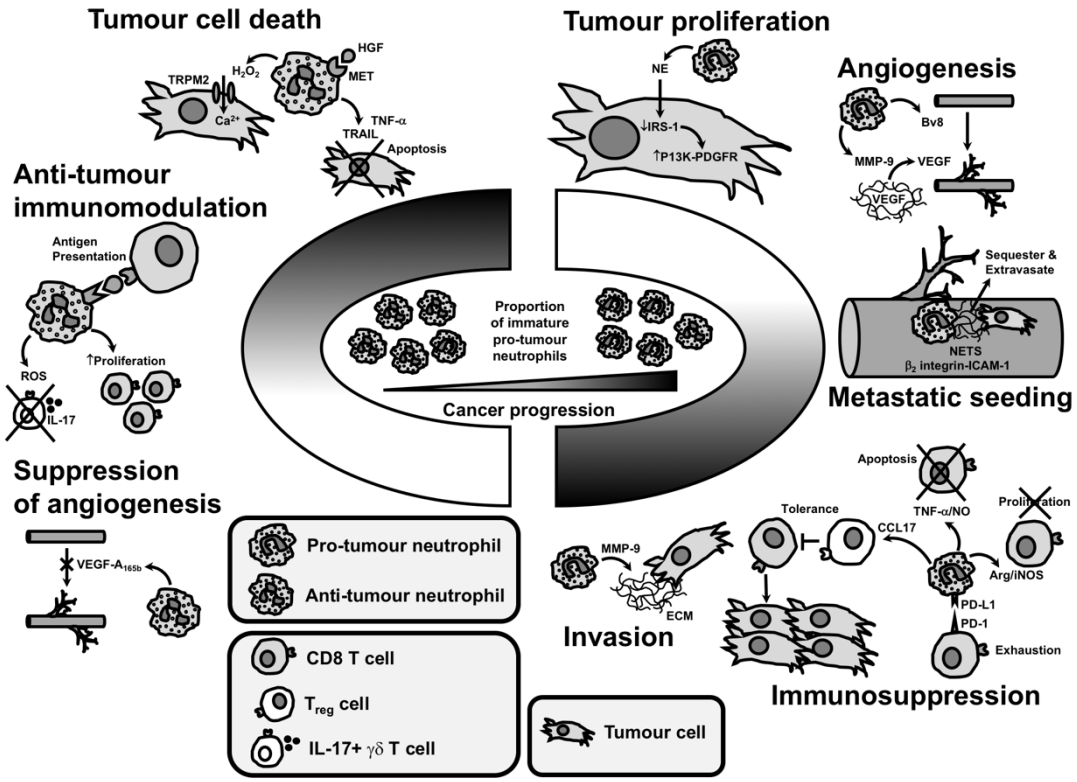

Figure 1.4 Mechanisms through which neutrophil subpopulations aid or abate tumourigenesis.

The proportion of pro- and anti-tumour neutrophils at any one time is in flux, with a degree of plasticity and a spectrum of activity. However, for cancers to progress this balance must begin to favour immature pro-tumour neutrophils.

1.2.7 Areas of agreement and controversy

Neutrophils are no longer seen as a simple first responder cell; they have complex multifaceted roles in all stages of malignancy with both pro- and anti-tumour roles. In cancer, neutrophils are a heterogeneous population and display plasticity. Several neutrophil subpopulations have been identified and are currently defined by a combination of features; density, maturity, surface markers, morphology and anatomical site.

A recent review article by the Eruslanov group highlights the ongoing areas of controversy regarding the role of neutrophils in cancer.[61] These mainly relate to 1) the limitations of translating murine tumour models to human pathology, and 2) the lack/quality of human data. These are addressed in turn, and examples given below.

Limitations of translating murine tumour models to human pathology

The most common form of murine model is transplantable tumours i.e. immortal cell lines that have undergone years of selective pressure and are chosen based on their ability to grow quickly when injected into the mouse. These tumours by definition have a very different natural history to the gradual evolution of a natural tumour, and therefore really only represent the later stages of malignancy. There are no shared neutrophil cellular markers between mouse and man. We do not know if immature LDN, G-MDSCs and N2 are the same cell population or not. N1/N2 polarisation has not been shown in human TAN, and it seems more likely that in fact there will be a continuum of behaviour rather than these two extremes. Are N2 neutrophils just immature cells recruited as a consequence of cancer and not a contributing cause?

Quality of human data

There is a lack of human tissue available from the later stages of cancer, as patients do not routinely have surgery. Furthermore, whilst peripheral blood may be more easily available from these patients (than solid tumour samples), the behavior of blood neutrophils may be completely different to that of TANs. When tumour samples are obtained, it must be noted that neutrophil function can be changed by

the process of disaggregation used to extract the neutrophils. Finally, in human studies, a lot has been attributed to ex-vivo T cell responses which may not reflect true physiology. For example, as previously described there are concerns about artefact that may be created by the methodologies used for ex-vivo T cell proliferation studies.

Conclusion

Overall, there needs to be an unpicking of the various neutrophil subpopulations, and a better understanding of their evolving roles as cancers progress, at both primary and metastatic sites.

1.2.8 Neutrophils as therapeutic targets in cancer

In terms of established therapies, neutrophils have been shown to be important players in the beneficial immune response to antibody-based cancer therapy,[79] photodynamic cancer therapy,[80] and Bacillus Calmette-Guerin immunotherapy.[81] However, a growing area of research is considering neutrophils as a therapeutic target themselves. Whilst the short-lived nature of neutrophils and their essential role in host defense against infection will need to be considered, nevertheless, targeted therapies relating to neutrophil recruitment, function and polarisation may be an attractive add-on therapy to conventional treatments (i.e. chemotherapy/radiotherapy) and newer immunotherapies. For example, in terms of neutrophil recruitment, there is interest in targeting the CXCR2 pathway.[82] Relating to neutrophil polarisation, there have been trials of TGF-β inhibitors as a cancer therapy.[83] With regard to direct neutrophil-tumour interaction, there has been interest in the use of neutrophil elastase inhibitors.[84]

Finally, an expanding area of interest is understanding how neutrophils respond to newer targeted cancer therapies. Inhibitors of the receptor Tyrosine kinase c-MET have been shown to inhibit neutrophil recruitment to tumours, with some concerned this may be detrimental,[30] but others hopeful of benefit.[85] As previously mentioned, neutrophils have been shown to express PD-L1, and therefore immune checkpoint inhibitors may have a role in reducing neutrophil suppression of T cell responses.

1.3 Lung cancer

1.3.1 Initiation of lung cancer

Around 7 out of 10 lung cancers are caused by smoking, which triggers genetic alterations in cells that can result in clonal proliferation.[86] Lung tumours themselves are composed of a heterogeneous mix of clonally expanded subpopulations, with distinct molecular features. The most common genetic mutations in smokers are found in the Kirsten rat sarcoma (KRAS) and tumour protein p53 (TP53) genes. The most common mutations in non-smokers are found in the epidermal growth factor receptor (EGFR), receptor tyrosine kinase (ROS1) and anaplastic lymphoma kinase (ALK) genes.[87]

1.3.2 Clinical classification, management and challenges

Lung cancer is the third most common cancer in the UK. Around 87% of lung cancers are histologically non-small cell lung cancer (NSCLC). It is common for patients to have advanced (stage IV) disease at the time of diagnosis. When this is the case, less than 20% survive one year or more. Primary lung cancers are classified as either small-cell lung cancer (SCLC) or non-small cell lung cancer (NSCLC). NSCLC further divides into adenocarcinoma (most common), squamous cell carcinoma and large cell carcinoma (uncommon). The most common sites of metastasis in lung cancer are elsewhere in the lung, the pleura (usually resulting in pleural effusion), bone, brain, adrenal glands, liver and extrathoracic lymph nodes. Treatment options depend upon the stage of the cancer and the performance status (fitness) of the patient. The main therapies include surgery, chemotherapy, radiotherapy, targeted cancer drugs (e.g. tyrosine kinase inhibitors), immunotherapy (e.g. programmed cell death protein 1 inhibitors), or symptom control. Diagnosis is often made when the disease has already metastasised. Metastatic burden is the major driver of morbidity and mortality. There is a need for more effective treatments of metastatic disease, in addition to finding better ways to make diagnoses earlier.[86]

1.3.3 Modulation of the immune system in lung cancer: programmed death-ligand 1 (PD-L1) and programmed cell death protein 1 (PD1)

T cells play a key role in host defence against cancer, by killing cancer cells. To carry out this function, T cells must become first become activated following antigen recognition. There are natural breaks ('immune checkpoints') for this immune response in order to prevent inappropriate T cell activity (e.g. autoimmunity): negative regulators of T cell activation include cytotoxic T lymphocyte antigen 4 (CTLA4) and programmed death protein 1 (PD1).[88] Cancers can express programmed death-ligand 1 (PD-L1 or B7-H1), which binds PD1, supressing T cell responses. Seminal work identified blockade of CTLA4,[89] and PD1/PD-L1,[90] as potential therapeutic targets, augmenting T cell responses to cancer. These discoveries have led to the clinical use of checkpoint inhibitors in lung cancer.

1.4 Summary and aims

Appropriate neutrophil responses are dependent upon a functioning balance of neutrophil production, release from the bone marrow, recruitment to sites of need, activation and appropriate action at said sites, and effective clearance afterward. Dysregulation of this finely tuned homeostatic system results in disease.

Neutrophils play an active role in cancer pathophysiology. They can be either pro- or anti-tumour, they form heterogeneous populations, and display plasticity. In cancer, neutrophil function appears to be dependent upon several factors including maturity and tissue microenvironment. Better understanding of these mechanisms may help to identify new immunomodulatory therapeutic targets.

Whilst neutrophil populations have been described in early stage human lung cancer (predominantly anti-tumour role), and animal models have demonstrated their importance in both pre-metastatic and established metastatic sites (predominantly pro-tumour role), to date, there is limited data regarding human neutrophil populations in advanced lung cancer. There is the need for a greater understanding of the interplay between extrinsic cell signals and intrinsic cell features, in determining neutrophil roles in cancer, and the subsequent effects on tumour outcome. For example, it is known that neutrophils can be polarised to pro- or anti-tumour phenotypes by environmental cytokines, but how neutrophil function is influenced by the extrinsic metastatic microenvironment in other ways, has not been fully delineated, nor how neutrophils interact with other immune cells and tumour cells at metastatic sites. In addition, there may be changes in the intrinsic features of neutrophils in cancer, that dictate their function.

This thesis aims to address the following questions:

1. How does the NSCLC metastatic environment influence neutrophil function?
2. What neutrophil populations are present in advanced NSCLC and do they have features specific to cancer?
3. Are there intrinsic properties of neutrophil populations in advanced NSCLC that determine their function?

This project utilises tissue from the NSCLC pleural metastatic site, as this provides a new and novel way of investigating neutrophil biology in the metastatic tumour microenvironment. The NSCLC pleural metastatic site is also routinely accessed clinically for diagnostic and therapeutic purposes, meaning tissue was frequently available for such work.

Chapter 2 Methods

2.1 Sample collection

2.1.1 Ethical approvals

Healthy donor participants were recruited from the University of Edinburgh Centre for Inflammation Research Blood Resource, ethical approval for which was granted by the Centre for Inflammation Research Blood Resource Management Committee. Study title: The Role of Inflammation in Human Immunity (AMREC 15-HV-013). Patient participants were recruited from NHS Lothian hospitals, ethical approval for which was granted by the NHS Lothian BioResource Tissue Governance Committee. Study title: Lung Cancer Characterisation to Develop Novel Molecular Stratification Imaging Probes for Lung Cancer (AMREC 15-ES-0094, SR419).

2.1.2 Permitted sampling from patients

Up to 500mL of pleural fluid was collected from patients undergoing diagnostic or therapeutic drainage of any pleural effusion as a routine part of their medical care. This tissue was surplus to diagnostic requirements and was taken from any excess that would otherwise have been discarded. An additional blood sample (up to 20mL) was taken concurrently. All patients gave written informed consent.

2.1.3 Patient selection criteria and confirmation of diagnoses

The shared exclusion criteria for all patients were: blood borne viruses, previous or current intravenous drug abuse, significant anaemia, steroid use or lack of capacity to give informed consent.

The diagnosis of NSCLC was confirmed by the combination of positive histology and supporting radiological imaging. Specific exclusion criteria for NSCLC: active cancer therapy or having undergone cancer therapy in the last 12 months.

The diagnosis of parapneumonic effusion was confirmed by the combination of: blood tests suggestive of infection, supporting radiological imaging and the identification of an exudate by Light's criteria (pleural fluid protein/ serum protein >0.5, or pleural fluid LDH/ serum LDH >0.6, or pleural fluid LDH >2/3rd of the serum LDH upper limit of normal). Specific exclusion criteria for pneumonia patients: known or suspected tuberculosis.

2.1.4 Healthy donor selection criteria

Healthy donors had to be fit and well. Exclusion criteria were: blood borne viruses, previous or current intravenous drug abuse, anaemia, blood clotting disorders, anticoagulant therapy, steroid use, under the age of 16 or infection in the last 2 weeks. All healthy donors gave written informed consent.

2.1.5 Blood collection method

Blood was drawn using a 21-gauge butterfly needle directly into 10mL S-Monovete® sodium citrate tubes (Sarstedt), or alternatively into a syringe. If drawn by syringe, 36mL of blood was immediately transferred into a 50mL polystyrene Falcon™ tube containing 4mL of 3.8% sodium citrate and mixed by gentle inversion. Samples were transported to the laboratory room temperature and processed within 2 hours.

2.1.6 Pleural fluid collection method

Pleural fluid was drawn by syringe and immediately transferred into polystyrene specimen containers. Samples were transported to the laboratory on ice and processed within 2 hours.

2.2 Sample processing

2.2.1 Isolation of blood normal-density neutrophils (NDN) and peripheral blood mononuclear cells (PBMCs) by density gradient

This is a modified version of the original protocol by Haslett et al.[91] Anticoagulated blood was centrifuged in a 50mL polystyrene Falcon™ tube at 350G for 20 minutes (acceleration 5, deceleration 5). The platelet rich plasma layer was carefully removed and transferred into a 15mL polystyrene Falcon™ tube and centrifuged at 1150G for 20 minutes at 4°C. The platelet-poor plasma supernatant was removed, aliquoted, flash frozen and stored at -80°C for future use. Meanwhile, the remaining erythrocytes and leukocytes in the 50mL polystyrene Falcon™ tube were separated from one another by differential sedimentation in 0.9% NaCl containing 0.72% Dextran-500 (Table 2.1), incubated for 25 minutes at 37°C.

Volume of blood taken (mL)	Volume of 6% Dextran added (mL)	Topped up with pre-warmed 0.9% sodium chloride to total volume of (mL)
20	3	25
40	6	50

Table 2.1: Dextran sedimentation preparations.

Thereafter, the leucocyte-rich upper later was aspirated and transferred to a fresh 50mL polystyrene Falcon™ tube and topped up to 40mL with pre-warmed 0.9% NaCl prior to centrifugation at 350G for 6 minutes (acceleration 9, deceleration 5) to pellet the leukocytes. A discontinuous Percoll™ (GE Healthcare) density gradient was then used to separate NDN and PBMCs. An isotonic stock solution of 90% Percoll™ was made by adding 10% volume of 10X DPBS (Sigma-Aldrich). 73%, 61% and 49% Percoll™ were made by dilution of the 90% stock with Gibco™ 1X DPBS (ThermoFisher) (Table 2.2).

Percoll™ concentration	90% Percoll™ (mL)	1X DPBS (mL)
73%	8.1	1.9
61%	6.8	3.2
49%	5.5	4.5

Table 2.2: Percoll™ preparations for blood (stock to make 3 gradients).

Gradients were made in 15mL polystyrene Falcon™ tubes. 3mL of 73% Percoll™ was pipetted into the bottom of the 15mL tube using a pastette, followed by 3mL of 61% gently layered on top. Finally, the leukocyte pellet was re-suspended in 3mL 49% Percoll™ and very carefully layered above the 61% layer. This gradient was then centrifuged at 720G for 20 minutes (acceleration 1, deceleration 0). The PBMC were harvested from the 49%/ 61% interface using a pastette, and transferred to a fresh 50mL polystyrene Falcon™ tube. The NDN were harvested from the 61%/ 73% interface and transferred to a different Falcon™ tube. The cells were then washed twice with Gibco™ 1X DPBS prior to use (centrifuged at 300G for 6 minutes (acceleration 9, deceleration 9)). Cell number was counted using a C-Chip Neubauer haemocytometer (NanoEnTek). NDN yield was consistently >1x10^6/ mL of blood donated. NDN purity was routinely >97%, determined by morphology on cytocentrifuge slide, with eosinophils being the predominant contaminant (Figure 2.1).

2.2.2 Cytocentrifuge slide preparation

Cytocentrifuge slides (Cytospins) were used in all experiments requiring examination of cellular morphology. 100μL of cell suspension was pipetted into reusable single cytofunnel cell concentrators (ThermoFisher), sandwiched together with a disposable filter card (ThermoFisher) and glass slide, using a metallic holder. This was centrifuged for 3 minutes at 300 rpm in a Cytospin 4 Cytocentrifuge (ThermoFisher). Slides were air-dried, fixed with 100% methanol, stained with Kwik-Diff™ (ThermoFisher) to visualise acidic and nuclear structures, and lastly glass coverslips mounted with DPX mountant (Sigma-Aldrich).

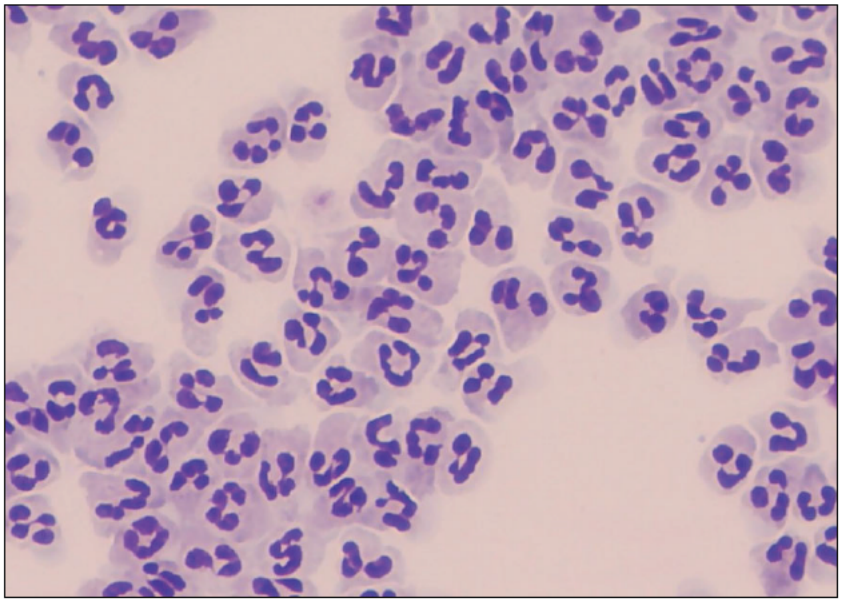

Figure 2.1: Representative Cytospin image demonstrating high neutrophil purity following extraction from the blood (40X magnification).

2.2.3 Isolation of whole blood neutrophils (WBN) using EasySep™ enrichment kit

For volumes of blood ≥20mL, WBN were isolated using the EasySep™ human neutrophil enrichment kit (Stemcell). Of note this product has now been discontinued, and has been replaced by the EasySep™ human neutrophil isolation kit. The samples were first prepared by following the protocol outlined in section 2.2.1, stopping at the point where the leukocytes were pelleted following dextran sedimentation. The leukocytes were counted using a C-Chip Neubauer haemocytometer, by taking an aliquot of the sample and staining with 3% acetic acid with methylene blue (Stemcell) to aid counting of nucleated cells (exclude any residual red cells).

The EasySep™ human neutrophil enrichment kit was then used as per the manufacturer's instructions. The leukocyte pellet was re-suspended in RoboSep™ buffer at a concentration of $5x10^7$/ mL, and transferred into 5mL polystyrene round-bottom tubes (maximum 2mL leukocyte suspension per tube). Isolation cocktail (tetrameric antibody complexes produced from mAb directed against CD2, CD3, CD9, CD19, CD36, CD56 and glycophorin A) was added at a concentration of 50μL/ mL of leukocyte suspension, the sample mixed, and then incubated at room temperature for 10 minutes. Nanoparticle beads were added at a concentration of 100μL/ mL of leukocyte suspension, the sample mixed, and then incubated at room temperature for 10 minutes. The sample was topped up to a total volume of 2.5mL with RoboSep™ buffer, gently pipetted up and down 2-3 times and placed into an EasySep™ magnet (Stemcell) (without lid) for 5 minutes. Following this, the magnet and tube were together inverted in one continuous movement, the contents (isolated WBN) pouring out into a 15mL polystyrene Falcon™ tube. The isolated WBN were pooled, and washed with Gibco™ 1X DPBS prior to counting and use. WBN yield was typically ≥$1x10^6$/ mL of blood donated (haemocytometer), with cell purity >99% (by morphology on cytocentrifuge slide).

2.2.4 Isolation of highly pure normal-density neutrophil (NDN) and low-density neutrophil (LDN) populations

Three different methods (a-c) were investigated, to find which provided the purest NDN an LDN populations:

a. Isolation of NDN and PBMC by density gradient (as per 2.2.1) followed by EasySep™ human neutrophil enrichment kit treatment of the NDN and PBMC separately, to give enriched NDN and LDN populations (in a similar fashion to the second part of 2.2.3).
b. Isolation of NDN and PBMC by density gradient (as per 2.2.1) followed by fluorescence-activated cell sorting, to give enriched NDN and LDN populations (in a similar fashion to 2.2.8).
c. Isolation of WBN using EasySep™ human neutrophil enrichment kit (as per 2.2.3) followed by discontinuous Percoll™ density gradient of WBN (73%/ 61%/ 49%) separating WBN into NDN and LDN populations (in a similar fashion to the gradient section of 2.2.1).

Purity of the resultant NDN and LDN populations was examined by flow cytometry (as per 2.6.1), due to the varying cell morphology of LDN making neutrophil identification on cytocentrifuge slide difficult. Neutrophils were defined by the combination of typical FSC/ SSC distribution, $CD66b^{+}$ and $CD15^{+}$. Method c was found to yield LDN with the highest purity, as demonstrated in Table 2.3 and Figure 2.2. Therefore, method c was used in all experiments requiring highly pure NDN and LDN populations.

Method	Purity NDN (%)	Purity LDN (%)
a	99.7	87.0
b	99.6	84.4
c	99.6	99.5

Table 2.3: Purity of NDN and LDN populations obtained, when isolated by three different methods.

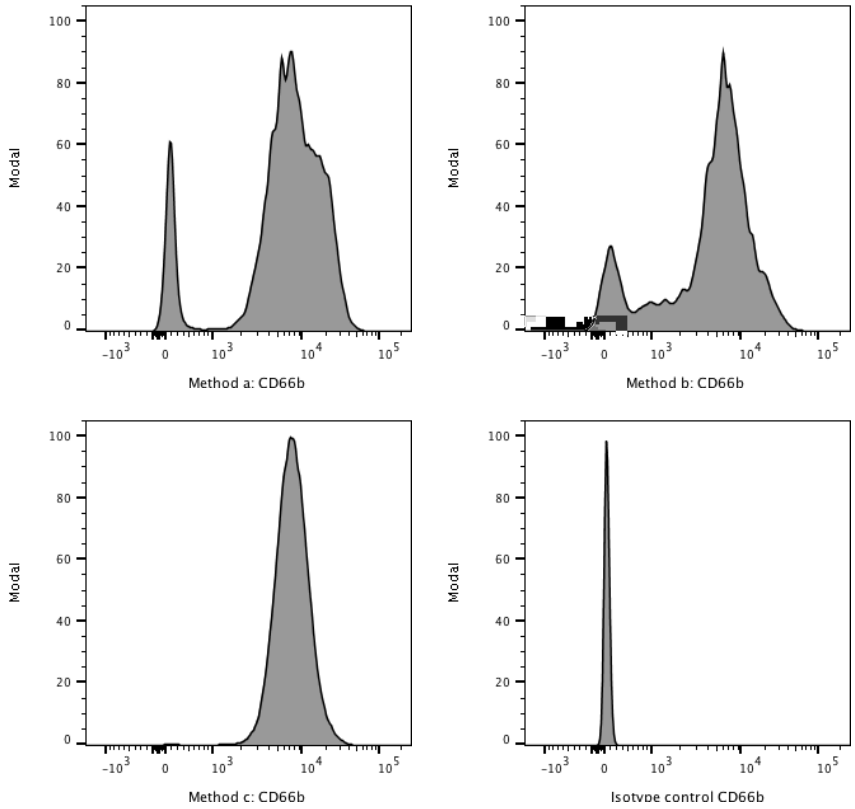

Figure 2.2: CD66b staining of LDN populations isolated by three different methods.

2.2.5 Isolation of whole blood neutrophils (WBN) and T cells from whole blood using EasySep™ direct kits

For volumes of blood <20mL, WBN were isolated using the EasySep™ direct human neutrophil isolation kit (Stemcell). T cells were separately isolated using the EasySep™ direct human T cell isolation kit (Stemcell). Both kits had a similar protocol. Anticoagulated whole blood was transferred into 5mL polystyrene round-bottom tubes (maximum 2.5mL per tube). The RapidSpheres™ were vortexed for 30 seconds. Isolation cocktail was added at a concentration of 50μL/ mL of blood, followed by RapidSpheres™ at a concentration of 50μL/ mL of blood, the sample mixed, and then incubated at room temperature for 5 minutes. The sample was topped up to a total volume of 2.5mL (T cell kit) or 5mL (neutrophil kit) with RoboSep™ buffer, gently pipetted up and down 2-3 times and placed into an EasySep™ magnet (without lid) for 5 minutes. Following this, the magnet and tube were together inverted in one continuous movement, the enriched contents pouring out into a new 5mL polystyrene round-bottom tube. The same volume of RapidSpheres™ as used in the first steps was added to the new tube containing the

enriched cells, the sample mixed, and then incubated at room temperature for 5 minutes. Next, the sample was placed into an EasySep™ magnet (without lid) for a further 5 minutes. Following this, the magnet and tube were together inverted in one continuous movement, the enriched contents pouring out into a 15mL polystyrene Falcon™ tube. The isolated cells were separately pooled, and washed with Gibco™ 1X DPBS prior to counting and use (centrifugation at 320G for 6 minutes (acceleration 9, deceleration 5)). Neutrophil yield was typically $\geq 1x10^6$/ mL of blood donated. T cell yield was typically $\geq 0.5x10^6$/ mL of blood donated (haemocytometer). Cell purity was >99% (by morphology on cytocentrifuge slide).

2.2.6 Processing of pleural fluid

Pleural fluid was processed immediately following collection. The sample was poured through 100μm Fisherbrand™ cell strainers (ThermoFisher) into 50mL polystyrene Falcon™ tubes, then centrifuged at 400G for 10 minutes at 4°C (acceleration 9, deceleration 9). The supernatant was removed, poured through 40μm Fisherbrand™ cell strainers (ThermoFisher) into 50mL polystyrene Falcon™ tubes, sterile-filtered using Millex®-GP 0.22μm polyethersulfone syringe filters (Sigma-Aldrich), aliquoted, flash frozen and stored at -80°C for future use (pleural fluid supernatant (PFS)). The cell pellets were pooled into an appropriate number of 50mL polystyrene Falcon™ tubes and re-pelleted prior to hypotonic red cell lysis. For red cell lysis, the cell pellet was re-suspended in 20mL of buffer A (0.2g NaCl in 100mL sterile water), the Falcon™ tube inverted ten times, 20mL of buffer B added (1.6g NaCl and 0.1g dextrose in 100mL sterile water), the Falcon™ tube inverted, then centrifuged at 350G for 6 minutes (acceleration 9, deceleration 5). The cells were then washed with Gibco™ 1X DPBS prior to use (centrifuged at 300G for 6 minutes (acceleration 9, deceleration 9). The leukocytes were counted using a C-Chip Neubauer haemocytometer, by taking an aliquot of the sample and staining with 3% acetic acid with methylene blue to aid counting of nucleated cells (exclude any residual red cells). Cytocentrifuge slides of the leukocyte suspension were also made.

2.2.7 Optimisation of pleural fluid neutrophil (PFN) isolation

Six different methods (a-f) were investigated, to find which provided the purest PFN population from the pleural fluid leukocyte population (isolated as per 2.2.6), with acceptable cell yield:

a. Discontinuous Percoll™ density gradient (73%/ 61%/ 49%, Table 2.2) (the same as that used for blood samples, see gradient section of 2.2.1). The gradient was constructed with 3mL in each layer, with the cells re-suspended in 49% Percoll™ at the top. This was centrifuged at 720G for 20 minutes (acceleration 1, deceleration 0). Neutrophils were expected to be found at the 61%/ 73% interface post centrifugation.
b. Discontinuous Percoll™ density gradient (78%/ 69%/ 52%, Table 2.4) (the same as that used for Broncho Alveolar lavage samples). The gradient was constructed with 3mL in each layer, with the cells re-suspended in 52% Percoll™ at the top. This was centrifuged at 1200G for 30 minutes (acceleration 1, deceleration 0). Neutrophils were expected to be found at the 69%/ 78% interface post centrifugation.
c. 4 layer discontinuous Percoll™ density gradient (54%/ 45%/ 36%/ 27%, Table 2.4) (as per Hamburger et al.[92]). The gradient was constructed with 3mL in each layer, except the top layer, which consisted of the cells re-suspended in 1mL of 27%. This was centrifuged at 800G for 30 minutes (acceleration 1, deceleration 0). Neutrophils were expected to be found in the cell pellet at the bottom of the gradient post centrifugation.
d. Ficoll-Paque PLUS™ (GE Healthcare) density gradient (as per Aleman et al.[93]). The gradient was constructed with 5mL Ficoll-Paque PLUS™ as a bottom layer, with the cells re-suspended in 5mL Gibco™ RPMI 1640 medium (ThermoFisher) on top. This was centrifuged at 840G for 20 minutes (acceleration 9, deceleration 0). Neutrophils were expected to be found in the cell pellet at the bottom of the gradient post centrifugation.
e. EasySep™ human neutrophil enrichment kit (in a similar fashion to the second part of 2.2.3).
f. Fluorescence-activated cell sorting (as per 2.2.8).

Percoll™ concentration	90% Percoll™ (mL)	1X DPBS (mL)
78%	8.7	1.3
69%	7.7	2.3
52%	5.8	4.2
54%	6.0	4.0
45%	5.0	4.0
36%	4.0	6.0
27%	3.0	7.0

Table 2.4: Percoll™ preparations for pleural fluid (stock to make 3 gradients).

Methods a-d were found to be inferior both in terms of cell yield and purity. There were also concerns that methods a-d would result in loss of any low-density PFN. Methods e and f were investigated head-to-head. Purity of the resultant PFN populations was examined by flow cytometry (as per 2.6.1). Neutrophils were defined by the combination of typical FSC/ SSC distribution, $CD66b^+$ and $CD15^+$. Fluorescence-activated cell sorting was found to yield PFN with the highest purity (Table 2.5 and Figure 2.3), and was used in all experiments requiring PFN.

Method	Purity PFN (%)
EasySep™ human neutrophil enrichment kit	85.7
Fluorescence-activated cell sorting	97.3

Table 2.5: Purity of PFN population obtained, when isolated by two different methods.

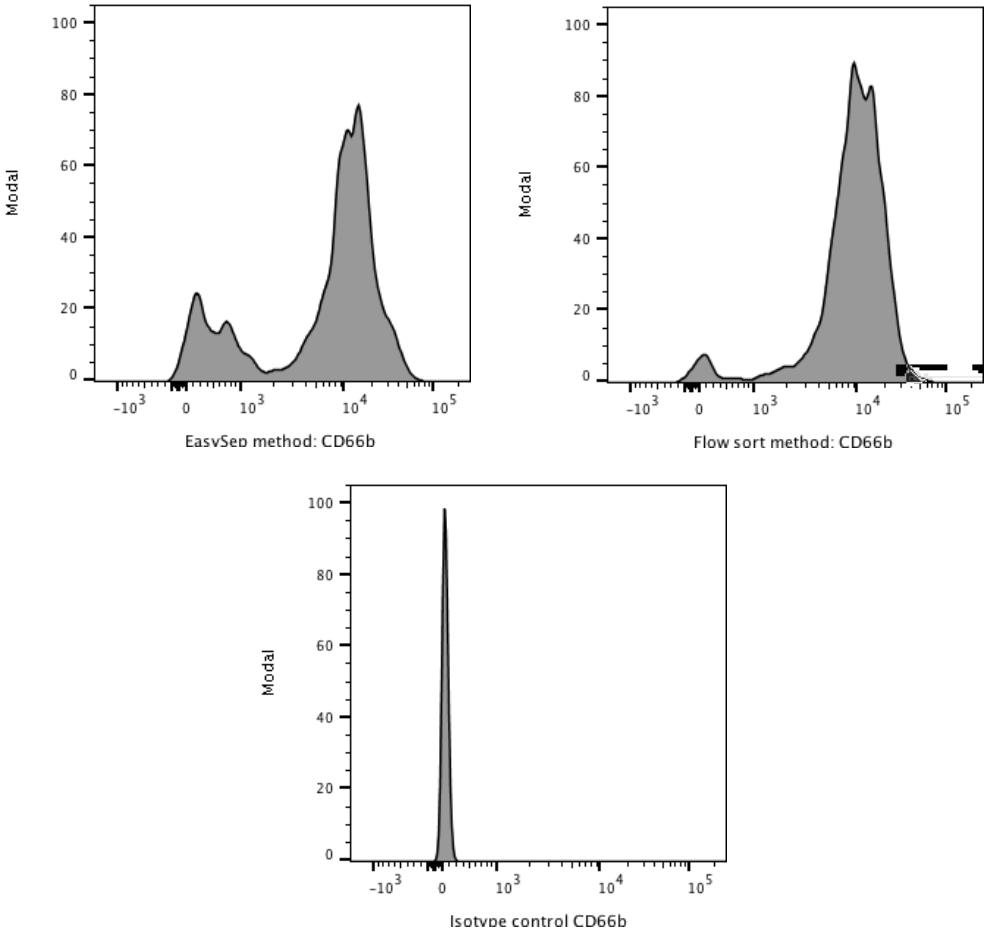

Figure 2.3: CD66b staining of PFN populations isolated by two different methods.

2.2.8 Isolation of highly pure pleural fluid neutrophils (PFN) by fluorescence-activated cell sorting

Pleural fluid leukocytes prepared as per 2.2.6 were pelleted and re-suspended in Gibco™ 1X DPBS (without FBS) at a concentration of $5x10^7$/ mL, then a maximum of 3mL transferred into a 5mL polystyrene round-bottom tube. Antibodies to CD3 and CD14 (BioLegend, Table 2.6) were each added at a concentration of 1μL/ $1x10^6$ leukocytes and the sample incubated for 30 minutes at 4-8°C protected from light. DAPI (ThermoFisher) at a working concentration of 100μg/ mL was added at 1:1000 (final concentration 0.1μg/ mL), immediately prior to fluorescence-activated cell sorting using the BD FACSAria™ Fusion flow cytometer running BD FACSDiva™ software version 8.0 (BectonDickinson). The gating strategy used is outlined in Figure 2.5. The cytometer was fitted with a 70μm nozzle. Samples were collected into 200μL of Gibco™ 1X DPBS (without FBS) in a 15mL polystyrene Falcon™ tube, with a maximum sorting time of 3 hours. The isolated neutrophils were washed with Gibco™ 1X DPBS, prior to counting (haemocytometer) and downstream use. This method provided neutrophils of a high purity (Table 2.5 and Figure 2.4).

Antigen	Fluorophore	Clone	Source	Product code
CD3	PE	HIT3a	BioLegend	300308
CD14	AF700	63D3	BioLegend	367114

Table 2.6: Antibodies used for fluorescence-activated cell sorting.

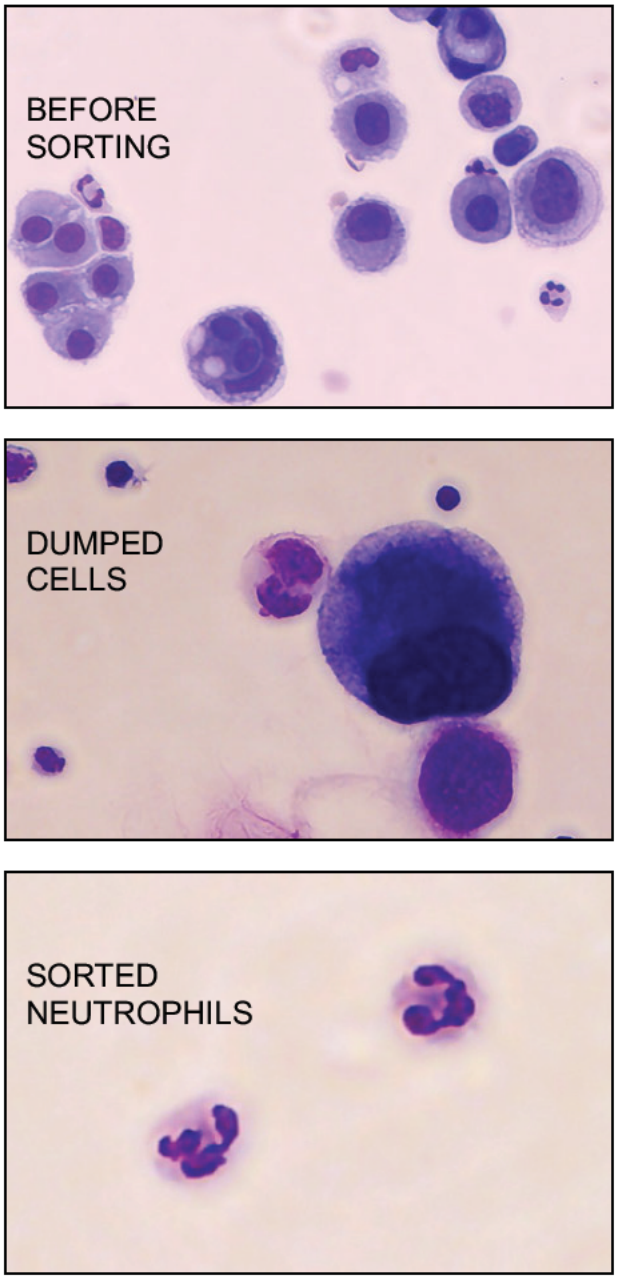

Figure 2.4: Images of pleural fluid cell populations before and after fluorescence-activated cell sorting (40X magnification).

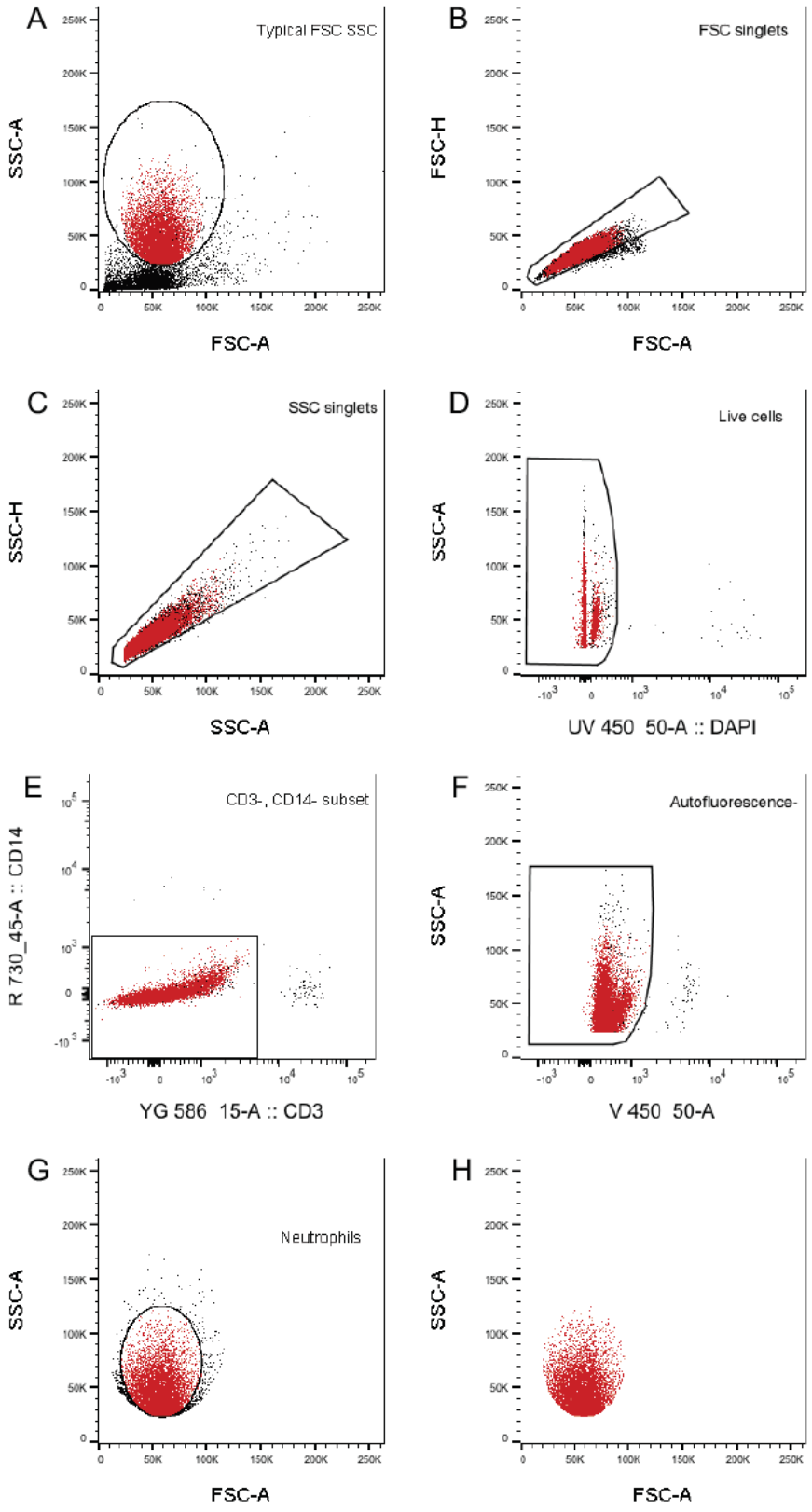

Figure 2.5: Fluorescence-activated cell sorting gating strategy.
Strategy shown in order (A-H). Back-gating of the final neutrophil population (H) is shown in red (A-G). CD3 and CD14 were used to exclude T cells and monocytes (E). Autofluorescence was used to exclude eosinophils[94] (F).

2.3 Cell culture conditions

2.3.1 Various media conditions

Glucose-free media: this was used for glucose-free cell culture experiments. It consisted of Gibco™ RPMI 1640 no glucose medium (2mM L-glutamine) (ThermoFisher), supplemented with 1% Gibco™ Penicillin-Streptomycin (ThermoFisher) and 10% Gibco™ dialysed FBS (ThermoFisher).

Glucose replete media: this was the standard media used for most cell culture experiments. It consisted of Gibco™ RPMI 1640 medium (2mM L-glutamine and 11mM D-glucose), supplemented with 1% Gibco™ Penicillin-Streptomycin and 10% FBS (PAN-Biotech) (or instead 10% Gibco™ dialysed FBS when for an experiment also including glucose-free conditions).

Media supplemented with pleural fluid supernatant (PFS): PFS was extracted as per 2.2.6. This was defrosted in a water bath at 37°C. Glucose-free media or glucose replete media was supplemented with 10% PFS, unless otherwise stated.

2.3.2 Normoxia (12kPa O_2) vs. hypoxia (4kPa O_2)

Normoxic cell culture (the standard condition unless otherwise stated) was carried out in a ThermoFisher Heraeus BB15 CO_2 incubator (O_2 21%, CO_2 5%, 37°C). Hypoxic cell culture was carried out in an Invivo$_2$ 400 hypoxic workstation (BakerRuskinn) (O_2 1%, CO_2 5%, 37°C). Culture media oxygen tension was confirmed by analysis using a RAPIDLab 348 blood gas system (Siemens). Mean PO_2 of hypoxic media from 20 different samples was 4.4kPa (95% confidence interval 4.1-4.7).

2.4 Assays of neutrophil function

2.4.1 Apoptosis by cellular morphology

Isolated neutrophils were re-suspended in appropriate media (2.3.1) at a concentration of $5x10^6$/ mL. The various experimental conditions were plated in triplicate, with $7.5x10^5$ neutrophils per well (96 well Corning™ Costar ™ plates (ThermoFisher)) and cultured for 8 or 20 hours. Following this, cytospins were formed (2.2.2). Apoptosis was assessed, by examining the cytospins with oil immersion light microscopy at 100X magnification, with the observer blinded to the experimental conditions. At least 300 neutrophils in total were counted per slide, to ascertain the percentage undergoing apoptosis. Apoptotic neutrophils were identified by typical morphology (Figure 2.6).

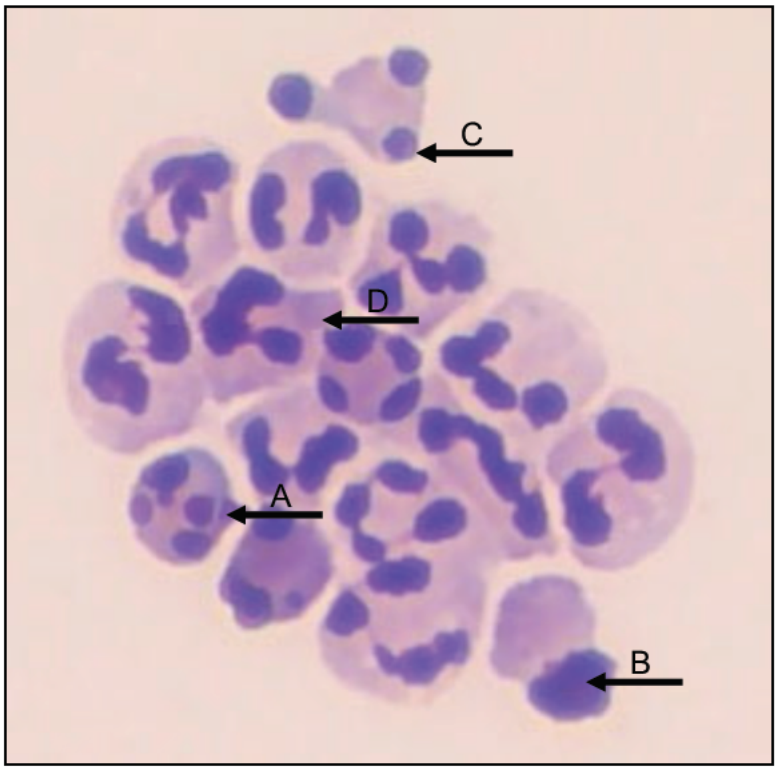

Figure 2.6: The typical morphological features of apoptotic neutrophils (100X magnification).
Cell shrinkage (A), nuclear pyknosis (B), formation of apoptotic bodies (C) and cell wall blebbing (D).

2.4.2 Apoptosis by flow cytometry

Apoptosis was also quantified by flow cytometry, using dual staining to categorise neutrophils into four groups (Table 2.7): viable (V), early apoptotic (EA), late apoptotic (LA) and dead/ necrotic (D). Annexin V binds phosphatidylserine residues, which are externalised to the neutrophil cell surface in early apoptosis. TO-PRO-3™ binds double-stranded nucleic acids, which are accessible to the stain when the cell wall is disrupted (late apoptosis) and destroyed (death/ necrosis).

	Annexin V	TO-PRO-3
Viable	-	-
Early apoptotic	+	-
Late apoptotic	+	+
Dead/ necrotic	-	+

Table 2.7: Annexin V and TO-PRO-3 staining features of apoptotic neutrophils.

Following culture, neutrophils were washed with Gibco™ 1X DPBS. 1X Annexin binding buffer was made by diluting 10X stock (BectonDickinson). PE conjugated Annexin V (BectonDickinson) was added to this buffer at a dilution of 1:25. The neutrophils were then re-suspended in 100μL of this staining buffer and incubated for 20 minutes at 4-8°C protected from light. Meanwhile, TO-PRO-3™ iodide (far-red fluorescence AF647-like) (ThermoFisher) stain was made up at a 1:3000 dilution with 1X Annexin binding buffer. 100μL of this TO-PRO-3™ stain was added to the neutrophils immediately before running each sample in a 5mL polystyrene round-bottom tube on the BD FACSCalibur™ (BectonDickinson) or alternatively the Attune™ NxT (ThermoFisher) flow cytometer. CellQuest Pro Software (BectonDickinson)/ Attune™ NxT software (ThermoFisher) was used for data acquisition of 10,000 'Singlets'. Data analysis was carried out using FlowJo 10.3 software (FlowJo). The gating strategy is outlined in Figure 2.7.

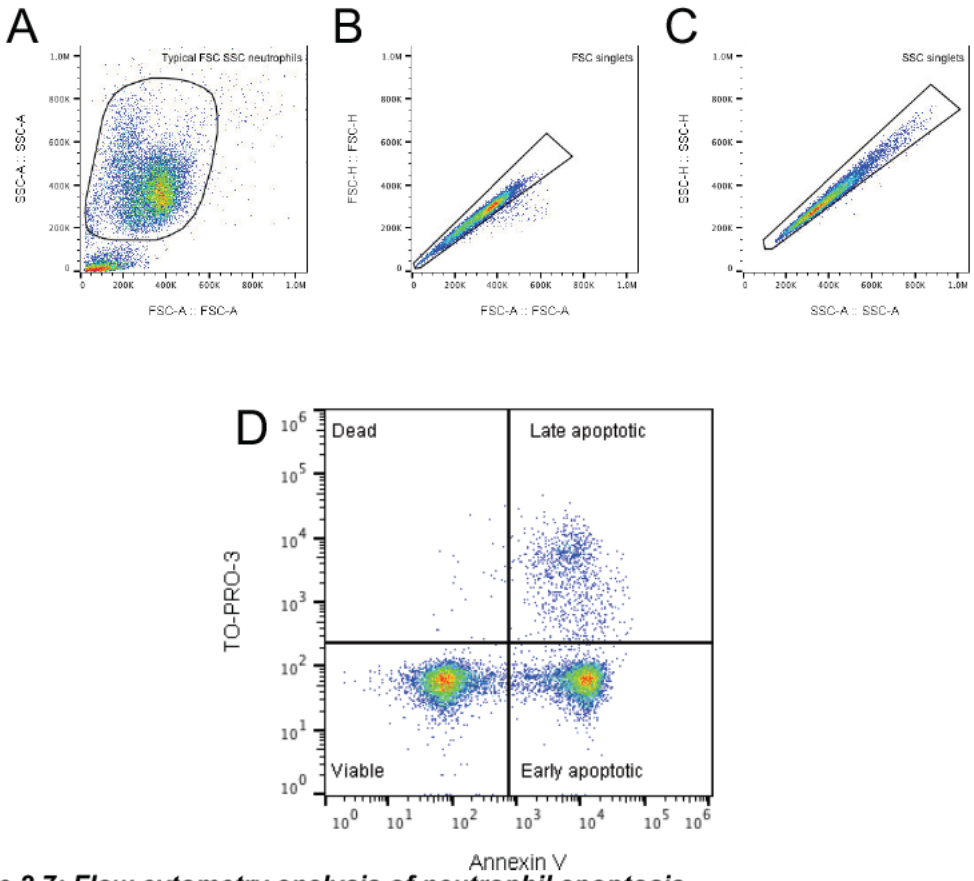

Figure 2.7: Flow cytometry analysis of neutrophil apoptosis.
The gating strategy is outlined in order (A-D).

2.4.3 Drugs used to manipulate neutrophil apoptosis

Drugs used to manipulate neutrophil apoptosis are listed in Table 2.8. Concentrations were based on previous studies. [95 96]

Name	Amount in culture media	Source	Product code
Recombinant TNFα	12.5ng/ mL	Bio-Techne	210-TA
LY294002 (PI3K inhibitor)	10μM	Stemcell	72152
Infliximab (INFLECTRA®)	100μg/ mL	Pfizer	N/A
TNFα monoclonal Ab	1μg/ mL	Bio-Techne	MAB210

Table 2.8: Drugs used to manipulate neutrophil apoptosis.

2.4.4 Phagocytosis

Phagocytosis of neutrophils was assessed using Zymosan A (Sigma-Aldrich). 1mg of Zymosan A was opsonised in 1mL Gibco™ dialysed FBS for 1 hour at 37°C with gentle agitation (contained In an Eppendorf® 1.5mL tube). The Zymosan A was then washed and re-suspended with 1mL Gibco™ 1X DPBS ready for use. Isolated neutrophils were re-suspended in appropriate media (2.3.1) at a concentration of $5x10^6$/ mL. The various experimental conditions were plated in triplicate, with $7.5x10^5$ neutrophils per well (96 well Corning™ Costar™ plates). Following 2 hours of culture, 3μL of Zymosan A stock was added to the wells (final concentration 20μg/ mL of media). After 15 minutes of exposure, cytospins were formed (2.2.2). Phagocytosis was assessed, by examining the cytospins with oil immersion light microscopy at 100X magnification (

Figure 2.8), with the observer blinded to the experimental conditions. At least 100 neutrophils in total were counted per slide, to ascertain the phagocytic index:

Phagocytic Index	=	Proportion of neutrophils that phagocytosed Zymosan A	*	Mean number of Zymosan A particles per neutrophil that phagocytosed

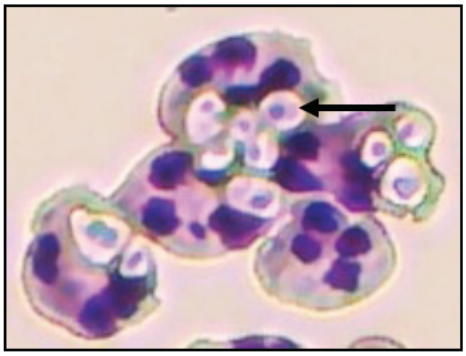

Figure 2.8: The morphological appearance of phagocytosed Zymosan A (100X magnification).

2.4.5 Neutrophil and T cell co-culture

Neutrophils and T cells were isolated separately from whole blood (see 2.2.5). T cells were re-suspended in Gibco™ 1X DPBS (without FBS) at a concentration of $1x10^6$/ mL and labelled with 1:1000 Cell Tracker™ Green CMFDA dye (FITC-like) (ThermoFisher) at 37°C for 30 minutes protected from light. Following this the T cells were washed with Gibco™ 1X DPBS prior to use. The T cells were cultured in 96 well Corning™ Costar™ plates, at a concentration of $1.5x10^5$ per well ($0.5x10^6$/ mL of final culture media), in glucose replete media (see 2.3.1) with varying ratios of neutrophils. T cells were activated with Dynabeads™ human T-activator CD3/ CD28 (ThermoFisher) at a ratio of 1:1 (round-bottom plate). Alternatively, T cells were activated with plate bound LEAF™ CD3 antibody (100μL per well of 1:200 dilution with Gibco™ 1X DPBS (without FBS) incubated overnight, then emptied out) and LEAF™ CD28 antibody (BioLegend) at 2μL/ mL of final culture media (flat-bottom plate). When a PD-L1 inhibitor was used (Human B7-H1 affinity purified polyclonal antibody (Bio-Techne)), this was at 10μg/ mL of final culture media.

After 72 hours of culture, Dynabeads™ were removed with a magnet, the samples transferred to 5mL polystyrene round-bottom tubes, and washed with staining buffer (Gibco™ 1X DPBS supplemented with 2% FBS). 50μL of antibody master mix was added to each sample, then the samples incubated at 4-8°C for 20 minutes protected from light. Master mix consisted of staining buffer with antibodies at concentrations listed in Table 2.9. Samples were then washed and re-suspended in 200μL staining buffer. DAPI at a working concentration of 100μg/ mL was added at 1:1000 (final concentration 0.1μg/ mL), just prior to running each sample on the BD LSRFortessa™ cell analyser (BectonDickinson). UltraComp eBeads (ThermoFisher) stained with single antibodies were used to set up compensations. Unstained and fluorescence minus one controls were also used. BD FACSDiva™ software version 8.0 was used for data acquisition of 10,000 '$CD8^+$'. Data analysis was carried out using FlowJo 10.3 software (including the proliferation tool). The gating strategy and proliferation tool are demonstrated in Figure 2.9.

Antigen	Fluorophore	Clone	Concentration	Source	Product code
CD15	BV421	W6D3	1:200	BioLegend	323039
CD62L	BV605	DREG-56	1:200	BioLegend	304833
CD3	BV785	SK7	1:200	BioLegend	344841
CD4	AF647	A161A1	1:200	BioLegend	357421
CD8	AF700	HIT8a	1:200	BioLegend	300919

Table 2.9: Antibodies used for neutrophil and T cell co-culture.

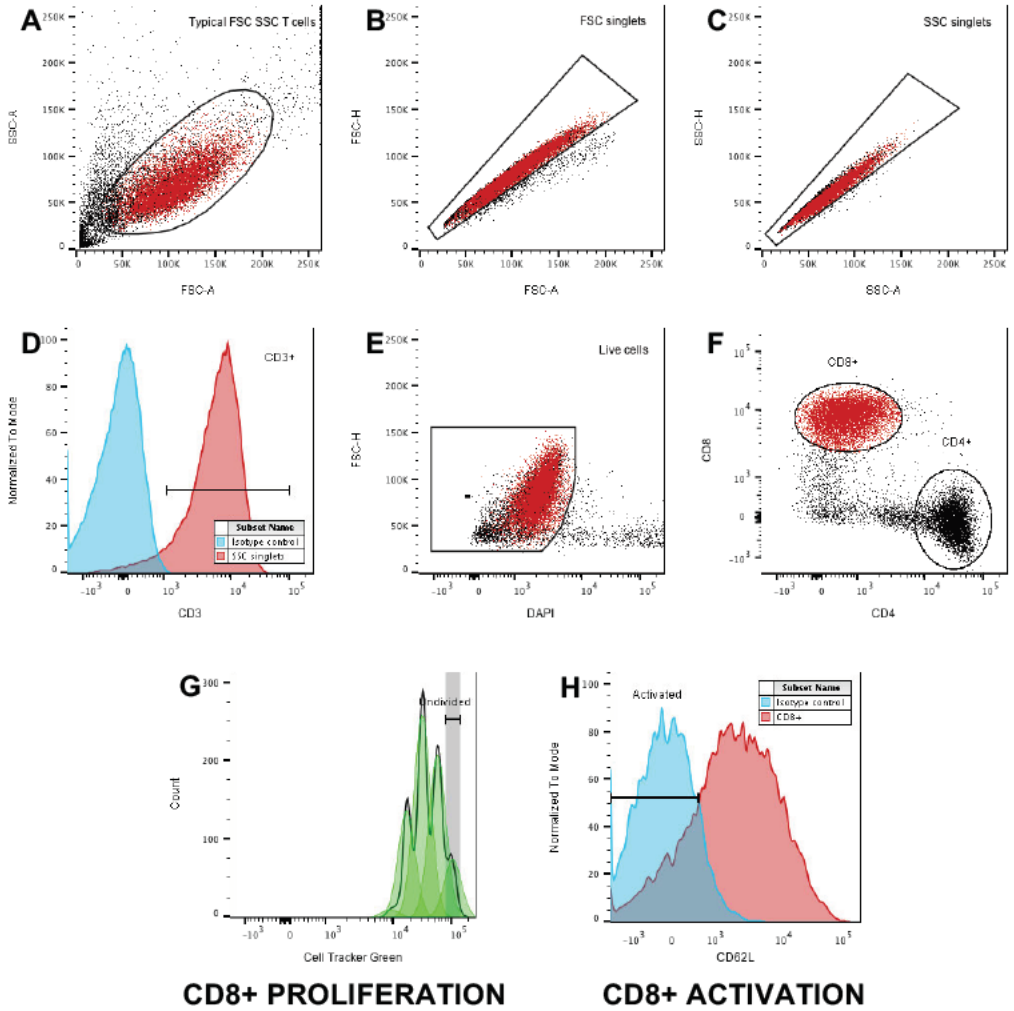

Figure 2.9: CD8⁺ T cell gating strategy.
Strategy shown in order (A-F). CD8 T cell population back-gating is shown in red. (G) FlowJo proliferation tool (model highlighted in green). (H) CD8 activation.

2.5 Analysis of pleural fluid supernatant (PFS)

2.5.1 Glucose measurement

PFS (and platelet-poor plasma) glucose levels were measured using a fluorometric assay kit (BioVision) as per the manufacturer's instructions. Samples were also sent at the time of the original procedure to the NHS Lothian hospital laboratory for glucose measurement (also protein and lactate dehydrogenase measurement) as a routine part of patient care. Hospital measurements and fluorometric assay measurements yielded similar results.

The fluorometric assay was performed using a 96-well flat-bottom plate (black). Each PFS was diluted to final concentrations of 1:500 and 1:1000 with assay buffer (diluted 1:50, then 5μL or 2.5μL added to each well, then made up to a total of 50μL/ well with assay buffer). The glucose standard was prepared to generate 0, 0.2, 0.4, 0.6, 0.8 and 1.0 nmol/ well standard curves. Reaction mix was added and the plate incubated for 5 minutes at room temperature, protected from light. Fluorescence was measured using the Infinite® M1000 microplate reader with i-control™ software (Tecan), excitation wavelength 535nm, emission wavelength 590nm.

Sample glucose concentration (mM) = A / B * C

(A: amount of glucose in the well (nmol), B: sample volume added (μL), C: sample dilution factor)

2.5.2 Human cytokine array

The human cytokine array was carried out by the Host and Tumour Profiling Unit (HTPU) at the Institute of Genetics and Molecular Medicine (IGMM), Edinburgh. The following protocol was provided by Kenneth Macleod.

The human cytokine array was a multiplexed ELISA-type assay, used to determine the relative expression of 64 cytokines, comparing 6 NSCLC PFS with 6 parapneumonic PFS.

A set of identical slides with 64 sub-arrays (one slide per sample) was prepared with each sub-array printed with a different capture antibody. Capture antibodies were

printed as 4 replicate spots on each sub-array (Figure 2.10). Array spotting was carried out with a 2470 Arrayer Platform (Aushon) using 185μm pins onto Oncyte Supernova 21x71mm slides (GraceBiolabs). Capture antibodies were printed at a concentration of 0.2mg/ mL in PBS supplemented with 0.05% Tween®20 (Sigma-Aldrich). Detection antibodies were diluted 1:500 from stocks in PBS containing Tween, 5% bovine serum albumin and 10% SuperG™ blocking buffer (GraceBiolabs).

Each slide (one per sample) was incubated with SuperBlock™ T20 (ThermoFisher) for 1 hour (all incubations and wash steps performed on a rocking platform). Each sample (1mL) was diluted with 2mL of PBS, making at total volume of 3mL that was incubated with a slide at 4°C overnight. A 'background control' slide using 3mL of PBS (containing no sample) was also created. Following overnight incubation, the slides were then washed three times for 5 minutes with PBS Tween, following which they were incubated with SuperG™ buffer for 10 minutes and then washed three times again with PBS Tween. The slides were clamped into the hybridisation cassette and incubated for 1 hour with detection antibodies (50μL per array). The slides were then washed three times for 5 minutes with PBS Tween, following which they were incubated with SuperG™ buffer for 10 minutes and then washed three times again with PBS Tween. They were then incubated for 30 minutes with Streptavidin 800 (Li-Cor) diluted 1:500 in PBS containing Tween, 5% bovine serum albumin and 10% SuperG™ blocking buffer. The slides were then washed three times for 5 minutes with PBS Tween, following which they were washed three times with PBS. After this they were washed with distilled water at room temperature, centrifuged for 5 minutes at 200G to dry, then air dried protected from light.

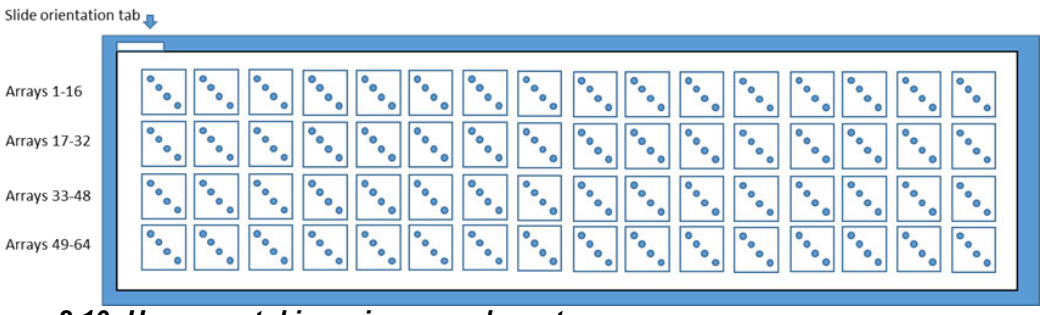

Figure 2.10: Human cytokine microarray layout.

Microarray images (Figure 2.11) were analysed using Mapix software (Innopsys). The feature (spot) diameter of the grid was set to 270μm. Net signal per feature was calculated by subtracting the median background signal intensity (from the area adjacent to the feature) from the average feature signal intensity. Relative fluorescence intensity values were corrected by subtracting the values obtained from the 'background control' slide. The mean of the for replicates was then calculated to give a final relative fluorescence intensity value for each cytokine for every sample.

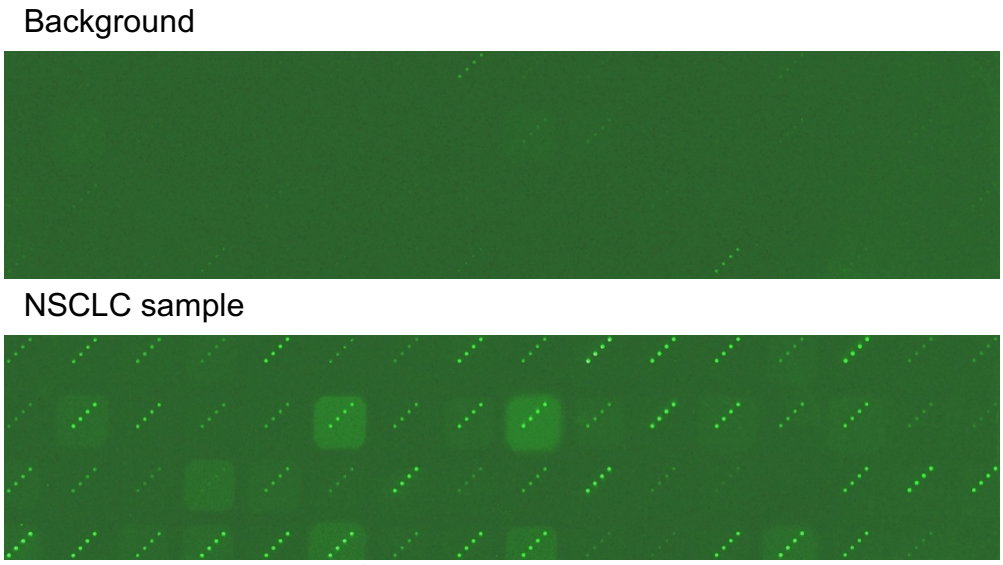

Figure 2.11: Microarray images from human cytokine array.

2.5.3 ELISA

DuoSet® ELISA sets, along with matching DuoSet® ancillary reagent kits, and as appropriate sample activation kits (TGFβ only) (Bio-Techne), were used to quantify TNFα, GM-CSF, IFNβ and TGFβ in PFS. Each ELISA was carried out as per the manufacturer's instructions, with PFS used undiluted.

For the TGFβ ELISA, the samples were activated immediately prior to the assay, by adding 20μL of 1 N HCl per 100μL of sample, mixing well, incubating for 10 minutes, then adding 20μL of 1.2 N NaOH/ 0.5 M HEPES per 100μL of sample to neutralise. 100μL per well of this final mix was then used as the 'sample'.

96-well microplates were prepared by coating them in 100μL of diluted capture antibody per well, sealing and incubating overnight at room temperature. The plates were then washed three times with wash buffer (same for every wash) and then blocked with 300μL per well of reagent diluent at room temperature for 1 hour. Following this, the plates were washed again before adding 100μL of sample/ standards per well, sealing and incubating for 2 hours at room temperature. Of note, a seven-point standard curve was prepared by using two-fold serial dilutions in reagent diluent. After a further wash, 100μL of diluted detection antibody per well was added, the plate sealed with a new adhesive strip and incubated for 2 hours at room temperature. A further wash was performed, followed by the addition of 100μL per well of working dilution of Streptavidin-HRP. The plate was sealed and incubated for 20 minutes at room temperature, protected from light. The plates were washed, 100μL per well of substrate solution was then added and incubated for 20 minutes at room temperature protected from light. 50μL of stop solution per well was then added and gently mixed. Optical density was then immediately determined using a BioTek Synergy™ HT microplate reader set to 450nm, using Gen5™ software (Agilent). Analysis of results was carried out using http://www.elisaanalysis.com, with four parameter logistic curve-fit.

2.6 Neutrophil phenotyping by flow cytometry

2.6.1 Neutrophil subpopulation identification

Following isolation (see 2.2), cells were re-suspended at a concentration of $1x10^7$/ mL in staining buffer (Gibco™ 1X DPBS supplemented with 2% FBS). 100μL ($1x10^6$ cells per sample) was transferred into 5mL polystyrene round-bottom tubes, and 100μL of antibody master mix added. This was incubated at 4-8°C for 20 minutes protected from light. Master mix consisted of staining buffer with antibodies at concentrations listed in Table 2.10. Samples were then washed and re-suspended in 200μL staining buffer. DAPI at a working concentration of 100μg/ mL was added at 1:1000 (final concentration 0.1μg/ mL), just prior to running each sample on the BD LSRFortessa™ cell analyser. UltraComp eBeads stained with single antibodies were used to set up compensations. Unstained and fluorescence minus one controls were also used. BD FACSDiva™ software version 8.0 was used for data acquisition of 10,000 'Viable Cells'. Data analysis was carried out using FlowJo 10.3 software. The gating strategy used to identify $CD66b^+CD11b^+CD15^+CD14^-CD49d^-$ neutrophils is demonstrated in Figure 2.12.

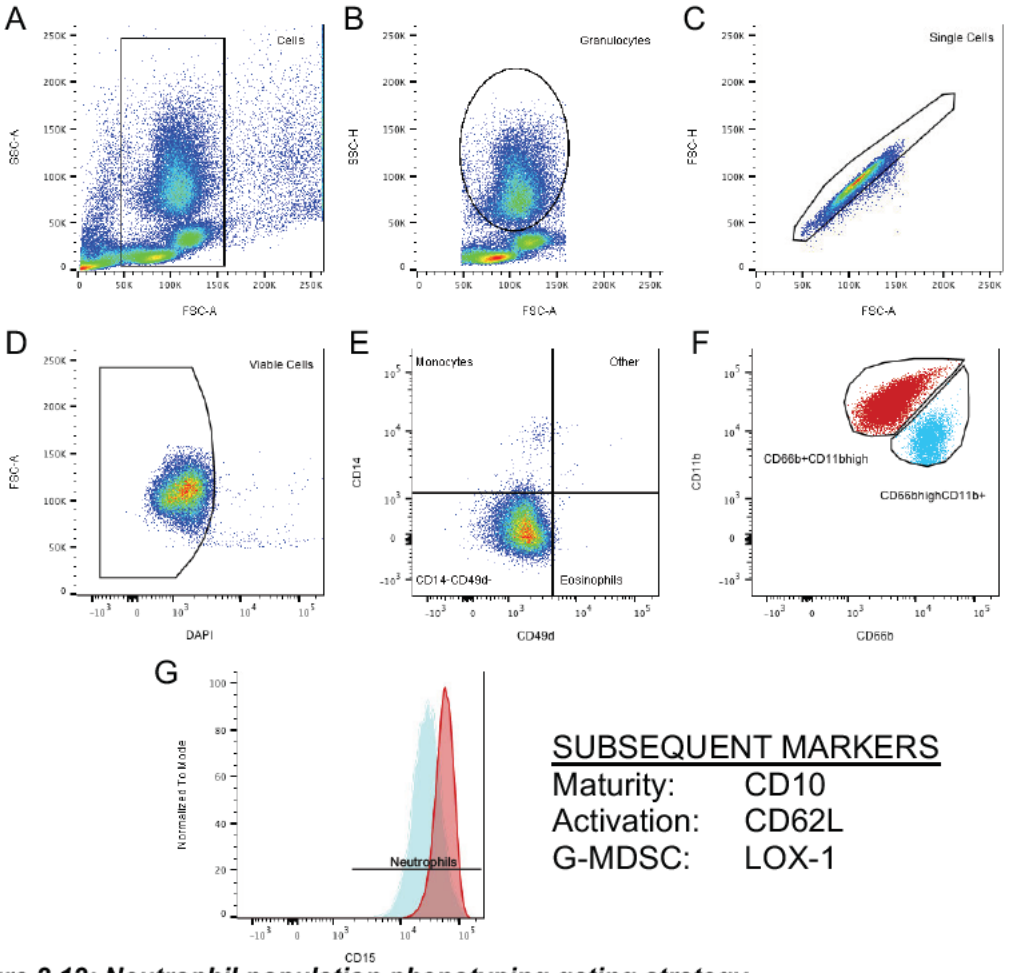

Figure 2.12: Neutrophil population phenotyping gating strategy.
Strategy shown in order (A-G)

Antigen	Fluorophore	Clone	Concentration	Source	Product code
CD11b	PE Cy7	ICRF44	1:20	BioLegend	301322
CD66b	FITC	G10F5	1:20	BioLegend	305104
CD15	BV421	W6D3	1:100	BioLegend	323039
CD14	AF700	63D3	1:20	BioLegend	367114
CD49d	PerCP Cy5.5	9F10	1:20	BioLegend	304312
CD10	APC Cy7	HI10a	1:20	BioLegend	312212
CD62L	BV605	DREG-56	1:20	BioLegend	304834
LOX-1	PE	15C4	1:20	BioLegend	358603

Table 2.10: Antibodies used for neutrophil population phenotyping.

2.6.2 Surface marker expression following PFS conditioning

Isolated healthy donor neutrophils (see 2.2.1) were cultured at a concentration of $5x10^6$/ mL ($7.5x10^5$ neutrophils per well in 96 well Corning™ Costar ™ plates) in glucose replete media ± PFS (see 2.3.1), for 3 hours in normoxia. Following this, samples were transferred to 5mL polystyrene round-bottom tubes and washed with staining buffer (Gibco™ 1X DPBS supplemented with 2% FBS). 100μL of antibody master mix was added to each sample, then the samples incubated at 4-8°C for 20 minutes protected from light. Master mix consisted of staining buffer with antibodies at concentrations listed in Table 2.11, or alternatively Table 2.12. Samples were then washed and re-suspended in 200μL staining buffer. Samples were run on the Attune™ NxT flow cytometer. Attune™ NxT software was used for data acquisition of 10,000 'Singlets' (neutrophils first gated based on FSC/ SCC). Fluorescence minus one controls were used. Data analysis was carried out using FlowJo 10.3 software.

Antigen	Fluorophore	Clone	Concentration	Source	Product code
PD-L1	PE	29E.2A3	1:20	BioLegend	329705

Table 2.11: Antibodies used to assess PD-L1 expression.

Antigen	Fluorophore	Clone	Concentration	Source	Product code
CD120a	APC	W15099A	1:20	BioLegend	369905
CD120b	PE	3G7A02	1:20	BioLegend	358403

Table 2.12: Antibodies used to assess TNFα receptor expression.

2.7 NanoString™

Transcriptomics is the study of RNA molecules within a cell. Messenger RNA indicates which genes are being actively expressed at that snap-shot in time. NanoString nCounter™ technology is a variation of a DNA microarray, that uses 'molecular barcodes' and imaging to detect and count targeted transcripts in one hybridisation reaction (individual capture probes to targeted gene transcripts are labelled with a reporter probe that has a specific fluorescent barcode). Differentially expressed genes can be identified by comparing cell populations.

2.7.1 Sample preparation

Highly pure neutrophil populations were isolated (see 2.2.4 and 2.2.8). Aliquots of $3x10^4$ neutrophils were transferred into 1.5mL Eppendorf® tubes and pelleted (2000 rpm for 6 minutes). The supernatant was removed, then each pellet re-suspended in 6μL of 1/3 lysis buffer (1 part RLT (Qiagen) in 2 parts Ultrapure™ RNAse free distilled water (ThermoFisher)). This was pipetted up and down (to mix) 20 times without making bubbles. The resultant lysate was flash frozen and stored at -80°C for use in the assay.

2.7.2 Protocol

The nCounter® human myeloid innate immunity panel (NanoString) was carried out by Alison Munro, at the Host and Tumour Profiling Unit (HTPU), Institute of Genetics and Molecular Medicine (IGMM), Edinburgh. NanoString™ was run according to the manufacturer's protocols. 5μL of each sample lysate was used. Hybridisation was at 65°C for 18 hours, ramped down to 4°C and held. The PrepStation was set at high sensitivity. The digital analyser was set at 555 fields of view (maximum resolution).

2.7.3 Data analysis

Raw data was processed using nSolver™ software version 4.0 (NanoString). All samples passed the in-built quality control measures. Data was then normalised, and a Log2 data matrix exported. Advanced analysis of this data matrix was then carried out with the help of Thomson Bioinformatics, Edinburgh (principal component analysis, heat maps, control boxplots, global Pearson correlations). Or Alternatively, using Excel (Microsoft) and Prism 8 (Graphpad) (differential expression). The DAVID 6.8 bioinformatics resource[97] was used for functional annotation/ biological process over-representation analysis.

2.8 Proteomics

Proteomics is the study of all the proteins of a cell. To a degree this reflects the transcriptome, however protein quantity at a snap-shot in time is not just regulated by expression of the relevant gene, but also by its rate of degradation, post-translational modification, etc. Proteins can then be considered in terms of their known interactions, cellular compartments and biological processes, using established databases. Differentially expressed proteins can be identified by comparing cell populations.

2.8.1 Neutrophil number determines the quantity of proteins that can be subsequently detected by proteomic analysis

As it was planned to use smaller pellets of neutrophils for proteomics experiments than the group had used previously, an optimisation experiment was carried out to investigate the effect of smaller pellet sizes on protein yield.

Neutrophils were extracted from healthy donor blood and matched pellets of three different sizes formed; $1.00x10^6$, $0.50x10^6$ and $0.25x10^6$ neutrophils. Samples were processed (*as per* the methods section of this thesis), before undergoing single shot analysis, or alternatively were fractionated (8 fractions) prior to analysis.

The total number of detected proteins decreased with smaller size neutrophil pellets both in single shot (Figure 2.13A) and fractionated (Figure 2.13B) samples. In addition, the number of detected proteins was approximately doubled to over 3500 following fractionation (Figure 2.13B). Lower abundance proteins were the ones no longer detected when smaller neutrophil pellets were used (Figure 2.13C).

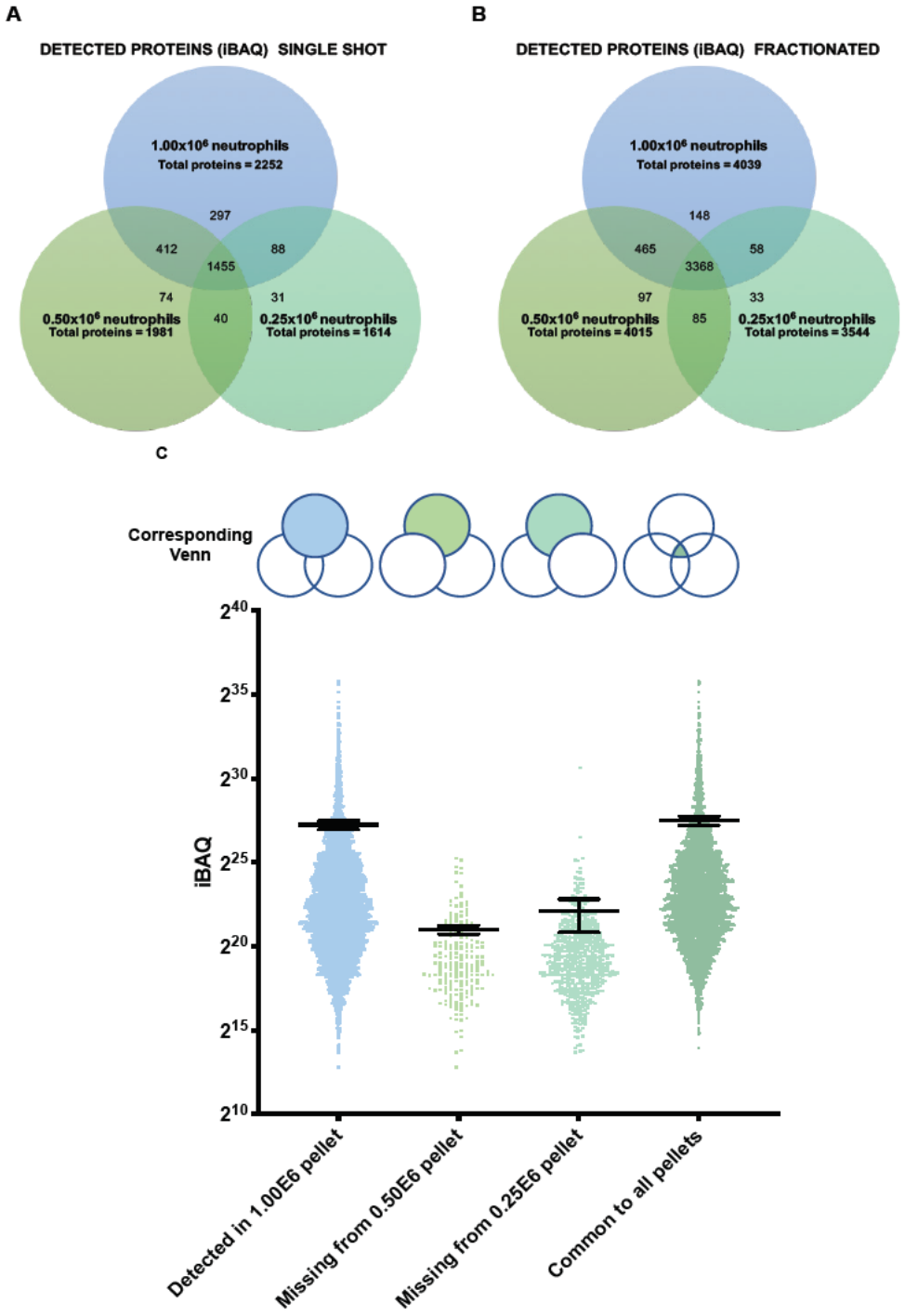

Figure 2.13: Fractionation of neutrophil proteomics samples leads to a greater number of detected proteins. Lower abundance proteins are not detected with smaller neutrophil pellet sizes.

Healthy donor blood matched neutrophil pellets of three different sizes were prepared for either single shot proteomic analysis, or fractionated prior to analysis (8 fractions). (A) Venn diagram of the number of detected proteins for each pellet size when single shot proteomic analysis was undertaken. (B) Venn diagram of the number of detected proteins for each pellet size when samples were fractionated prior to analysis. (C) The proteins that were no longer detected when smaller neutrophil pellets were used for proteomics. Data represents individual proteins and mean ± SEM.

2.8.2 Sample preparation

Highly pure neutrophil populations were isolated (see 2.2.4 and 2.2.8). Aliquots of $2.5x10^5$ neutrophils were transferred into 1.5mL Eppendorf® low bind tubes and pelleted (2000 rpm for 6 minutes). The supernatant was removed, then each pellet was flash frozen and stored at -80°C prior to subsequent use.

2.8.3 Protocol

The following protocol was provided by, and carried out with the help of Andy Howden, School of Life Sciences, University of Dundee.[98] The protocol and buffers are summarised in Figure 2.14 and Table 2.13.

Stock	Lysis buffer	Digest buffer
20% SDS	1000µL (4% final concentration)	10µL (0.1% final concentration)
0.5M TCEP	100µL (10mM final)	-
1M TEAB	250µL (50mM final)	100µL (50mM final)
1M $CaCl_2$	-	2µL (1mM final)
H_2O	3650µL	1888µL

Table 2.13: Proteomic sample buffers.
SDS, sodium dodecyl sulphate; TCEP, tris (2-carboxyethyl) phosphine hydrochloride; TEAB, tetraethylammonium bromide.

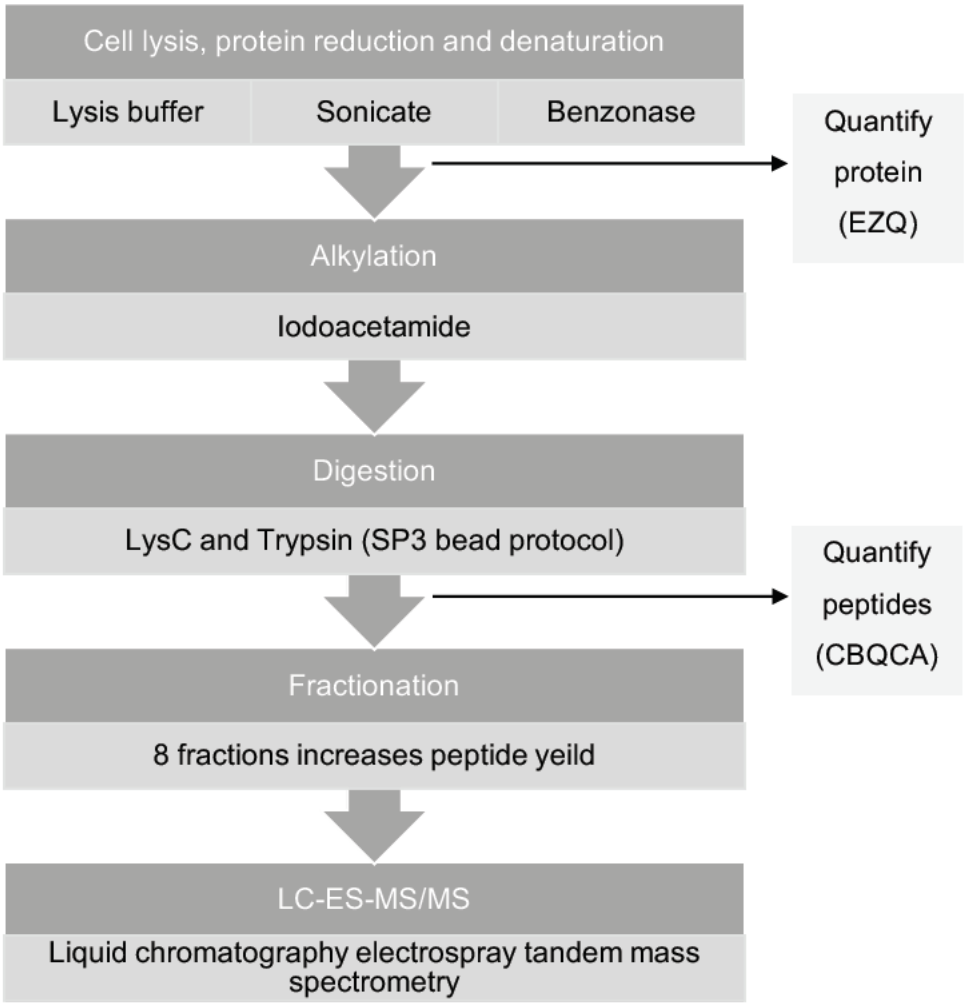

Figure 2.14: Proteomic sample protocol.

The pellets of $2.5x10^5$ highly pure neutrophils were lysed in 400μL lysis buffer and boiled for 5 minutes shaking at 500rpm (Eppendorf® Thermomixer). Samples underwent 15 minutes of sonication (BioRuptor® (Diagenode), cycles of 30 seconds on then 30 seconds off), then 1μL benzonase was added, followed by incubation for 15 minutes at 37°C. Protein concentration was estimated using the EZQ™ protein quantification kit (ThermoFIsher) as per the manufacturer instructions.

Iodoacetamide was then added as an alkylating agent, at a working concentration of 20mM and the samples incubated at room temperature protected from light for 1 hour. In-solution digestion was carried out using the SP3 beads protocol[99] with 65μL digest buffer containing 1μg LysC (Promega) per 100μg protein, incubated overnight at 37°C shaking at 500rpm (Eppendorf® Thermomixer). Followed by 1μg Trypsin (Promega) per 100μg protein, incubated overnight at 37°C shaking at 500rpm. Peptides were eluted by adding 189μL of 2% DMSO in water and sonicating the samples for 5 minutes (cycles of 30 seconds on then 30 seconds off). Beads were removed with a magnet leaving a supernatant containing peptides. The supernatant was then centrifuged to remove non-magnetic bead debris.

Peptides would then normally be quantified by CBQCA assay (ThermoFisher), to enable accurate dilution of samples to a concentration of 1μg per 15μL with 5% formic acid prior to single shot analysis. However, during optimisation experiments, the CBQCA assay was found to be redundant, due to the low levels of peptide obtained, making quantification inaccurate. Furthermore, fractionation yielded a much greater number of proteins compared with single shot analysis in optimisation experiments. Therefore, the CBQCA assay was not used, and to prepare samples for fractionation 21μL of 50% formic acid was added (to give a total volume of 210μL per sample, 5% working concentration of formic acid).

Samples were subsequently fractionated using high pH reverse phase liquid chromatography. 200μL of sample was loaded onto a 2.1mmx150mm XBridge™ Peptide BEH C18 column with 3.5μm particles (Waters). Using a Dionex UltiMate™ 3000 system (ThermoFisher), the samples were separated using a 25-minute multistep gradient, of buffers A (10mM ammonium formate at pH 9 in 2% acetonitrile) and B (10mM ammonium formate pH 9 in 80% acetonitrile), at a flow rate of 0.3mL per minute. Peptides were separated into 16 fractions which were consolidated into 8 fractions. Fractionated peptides were dried in vacuo then re-suspended in 40μL of 5% formic acid for analysis by LC-ES-MS/MS.

LC-ES-MS/MS was carried out at the Proteomics Facility, School of Life Sciences, University of Dundee. 15μL of each fraction was injected onto a Q Exactive™ Plus mass spectrometer (ThermoFisher). Samples were washed with 0.1% formic acid (10μL per minute) for 5 minutes prior to valve switch on an Acclaim™ PepMap™ 100 nanoViper™ C18 trap column (100μm inner diameter, 2cm) (ThermoFisher).

Peptides were eluted onto an EASY-Spray™ PepMap™ RSLC nanoViper™ C18, 2μm column (75μm, 50cm) (ThermoFisher), using the buffer conditions summarised in Table 2.14, at a flow rate of 0.3μL per minute.

Time (minutes)	% of buffer (80% acetonitrile in 0.1% formic acid)
0-5	2 to 5
5-130	5 to 35
130-132	35 to 98
132-152	98
152-153	98 to 2
153-170	Equilibrated in 2

Table 2.14: Buffer conditions used in LC-ES-MS/MS.

The eluting peptides were electrosprayed into a Q Exactive™ Plus mass spectrometer using an EASY-Spray™ nanoelectrospray ion source at 50° and a source voltage of 2kV (ThermoFIsher). The mass spectrometer was operated in positive ion mode. Data was collected using data-dependent acquisition: the 15 most intense peptide ions from the preview scan were fragmented by higher-energy collisional dissociation. The following settings were applied. MS1 scan resolution: $7x10^4$; MS1 AGC target: $1x10^6$; MS1 maximum IT: 20ms; MS1 scan range: 350-1600 Th; MS2 scan resolution: $1.75x10^4$; MS2 AGC target: $2x10^5$; MS2 maximum IT: 100ms; isolation window: 1.4 Th; first fixed mass: 200 Th; NCE: 27; minimum AGC target: $2x10^3$; only charge states 2 to 6 considered; peptide match: preferred; exclude isotopes: on; dynamic exclusion: 45s.

2.8.4 Data analysis

Raw data was processed using MaxQuant Software 1.6.2.6.[100 101] The resultant protein groups data matrix was then imported into Perseus Software 1.6.2.3.[102] In Perseus, several quality control measures were undertaken (removal of proteins only identified by site, reverse and potential contaminants), the proteins were functionally annotated and the data Log2 transformed. Pairwise comparisons were made between NSCLC neutrophil subpopulations and the healthy donor control group. To be included in analysis, a protein had to be present in a minimum of 3 out of 5 samples in one of the pairwise groups (i.e. control or NSCLC subpopulation). Imputation was then carried out to replace missing values (from a normal distribution). Where estimated copy numbers, concentrations and mass were required, these were added using the Perseus proteomic ruler plug-in. Perseus tools were also used to carry out principal component analysis and global Pearson correlations. Perseus matrices were then exported for further analysis using Excel and Prism 8 (e.g. differential expression). The DAVID 6.8 bioinformatics resource[97] was used for biological process over-representation analysis. Heatmaps were created using https://software.broadinstitute.org/morpheus. Network analysis was carried out using GeneMania.[103]

2.9 Statistical analysis

Statistical analysis was performed using Prism 8 or Excel. Data was assumed to follow a non-parametric distribution when sample size was insufficient to test for normality ($n<8$). Large data sets (Human cytokine array, NanoString™ and Proteomics) were normally distributed. When comparing two normally distributed groups, significance testing was performed using a t-test and summary data was expressed as mean ± SEM. When comparing two groups with non-parametric distribution, significance testing was performed using a Mann-Whitney/ Wilcoxon test and summary data was expressed as median ± interquartile range. Correlation of data was examined using Pearson's test (normally distributed) or Spearman's test (non-parametric). Results were considered significantly different when $p<0.05$.

In some experiments where >2 groups were being compared, Wilcoxon tests were used instead of a Friedman test e.g. when comparing any added effect of PFS versus no PFS (alternatively, glucose versus no glucose) in culture media, upon the apoptosis of healthy donor neutrophils in normoxia or hypoxia. This was because the 'planned comparisons' were within group (i.e. PFS versus no PFS in normoxia, PFS versus no PFS in hypoxia). It was already known that hypoxia has a survival advantage over normoxia. The primary aim was not to look at any other comparisons (of the 6 pairs available). Friedman with Dunn's multiple comparisons was not chosen as it would test the null hypothesis 'all groups means are the same' and would therefore certainly have a $p<0.05$ (due to hypoxic survival). Dunn's multiple comparisons would be too strict a test, as it would correct for all 6 comparisons (when the 'planned comparisons' were only 2 of the 6 pairs), leading to an unacceptable chance of a Type II error. Using an uncorrected Dunn's test for 'planned comparisons' only would have been another option, but was less suitable to the question being asked than using Wilcoxon (as Dunn's would be a post-hoc test for the Friedman test, that as discussed, would not test a suitable null hypothesis).

2.10 Materials list

Product	Source	Product code
3% acetic acid with methylene blue	Stemcell	07060
Annexin V binding buffer 10X concentrate	BectonDickinson	556454
Annexin V PE	BectonDickinson	556421
C-Chip haemocytometer	NanoEnTek	DHC-N01
Cell Tracker™ Green CMFDA dye	ThermoFisher	C7025
DAPI	ThermoFisher	D3571
10X DBPS	Sigma-Aldrich	D1408
DPX mountant	Sigma-Aldrich	06522
DuoSet® ELISA human GM-CSF	Bio-Techne	DY215/ DY008
DuoSet® ELISA human IFNβ	Bio-Techne	DY814/ DY008
DuoSet® ELISA human TGFβ	Bio-Techne	DY240/ DY007/ DY010
DuoSet® ELISA human TNFα	Bio-Techne	DY210/ DY008
Dynabeads™ human T-activator CD3/ CD28	ThermoFisher	11161D
EasySep™ direct human neutrophil isolation kit	Stemcell	19666
EasySep™ direct human T cell isolation kit (Stemcell)	Stemcell	19661
EasySep™ human neutrophil enrichment kit (discontinued, now EasySep™ human neutrophil isolation kit)	Stemcell	19257
EasySep™ magnet	Stemcell	18000
EZQ™ protein quantification kit	ThermoFisher	R33200
FBS Good Forte (EU approved) heat inactivated	PAN-Biotech	P30-19475
Ficoll-Paque PLUS™	GE Healthcare	17-1440-02
Fisherbrand™ cell strainers (40μm/ 100μm)	ThermoFisher	22363547/ 22363549

Gibco™ dialysed FBS	ThermoFIsher	26400-044
Gibco™ 1X DPBS	ThermoFisher	14190-144
Gibco™ Penicillin-Streptomycin	ThermoFisher	15140-163
Gibco™ RPMI 1640 medium	ThermoFisher	21875034
Gibco™ RPMI 1640 no glucose medium	ThermoFisher	11879020
Glucose colorimetric/ fluorometric assay kit	BioVision	K606-100
Human B7-H1 affinity purified polyclonal antibody	Bio-Techne	AF156
Kwik-Diff™ (ThermoFisher)	ThermoFIsher	9990700
LEAF™ purified anti-human CD3 (HIT3a)	BioLegend	300314
LEAF™ purified anti-human CD28 (CD28.2)	BioLegend	302914
Millex®-GP 0.22μm polyethersulfone syringe filter	Sigma-Aldrich	SLGP033RS
nCounter® human myeloid innate immunity panel	NanoString	115000171/ 100052
Percoll™	GE Healthcare	17-0891-01
RLT	Qiagen	79216
RoboSep™ buffer	Stemcell	20104
S-Monovete® sodium citrate tubes	Sarstedt	02.1067.001
Streptavidin 800	Li-Cor	926-32230
SuperBlock™ T20	ThermoFisher	37536
SuperG™ blocking buffer	GraceBiolabs	105101
TO-PRO-3™ iodide	ThermoFisher	T3605
Tween®20	Sigma-Aldrich	9005-64-5
UltraComp eBeads	ThermoFisher	01-2222-42
Ultrapure™ RNAse free distilled water	ThermoFisher	10977-035
Zymosan A	Sigma-Aldrich	Z4250

Chapter 3 The NSCLC pleural environment influences neutrophil function

3.1 Introduction

3.1.1 Neutrophil function is modulated in response to the local environment, which is highly relevant at the metastatic site

It is well known that metastatic tumour sites are often hypoxic, glucose deplete, and rich in cytokines.[32] These features of the tumour microenvironment will have significant impact upon the function of recruited neutrophils. For example, key neutrophil functions such as phagocytosis and apoptosis are energy-dependent processes. Such microenvironmental features, have not yet been fully explored in human cancer models.

Oxygen availability

Oxygen sensing pathways regulate neutrophil function and survival responses.[71 72 104 105] Hypoxia acts as a neutrophil survival signal.[14] This is controlled by hypoxia-inducible factors (HIFs) and they in turn are regulated by prolyl hydroxylase domain enzymes (PHDs) and factor inhibiting HIF (FIH). In oxygen-replete conditions PHDs hydroxylate the HIFα subunit. This targets it for proteosomal degradation by von Hippel-Lindau (VHL) protein, putting a halt to its downstream signalling. FIH can hydroxylate asparagine 803 on the HIFα subunit, preventing its binding to transcriptional co-factor p300/CBP. In hypoxia, the PHDs are inactive, HIFα binds HIFβ and p300/CBP, and this complex activates hypoxia response elements (HREs) stimulating gene transcription (Figure 3.1 adapted from Watts et al.[106]). Neutrophil hypoxic survival is driven by HIF-1α-dependent NF-κB activity.[71]

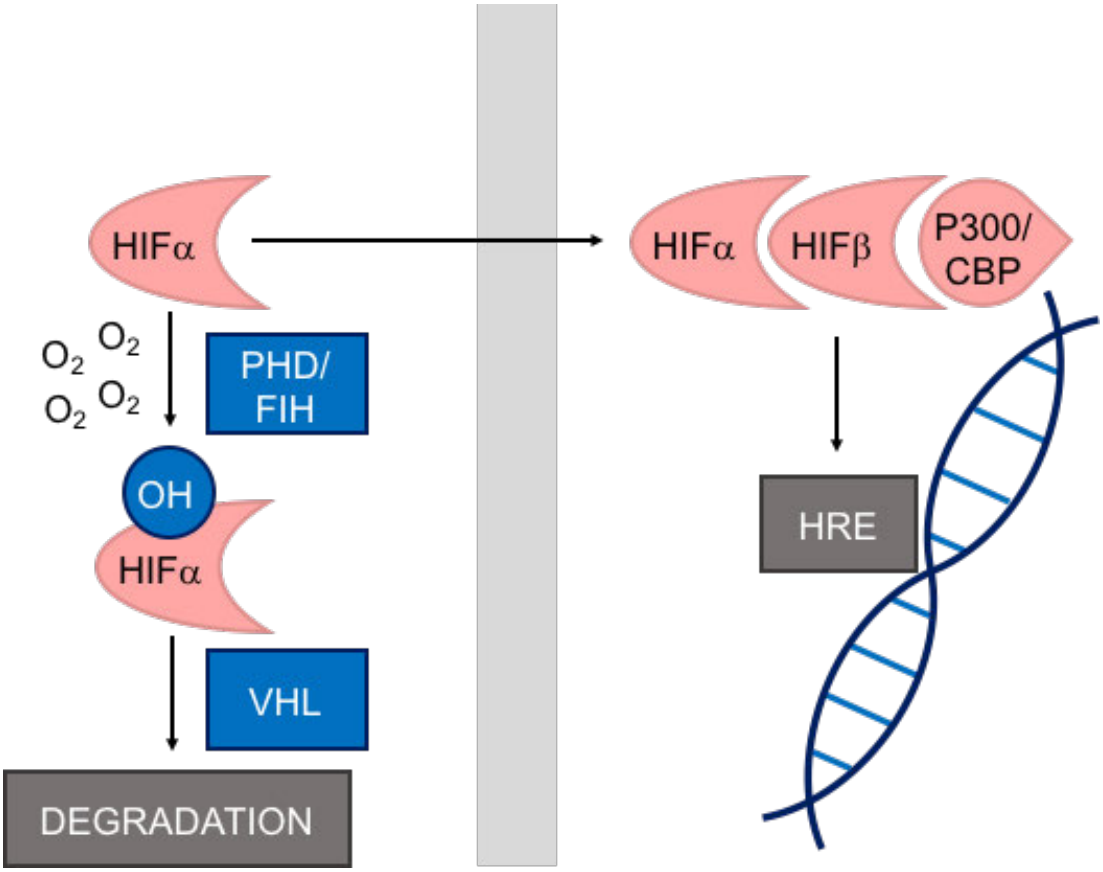

Figure 3.1: The response to hypoxia is regulated by hypoxia-inducible factors (HIFs). *In oxygen-replete conditions prolyl hydroxylase domain enzymes (PHDs) hydroxylate the HIFα subunit. This targets it for proteosomal degradation by von Hippel-Lindau (VHL) protein, putting a halt to its downstream signalling. In hypoxia, the PHDs are inactive, HIFα binds HIFβ and p300/CBP, and this complex activates hypoxia response elements (HREs) stimulating gene transcription (adapted from Watts et al.[106]).*

Metabolic substrate availability

Neutrophils contain few mitochondria and are traditionally viewed as being dependent upon glycolysis for their energy source. Hypoxia promotes glucose uptake and glycogen accumulation in neutrophils. When neutrophils are cultured in hypoxia, removal of glucose from the culture media or pharmacological inhibition of glycolysis, both result in loss of hypoxic survival.[72]

There is now however increasing evidence that certain neutrophil populations refute this dogma, utilising other forms of metabolism. In murine models of cancer, tumour-infiltrating granulocytic myeloid-derived suppressor cells (G-MDSCs), display increased fatty acid uptake and fatty acid oxidation.[78] These G-MDSCs are thus able to circumvent nutritional limitations (i.e. low glucose) within their local tissue

environment, and through mitochondrial fatty acid oxidation are able to support immunosuppressive NADPH oxidase-dependent reactive oxygen species production.[74] In addition, immunosuppressive activity of these cells may be mediated by fatty acid transport protein 2-dependent prostaglandin E_2 synthesis.[75] Finally, in the absence of glucose, murine immature low density neutrophils (which are likely to be one and the same as G-MDSC) utilise glutamine and proline to support pro-metastatic NETosis.[77]

Cytokines in the microenvironment

Neutrophils can be polarised to pro- or anti-tumour phenotypes in response to cytokines within their microenvironment, such as TGFβ and IFNβ.[25 26 58] Studies that emulate the tumour microenvironment *in vitro* by culturing neutrophils in media conditioned by cancer tissue or adding cytokines that are known to be present, have shown changes in neutrophil apoptosis and neutrophil-T cell interactions. However, such studies have been mainly limited to cancer cell lines or mouse models, and have been carried out with ex-vivo human tissue infrequently, e.g. from early stage lung cancer,[46 47] early and late stage gastric cancer,[43 107] and ovarian malignant ascites.[108] What's more, the mechanisms underlying these changes in neutrophil behaviour have not been fully decoded.

3.1.2 Pleural effusion: a metastatic environment in NSCLC

Mortality in patients with NSCLC most commonly relates to metastatic burden. It is therefore important to gain a better understanding of the mechanisms that permit metastatic tumour progression, and which features of the metastatic environment act as drivers.

Pathophysiology and significance of pleural effusion in NSCLC

In health, the pleural space between the visceral pleural membrane (outer lung lining) and parietal pleural membrane (inner chest wall lining) is filled by a <10mL of pleural fluid. This enables the lung to freely expand and contract with inspiration and

expiration, without friction. In advanced NSCLC patients can develop a much larger collection of pleural fluid (pleural effusion). The exact pathophysiological mechanisms underpinning this fluid accumulation are not fully understood, but there are thought to be three key factors. Firstly, there is increased permeability and leak from pleural membrane capillaries. Secondly, there is imbalance in oncotic and hydrostatic pressures between the vasculature and the pleural space. Thirdly, there is obstruction of lymphatic drainage. In advanced NSCLC, metastatic tumour deposits form on both pleural membranes, tumour cells float freely in the pleural fluid and there is an inflammatory response with infiltration of immune cells, including neutrophils, into the pleural space. All of these processes contribute to the three key factors already described.[109]

The lung does not have any pain-sensing nerves; therefore, the first symptoms of NSCLC are often later in the disease process, with cough, haemoptysis, weight loss, shortness of breath or pain from metastatic sites (typically bone or liver). When pleural effusions become large, this causes compression of the underlying lung, leading to severe breathlessness. Therefore, for symptomatic relief, clinicians drain these effusions, also providing tissue from which a histological diagnosis may be made. Regrettably, NSCLC patients that first present to medical services with shortness of breath due to malignant pleural effusion, already have incurable stage IV disease with a median survival of around 3 months.

Measurement of pleural fluid metabolites and cytokines is used to aid diagnosis and guide prognosis for pleural effusions

NSCLC is the most common cause of malignant pleural effusion, but there are many other causes of pleural effusions (benign and malignant); examples are listed in Table 3.1. Historically, many studies looking into the components that make up pleural fluid (e.g. metabolites, cells and cytokines), have been carried out in order to help distinguish between said causes i.e. to aid diagnosis. Light et al.[110] set out criteria based on pleural fluid protein and lactate dehydrogenase levels, that have been universally clinically accepted as the basis by which to define pleural effusions as either transudative or exudative. The gold standard test to confirm malignant pleural effusion is positive pleural fluid cytology for malignant cells.

Causes of pleural effusions: transudates (protein-poor)	Causes of pleural effusions: exudates (protein-rich)
Heart failure	Pneumonia
Liver failure	Metastatic malignancy (lung, breast, lymphoma, genitourinary, gastrointestinal)
Renal failure	Tuberculosis
Hypothyroidism	Lung infarction (pulmonary embolus)
	Rheumatological conditions and vasculitides
	Pancreatitis
	Oesophageal rupture
	Drug induced
	Post (intrathoracic) surgery

Table 3.1: Causes of pleural effusions.

Pleural biomarkers have more recently been explored in order to help define prognosis and aid treatment decisions in pleural effusion e.g. whether to insert a long-term indwelling pleural drainage catheter. This work led to the creation of the LENT survival score for malignant pleural effusion (pleural fluid **L**actate dehydrogenase, **E**astern cooperative oncology group performance status, **N**eutrophil-to-lymphocyte ratio, **T**umour type).[111] Latterly, the PROMISE clinical score has been shown to predict survival and pleurodesis response in patients with malignant pleural effusion (chemotherapy, radiotherapy, haemoglobin, white blood cell count, C-reactive protein, performance status, cancer type).[112] However, whilst these scores are useful clinically, they do not give insight into the mechanisms that permit metastatic tumour progression at the pleural site.

Malignant pleural effusions have a reduced partial pressure of oxygen, and variable glucose levels

Oxygen diffuses from the air into the blood stream, is transported around the body by haemoglobin in the blood and then disperses into tissues. Each of these steps has inherent inefficiencies; resultantly the partial pressure of oxygen drops significantly between the air and tissues (Figure 3.2). The partial pressure of oxygen in malignant pleural effusions has been measured to be 18-48% of that found in arterial blood,[113] with a mean value of 3-5kPa.[114-116] Malignant pleural effusions are oxygen deplete. Pleural fluid acidification and reduction in glucose in the acute setting is pathognomonic of infection/ empyema. However, pleural fluid pH and glucose can also fall in malignant pleural effusion over time.[109 114 117 118]

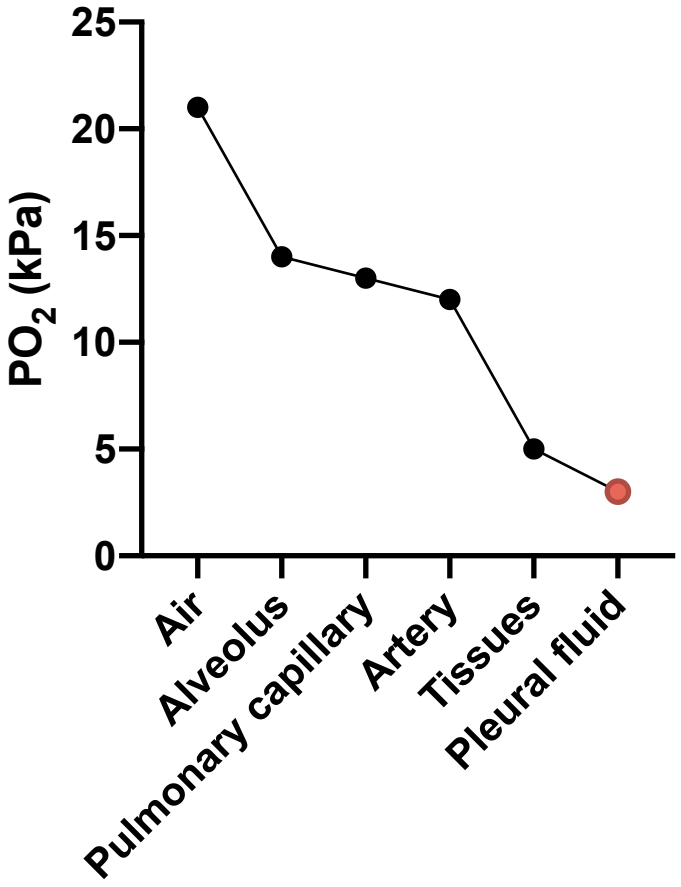

Figure 3.2: The oxygen cascade.
The partial pressure of oxygen reduces sequentially as the distance travelled from its source in the atmosphere into the tissues increases. Pleural fluid has a PO_2 of 3-5kPa.[114-116]

There is the clinical potential to inject therapies into the pleural space, in order to modulate the malignant immune environment

As the pleural space is easily accessible by needle when a pleural effusion is present, there has been the recognition that there is the potential to inject therapies into it. This has the benefit of making the treatment localised, limiting systemic side-effects. Trials to date have focussed on modulating the malignant pleural immune environment, whether it be the introduction of genetically engineered T cells (chimeric antigen receptor T cells), inhibitor drugs or cytokines.[119] Of note, there has been some success with IFNβ gene transfer,[120] a cytokine known to polarise neutrophils to an anti-tumour phenotype.[26]

3.1.3 Summary

Mortality in patients with NSCLC most commonly relates to metastatic burden. It is therefore important to gain a better understanding of the mechanisms that permit metastatic tumour progression, and which features of the metastatic environment act as drivers. Oxygen availability, metabolic substrate availability and cytokines in the microenvironment will determine neutrophil responses at the metastatic site in cancer. Pleural effusions are metastatic sites in NSCLC. They are low in oxygen and have variable glucose availability, and therefore share similarities with other metastatic sites. Pleural effusions are often drained for diagnostic or symptomatic purposes, providing tissue that can be used experimentally. Tissue from metastatic sites in human cancers has been infrequently used in the past due to lack of availability. Therefore, using NSCLC pleural fluid could provide novel insights into how the metastatic environment influences neutrophil function, with possible impacts on cancer outcome. Using pleural fluid from patients with pneumonia could also add information regarding the differences between cancer and non-cancer states. Finally, there is the potential that if new therapeutic targets were identified, drugs could be injected directly into the pleural space.

3.1.4 Hypotheses

I hypothesised that the NSCLC pleural environment influences the function of neutrophils that have been recruited to this metastatic site, leading to an inappropriate and ineffective chronic inflammatory response to malignancy. I further hypothesised that the features of the NSCLC pleural environment would differ from those seen in pneumonia, an acute inflammatory condition that commonly, when treated supportively with antibiotics, results in appropriate and effective immune resolution.

3.1.5 Aims

To explore how NSCLC pleural fluid influences the function of neutrophils that have migrated to this space, and establish whether this results in a pro- or anti-tumour neutrophil behaviour. To elucidate the underlying mechanisms modulating the neutrophil immune response at this metastatic site in NSCLC. To define cancer-specific features of the NSCLC pleural environment that may impact upon tumour progression.

3.2 Results

3.2.1 Features of NSCLC patients

33 NSCLC patients were recruited to the study. Patient demographics are listed in Table 3.2. Of note, patients typically had a high blood neutrophil-to-lymphocyte ratio and an extensive smoking history. In terms of confirming the diagnosis of NSCLC, in addition to suggestive radiology, pleural fluid protein was >0.5 that of the matched serum, confirming the pleural effusions to be exudative as per Light's criteria[110] (Figure 3.3A). Furthermore, the majority of patients recruited had positive pleural fluid histology and the remainder had a positive tissue biopsy (via bronchoscopy or computerised tomography-guidance) (Figure 3.3B). With regard to treatment decisions and outcome, most patients were managed conservatively (Figure 3.3C) and median patient survival was 73 days (Figure 3.3D).

NSCLC patient demographics	
Number recruited (n)	33
Age (years)	73 (49-94)
Sex (male)	19 (57.6%)
NLR (<4 in health)	6.8 (2.4-19.0)
Current or ex-smoker	30 (90.9%)
Pack years	50 (5-60)

Table 3.2: NSCLC patient demographics.
Data represents number (percentage) or median (full range of values).

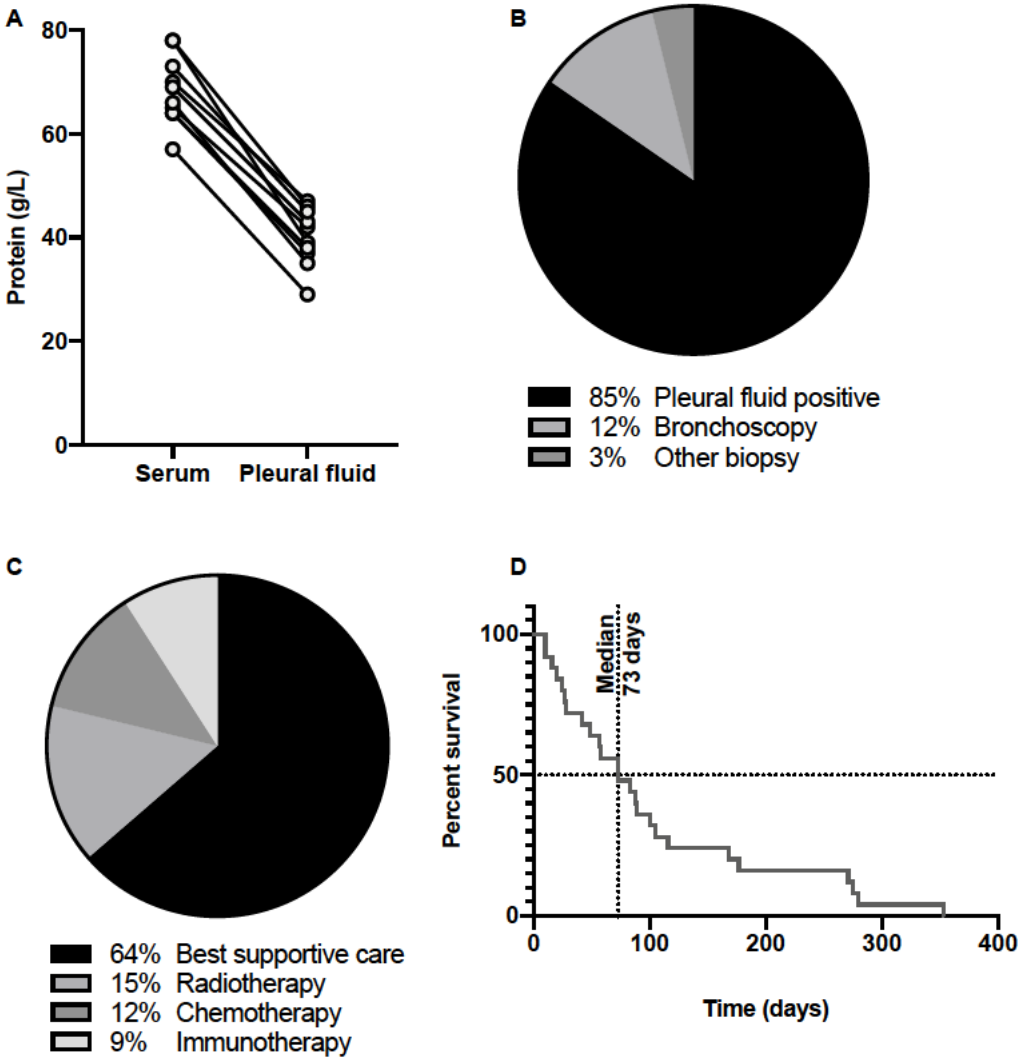

Figure 3.3: NSCLC patient diagnostic features, treatment decisions and survival. *(A) Pleural fluid and matched serum protein measured in recruited patients (n=10). Data represents individual values. (B) How the histological diagnosis of NSCLC was confirmed in recruited patients. (C) The treatment decisions made with recruited patients. (D) NSCLC patient overall survival (n=25).*

3.2.2 NSCLC and parapneumonic pleural fluid supernatant glucose is lower than matched serum

To establish the magnitude of glucose deprivation in NSCLC and parapneumonic plural effusions, levels were measured in matched serum and pleural fluid samples. Both were measured as a routine part of care in the hospital laboratories. Repeat measures were also taken in our laboratory by fluorometric assay. Whilst glucose levels were significantly lower in pleural fluid than the blood (Figure 3.4), no pleural samples were severely depleted of glucose (i.e. less than 3nM glucose per μL).

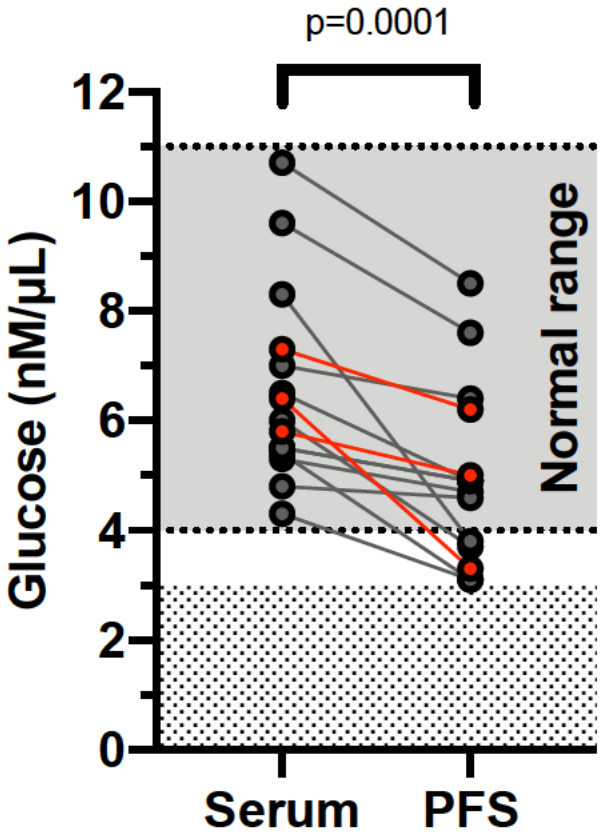

Figure 3.4: NSCLC and parapneumonic pleural fluid supernatant glucose is lower than matched serum.
Pleural fluid supernatant (PFS) and matched serum glucose measured from patients with NSCLC (●) n=12 and pneumonia (●) n=3 Dotted lines and grey shading indicate the normal range (non-fasting) for serum glucose (4-11nM/μL). Dotted shading indicates hypoglycaemic range (<3nMμ/μL). Analysed by paired t-test (passed Anderson-Darling normality test). Data represents individual values.

3.2.3 Modelling the NSCLC pleural metastatic environment

In order to address the hypotheses regarding the NSCLC pleural metastatic environment, two main approaches were taken. Firstly, the environment was modelled *in vitro* by culturing healthy donor blood neutrophils (or alternatively NSCLC blood neutrophils) in conditions emulating the pleural space and observing the impact of these manipulations (i.e. oxygen/ glucose availability and cell conditioning with pleural fluid supernatant) upon neutrophil functional readouts (i.e. apoptosis, phagocytosis and interaction with the adaptive immunity). Secondly, features of the NSCLC pleural environment were directly compared with those of pneumonia, to elucidate differences that may be of mechanistic importance in determining neutrophil functional outcome.

It was noted that glucose replete media, had a much higher concentration of glucose than that found in the serum and matched pleural fluid supernatant of patients (Figure 3.5). However, there was also a reasonable amount of variation in patient serum and pleural fluid supernatant glucose concentrations. Therefore, to elucidate if there were glucose-dependent neutrophil functional phenotypes, and to ensure that any subtle changes were not missed, in the *in vitro* models, culture in glucose-replete media was compared with culture in media that had no glucose at all.

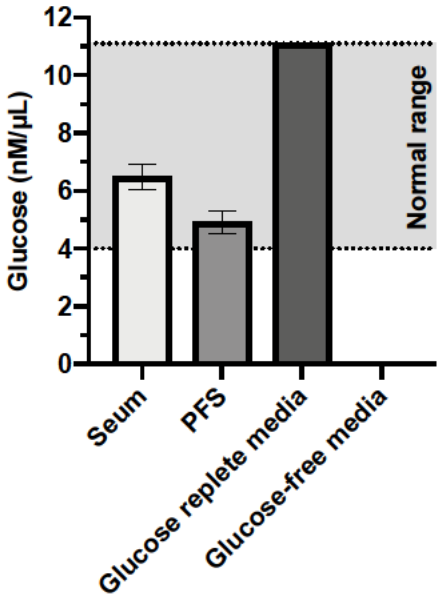

Figure 3.5: The glucose concentration of standard glucose replete culture media is much higher than that found in the serum and pleural fluid of patients.
Mean glucose concentration in matched serum and pleural fluid supernatant (PFS) of patients (n=15) is much lower than that of standard culture media. Standard culture media has a glucose concentration at the upper end of the normal range (non-fasting) for serum glucose. Data represents mean ± SEM.

3.2.4 Glucose availability regulates neutrophil apoptosis

To investigate the impact of glucose availability upon neutrophil apoptosis, blood neutrophils were cultured in media that was either glucose replete or glucose-free, with normal oxygen availability (21% O_2 in atmosphere, 12kPa in media) or alternatively hypoxia (1% O_2 in atmosphere, 4kPa in media). Apoptosis was measured at early (8-hour) and late (20-hour) time points. Apoptosis was quantified by cellular morphology (pyknotic nuclei) or by flow cytometry (positive Annexin V staining).

At 20 hours, deprivation of glucose was found to have a diametric effect upon apoptosis, dependent on oxygen availability (Figure 3.6A and B). In normoxia, glucose deprivation was pro-survival (median 36.0% apoptosis versus 70.6% apoptosis, p=0.0312), whereas in hypoxia it was pro-apoptotic (median 84.5% apoptosis versus 42.5% apoptosis, p=0.0312) (also resulting in cell loss). This was seen in both healthy donor (Figure 3.6A and B) and NSCLC blood neutrophils (Figure 3.7). At the earlier time point of 8 hours (Figure 3.6C) glucose deprivation did not have a significant impact upon apoptosis.

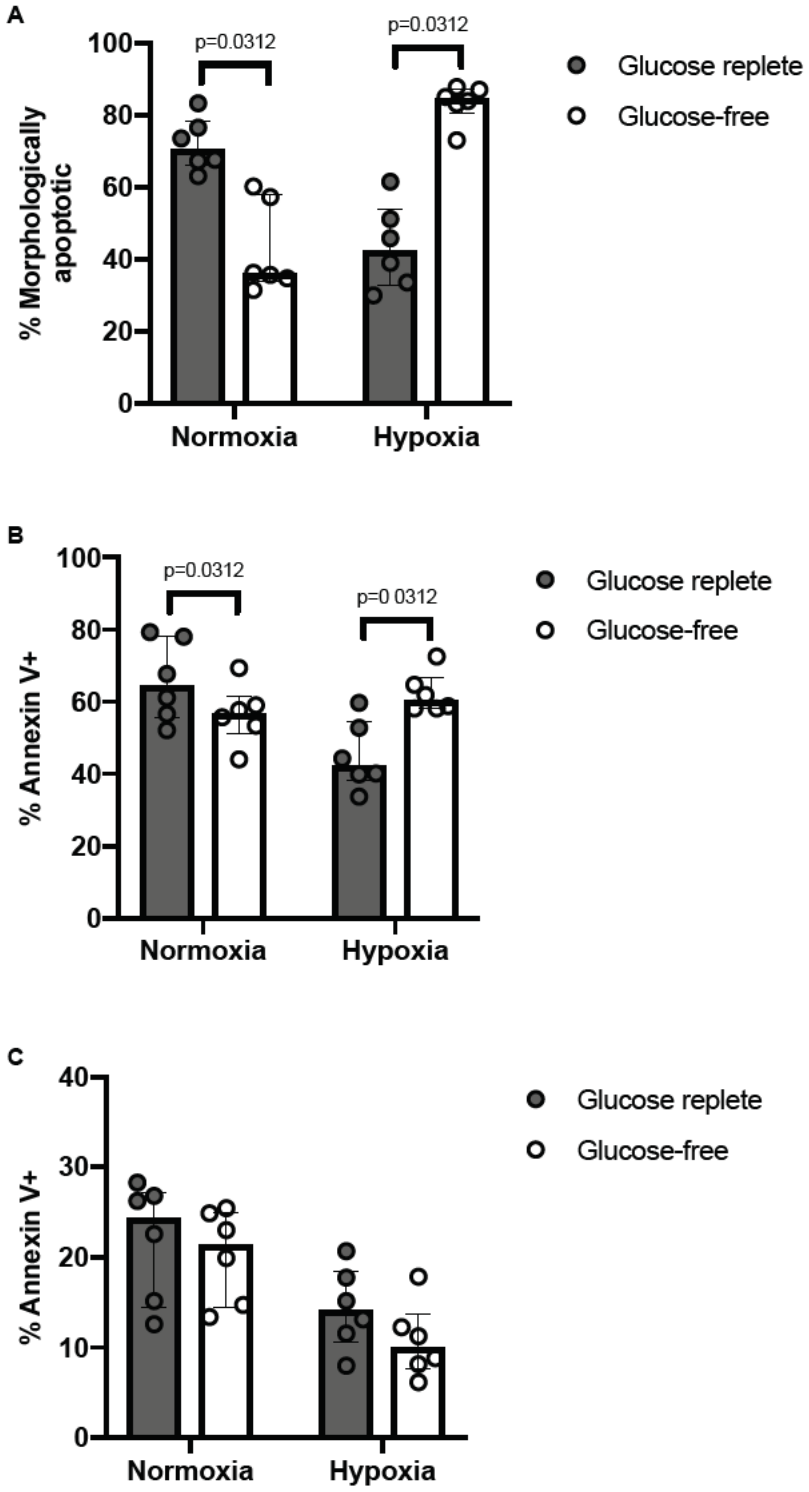

Figure 3.6: Glucose availability regulates healthy donor normal-density neutrophil apoptosis.

Apoptosis measured in healthy donor normal-density neutrophils cultured in media ± glucose (indicated by colour fill), with normal oxygen availability or alternatively hypoxia. (A) 20-hour apoptosis measured by cellular morphology, n=6. (B) 20-hour apoptosis measured by flow cytometry, n=6. (C) 8-hour apoptosis measured by flow cytometry, n=6. (A-C) Analysed by Wilcoxon test. Data represents individual values (average of at least two replicates) and median ± IQR.

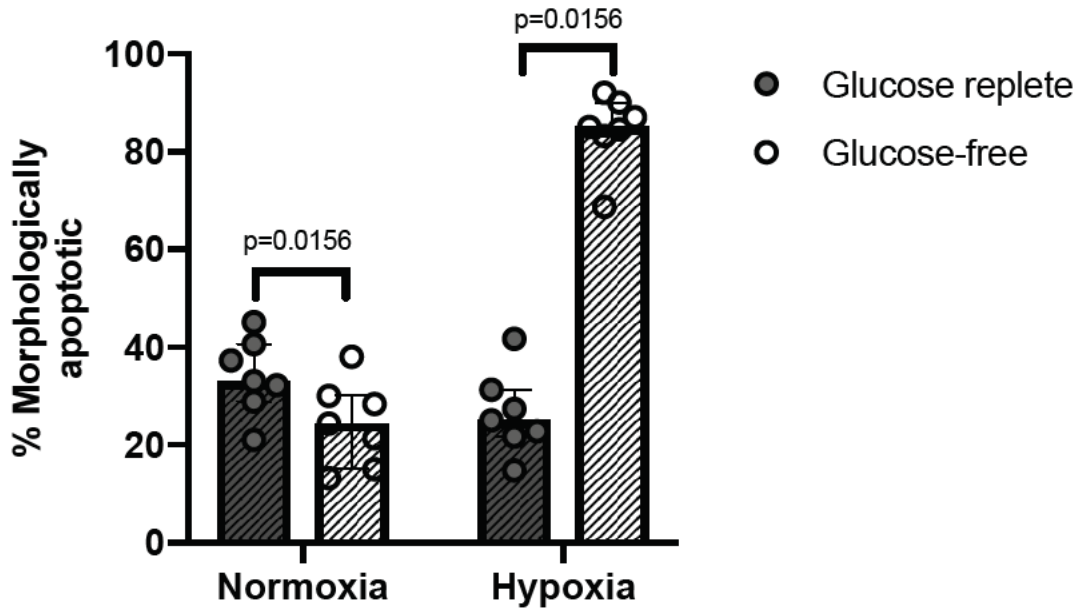

Figure 3.7: Glucose availability regulates NSCLC whole blood neutrophil apoptosis. *Apoptosis measured in NSCLC whole blood neutrophils (indicated by striped shading) cultured in media ± glucose (indicated by colour fill), with normal oxygen availability or alternatively hypoxia. Apoptosis measured by cellular morphology at 20 hours, n=7. Analysed by Wilcoxon test. Data represents individual values and median ± IQR.*

3.2.5 Neutrophil phagocytic capacity is preserved in glucose deprivation

In order to interrogate whether glucose availability determines the phagocytic capability of neutrophils, blood neutrophils were cultured in media that was either glucose replete or glucose-free, with normal oxygen availability or alternatively hypoxia. Phagocytosis was assessed by exposure to Zymosan A for 15 minutes, and measured by cellular morphology. Neutrophil phagocytic capacity was preserved in glucose deprivation (Figure 3.8).

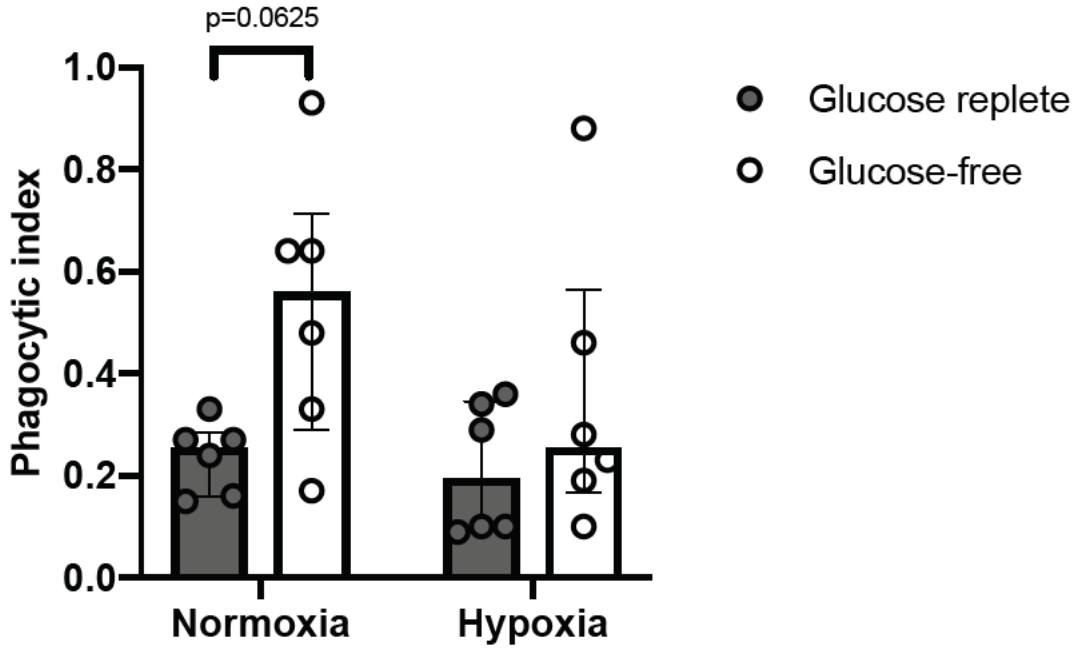

Figure 3.8: Neutrophil phagocytic capacity is preserved in glucose depletion. *Phagocytosis of Zymosan A measured in healthy donor normal-density neutrophils cultured in media ± glucose (indicated by colour fill), with normal oxygen availability or alternatively hypoxia, n=6. Analysed by Wilcoxon test. Data represents individual values (average of at least two replicates) and median ± IQR.*

3.2.6 NSCLC pleural fluid supernatant acts as a survival signal to neutrophils

To study whether other signals within NSCLC pleural fluid supernatant itself (e.g. cytokines) condition neutrophil survival, healthy donor blood neutrophils were cultured in media supplemented with pleural fluid supernatant in normal oxygen availability or alternatively hypoxia. Apoptosis was quantified by cellular morphology (pyknotic nuclei) or by flow cytometry (positive Annexin V staining).

In normoxia, NSCLC pleural fluid supernatant reduced the rate of apoptosis of healthy donor blood neutrophils at 20 hours. This effect was seen with 10% pleural fluid supernatant supplementation of culture media, with no added survival benefit of higher concentrations (median 29.9% apoptosis versus 60.0% apoptosis, p=0.0156) (Figure 3.9A). Pleural fluid supernatant was therefore used at a concentration of 10% in all subsequent *in vitro* neutrophil functional assays investigating its role. In hypoxia, 10% pleural fluid supernatant did not have any additional added effect on the rate of apoptosis of healthy donor blood neutrophils (Figure 3.9B and C).

A concern subsequently, was that NSCLC pleural fluid supernatant might induce healthy donor blood neutrophil necrosis/ cell loss, which was then not detected by the apoptosis quantification methods used, leading to a false result. Flow cytometry plots at 20 hours did not suggest this (Figure 3.10A and B), however to resolve this question, neutrophil counts were taken following 20 hours of culture with pleural fluid supernatant (Figure 3.10C). These counts were found to be identical to those taken following 20 hours culture without pleural fluid supernatant.

A final supplementary investigation, was to assess whether NSCLC pleural fluid supernatant had any additional impact on the pro-survival signal of glucose deprivation in normoxia, which It did not (Figure 3.11).

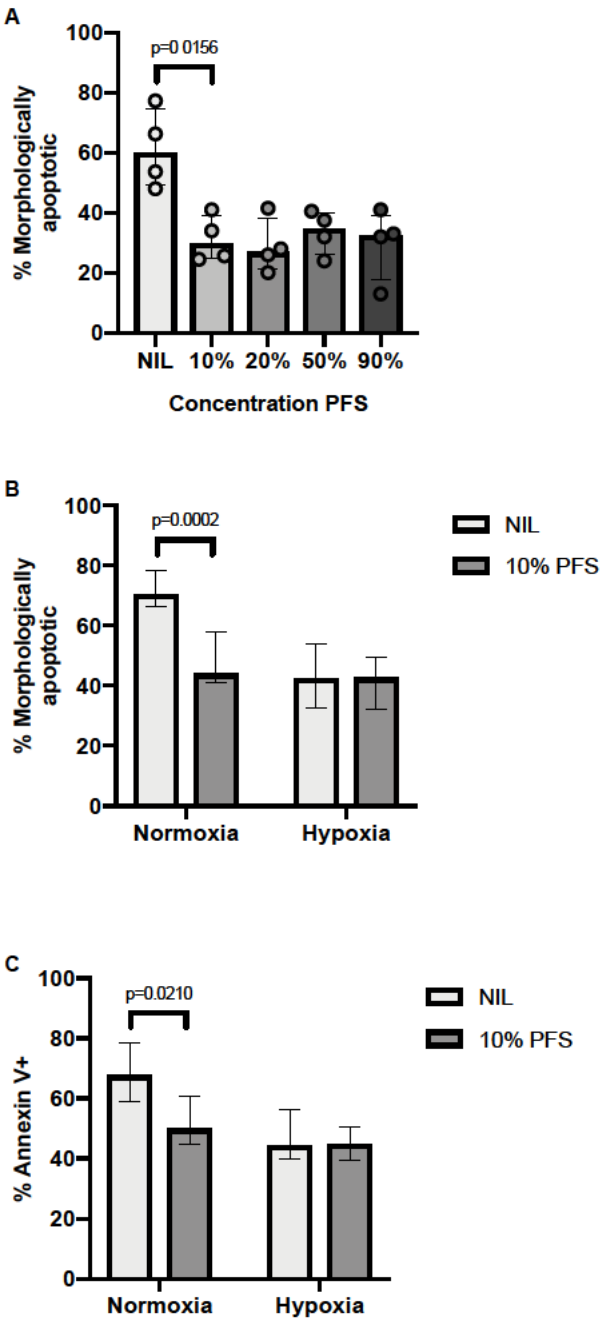

Figure 3.9: NSCLC pleural fluid supernatant acts as a survival signal to healthy donor normal-density neutrophils.
Apoptosis at 20 hours was measured in healthy donor normal density neutrophils cultured in media ± NSCLC pleural fluid supernatant (PFS) (indicated by colour fill), with normal oxygen availability or alternatively hypoxia. (A) Apoptosis measured by cellular morphology, following neutrophil culture with varying concentrations of pleural fluid supernatant, n=4 (normoxia only). (B) Apoptosis measured by cellular morphology, following neutrophil culture ± 10% pleural fluid supernatant, n=6 (each donor tested against two different pleural fluid supernatants). (C) Apoptosis measured by flow cytometry, following neutrophil culture ± 10% pleural fluid supernatant, n=5 (each donor tested against two different pleural fluid supernatants). (A) Analysed by Friedman test and Dunn's multiple comparisons. Analysed by Mann-Whitney test (B and C). Data represents individual values (average of at least two replicates) and median ± IQR.

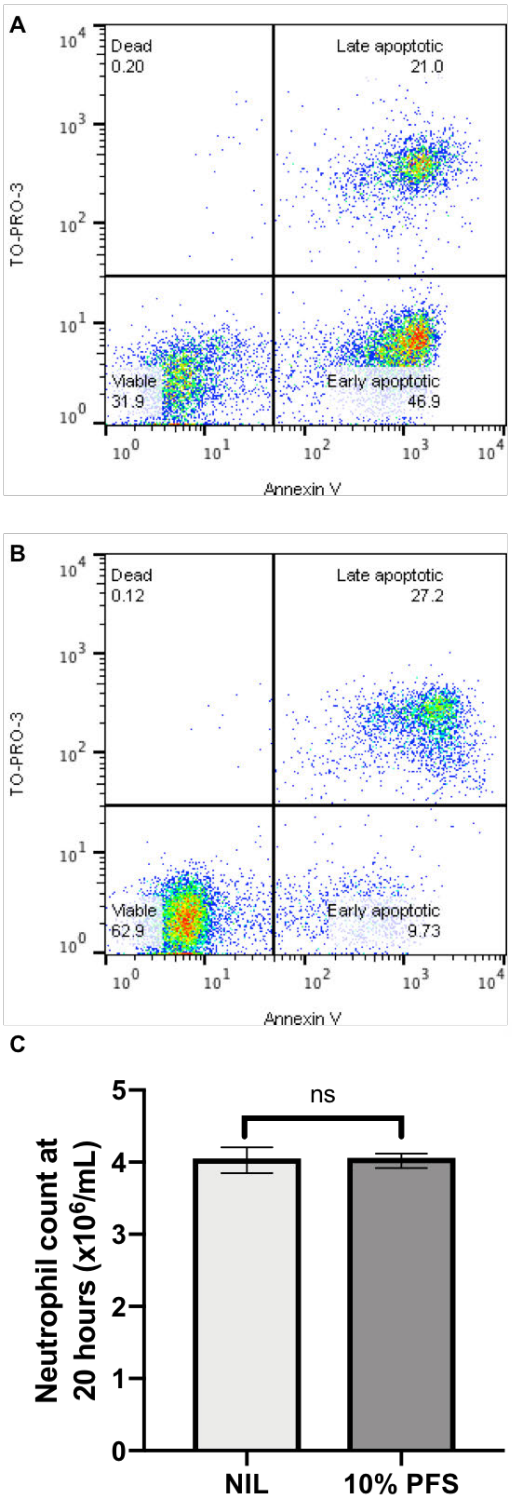

Figure 3.10: NSCLC pleural fluid supernatant does not induce healthy donor normal-density neutrophil necrosis/ cell loss.
Representative flow cytometry plots of the 20-hour apoptosis of healthy donor normal-density neutrophils cultured in normoxia in the absence (A) or presence (B) of NSCLC pleural fluid supernatant. (C) Neutrophil counts taken (Neubauer haemocytometer) following 20 hours of cell culture ± 10% NSCLC pleural fluid supernatant (PFS), n=4 (each donor tested against two different pleural fluid supernatants). Analysed by Mann-Whitney test. Summary data represents median ± IQR.

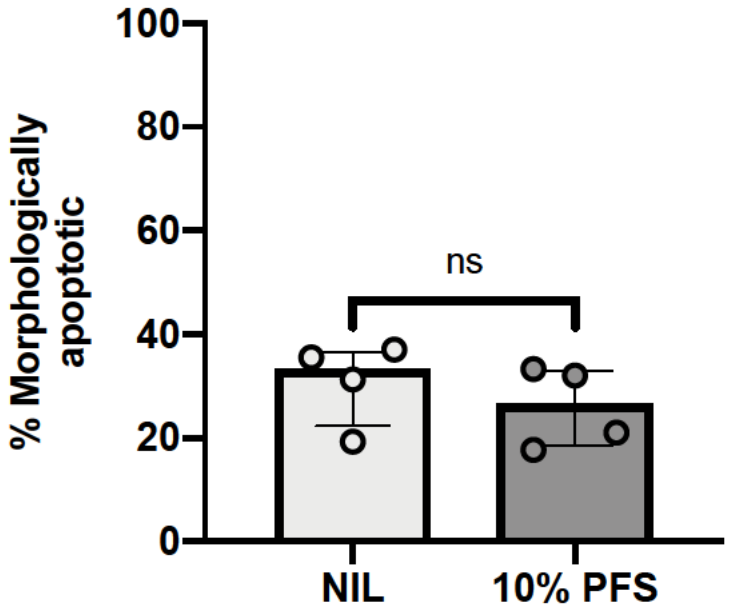

Figure 3.11: NSCLC pleural fluid supernatant does not have any added effect on the apoptosis of healthy donor normal-density neutrophils in glucose-free media.
Apoptosis at 20 hours was measured by cellular morphology in healthy donor normal-density neutrophils cultured in glucose-free media ± NSCLC pleural fluid supernatant with normal oxygen availability, n=4 (4 different donors, each tested against a different pleural fluid supernatant). Analysed by Wilcoxon test. Data represents individual values (average of at least two replicates) and median ± IQR.

3.2.7 NSCLC pleural fluid supernatant stimulates neutrophil phagocytosis of Zymosan A via opsonisation

To consider whether NSCLC pleural fluid supernatant aided or abrogated the phagocytic capacity of neutrophils, healthy donor blood neutrophils were cultured in media supplemented with pleural fluid supernatant in normal oxygen availability or alternatively hypoxia. Phagocytosis was assessed by exposure to Zymosan A for 15 minutes, and measured by cellular morphology. NSCLC pleural fluid supernatant increased the phagocytosis of healthy donor blood neutrophils (Figure 3.12A, C and D). However, it was thought this may be an opsonisation effect, which was supported when a similar result was obtained by adding non-autologous serum to the culture media (Figure 3.12B), $p=0.8438$.

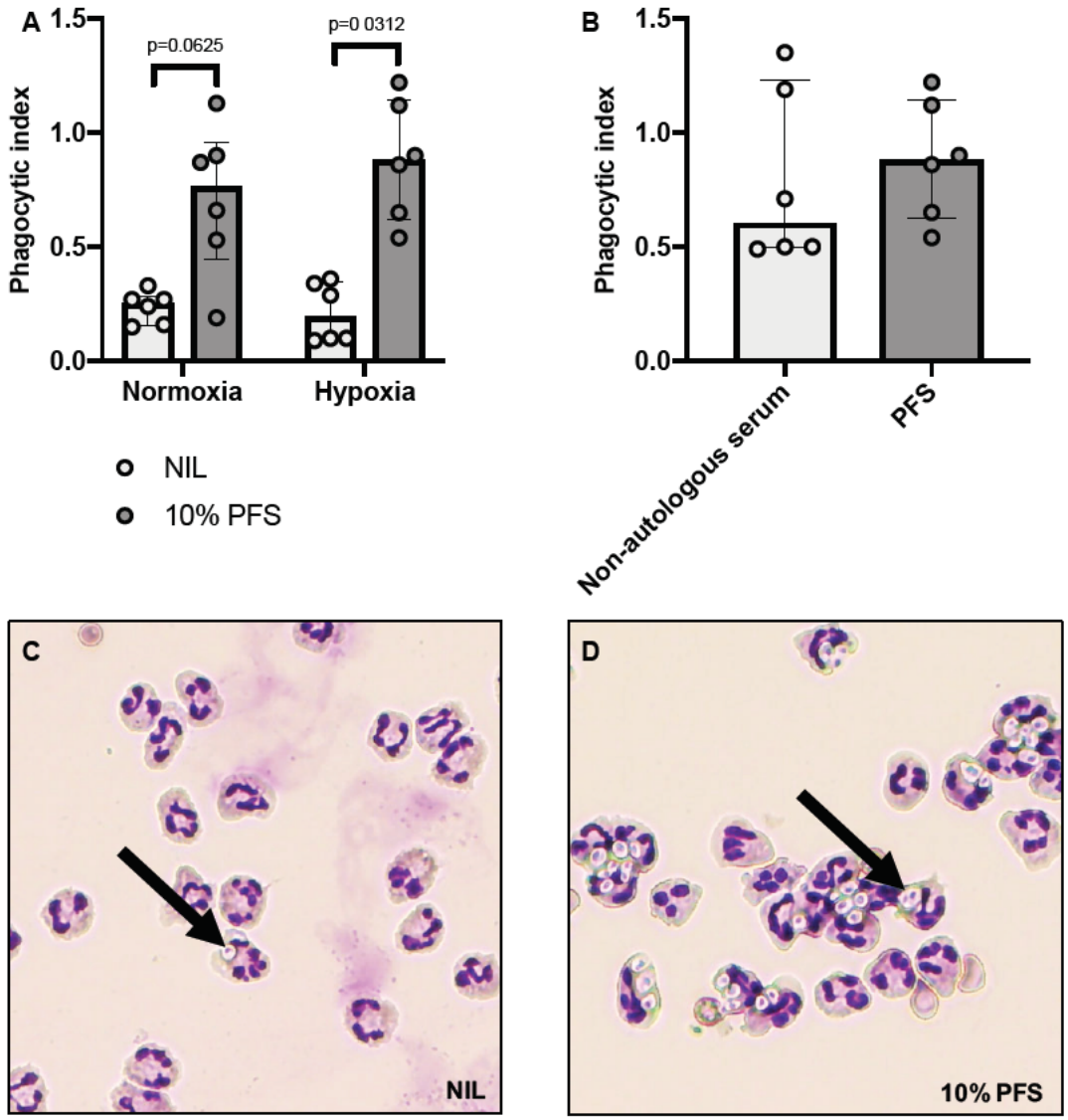

Figure 3.12: Evidence that NSCLC pleural fluid supernatant stimulates healthy donor normal-density neutrophil phagocytosis of Zymosan A via opsonisation.
(A) Phagocytosis of Zymosan A measured in healthy donor normal-density neutrophils cultured in media ± NSCLC pleural fluid supernatant (PFS) (indicated by colour fill), with normal oxygen availability or alternatively hypoxia, n=6. (B) Phagocytosis of Zymosan A measured in healthy donor normal-density neutrophils cultured in normoxia, with media containing either 10% non-autologous serum or 10% NSCLC pleural fluid supernatant. Representative cytospin images (40X magnification) of Zymosan A phagocytosis by neutrophils (arrows) in the absence (C) or presence (D) of 10% NSCLC pleural fluid supernatant. (A and B) Analysed by Wilcoxon test. Data represents individual values (average of at least two replicates) and median ± IQR.

3.2.8 NSCLC pleural fluid supernatant conditions neutrophils to inhibit $CD8^+$ T cells via PD-L1

To examine the impact of NSCLC pleural fluid supernatant upon interactions between the innate and adaptive immunity, a neutrophil-T cell co-culture was utilised. Healthy donor blood Cell Tracker Green™ labelled T cells stimulated with CD3/CD28, were cultured with varying ratios of healthy donor blood neutrophils in the presence or absence of 10% NSCLC pleural fluid supernatant. $CD8^+$ T cell proliferation and activation was measured after 72 hours by flow cytometry (Cell Tracker Green and FlowJo proliferation tool, CD62L staining). NSCLC pleural fluid supernatant did not inhibit $CD8^+$ T cell proliferation on its own, but did condition neutrophils to inhibit $CD8^+$ T cell proliferation (median 7.6% proliferation versus 43.9% proliferation, p=0.0286) (Figure 3.13A and B). Neutrophils conditioned by NSCLC pleural fluid supernatant also triggered a corresponding reduction in $CD8^+$ T cell activation (median 13.5% activated versus 38.9% activated, although not statistically significant p=0.0571) (Figure 3.13C and D). In addition, the data in Figure 3.13 suggested that increasing ratios of neutrophils may inhibit $CD8^+$ T cell proliferation on their own, even before the addition of pleural fluid supernatant (although not statistically significant). As there has been some concern in the literature that this may be an experimental artefact when Dynabeads™ are used for T cell stimulation,[41] the experiment was repeated using plate bound LEAF™ antibody, confirming that this observation was not artefactual (Figure 3.14).

Next, a mechanism to explain the T cell suppression by NSCLC pleural fluid supernatant-conditioned neutrophils was sought. Neutrophil surface expression of PD-L1 was found to be augmented by exposure to NSCLC pleural fluid supernatant (median fluorescence 1363 versus 873, p=0.0312) (Figure 3.15A and B). Furthermore, when the neutrophil-T cell co-culture was repeated with a PD-L1 inhibitor (Figure 3.15C), there was partial reversal of the $CD8^+$ T cell suppression (median 18.3% proliferation versus 3.9% proliferation, baseline 54.2%, p=0.0312).

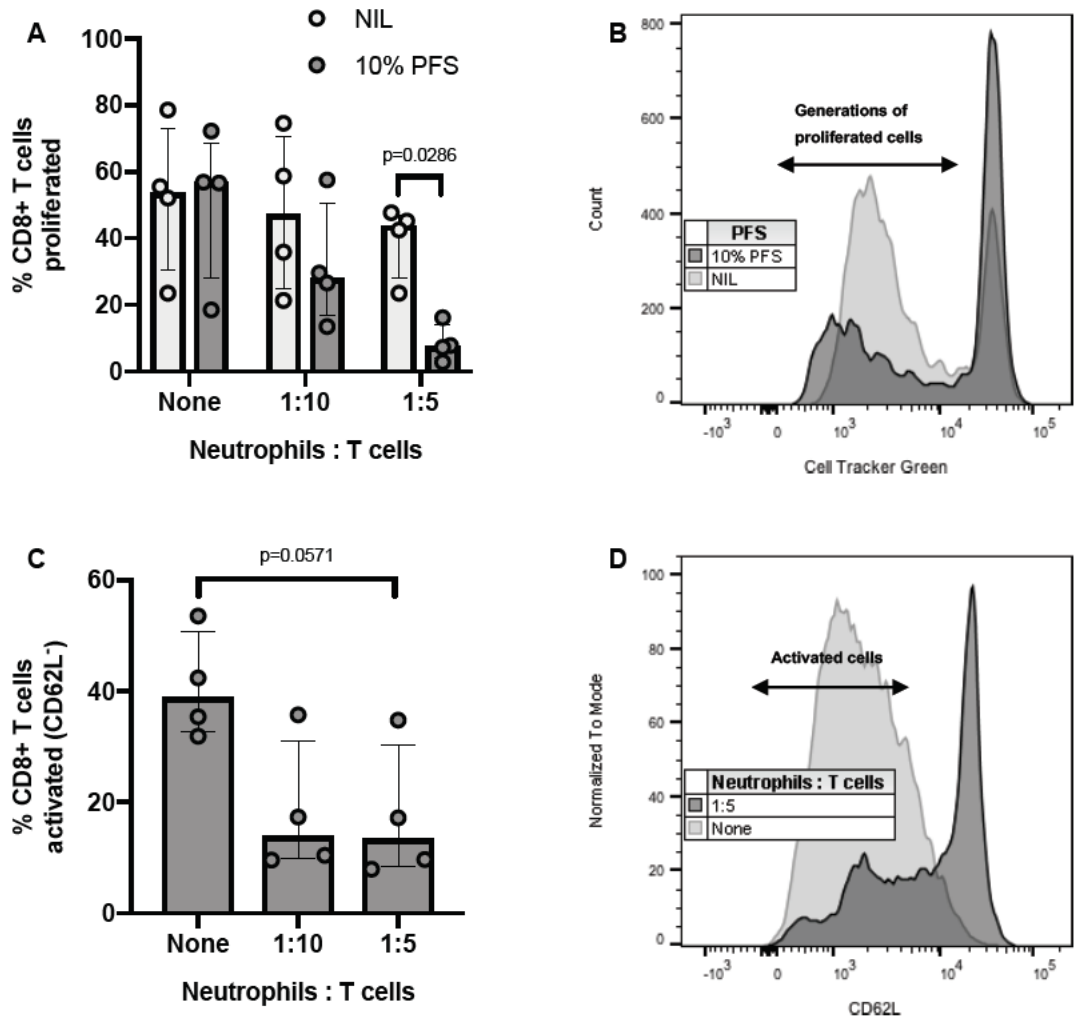

Figure 3.13: NSCLC pleural fluid supernatant conditions healthy donor neutrophils to inhibit CD8$^+$ T cell proliferation and activation.
(A) CD8 T cell 72-hour proliferation measured in healthy donor cells stimulated with CD3/CD28 Dynabeads™ and cultured with varying ratios of heathy donor neutrophils ± 10% NSCLC pleural fluid supernatant (PFS) (indicated by colour fill), n=4. (B) Representative flow cytometry histogram of CD8 proliferation, following culture with neutrophils at a ratio 1:5 ± 10% NSCLC pleural fluid supernatant (indicated by colour fill). Undivided cells are seen as a peak on the right, each subsequent generation of divided cells forming an additional peak to the left, with peak height indicating cell number. (C) The activation of CD8 T cells cultured with 10% NSCLC pleural fluid supernatant ± neutrophils of varying ratios, n=4. (D) Representative flow cytometry histogram of CD8 T cell activation following culture with 10% NSCLC pleural fluid supernatant and neutrophils at a ratio of 1:5 (indicated by colour fill). (A and C) Analysed by Mann-Whitney test. Data represents individual values and median ± IQR.

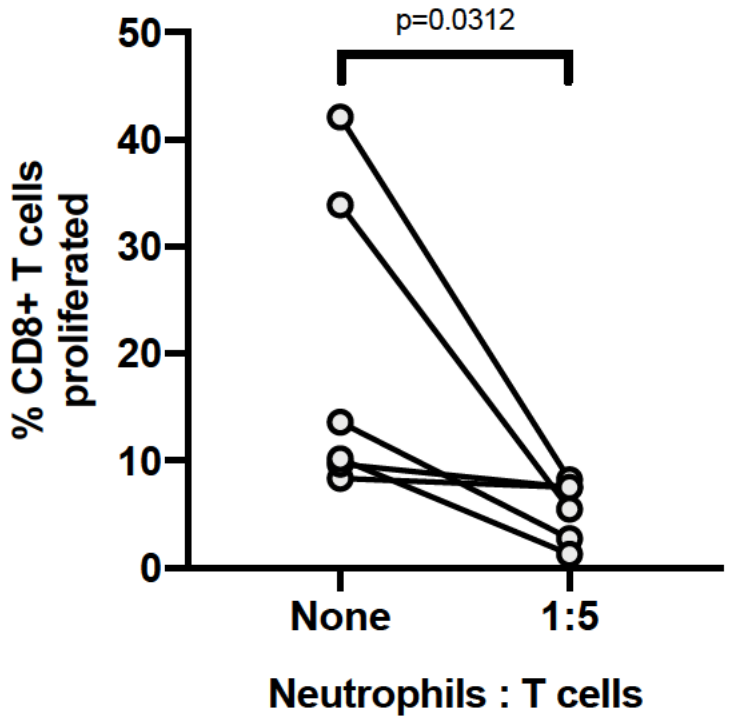

Figure 3.14: Healthy donor neutrophils inhibit CD8$^+$ T cell proliferation.
CD8 T cell 72-hour proliferation measured in healthy donor cells stimulated with plate bound LEAF™ CD3 antibody and LEAF™ CD28 antibody, and cultured ± heathy donor neutrophils at a ratio of 1:5, n=6. Analysed by Wilcoxon test. Data represents individual paired values.

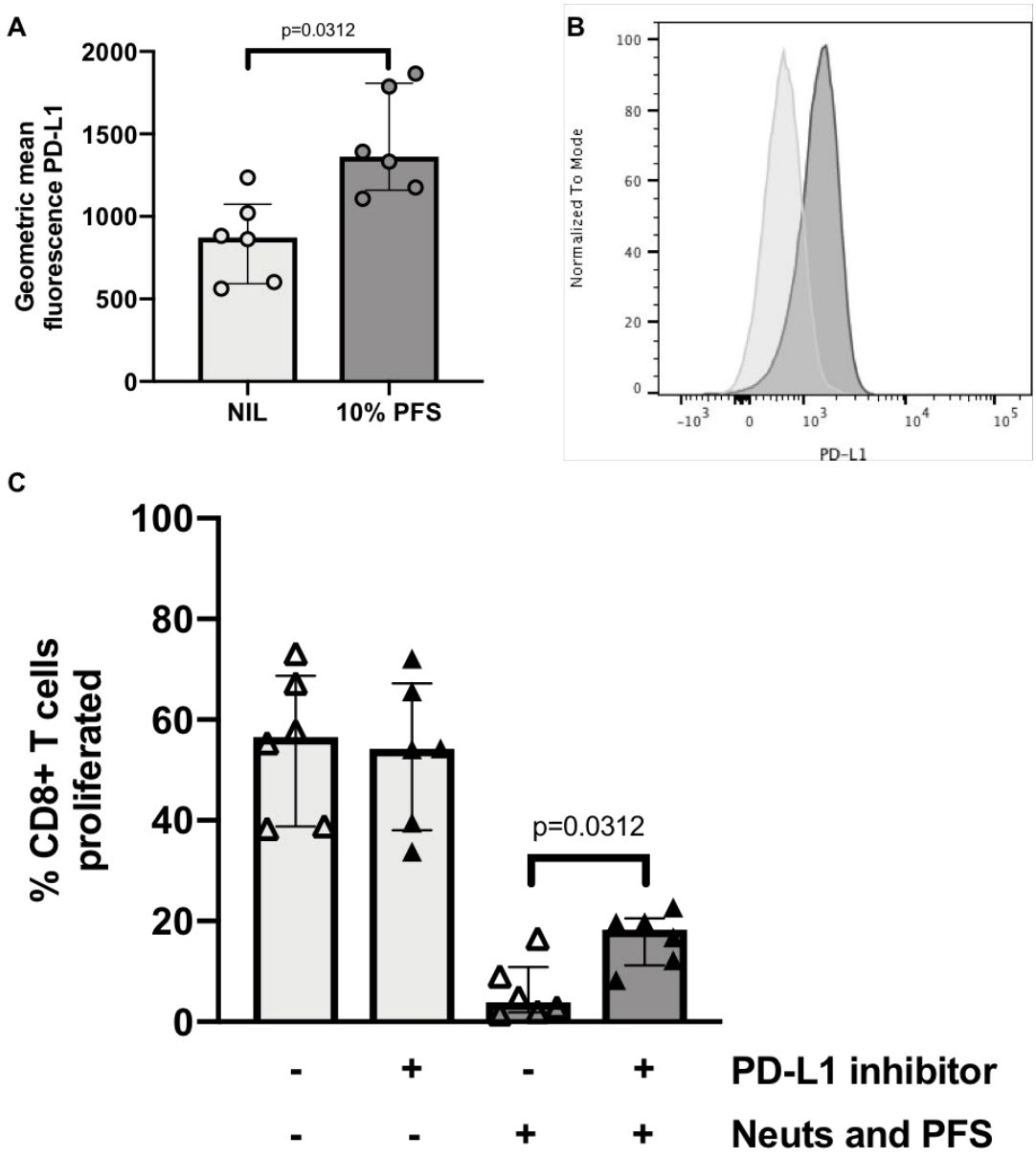

Figure 3.15: NSCLC PFS conditions healthy donor neutrophils to inhibit CD8$^+$ T cell proliferation via PD-L1.

(A) Healthy donor neutrophils were cultured ± 10% NSCLC pleural fluid supernatant (PFS) (indicated by colour fill) for 3 hours, n=6. (B) Representative PD-L1 histogram of data shown in A. (C) CD8 T cell 72-hour proliferation measured in healthy donor cells stimulated with CD3/CD28 Dynabeads™ and cultured with or without heathy donor neutrophils (ratio 1:5) together with 10% NSCLC pleural fluid supernatant (indicated by bar colour fill) ± PD-L1 inhibitor (indicated by triangle colour fill), n=6. Analysed by Wilcoxon test. Data represents individual values and median ± IQR (different donors, each tested against a different pleural fluid supernatant).

3.2.9 The N2-polarising cytokine TGFβ is present in NSCLC pleural fluid supernatant

To determine whether NSCLC pleural fluid supernatant contained cytokines already described to polarise neutrophils to either pro- or anti-tumour phenotypes, [25 26] TGFβ and IFNβ were quantified by ELISA (Figure 3.16). The N1 (anti-tumour) polarising cytokine IFNβ, was detected at low levels. The N2 (pro-tumour) polarising cytokine TGFβ was present at higher concentrations.

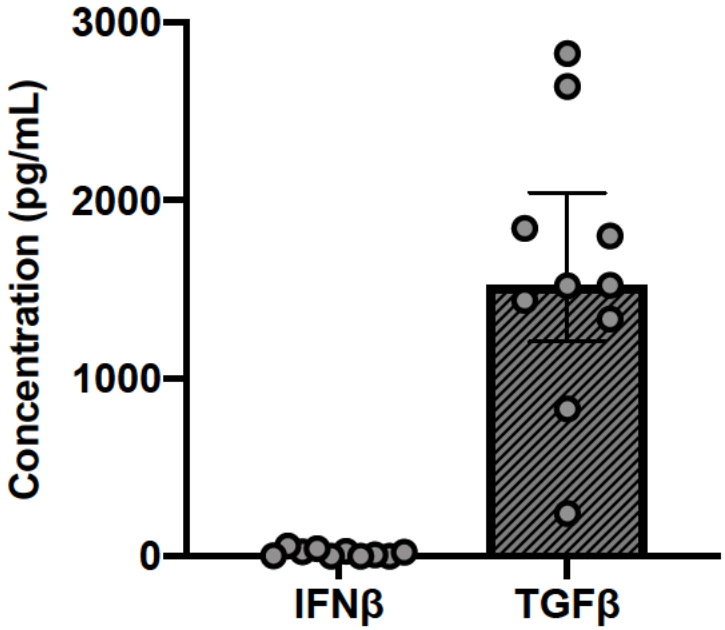

Figure 3.16: The N2-polarising cytokine TGFβ is present in NSCLC pleural fluid supernatant.

The N1-polarising cytokine IFNβ and N2-polarising cytokine TGFβ were both measured in NSCLC pleural fluid supernatant by ELISA (n=10 different pleural fluid supernatants). Data represents individual values (average of at least two replicates) and median ± IQR.

3.2.10 Neither pneumonia pleural fluid supernatant nor non-autologous serum act as a survival signal

To affirm whether the pro-survival effect of NSCLC pleural fluid supernatant upon healthy donor blood neutrophils was NSCLC-specific, the apoptosis studies described in 3.2.6, were repeated using pneumonia pleural fluid supernatant or alternatively non-autologous serum. At the concentration of 10% in culture media, pneumonia pleural fluid supernatant did not change neutrophil apoptosis (Figure 3.17A-C), and at higher concentrations it increased apoptosis (median 65.9% apoptosis versus 54.6% apoptosis, p=0.0373) (Figure 3.17A). Non-autologous serum had no impact upon healthy donor blood neutrophil apoptosis (Figure 3.18A and B). The phenomenon was therefore specific to the NSCLC pleural fluid environment.

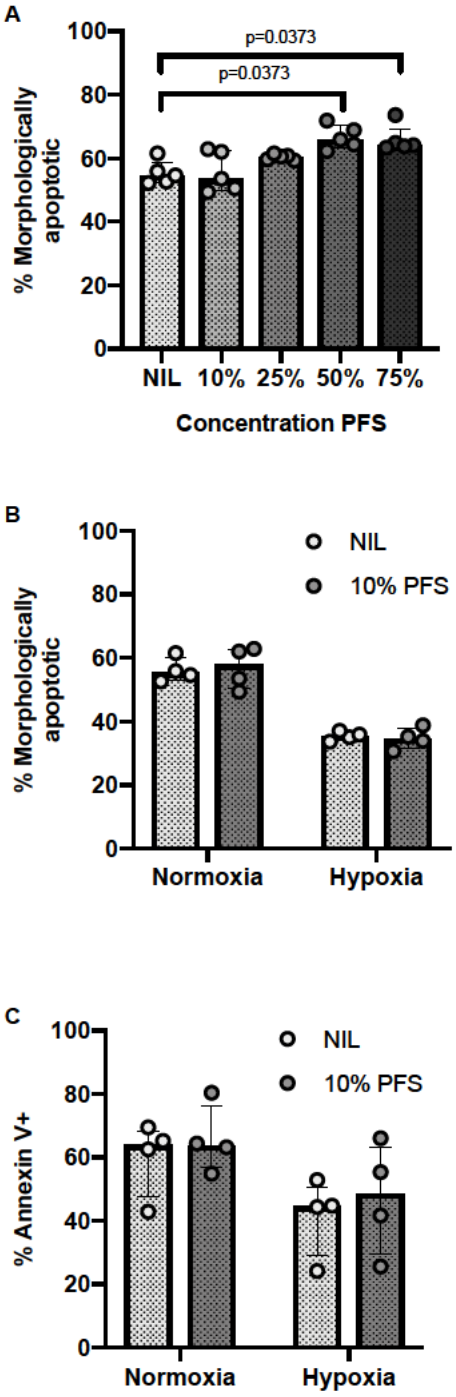

Figure 3.17: Pneumonia pleural fluid supernatant does not act as a survival signal to healthy donor normal-density neutrophils.
Apoptosis at 20 hours was measured in healthy donor normal-density neutrophils cultured in media ± pneumonia pleural fluid supernatant (PFS) (indicated by colour fill), with normal oxygen availability or alternatively hypoxia. (A) Apoptosis measured by cellular morphology, following neutrophil culture with varying concentrations of pleural fluid supernatant, n=5 (normoxia only). (B) Apoptosis measured by cellular morphology, following neutrophil culture ± 10% pleural fluid supernatant, n=4. (C) Apoptosis measured by flow cytometry, following neutrophil culture ± 10% pleural fluid supernatant, n=4. (A) Analysed by Friedman test (p=0.0093) and Dunn's multiple comparisons. Analysed by Wilcoxon test (B and C). Data represents individual values (average of at least two replicates) and median ± IQR.

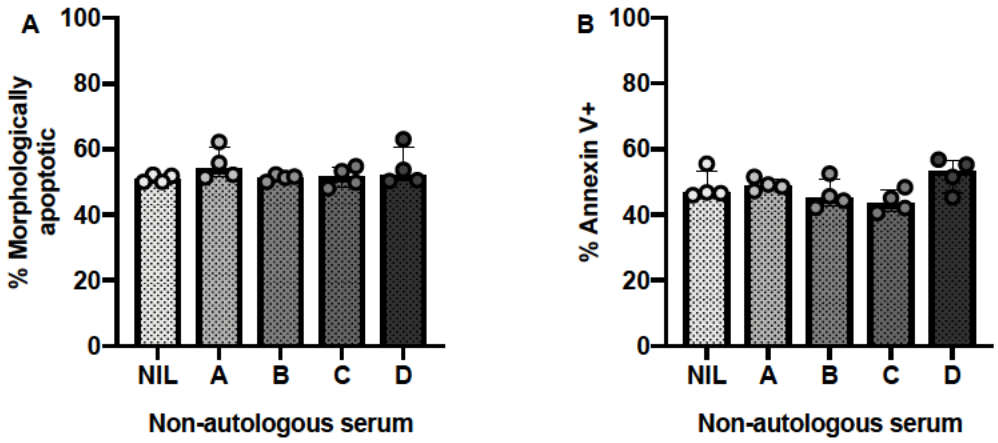

Figure 3.18: Non-autologous serum does not act as a survival signal to healthy donor normal-density neutrophils.
Apoptosis at 20 hours was measured in healthy donor normal-density neutrophils cultured in media ± 10% non-autologous serum with normal oxygen availability. (A) Apoptosis measured by cellular morphology, n=4. (B) Apoptosis measured by flow cytometry, n=4. Analysed by Friedman test and Dunn's multiple comparisons. Data represents individual values (average of at least two replicates) and median ± IQR.

3.2.11 The pleural fluid supernatant cytokine profile in NSCLC differs to pneumonia, with N2 and pro-survival features

To explore what signals in the pleural fluid supernatant may be responsible for manipulating neutrophil function, and to elucidate differences between NSCLC and pneumonia pleural fluid supernatant that may be of mechanistic importance in determining disease outcome, a human cytokine array was performed. This quantified the relative expression of 64 cytokines in NSCLC pleural fluid supernatant versus pneumonia pleural fluid supernatant (relative rather than absolute quantification). Despite significant heterogeneity between samples, clear patterns of differential expression were observed (Figure 3.19). Cytokines associated with immune tolerance, neutrophil survival and immune checkpoint (N2 features) were expressed at higher levels in NSCLC pleural fluid supernatant when compared with pneumonia pleural fluid supernatant (Figure 3.20). Cytokines associated with neutrophil chemotaxis and acute response (N1 features) were lower in NSCLC. In addition, TNFα was identified as a candidate neutrophil survival signal. When absolute quantification of TNFα was then subsequently measured in pleural fluid supernatant by ELISA, the levels in NSCLC were found to be higher than those in pneumonia (Figure 3.21).

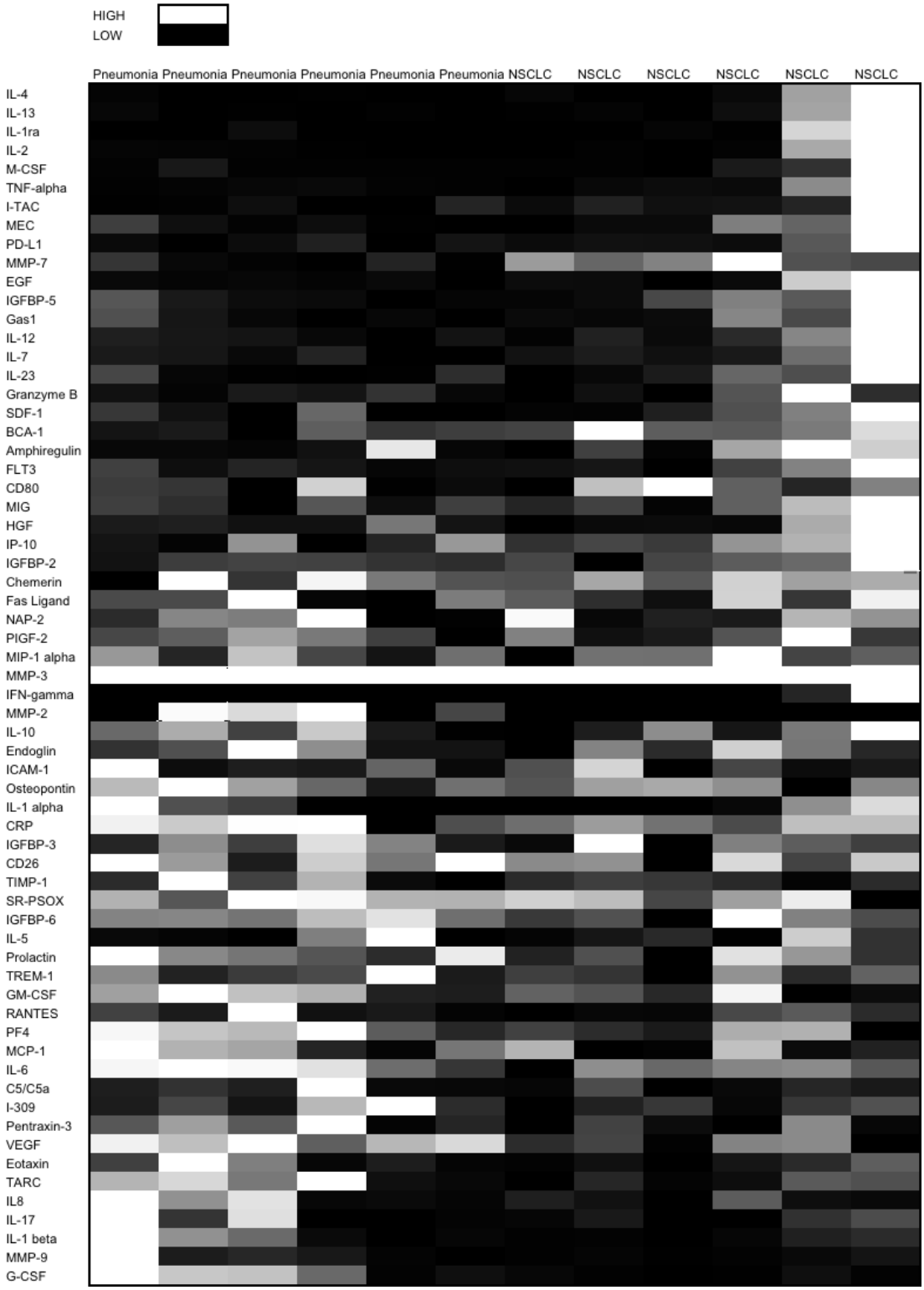

Figure 3.19: Heat map showing relative expression of 64 pleural fluid supernatant cytokines in NSCLC versus pneumonia.

The relative expression of 64 pleural fluid supernatant cytokines in NSCLC versus pneumonia was measured by human cytokine array (n=6 each group). Heat map colour shades based upon relative fluorescence intensity values.

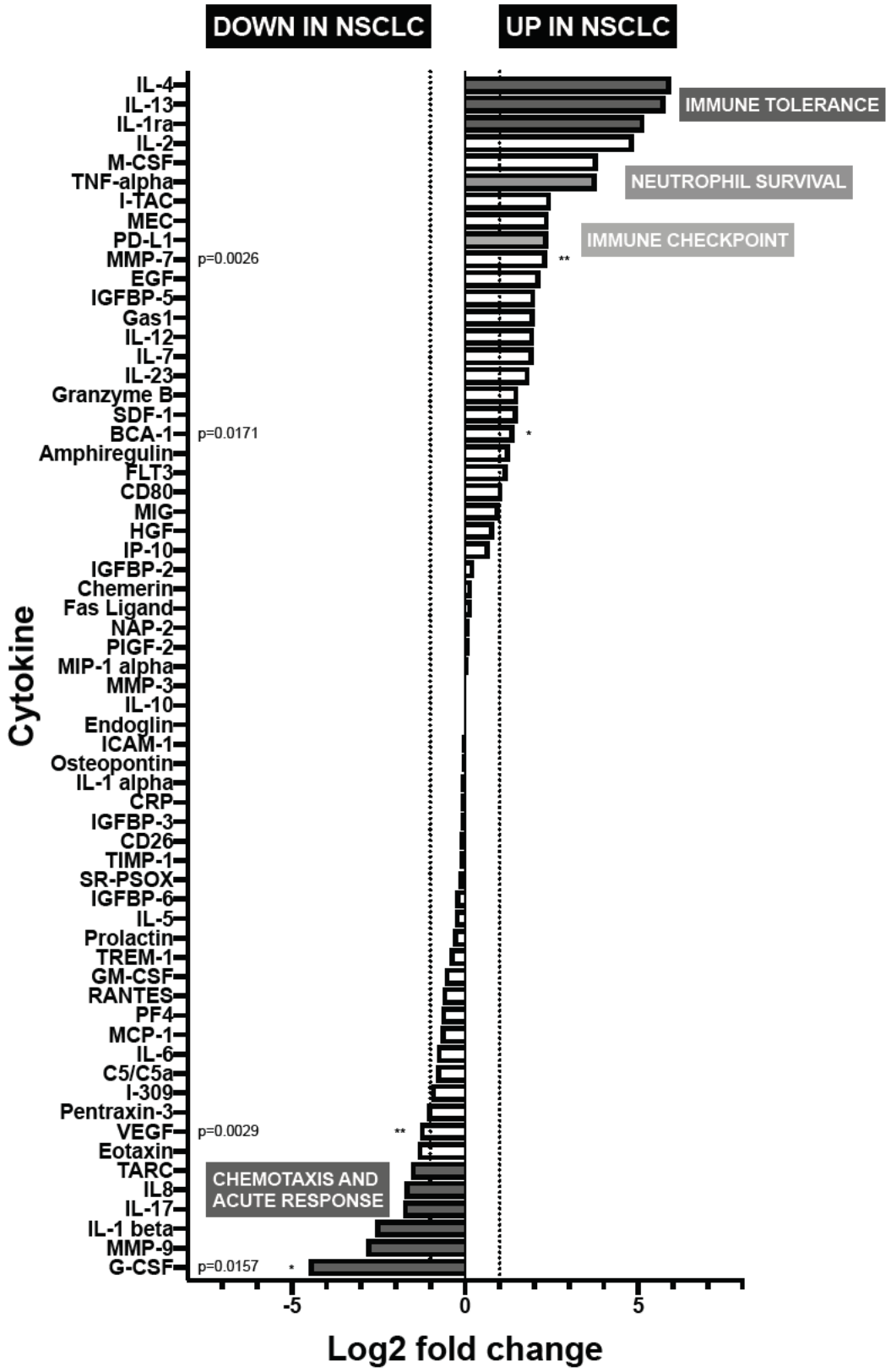

Figure 3.20: Fold change difference between pleural fluid supernatant cytokines in NSCLC versus pneumonia.

The relative expression of pleural fluid supernatant cytokines in NSCLC versus pneumonia was measured by human cytokine array (n=6 each group). Analysed by t-test, with statistically significant results marked by asterisk. Data represents mean values.

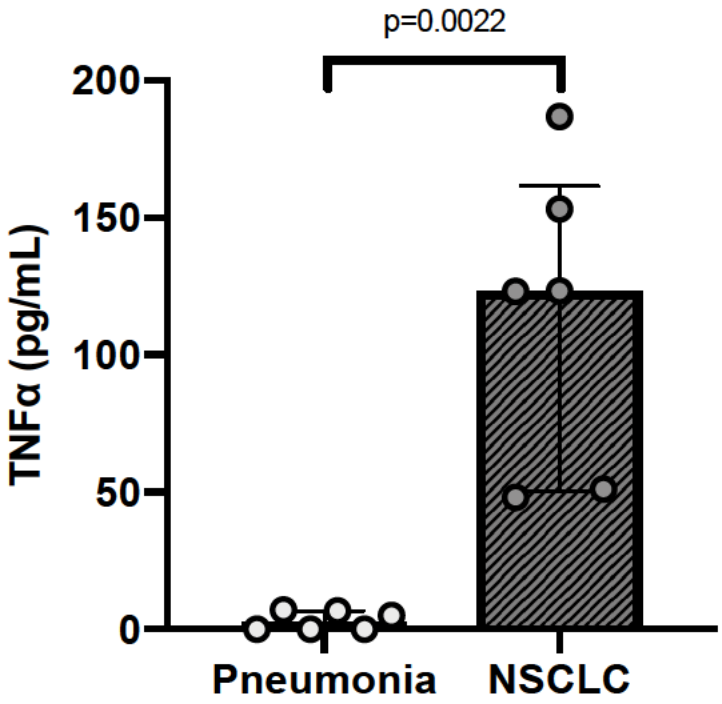

Figure 3.21: NSCLC pleural fluid supernatant TNFα levels are higher than those seen in pneumonia.

TNFα levels were measured by ELISA, in pleural fluid supernatant from patients with NSCLC and pneumonia, n=6. Data represents individual values (average of at least two replicates) and median ± IQR.

3.2.12 The NSCLC pleural fluid supernatant neutrophil survival signal is TNFα

Several experiments were carried out to cross-examine whether TNFα was indeed the NSCLC pleural fluid supernatant neutrophil survival signal. It is known that TNFα has a biphasic effect on neutrophil apoptosis, with a pro-apoptotic effect at earlier time points (via the CD120a) but an overall pro-survival effect at later time points (CD120b mediated).[95] The healthy donor blood neutrophil experiments described in 3.2.6 were therefore repeated with an earlier time point of 8 hours.

These experiments demonstrated that the healthy donor blood neutrophil apoptosis response to NSCLC pleural fluid supernatant was indeed biphasic. Apoptosis of healthy donor blood neutrophils was increased at 8 hours, following exposure to pleural fluid supernatant (median 32.9% apoptosis versus 24.4% apoptosis, p=0.0182) (Figure 3.22A). Furthermore, the magnitude of the pro-apoptotic effect of NSCLC pleural fluid supernatant seen at the 8-hour time point, and the magnitude of the pro-survival effect of NSCLC pleural fluid supernatant seen at the 20-hour time point was proportional to the concentration of TNFα in the pleural fluid supernatant (Figure 3.22B and C)

Next it was observed that NSCLC pleural fluid supernatant induced changes in healthy donor neutrophil TNFα surface receptor expression, favouring higher levels of the pro-survival receptor CD120b (median fluorescence 426 versus 362, p=0.0312) (Figure 3.23A-C). Finally, further evidence that the NSCLC pleural fluid supernatant neutrophil survival signal is TNFα came from using inhibitors of TNFα downstream signalling (Figure 3.24) and direct TNFα inhibitors, that reversed both the 8-hour (Figure 3.25A and B) and 20-hour (Figure 3.26A and B) healthy donor neutrophil NSCLC pleural fluid supernatant- induced apoptosis phenotypes.

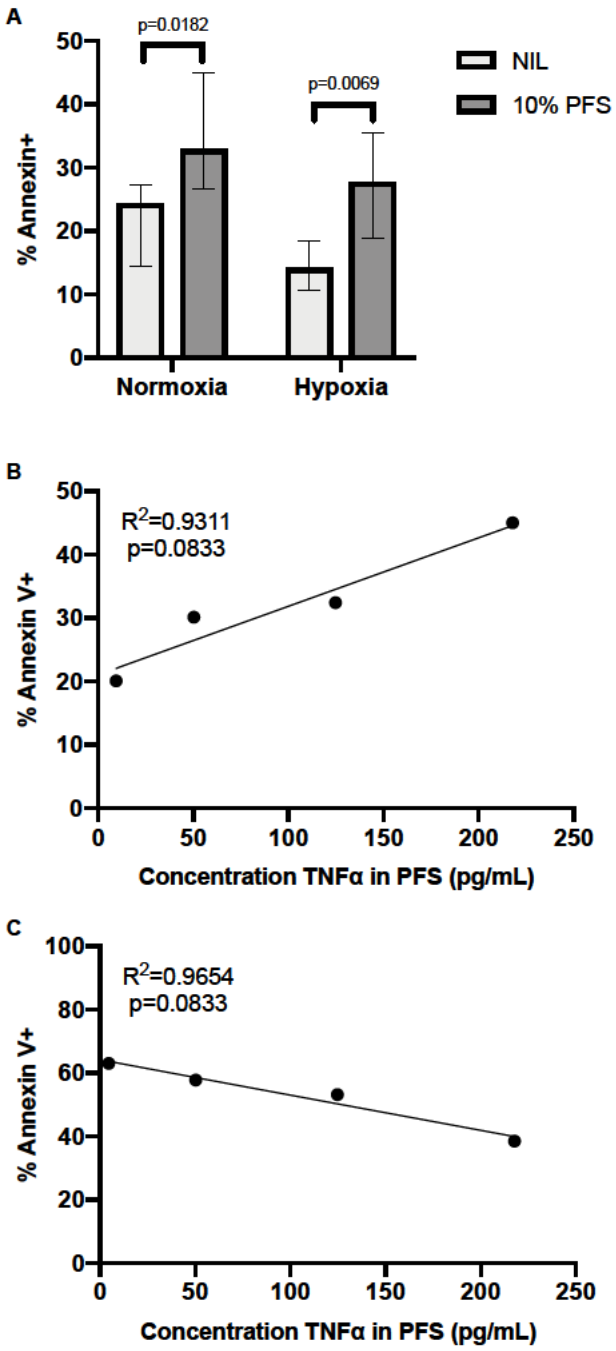

Figure 3.22: The healthy donor normal-density neutrophil survival response to NSCLC pleural fluid supernatant is biphasic and correlates to TNFα concentration in the pleural fluid supernatant.

(A) Apoptosis at 8 hours measured by flow cytometry in healthy donor normal-density neutrophils cultured in media ± 10% NSCLC pleural fluid supernatant (PFS) (indicated by colour fill), with normal oxygen availability or alternatively hypoxia, n=6 (each donor tested against two different pleural fluid supernatants). (B and C) Concentration of TNFα in four different pleural fluid supernatants used (measured by ELISA) was plotted against the mean healthy donor normal-density neutrophil 8-hour apoptosis (B) or 20-hour apoptosis (C) (both measured by flow cytometry), resulting from culture with the matched pleural fluid supernatant. Analysed by Mann-Whitney test and summary data represents median ± IQR (A). Analysed by Spearman correlation and summary data represents mean apoptosis values with slope plotted by linear regression (B and C).

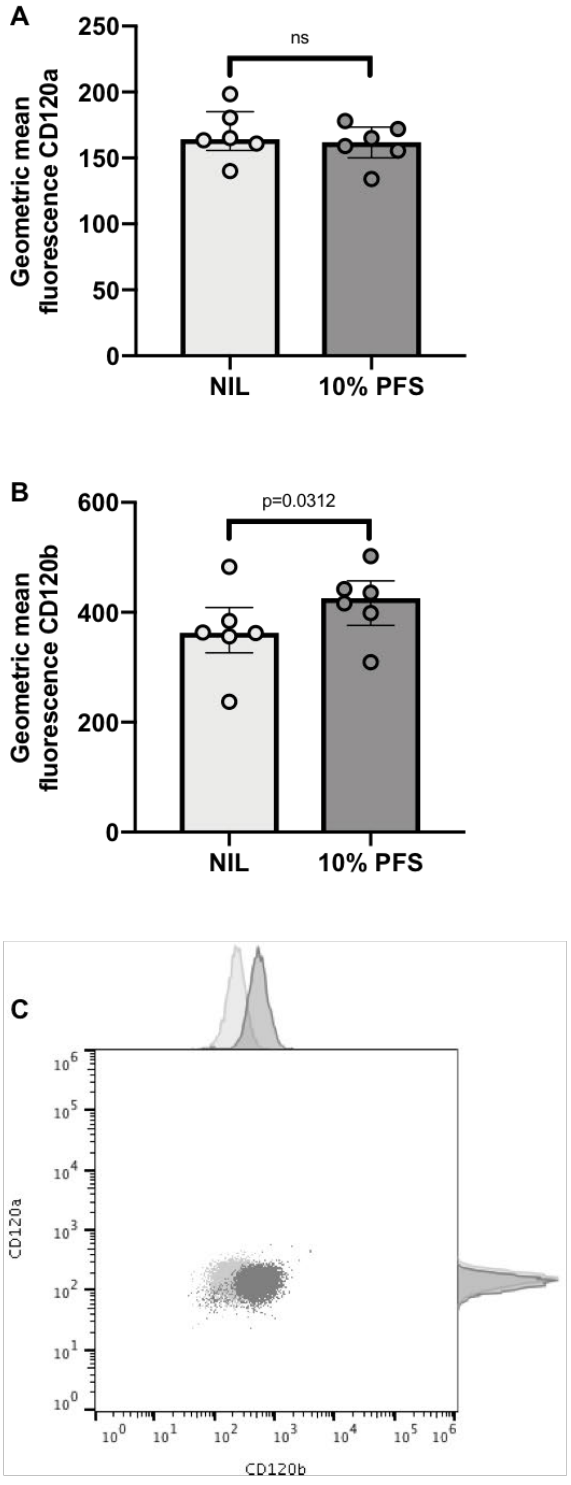

Figure 3.23: NSCLC pleural fluid supernatant induces changes in healthy donor neutrophil TNFα surface receptor CD120b expression.

Healthy donor neutrophils were cultured ± 10% NSCLC pleural fluid supernatant (PFS) (indicated by colour fill) for 3 hours, n=6. (A) CD120a surface expression. (B) CD120b surface expression. (C) Representative dot plots/ histograms. Analysed by Wilcoxon test. Data represents individual values and median ± IQR (A and B).

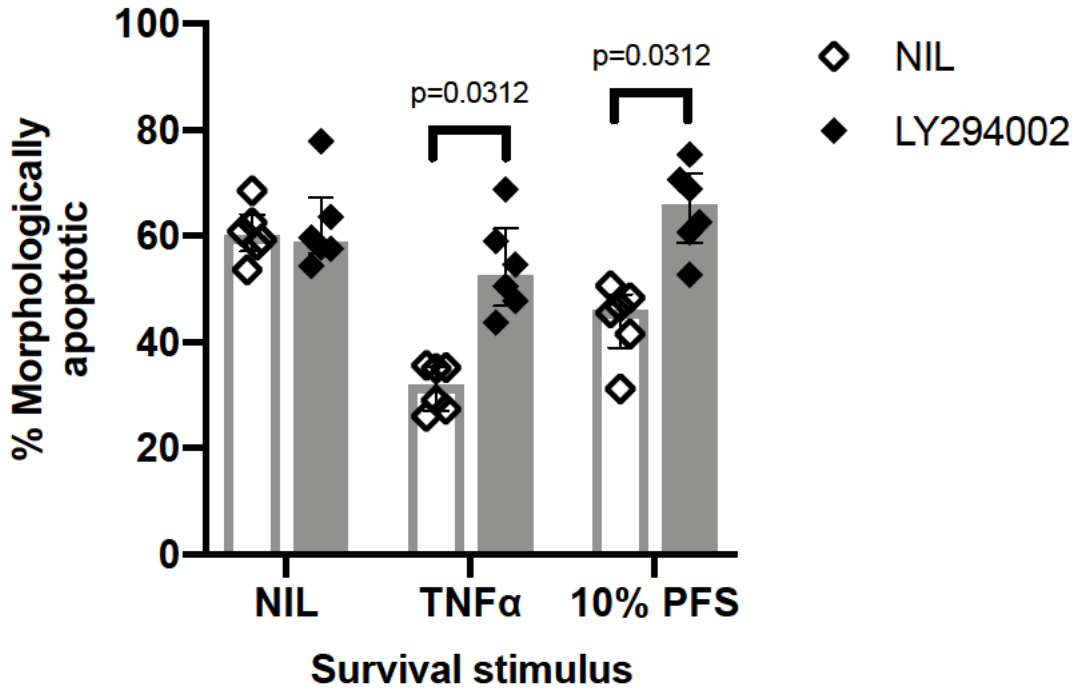

Figure 3.24: The 20-hour pro-survival effect of NSCLC pleural fluid supernatant on healthy donor normal-density neutrophils is reversed by the PI3K inhibitor LY294002. *Apoptosis at 20 hours was measured by cellular morphology in healthy donor normal-density neutrophils cultured in normoxic media with or without recombinant TNFα or alternatively 10% NSCLC pleural fluid supernatant (PFS), and ± the PI3K inhibitor LY294002 (indicated by filled diamonds and bars), n=6. Analysed by Wilcoxon test. Data represents individual values (average of at least two replicates) and median ± IQR.*

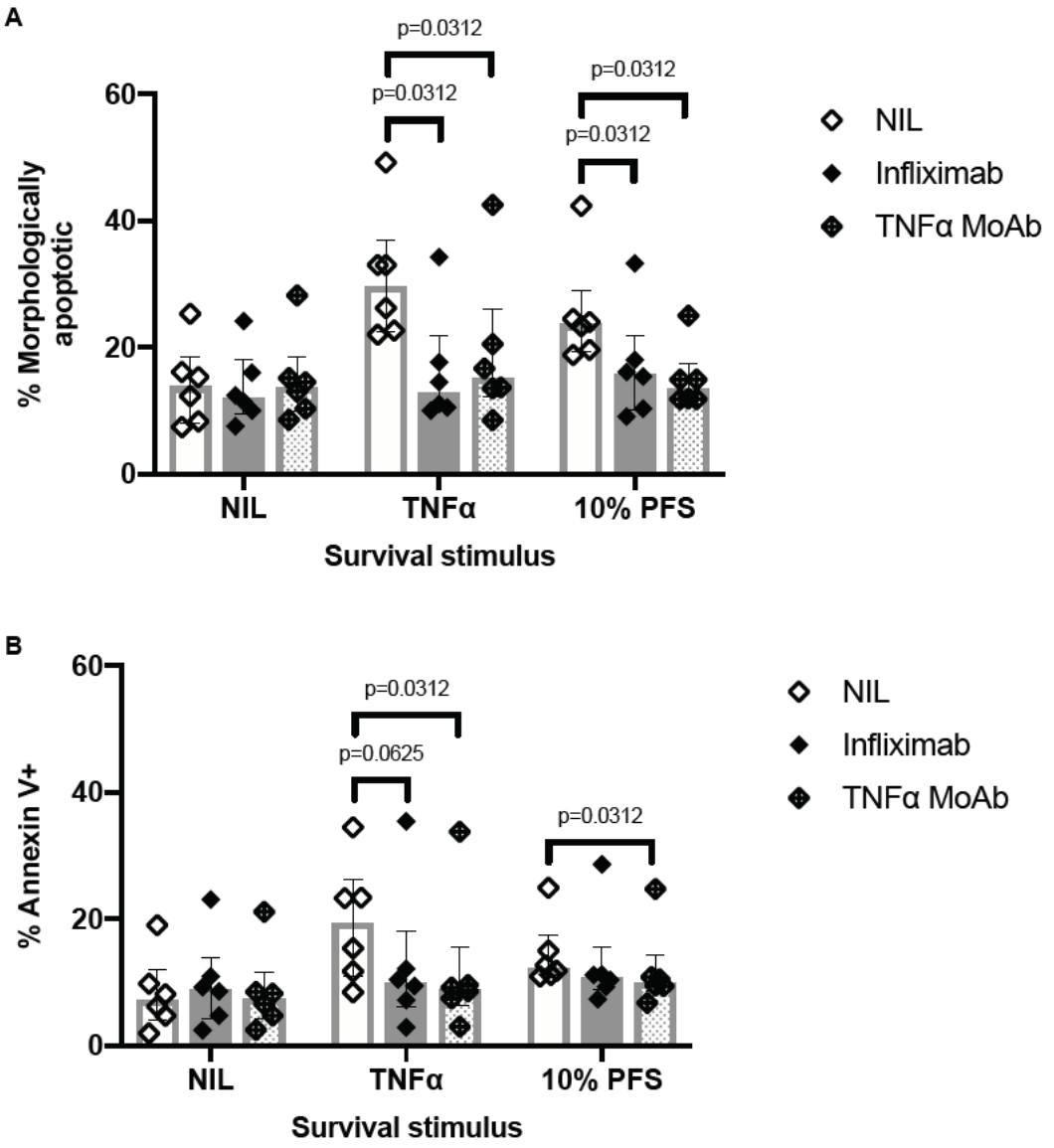

Figure 3.25: The 8-hour pro-apoptotic effect of NSCLC pleural fluid supernatant on healthy donor normal-density neutrophils is reversed by TNFα inhibitors.
Apoptosis at 8 hours was measured in healthy donor normal density neutrophils cultured in normoxic media with or without recombinant TNFα or alternatively 10% NSCLC pleural fluid supernatant (PFS), and ± the TNFα inhibitor Infliximab (indicated by filled diamonds and bars) or alternatively TNFα monoclonal antibody (MoAb) (indicated by crossed diamonds and dotted bars). (A) Measured by cellular morphology, n=6. (B) Measured by flow cytometry, n=6. Analysed by Wilcoxon test. Data represents individual values (average of at least two replicates) and median ± IQR.

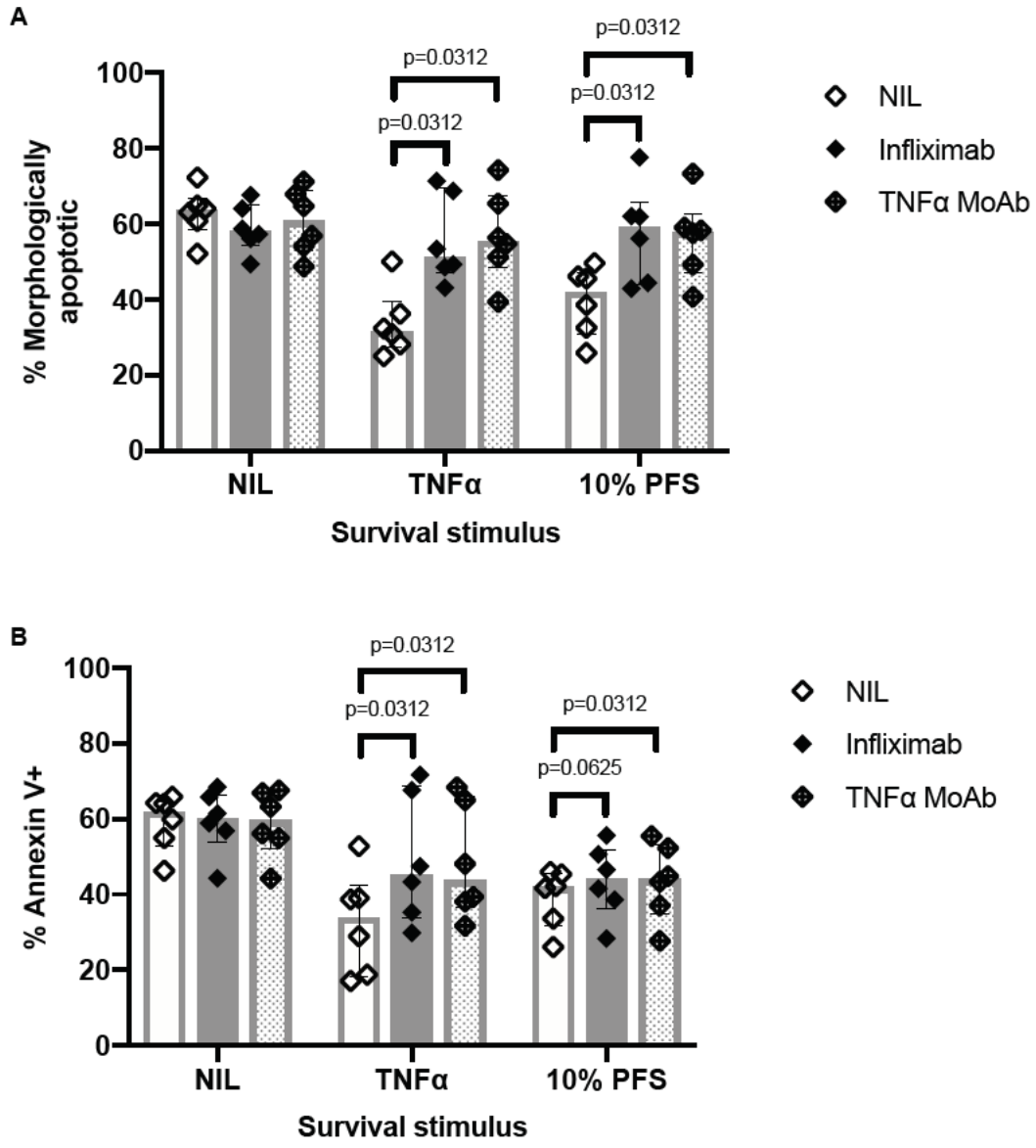

Figure 3.26: The 20-hour pro-survival effect of NSCLC pleural fluid supernatant on healthy donor normal-density neutrophils is reversed by TNFα inhibitors.
Apoptosis at 20 hours was measured in healthy donor normal density neutrophils cultured in normoxic media with or without recombinant TNFα or alternatively 10% NSCLC pleural fluid supernatant (PFS), and ± the TNFα inhibitor Infliximab (indicated by filled diamonds and bars) or alternatively TNFα monoclonal antibody (MoAb) (indicated by crossed diamonds and dotted bars). (A) Measured by cellular morphology, n=6. (B) Measured by flow cytometry, n=6. Analysed by Wilcoxon test. Data represents individual values (average of at least two replicates) and median ± IQR.

3.2.13 TNFα monoclonal antibody does not reverse pleural fluid supernatant-conditioned neutrophil inhibition of CD8$^+$ T cell proliferation

The neutrophil-T cell co-culture experiment described in 3.2.8 was repeated with the presence or absence of TNFα monoclonal antibody (Figure 3.27). TNFα monoclonal antibody did not reverse the suppression of CD8$^+$ T cell proliferation by neutrophils conditioned with pleural fluid supernatant.

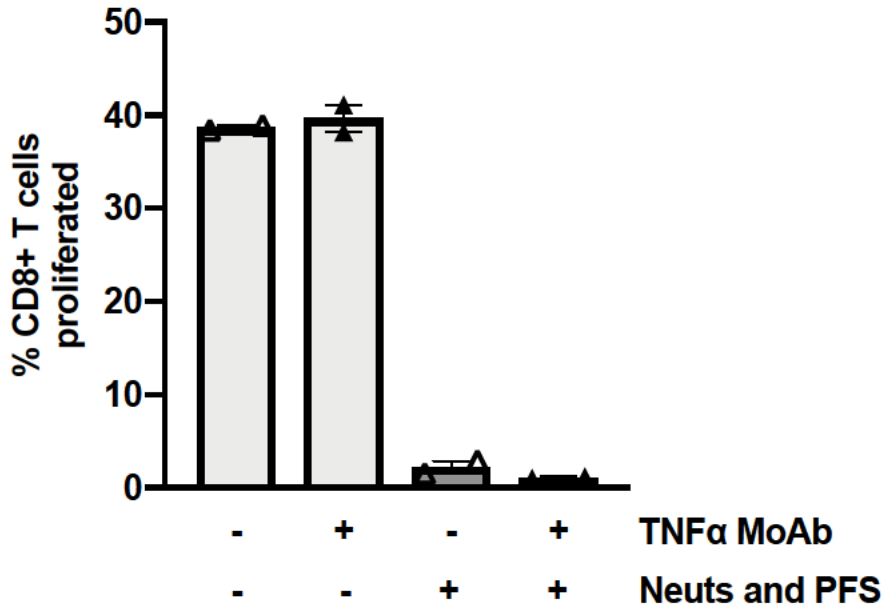

Figure 3.27: TNFα monoclonal antibody does not reverse the suppression of CD8$^+$ T cell proliferation by neutrophils conditioned with pleural fluid supernatant.
CD8 T cell 72-hour proliferation measured in healthy donor cells stimulated with CD3/CD28 Dynabeads™ and cultured with or without heathy donor neutrophils (ratio 1:5) together with 10% NSCLC pleural fluid supernatant (indicated by bar colour fill) ± TNFα monoclonal antibody (1μg/ mL final concentration) (indicated by triangle colour fill), n=2. Analysed by Wilcoxon test. Data represents individual values and median ± IQR.

3.3 Discussion

3.3.1 NSCLC study population

The NSCLC patients recruited to this study were representative of the wider population. They had features that would be expected, such as a significantly raised NLR and extensive smoking history. All patients included in analysis had positive histology for NSCLC. Only 1/3rd of patients received active treatment for their cancer (radiotherapy, chemotherapy or immunotherapy), which is typical for this group. Median survival of 73 days is slightly shorter than the 3 months that is widely anticipated, suggesting that this population may have had slightly more advanced disease.

3.3.2 The metastatic environment impacts upon neutrophil function

The data in this chapter confirms that there are several signals within the NSCLC pleural metastatic environment that influence neutrophil function. Key functions that are altered in this model include pro-survival and immunosuppressive neutrophil phenotypes. Hypoxia is a key driver of neutrophil survival, alongside TNFα signalling. As previously shown by our group, when neutrophils are cultured in hypoxia, removal of glucose from the culture media results in loss of hypoxic survival.[72] This is a result of neutrophil dependency on glycolysis. However, of note, glucose is still available in the NSCLC metastatic site, which could be viewed as a surprising finding, considering the number of cells that would be expected to utilise glucose in this space. It would be interesting to explore in future work if glucose is in fact not being consumed by neutrophils in this setting (in contrast to pneumonia pleural fluid neutrophils), and whether other forms of metabolism e.g. fatty acid oxidation, are being used by neutrophils. Phagocytosis does not seem to be effected in this model of the pleural environment, which could aid anti-tumour responses, however this may not be the best measure of anti-tumour activity, as the mechanism by which neutrophils are most commonly described to be anti-tumour (in early cancers) is through cytotoxicity.[55 121]

3.3.3 TNFα modulates neutrophil apoptosis in advanced NSCLC

TNFα is a well-known modulator of neutrophil apoptosis,[13] with a biphasic response. TNFα is pro-apoptotic at early time points via CD120a (TNFR1) and pro-survival at later time points through CD120b (TNFR2).[95 122] Pro-survival TNFα signalling is via PI3K-Akt-NF-κB and p38-MAPK pathways.[96 123] TNFα is known to be present in early stage human NSCLC tumours,[124] and is also present at metastatic sites (as is shown here in advanced NSCLC). The source of TNFα in NSCLC pleural fluid supernatant has not been established in this body of work; it can be released by multiple cell types including macrophages, T cells, eosinophils and neutrophils. It is therefore likely that there are multiple sources of TNFα in NSCLC pleural fluid supernatant.

Of interest, it has been shown previously that chronic production of TNFα in the tumour microenvironment increases neutrophil recruitment, through IL-17 production by CD4+ T cells,[125] $CD8^+$ T cells can increase neutrophil survival *in vitro* via release of TNFα,[126] and there is evidence that the TNFα p38-MAPK axis is important for neutrophil survival in head and neck cancers.[127]

However, the data in this chapter provides novel insights into the role TNFα may be playing in sustaining neutrophilic inflammation at the NSCLC pleural metastatic site, with evidence derived by utilising NSCLC patient tissue, rather than cell lines or animal models. The data shows that NSCLC pleural fluid supernatant makes neutrophils pro-survival and the response is proportional to the quantity of TNFα within the pleural fluid supernatant. Additionally, neutrophil surface expression of TNFα receptors is altered following exposure to pleural fluid supernatant. Finally, the pleural fluid supernatant- induced survival phenotype is reversed by TNFα pathway inhibitors.

The data in this chapter also shows that NSCLC pleural fluid supernatant conditions neutrophils to inhibit $CD8^+$ T cells via PD-L1. PD1/PD-L1 immune checkpoint inhibitors are used clinically to treat NSCLC; but this is based upon the fact that tumour cells have been shown to express PD-L1. Whilst it has been previously shown that neutrophils can be conditioned to express PD-L1 in human studies of gastric cancer[43 107] and ovarian malignant ascites,[108] this has never been shown

before in lung cancer. Of note, one study has demonstrated TNFα to induce neutrophil PD-L1 expression,[128] however in this chapter when a TNFα inhibitor was used, the suppression of $CD8^+$ T cell proliferation by neutrophils conditioned with pleural fluid supernatant was not reversed, suggesting that this is not a key mechanism here (although the expression of PD-L1 on neutrophils conditioned with pleural fluid supernatant in the presence of TNFα inhibitor was not measured, and could form a future experiment). The fact that a PD-L1 inhibitor did not completely reverse the phenotype either, raises the question of other mechanisms being involved in T cell suppression. Neutrophils have been described to inhibit T cells in many other ways, for example through release of proteases, reactive oxygen species and arginase.[40 129]

The wider implications of the biphasic neutrophil apoptosis response in this setting requires further interrogation. For instance, it is not known whether TNFα is selecting out particular neutrophil populations for survival. For example, do older neutrophils undergo apoptosis in response to TNFα at the early time-point and younger neutrophils become pro-survival?

The next question, is whether TNFα could be used as a therapeutic target. This is a complex issue, as TNFα-related neutrophil behaviour is context dependent.[17] For example, in favour of TNFα inhibition would be evidence that tumour associated neutrophils induce T cell apoptosis via TNFα,[42] and that transmembrane TNFα (precursor of the soluble form) promotes suppressive activities of MDSCs through CD120b.[130] However in contrast to this, we also know that TNFα can induce tumour apoptosis,[31] and mediates neutrophil cytotoxicity in breast cancer.[131] Furthermore, in the context of malignant pleural effusion, the injection of intrapleural recombinant TNF may in fact be beneficial.[132] Therefore more research is needed.

3.3.4 There are differences in the pleural environment in NSCLC compared with pneumonia

The data in this chapter demonstrates that the NSCLC pleural environment differs significantly from that of pneumonia. Neutrophils do not gain a survival benefit following exposure to pneumonia pleural fluid supernatant, indicating that this phenotype is NSCLC specific. The human cytokine array and ELISA data suggest that the NSCLC environment, in contrast to pneumonia, would favour a phenotype of sustained and immunosuppressive inflammation. If this phenotype were to prevail, it would lead to an ineffective response in the face of progressing NSCLC metastasis. TGFβ has commonly been noted to be raised in cancer microenvironments, and of note, in addition to its likely polarising effect upon neutrophils in NSCLC pleural fluid, it has previously been observed that TGFβ derived from macrophages impairs T cells in malignant pleural effusion.[133]

Reassuringly, many of the differences in cytokine profile seen between NSCLC pleural fluid supernatant and pneumonia pleural fluid supernatant fit with previous data. For example IL-8[134] and MMP-9[135] have previously been shown to be lower in malignant pleural effusions when compared with effusions secondary to infection. One striking difference on first inspection, when comparing the cytokine data shown in this chapter with previous data, is that many research groups have found TNFα to be lower in malignant pleural effusion than it is in effusions secondary to infection.[136-139] This contradictory finding can however be explained by the case mix of patients in these other studies; they use pleural effusions from patients infected with tuberculosis. Tuberculosis is a chronic infection, with a very different immune profile and disease course, when compared with a standard bacterial pneumonia with parapneumonic effusion. In this study, tuberculous pleural effusions were excluded. It must be noted, that the previous studies were also looking for cytokine profiles that might distinguish tuberculous pleural effusions in particular, as they can be hard to confirm diagnostically.

3.3.5 Summary

In summary, this chapter provides evidence that the NSCLC pleural environment conditions neutrophils into a state of persistent counterproductive inflammation (Figure 3.28). This is likely to permit cancer progression. TNFα and hypoxia act as pro-survival signals leading to neutrophil persistence. NSCLC pleural fluid conditions neutrophils to suppress $CD8^+$ T cells through mechanisms that include PD-L1 expression. Finally, the cytokine profile of the NSCLC environment differs significantly from that seen in pneumonia, and this leads to differences in neutrophil function e.g. apoptosis.

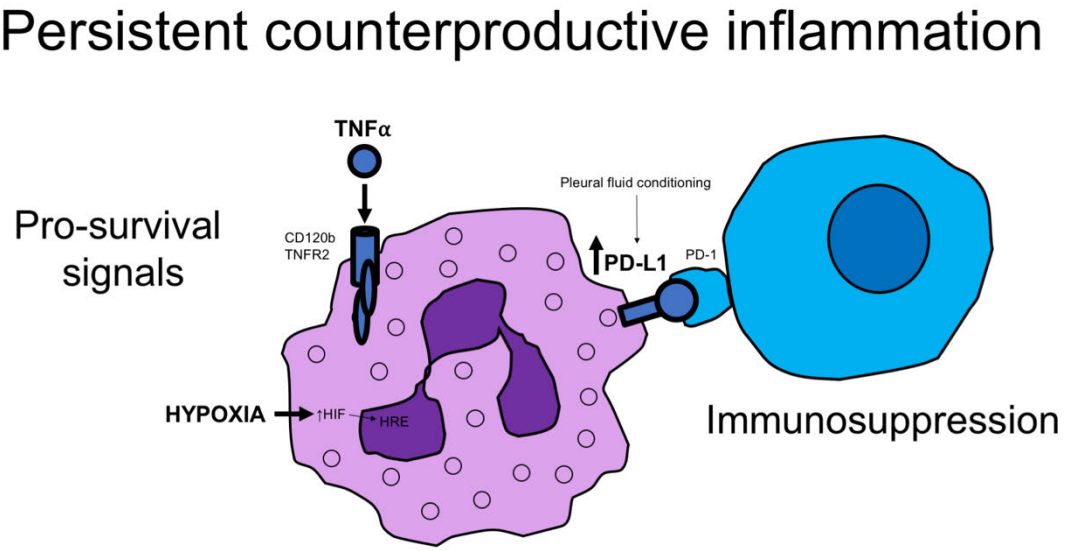

Figure 3.28: The NSCLC pleural environment conditions neutrophils into a state of persistent counterproductive inflammation.
Summary of findings from this chapter. TNFα and hypoxia act as pro-survival signals leading to neutrophil persistence. NSCLC pleural fluid conditions neutrophils to suppress CD8 T cells through mechanisms that include PD-L1 expression.

Chapter 4 There are cancer-specific neutrophil populations in advanced NSCLC

4.1 Introduction

Appropriate neutrophil responses are dependent upon a functioning balance of neutrophil production, release from the bone marrow, recruitment to sites of need, activation and appropriate action at target sites, and effective clearance afterward. Whilst neutrophils have been described to have anti-tumour function at the primary site in cancer, it appears they are detrimental at sites of metastasis. It is likely that dysregulation of the neutrophil homeostatic processes described above, contributes to cancer progression and worse outcome,[17] however the mechanisms are not fully known.

4.1.1 Immature neutrophil populations in cancer (dysregulation of bone marrow release/ recruitment)

During times of acute inflammation e.g. infection, there is 'left shift' in the blood neutrophil population, with release of immature non-dividing cells into the circulation.[4] Neutrophils are mobilised from the bone marrow by signals including granulocyte colony-stimulating factor, as part of the normal physiological response, and in this context usually have appropriate function, leading to timely resolution of the insult. In cancer, neutrophil recruitment signals become chronic, and the proportion of immature neutrophils in the circulation increases. These neutrophils are low-density and accumulate into a separate layer when blood is processed using a density gradient. Low-density immature blood neutrophils have nuclear morphology in keeping with the banded neutrophil stage of development, are long-lived, and immunosuppressive. They are likely to be the same cell population as granulocytic myeloid-derived suppressor cells that have been described elsewhere. Mature low-density blood neutrophils are also found in cancer, the exact role of which needs to be further explored. Increasing proportions of the pro-tumour low-density immature neutrophil population as cancers progress, will contribute to disease progression[58 59]

However, whilst there are many descriptions of low-density blood neutrophils in human cancers and animal models, there is a lack of data regarding how they relate to neutrophil populations found at the primary and metastatic cancer sites. The failure to identify distinguishing cell surface makers is often the given reason.

4.1.2 Flow cytometry neutrophil markers in cancer

As outlined above, distinguishing cell surface markers for immature low-density blood neutrophils/ granulocytic myeloid-derived suppressor cells are poorly defined. As these are considered to be immature cells recruited from the bone marrow, it is useful to consider granulopoiesis. Changes in surface markers during neutrophil development are outlined in Table 4.1 (created using data from two papers[2 140]). Useful markers of neutrophil maturity in mouse and man have also been recently well summarised by Mackey et al. and Hidalgo et al.[2 63]

Of note, low levels of CD10 or CD16 are usually used to identify immature neutrophils in humans, and have been used to distinguish between mature and immature low-density blood neutrophils.[62] CD66b and CD15 are typically used as neutrophil-specific markers, with some noting low-density blood neutrophils to have higher CD66b than normal-density blood neutrophils from the same patients.[58] CD14 is universally used to exclude monocytic cells. CD33 has been used previously for myeloid-derived suppressor cells, but does not distinguish them from neutrophils.[64]

In terms of markers not mentioned in Table 4.1, shedding of CD62L is a marker of neutrophil activation and immature low-density blood neutrophils have been described as $CD62L^{-}$.[2]

Progressive stages of development (left to right)	Granulocyte macrophage progenitor	Promyelocyte	Myelocyte	Metamyelocyte	Banded neutrophil	Mature neutrophil
	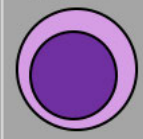	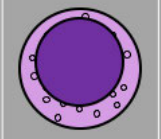		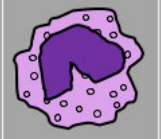	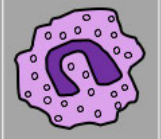	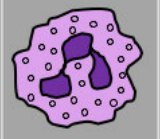
Dividing cell	Yes	Yes	Yes	No	No	No
CD66b	-	+++	+++	++	++	++
CD11b	-	-	++	++	++	++
CD15	-	+++	+++	+++	+++	+++
CD14	-	-	-	-	-	-
CD10	-	-	-	-	-	++
CD16	-	-	-	+	++	+++
CD33	+++	+++	++	+	+	+

Table 4.1: Changes in surface marker expression during neutrophil development. *CD66b and CD15 are typically used as neutrophil-specific markers. Levels of CD10 or CD16 are used to identify immature neutrophils. CD14 is used to identify monocytic cells. CD33 has been used previously to identify myeloid-derived suppressor cells (created using data from two papers[2,140]).*

4.1.3 Lectin-type oxidised low-density lipoprotein receptor 1 (LOX-1): a new marker

Lectin-type oxidised low-density lipoprotein receptor 1 (LOX-1) is proving to be a useful marker of immature low-density blood neutrophils/ granulocytic myeloid-derived suppressor cells. LOX-1 is a 50kDa transmembrane glycoprotein encoded by the OLR1 gene. It binds oxidised low-density lipoprotein. Expression is thought to be upregulated on the surface of immature low-density blood neutrophils/ granulocytic myeloid-derived suppressor cells by endoplasmic reticulum stress, and is associated with immunosuppressive activity of these cells.[65] Uptake of lipoproteins could also provide the fuel source for fatty acid oxidation, which has been observed to be an important energy source for granulocytic myeloid-derived suppressor cells.[78] Indeed low-density neutrophils may be low-density due to lipoprotein content.

4.1.4 Neutrophil persistence in cancer

It has been established for a long time that circulating neutrophils in patients with cancer have a long half-life (i.e. persist).[141] This may be of key importance, as ineffective neutrophil clearance at the target site may lead to prolonged and detrimental inflammation, resulting in worse outcome.[142] Many mechanisms can contribute to neutrophil apoptosis/death and clearance, and are described in the main introduction of this thesis. Neutrophil survival may be a result of extrinsic microenvironmental signals,[13] but could also be a product of intrinsic programming. This has not been fully unpicked in cancer, nor have the apoptosis phenotypes of different neutrophil populations/ subpopulations been fully described in cancer.

4.1.5 Neutrophil function at metastatic sites (dysfunctional action at target sites)

The understanding of neutrophil function at metastatic sites has improved greatly, but limitations to the data do remain. In terms of human studies, it is very difficult to obtain tissue from metastatic sites, as often it is not appropriate ethically. Therefore, most papers, alike the first results chapter of this thesis, have used circulating neutrophils, emulating the tumour/ metastatic site by culturing these cells with cytokines, or tumour-conditioned media.[43 107 108 128] Whilst this has provided useful insights, attributing the functional outcomes of these cells to what happens at the metastatic site, must be done with caution. In rare cases where metastatic tumour has been obtained from patients e.g. lung metastases from breast cancer,[143] studies of the whole tissue e.g. immunohistochemistry, tend to have been carried out. Whilst neutrophils have been extracted from primary human tumours for closer study,[46 47] this has not been done to date with metastatic tissue in humans. Mouse models have provided further insights. Indeed, the concept of neutrophils being important to metastasis has been proven by experiments where neutrophil recruitment was blocked or neutrophils were depleted.[54 82] Of note, the predominant model used has been lung metastasis in breast cancer (4T1/ KEP). The 4T1 mammary carcinoma is a transplantable tumour cell line that is highly invasive and spontaneously metastasises to the mouse lung. The 4T1 model has shown immature neutrophils to be important in angiogenesis at the metastatic site and to supress interferon gamma.[144] Building upon this work, type I interferon knock-out mice were shown to develop worse lung metastases.[145] Furthermore, 4T1 breast cancer cells induce neutrophils to release neutrophil extracellular traps that promote metastasis.[143] The KEP breast cancer model (a conditional model of invasive lobular breast cancer, K14cre;$Cdh1^{F/F}$;$Trp53^{F/F}$) was used to find that tumour produces Interleukin-1β, that stimulates pro-tumour $\gamma\delta$ T cells to express interleukin-17, leading to granulocyte colony-stimulating factor-dependent expansion and polarisation of immature neutrophils, that supress CD8 T cells via inducible nitric oxide synthase, permitting metastasis in the lung.[146] Nonetheless, as in human studies, many of these animal studies use circulating or bone marrow neutrophils, rather than neutrophils from the metastatic site. Studies that extract neutrophils from metastatic tissue in animals are more infrequent, for example Wang et al. showed immature neutrophils from the pre-metastatic liver in a metastatic colorectal cancer model, stimulated tumour cell survival.[147]

4.1.6 Summary

Whilst neutrophils have been phenotyped in several metastatic animal models, human data is limited. Studying neutrophils from the blood and pleural fluid (metastatic site) in advanced NSCLC, should provide novel insights into how the populations correlate across compartments, and their features. Comparing the populations to those found in pneumonia, will identify characteristics that are cancer-specific, and that may have implications for disease outcome. Immature neutrophil populations are of key interest, and the markers CD66b, CD11b, CD15, CD10, CD62L and LOX-1^{+} may be of help in defining them further. To date, the balance of the cell-extrinsic and intrinsic drivers of neutrophil survival in cancer, have not been delineated.

4.1.7 Hypotheses

I hypothesised that there would be an expanded population of low-density immature blood neutrophils in advanced NSCLC, that would have an immunosuppressive phenotype. I further hypothesised that these low-density neutrophils would have distinct morphological appearances and expression of surface markers. Additionally, I hypothesised that there would be evidence for these neutrophils migrating into the pleural space, and that the neutrophil populations identified in NSCLC would have phenotypical differences from those found in other conditions e.g. pneumonia.

4.1.8 Aims

To identify and define the neutrophil populations present in the blood and pleural fluid of NSCLC patients; in terms of density, morphological appearances and flow cytometry surface marker expression. To find evidence that these NSCLC neutrophil populations are functionally distinct, with implications for disease outcome. To extract neutrophils from the pleural metastatic site for study.

4.2 Results

4.2.1 Terminology used for neutrophil populations

In this chapter, several neutrophil populations are described. The methods chapter of this thesis describes in full detail how each was harvested from samples. However, to aid interpretation of the results that follow, a brief overview is given below:

Whole blood neutrophils (WBN) are blood neutrophils of all densities (not separated), and were obtained using EasySep™ kits.

Normal-density neutrophils (NDN) are blood neutrophils, defined by the layer in which they resided following a discontinuous Percoll™ density gradient separation.

Low-density neutrophils (LDN) are blood neutrophils, defined by the layer in which they resided following a discontinuous Percoll™ density gradient separation.

Pleural fluid neutrophils (PFN) are neutrophils that were found in the pleural fluid, and when extracted, this was by fluorescence-activated cell sorting.

Healthy donor neutrophils (HD) refers to blood neutrophils from healthy donors, harvested by matching method (EasySep™ kit and/or density gradient)

4.2.2 Neutrophils are present in NSCLC pleural fluid

To confirm that neutrophils were indeed present in NSCLC pleural fluid, cytospins of unprocessed pleural fluid were made (Figure 4.1A). Neutrophils were then identified by their typical morphology, with multi-lobed nuclei. Neutrophils were then quantified from pleural fluid by flow cytometry using cell markers $CD66b^{+}CD11b^{+}CD15^{+}CD14^{-}CD49d^{-}$ and found to form 9% (mean) of pleural fluid leukocytes (Figure 4.1B).

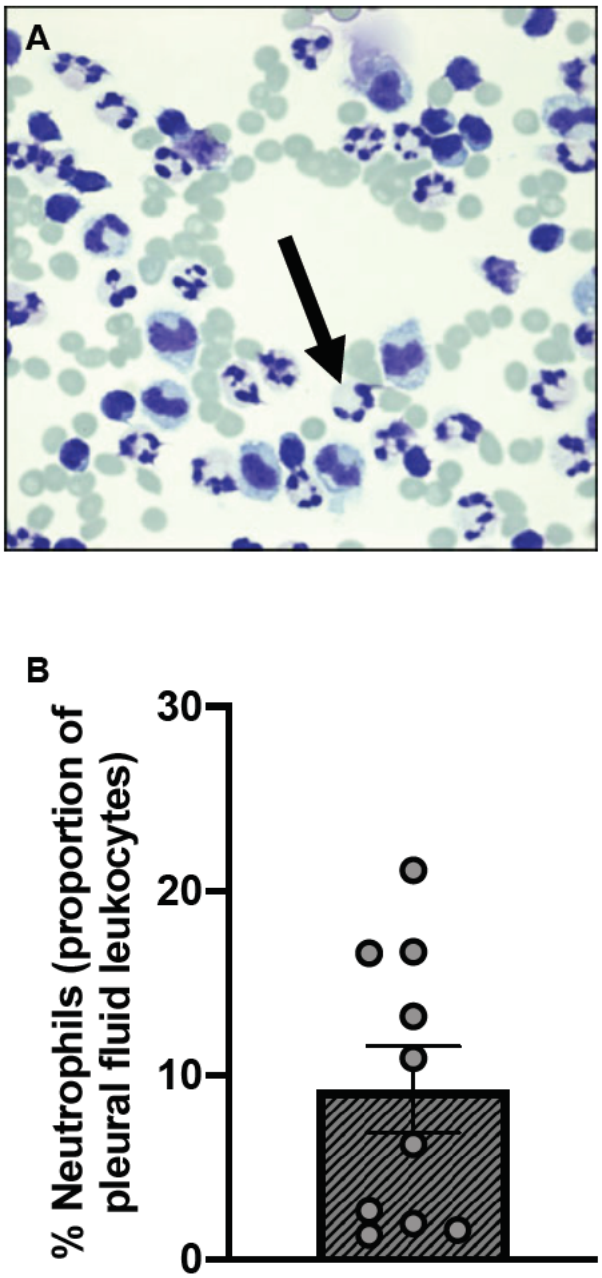

Figure 4.1: Neutrophils are present in NSCLC pleural fluid, forming 9% of pleural fluid leukocytes.
(A) Representative cytospin of unprocessed NSCLC pleural fluid, example neutrophil indicated with an arrow (40X magnification). (B) The proportion of neutrophils in NSCLC pleural fluid quantified by flow cytometry, n=10. Data represents individual values and mean ± SEM (passed D'Agostino and Pearson normality test).

4.2.3 There is an expanded population of low-density blood neutrophils in advanced NSCLC, that migrate into NSCLC pleural fluid

In order to address whether an expanded population of low-density blood neutrophils was indeed present in NSCLC, blood leukocytes from NSCLC patients and healthy donors were each separated by discontinuous Percoll™ density gradient into normal-density neutrophil and peripheral blood mononuclear cell (low-density) layers. Low-density neutrophils were identified in the peripheral blood mononuclear cell layer by flow cytometry using cell markers $CD66b^{+}CD11b^{+}CD15^{+}CD14^{-}CD49d^{-}$ and the quantity expressed as a percentage of the total layer (Figure 4.2). In health neutrophils formed <2% of cells, whereas in NSCLC neutrophils formed 11% (mean), p=0.0067.

Next, the morphology of NSCLC low-density blood neutrophils was examined. NSCLC whole blood neutrophils were separated by discontinuous Percoll™ density gradient into normal-density and low-density neutrophils and cytospins made. When examining the morphological appearance of low-density neutrophils, the population was seen to consist a mixture of both immature banded and mature segmented cells (Figure 4.3A). In contrast, normal-density neutrophils were all mature in appearance. In addition, the magnitude of the low-density neutrophil population as a proportion of total neutrophils within the blood was determined by counting the number of neutrophils in the low-density layer (Neubauer haemocytometer) and dividing this by the sum of the number of neutrophils in the low- and normal-density layers. Low-density neutrophils were found to form 9% (mean) of NSCLC whole blood neutrophils (Figure 4.3B).

The cytospin morphology of NSCLC low-density blood neutrophils (Figure 4.4A) was compared with matched pleural fluid leukocytes (Figure 4.4B) to see if similar immature banded-nuclei neutrophils could be seen in both. This was indeed the case, providing some evidence that NSCLC low-density blood neutrophils migrate into NSCLC pleural fluid.

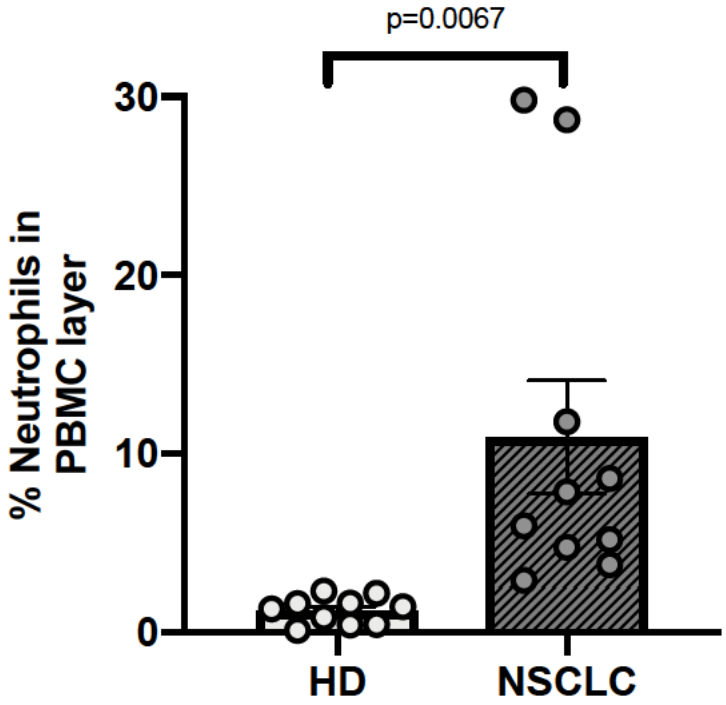

Figure 4.2: Low-density blood neutrophils are scarce in health, but form an expanded population in NSCLC.
The proportion of neutrophils in the peripheral blood mononuclear cell (low-density) layer of blood in healthy donors (HD) and NSCLC patients, quantified by flow cytometry, n=10. Analysed by unpaired t-test (passed D'Agostino and Pearson normality test). Data represents individual values and mean ± SEM.

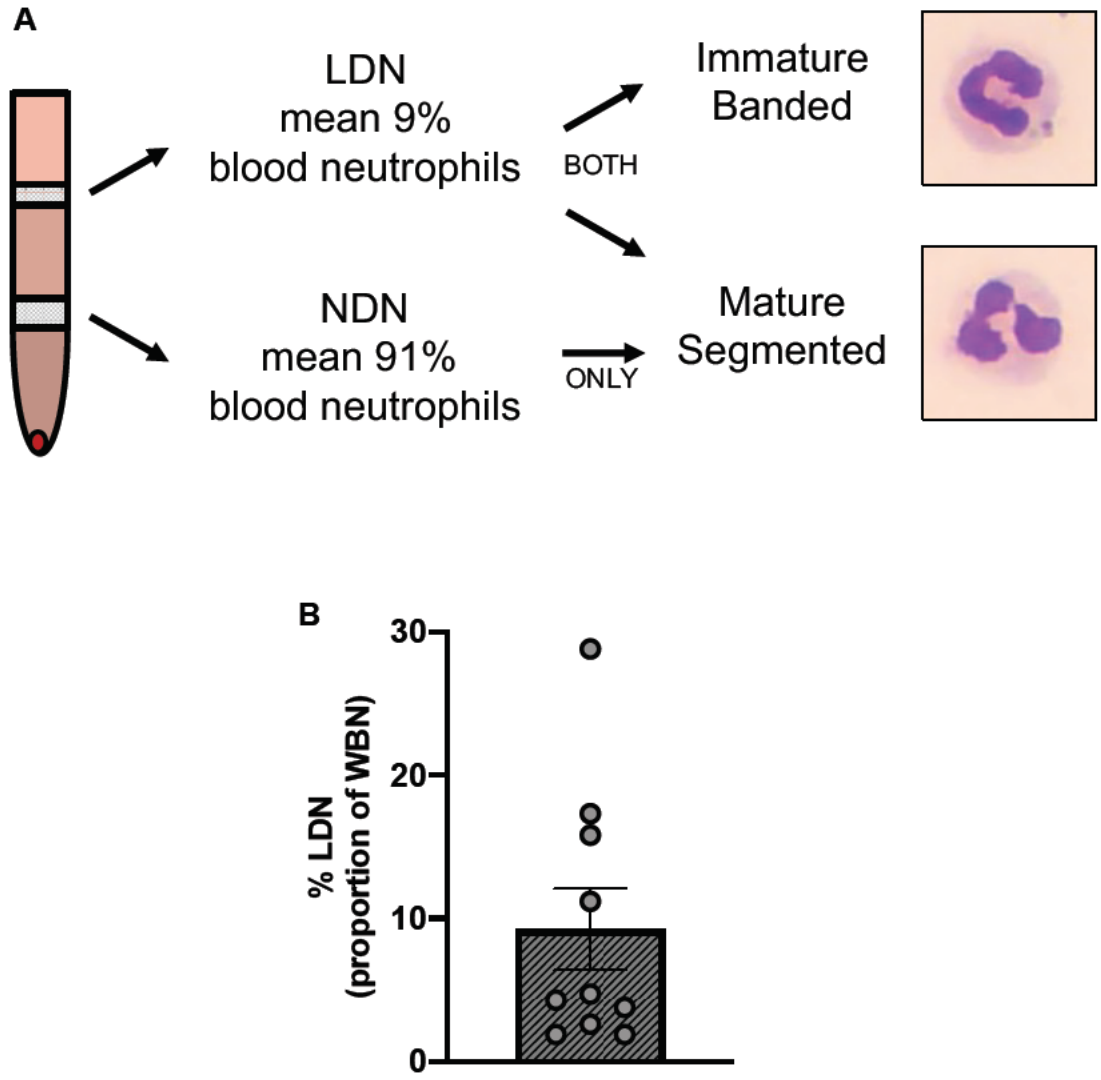

Figure 4.3: NSCLC blood neutrophils and have mixed morphology and low-density neutrophils form 9% of the whole blood neutrophil population.
(A) Morphology of NSCLC blood neutrophils with regard to density. (B) Low-density neutrophils as a proportion of the total NSCLC whole blood neutrophil population, n=10. Data represents individual values and mean ± SEM (passed D'Agostino and Pearson normality test). LDN, low-density neutrophils; NDN, normal-density neutrophils.

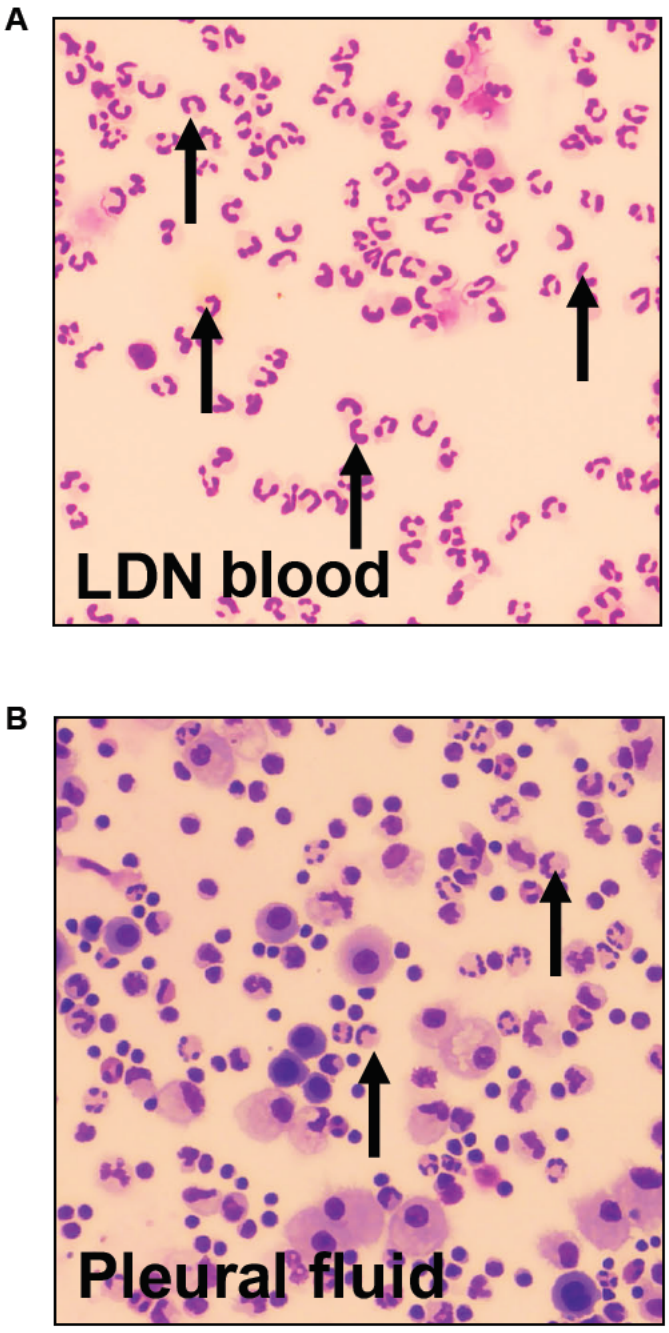

Figure 4.4: Immature neutrophils with banded nuclei form a subpopulation of both the NSCLC low-density blood neutrophil and NSCLC pleural fluid leukocyte populations. *Cytospins (40X magnification) of NSCLC low-density blood neutrophils (LDN) (A) and NSCLC pleural fluid leukocytes (B). Examples of immature neutrophils with banded nuclei are indicated with arrows.*

4.2.4 Flow cytometry further defines a CD66b^{high} neutrophil subpopulation in NSCLC

To investigate whether NSCLC neutrophil populations could be further defined by surface marker expression, healthy donor blood neutrophils (HD) were compared with NSCLC normal-density blood neutrophils (NDN), NSCLC low-density blood neutrophils (LDN) and NSCLC pleural fluid neutrophils (PFN) by flow cytometry.

A CD66b^{high}CD11b^{+}CD15^{+}CD14^{-}CD49d^{-} neutrophil subpopulation was identified by flow cytometry (for gating strategy, see Methods Figure 2.12), forming 13% (mean) of the NSCLC LDN population. It was also detected in the NSCLC PFN population, but was negligible in NSCLC NDN and HD (Figure 4.5A-D).

The CD66b^{high}CD11b^{+}CD15^{+}CD14^{-}CD49d^{-} NSCLC LDN subpopulation was further examined by flow cytometry to see if there were any other surface markers that phenotypically distinguished it from the rest of the NSCLC LDN population (CD66b^{+}CD11b^{high}CD15^{+}CD14^{-}CD49d^{-} neutrophils). Expression of the maturity marker CD10 was lower in CD66^{high} neutrophils than CD66b^{+} indicating that they are more immature (Figure 4.6A and B), p=0.0039. The activation marker CD62L was lower in CD66^{high} neutrophils than CD66b^{+} indicating that they are more activated (Figure 4.6C and D), p<0.0001. Finally, CD66^{high} neutrophils were also positive for the G-MDSC marker LOX-1 (Figure 4.6E and F).

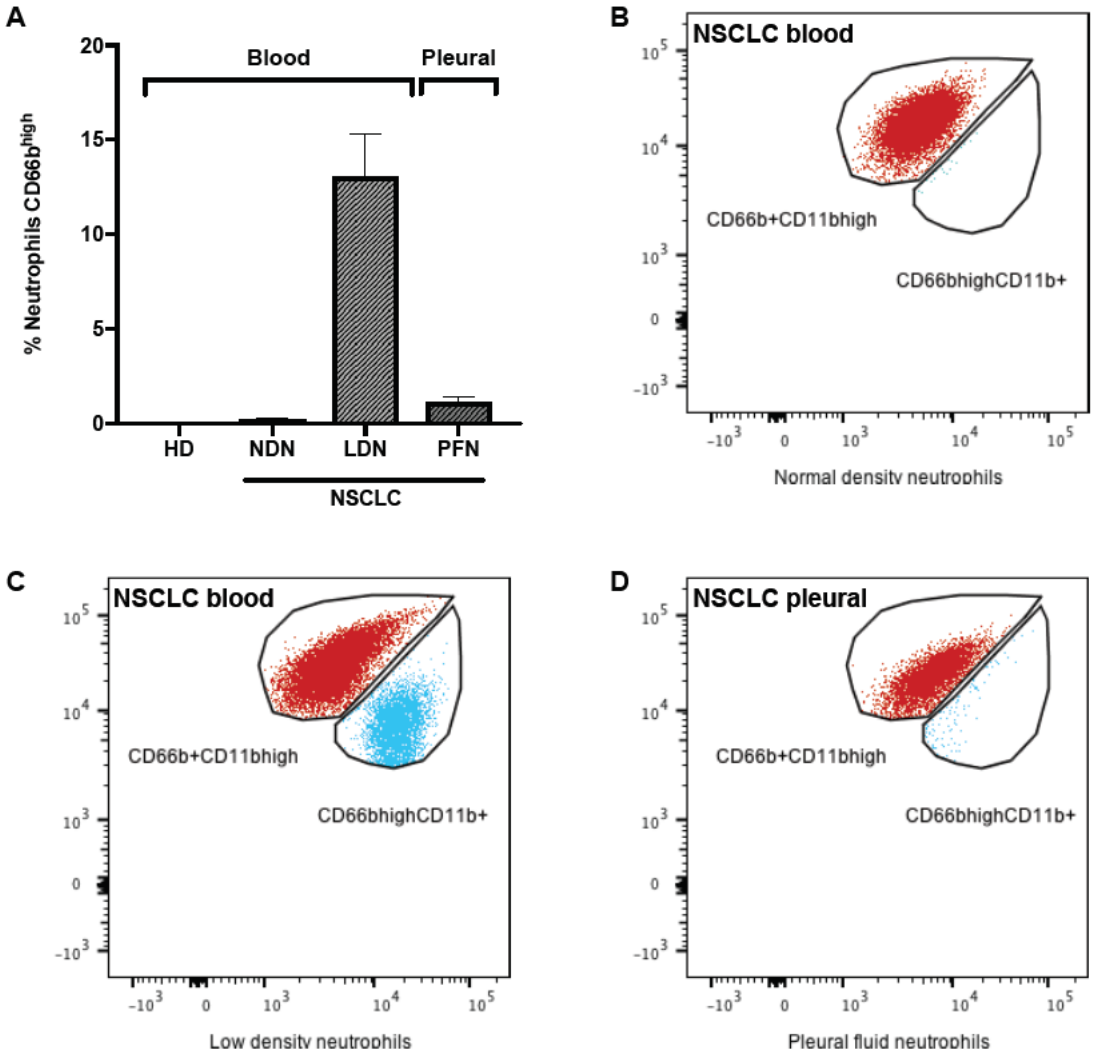

Figure 4.5: NSCLC low-density blood neutrophils and NSCLC pleural fluid neutrophils have a CD66^{high} subpopulation that is not present in NSCLC normal-density blood neutrophils nor healthy donor blood neutrophils.
(A) Number of CD66b^{high}CD11b CD15 CD14^{-}CD49d^{-} neutrophils as a proportion of each neutrophil population, n=9. (B-D) Representative flow cytometry dot plots, illustrating the quantity of CD66b^{high} neutrophils (blue) in each NSCLC neutrophil population. Data represents mean ± SEM (passed D'Agostino and Pearson normality test). HD, healthy donor neutrophils; NDN, normal-density neutrophils; LDN, low-density neutrophils; PFN, pleural fluid neutrophils. For gating strategy, see Methods Figure 2.12.

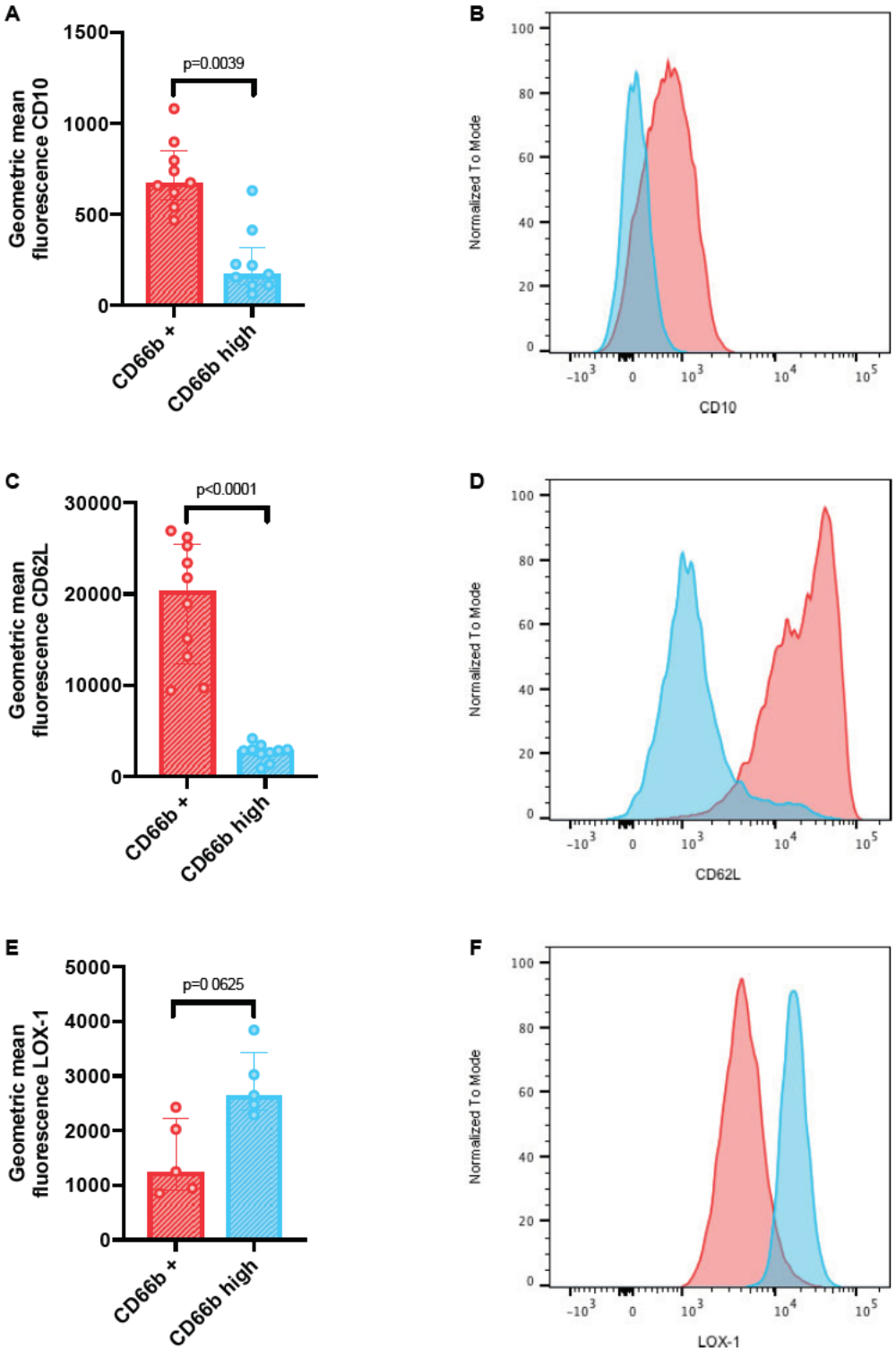

Figure 4.6: CD66^{high} NSCLC low-density blood neutrophils are immature, activated and positive for G-MDSC marker LOX-1.
Relative expression of surface markers by flow cytometry, in CD66^{high} versus CD66 NSCLC low-density blood neutrophils. (A) CD10, n=9. (B) Representative CD10 histogram. (C) CD62L, n=10. (D) Representative CD62L histogram. (E) LOX-1, n=5. (F) Representative LOX-1 histogram. Analysed by Wilcoxon test (A and E) or paired t-test (C) (passed D'Agostino and Pearson normality test). Data represents individual values and median ± IQR (A and E) or mean ± SEM (C).

4.2.5 Neutrophil populations in pneumonia differ from NSCLC

In order to interrogate whether the neutrophil populations found in NSCLC were unique to this disease state, the same set of phenotyping experiments was repeated with blood and pleural fluid neutrophils from patients with pneumonia.

The proportion of neutrophils in the peripheral blood mononuclear cell (PBMC) (low-density) layer of pneumonia patient blood was quantified by flow cytometry, again using cell markers $CD66b^{+}CD11b^{+}CD15^{+}CD14^{-}CD49d^{-}$, and was revealed to be 12% (Figure 4.7A). Whilst this was similar to that found in NSCLC (Figure 4.2), when the quantity of pneumonia low-density blood neutrophils was calculated as a proportion of pneumonia total blood neutrophils (Figure 4.7B), it was calculated to be 3%, which was $1/3^{rd}$ of that seen in NSCLC (Figure 4.3B).

The proportion of neutrophils in pneumonia pleural fluid was quantified by flow cytometry using the same cell markers. This was found to be 68% of pneumonia pleural fluid leukocytes (Figure 4.7C), around seven and a half times greater than observed in NSCLC (Figure 4.1B).

Measured by flow cytometry, a $CD66b^{high}CD11b^{+}CD15^{+}CD14^{-}CD49d^{-}$ subpopulation was present in pneumonia low-density blood neutrophils (Figure 4.7D). This subpopulation was not seen in the normal-density blood neutrophil population, in a similar manner to the observations in NSCLC (Figure 4.5A). However, in contrast to NSCLC, the $CD66b^{high}$ subpopulation was not detected in the pneumonia pleural fluid neutrophil population.

Lastly, when the $CD66b^{high}$ and $CD66b^{+}$ pneumonia low-density blood neutrophil subpopulations were further interrogated for expression of surface markers CD10 (Figure 4.7E) and CD62L (Figure 4.7F), the data indicated that the $CD66b^{high}$ neutrophils were immature (CD10 low) and activated (CD62L low). This was similar to what was seen in NSCLC (Figure 4.6A and C).

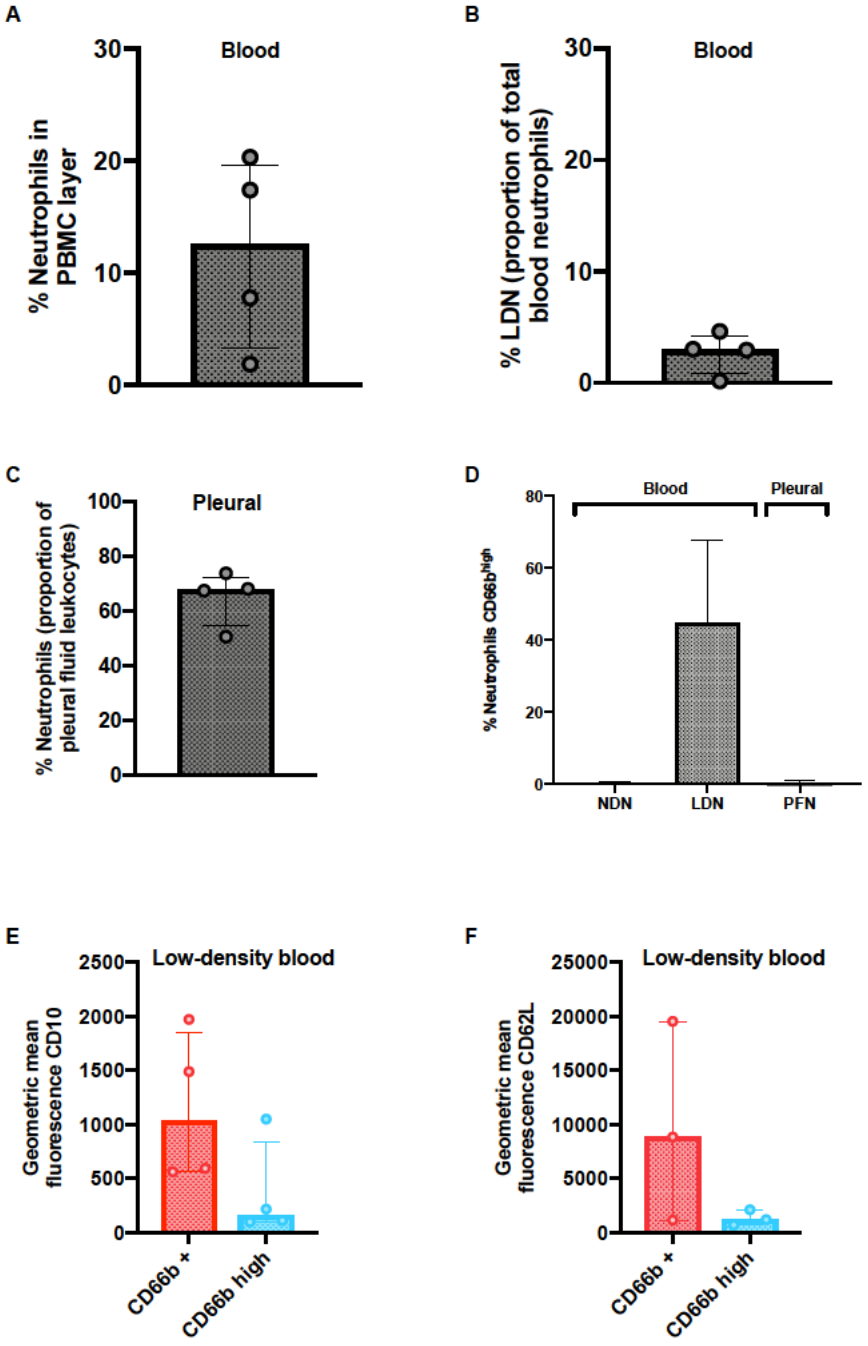

Figure 4.7: Quantification and flow cytometry features of neutrophil populations in pneumonia.

(A) Proportion of neutrophils in the low-density layer of blood (PBMC layer) in pneumonia patients, n=4. (B) Quantity of pneumonia low-density blood neutrophils calculated as a proportion of pneumonia total blood neutrophils, n=4. (C) Proportion of neutrophils in pneumonia pleural fluid, n=4. (D) Number of CD66b^{high}CD11b^{+} CD15^{+} CD14^{-}CD49d^{-} neutrophils as a proportion of each pneumonia neutrophil population, n=4. (E and F) Relative expression of surface markers by flow cytometry, in CD66^{high} versus CD66^{+} pneumonia low-density blood neutrophils. (E) CD10, n=4. (F) CD62L, n=3. Data represents individual values and median ± IQR. NDN, normal-density neutrophils; LDN, low-density neutrophils; PFN, pleural fluid neutrophils.

4.2.6 NSCLC and pneumonia whole blood neutrophils have different apoptosis phenotypes

Apoptosis was used as a functional readout by which to examine neutrophils from NSCLC and pneumonia. Whole blood neutrophils were extracted from NSCLC patients, pneumonia patients and healthy donors (HD). These neutrophils were then cultured *in vitro* for 20 hours, and apoptosis measured by cellular morphology (identified by pyknotic nuclei) or alternatively flow cytometry (positive Annexin V staining).

Measured by flow cytometry, NSCLC whole blood neutrophils were pro-survival when compared with HD at 20 hours (median 33.2% apoptosis versus 51.5% apoptosis, p=0.0286) (Figure 4.8A-C). There was also an identical result when apoptosis was measured by cellular morphology (Figure 4.9A). In contrast, pneumonia whole blood neutrophils had a similar rate of apoptosis to HD (Figure 4.9B).

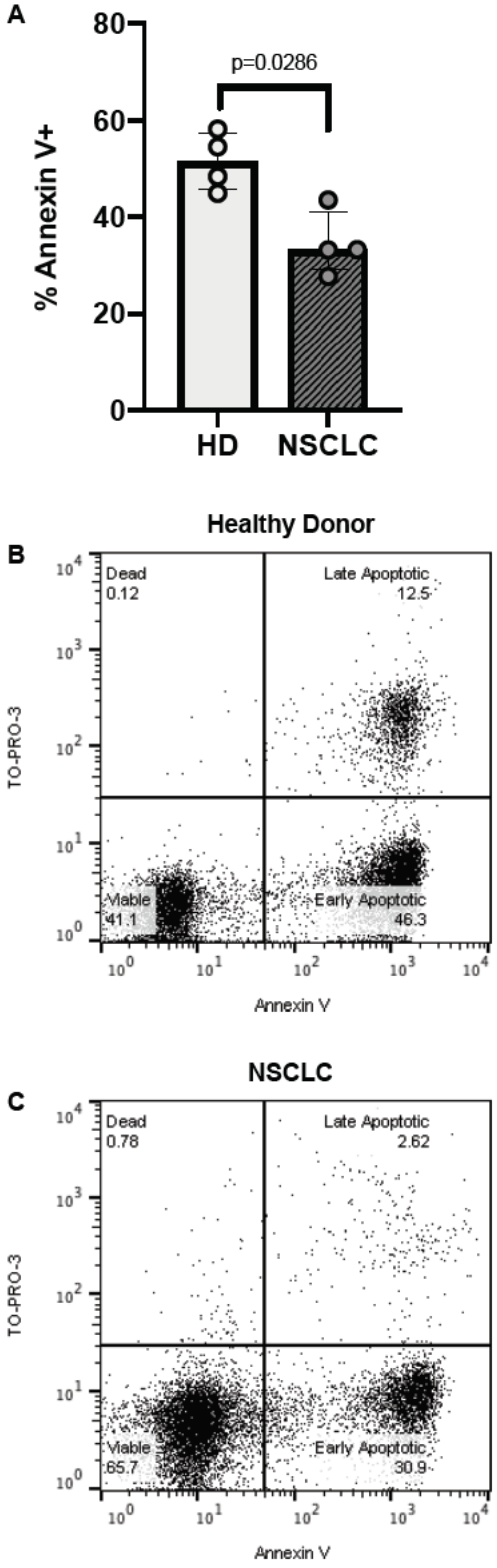

Figure 4.8: NSCLC whole blood neutrophils are pro-survival.
(A) Proportion of apoptotic neutrophils after 20 hours of culture, healthy donor whole blood neutrophils (HD) versus NSCLC whole blood neutrophils, n=4. (B and C) Representative flow cytometry dot plots of whole blood neutrophil 20-hour apoptosis. Analysed by Mann-Whitney test. Data represents individual values (average of at least two replicates) and median ± IQR.

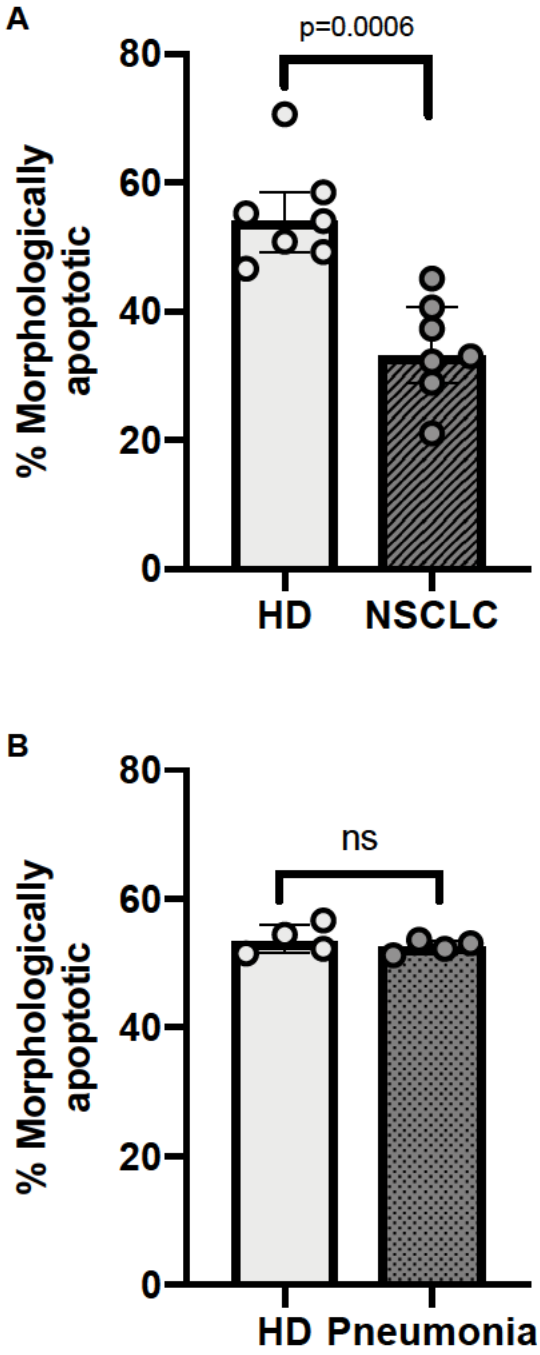

*Figure **4.9: When compared with healthy donor (HD) whole blood neutrophils, NSCLC whole blood neutrophils resist apoptosis, pneumonia whole blood neutrophils do not.** (A) Proportion of apoptotic neutrophils after 20 hours of culture, healthy donor whole blood neutrophils versus NSCLC, n=7. (B) Proportion of apoptotic neutrophils after 20 hours of culture, health donor whole blood neutrophils versus pneumonia, n=4. Analysed by Mann-Whitney test. Data represents individual values (average of at least two replicates) and median ± IQR.*

4.2.7 All NSCLC neutrophil populations are pro-survival

To determine if the pro-survival phenotype of NSCLC whole blood neutrophils was maintained in neutrophils that had migrated into the NSCLC pleural space, the apoptosis of NSCLC pleural fluid neutrophils was measured, and compared with that of healthy donor blood neutrophils. Furthermore, the apoptosis of NSCLC normal-density and low-density blood neutrophils was examined to extrapolate if one or both contributed to the NSCLC whole blood neutrophil pro-survival phenotype. Isolated NSCLC and healthy donor neutrophil populations were cultured *in vitro* and apoptosis measured at 20-hours by flow cytometry (Annexin V staining). All NSCLC neutrophil populations had a survival advantage at 20 hours compared with healthy donor blood neutrophils (Figure 4.10A).

Of note, when the 20-hour apoptosis flow cytometry dot plots of NSCLC neutrophil populations were examined (e.g. Figure 4.10B) it was noted that almost all NSCLC neutrophils that had entered apoptosis were at an early stage (TO-PRO-3 negative).

Furthermore, it was noted in the NSCLC pleural environment chapter of this thesis that neutrophils in conditions modelling the NSCLC pleural environment became pro-survival via TNFα signalling, with upregulation of CD120b surface expression. The surface expression of CD120b was therefore measured by flow cytometry in all NSCLC neutrophil populations (Figure 4.10C). Surface expression of CD120b was higher in NSCLC low-density blood neutrophils and NSCLC pleural fluid neutrophils than that found in healthy donor blood neutrophils.

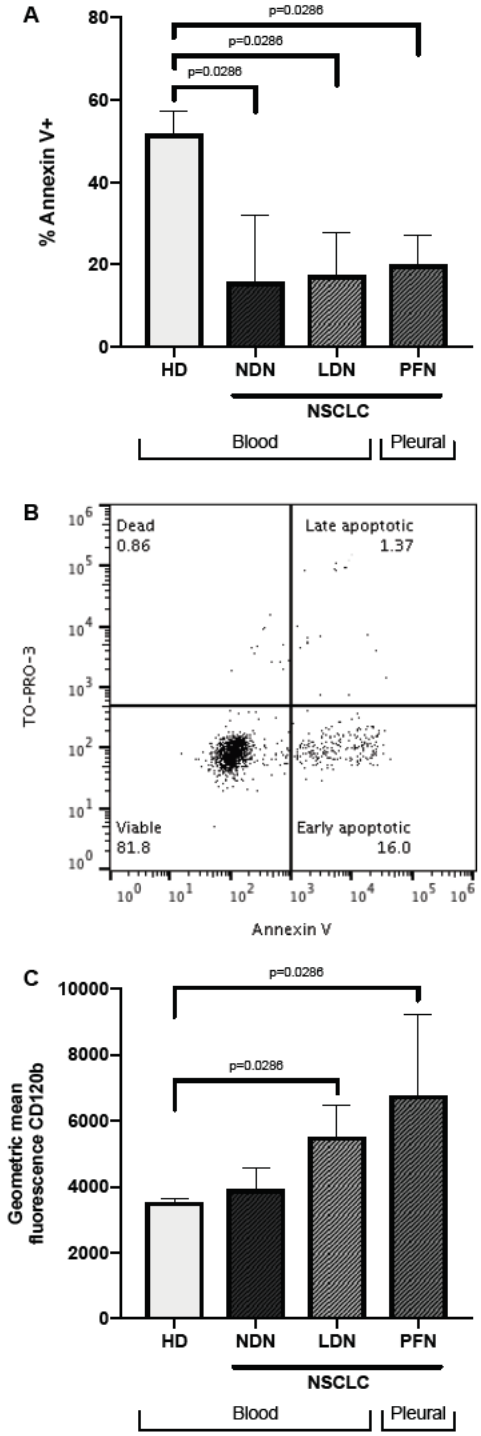

Figure 4.10: NSCLC neutrophil populations are all pro-survival. NSCLC low-density blood neutrophils and NSCLC pleural fluid neutrophils have altered surface expression of CD120b.
(A) 20-hour apoptosis of NSCLC neutrophil populations versus healthy donor blood neutrophils, measured by flow cytometry (Annexin V staining), n=4. (B) Representative flow cytometry dot plot of NSCLC pleural fluid neutrophil 20-hour apoptosis. (C) Surface expression of CD120b in freshly isolated NSCLC neutrophil populations versus healthy donor blood neutrophils, n=4. Data analysed by Mann-Whitney test. Data represents median ± IQR. HD, healthy donor neutrophils; NDN, normal-density neutrophils; LDN, low-density neutrophils; PFN, pleural fluid neutrophils.

4.2.8 Not all environmental signals that impact upon healthy donor neutrophil survival impact upon NSCLC neutrophil survival at 20 hours

In the NSCLC pleural environment chapter of this thesis, it was noted that NSCLC pleural fluid supernatant acted as a survival signal to healthy donor blood neutrophils. Hypoxia also acted as a survival signal to healthy donor blood neutrophils in glucose replete conditions, but when hypoxia was combined with glucose-free conditions, this resulted in cell death (of key importance to note, is that the pleural environment is NOT entirely glucose-free, but does have glucose levels lower than serum).

To investigate whether the NSCLC pleural environment acts as an additional survival signal to NSCLC neutrophils that have migrated from the blood into the pleural space, NSCLC whole blood neutrophils were cultured *in vitro* with or without autologous pleural fluid supernatant in normoxia, or alternatively hypoxia (glucose replete media). Apoptosis was measured at 20 hours by morphological appearances (pyknotic nuclei). In normoxia there was no added survival effect of autologous pleural fluid supernatant (Figure 4.11A). In hypoxia, there was no added survival effect of autologous pleural fluid supernatant either (Figure 4.11B). For completeness, the NSCLC pleural fluid supernatants used in the above experiments were used for healthy donor whole blood neutrophil apoptosis cultures, confirming that despite not having an added survival effect on autologous NSCLC whole blood neutrophils, they were indeed survival signals for healthy donor whole blood neutrophils (Figure 4.11C).

As was found with healthy donor blood neutrophils, NSCLC whole blood neutrophils had a reduced rate of apoptosis when exposed to hypoxia in glucose replete conditions (Figure 4.12A), but when hypoxia was combined with glucose-free conditions, this resulted in cell death (Figure 4.12B).

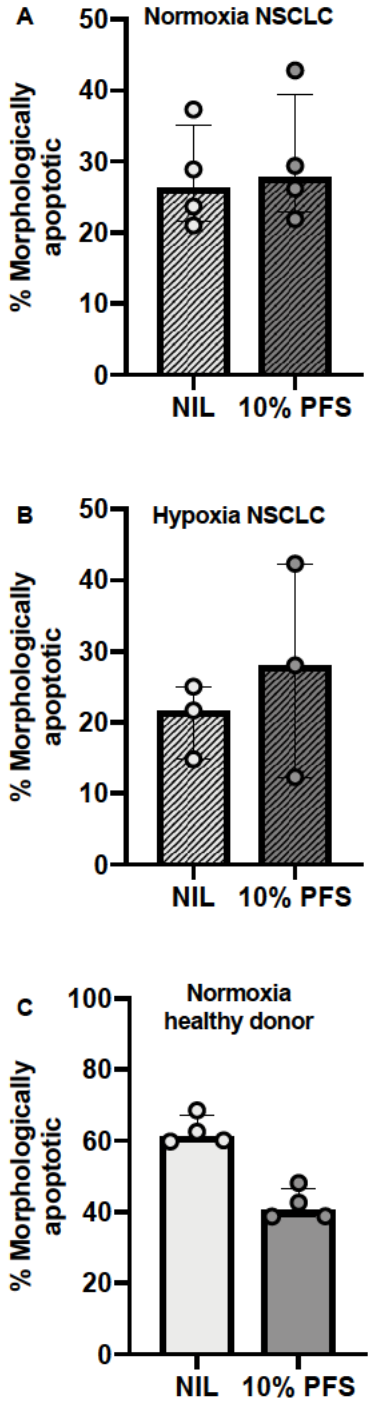

Figure 4.11: Autologous NSCLC pleural fluid supernatant has no added effect upon the survival of NSCLC whole blood neutrophils.
(A) 20-hour apoptosis of NSCLC whole blood neutrophils cultured with or without autologous pleural fluid supernatant in normoxia, n=4. (B) 20-hour apoptosis of NSCLC whole blood neutrophils cultured with or without autologous pleural fluid supernatant in hypoxia, n=3. (C) 20-hour apoptosis of healthy donor whole blood neutrophils cultured with the NSCLC pleural fluid supernatants used in experiment A, n=4. Data analysed by Wilcoxon test. Data represents individual values (average of at least two replicates) and median ± IQR. Striped shading indicates NSCLC neutrophils, darker bar colour fill indicates the presence of pleural fluid supernatant.

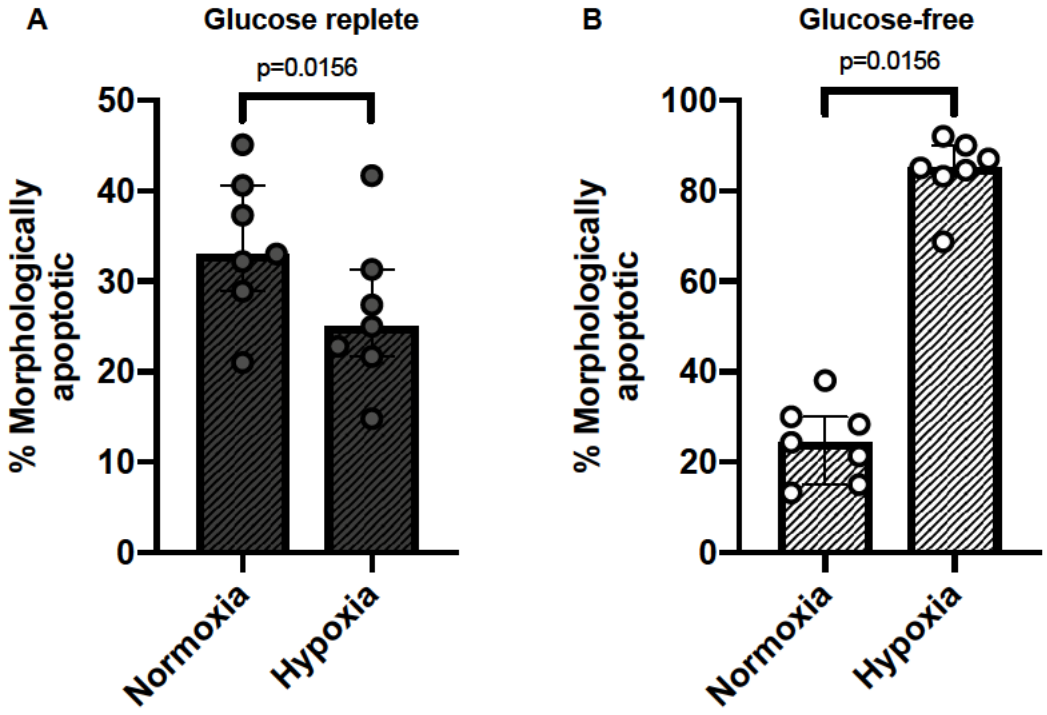

Figure 4.12: Hypoxia acts as a survival signal to NSCLC whole blood neutrophils in glucose replete conditions.
(A) 20-hour apoptosis of NSCLC whole blood neutrophils cultured in glucose replete media, with normoxia or hypoxia, n=7. (B) 20-hour apoptosis of NSCLC whole blood neutrophils cultured in glucose-free media, with normoxia or hypoxia, n=7. Data analysed by Wilcoxon test. Data represents individual values (average of at least two replicates) and median ± IQR.

4.2.9 Apoptosis of pneumonia patient whole blood neutrophils is not reduced by autologous pleural fluid supernatant

To investigate whether the pneumonia pleural environment acts as an additional survival signal to pneumonia patient neutrophils that have migrated from the blood into the pleural space, pneumonia patient whole blood neutrophils were cultured *in vitro* with or without autologous pleural fluid supernatant in normoxia (glucose replete media). Apoptosis was measured at 20 hours by morphological appearances (pyknotic nuclei). The rate of apoptosis was not reduced (Figure 4.13).

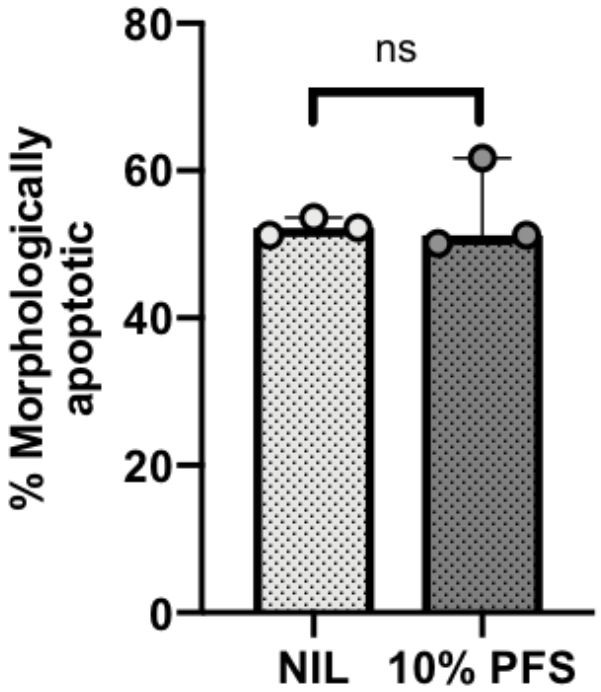

Figure 4.13: Apoptosis of pneumonia patient whole blood neutrophils is not reduced by autologous pleural fluid supernatant.
20-hour apoptosis of pneumonia patient whole blood neutrophils cultured with or without autologous pleural fluid supernatant in normoxia, n=3. Data analysed by Wilcoxon test. Data represents individual values (average of at least two replicates) and median ± IQR. Dotted shading indicates NSCLC neutrophils, darker bar colour fill indicates the presence of pleural fluid supernatant.

4.2.10 NSCLC whole blood neutrophils have preserved phagocytosis

To examine whether the phagocytic capacity of NSCLC neutrophils is preserved, whole blood neutrophils from NSCLC patients and healthy donors (HD) were exposed to Zymosan A *in vitro* for 15 minutes and then cytospins made. These slides were then inspected in order to calculate phagocytic index. Phagocytosis was similar in both groups (Figure 4.14).

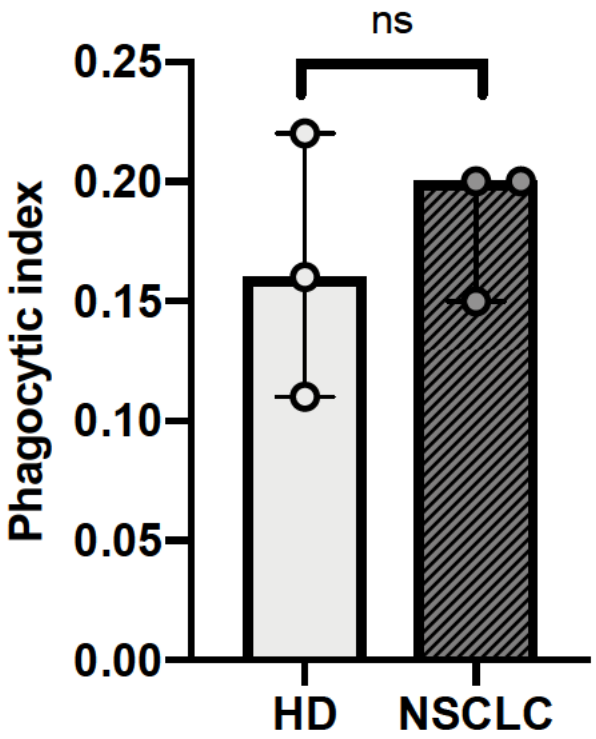

Figure 4.14: NSCLC whole blood neutrophils display a similar rate of phagocytosis when compared with healthy donor (HD) whole blood neutrophils.
Phagocytosis of Zymosan A measured in NSCLC whole blood neutrophils and healthy donor whole blood neutrophils, n=3. Data analysed by Mann-Whitney test. Data represents individual values (average of at least two replicates) and median ± IQR.

4.2.11 NSCLC neutrophil populations express PD-L1

As a readout of whether NSCLC neutrophil populations may be immunosuppressive to T cells, PD-L1 expression was measured in freshly isolated neutrophils by flow cytometry. All NSCLC neutrophil populations expressed PD-L1 on the majority of cells, whereas PD-L1 was expressed at very low levels on healthy donor blood neutrophils (Figure 4.15).

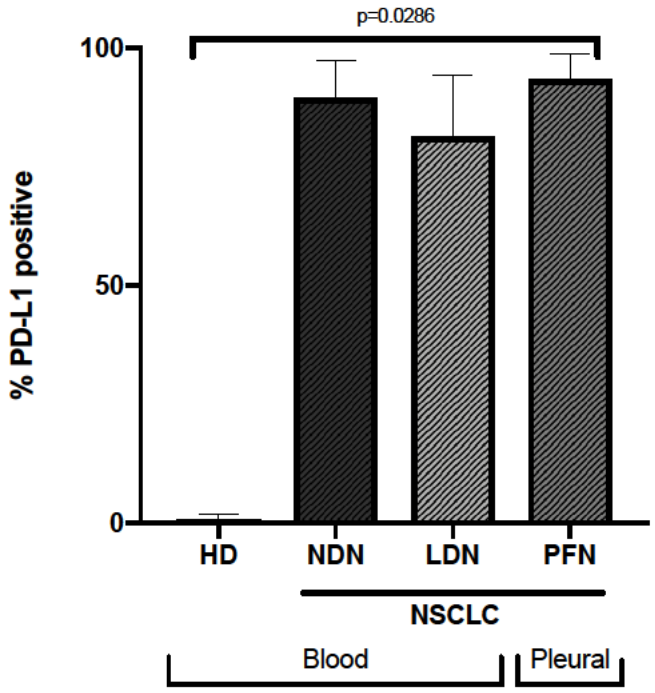

Figure 4.15: NSCLC neutrophil populations express PD-L1.
PD-L1 expression measured by flow cytometry in NSCLC neutrophil populations and healthy donor blood neutrophils, n=4. Data analysed comparing each NSCLC neutrophil population to healthy donor blood neutrophils by Mann-Whitney test. Data represents individual values and median ± IQR. HD, healthy donor neutrophils; NDN, normal-density neutrophils; LDN, low-density neutrophils; PFN, pleural fluid neutrophils.

4.3 Discussion

Neutrophils have been widely reported to be present in malignant pleural effusions,[92 93 109 133 134 148-155] but whether they are able to carry out normal host defence functions, and the mechanistic role they may play in cancer pathophysiology at this metastatic site, have to date been largely neglected. Furthermore, whilst there has been some interest in the use of flow cytometry phenotyping to identify the different leukocyte populations in malignant pleural effusion,[151] the data in this chapter provide more detailed insights into neutrophil populations, their function, and their correlations across the different cell compartments (i.e. blood versus pleural space) in advanced NSCLC.

4.3.1 Advanced NSCLC neutrophil population quantification

Here it is reported that neutrophils form up to 21% (mean 9%) of pleural fluid leukocytes in NSCLC. This is in keeping with previous studies which have shown neutrophils to form 12-31% (mean) of pleural fluid leukocytes in malignant pleural effusion.[133 134 149 152] Indeed, it is typical for neutrophils to constitute <25% of this cell population.[109] However, whilst neutrophils form a minority cell population in malignant pleural effusion, it is key to note that as their proportion increases, patient prognosis worsens.[153]

Next the data in this chapter confirms the presence of low-density neutrophils in the blood of advanced NSCLC patients. This is a population that is present at negligible levels in health. Advanced NSCLC low-density neutrophils were quantified as forming 11% (mean) of the peripheral blood mononuclear cell layer (low-density layer) and 9% (mean) of total blood neutrophils. This is similar to what has been found previously; Liu et al. studied the blood of patients with stage III and IV lung cancer and found an increased ratio of low-density to high-density neutrophils compared with healthy donors, and Sagiv et al. studied blood from patients with lung or breast cancer (stage not specified), reporting low-density neutrophils to form 19% of the low-density blood fraction and 4% of total blood neutrophils.[58 156] In addition, G-MDSCs have been described to constitute 9% of immune cells in stage III-IV lung cancer, with increasing levels correlating with worse overall survival.[157]

4.3.2 Defining advanced NSCLC neutrophil subpopulations by morphology and flow cytometry

In terms of cellular morphology, this chapter describes NSCLC low-density blood neutrophils to be a mixed population of both mature cells (segmented nuclei) and immature cells (banded nuclei). These immature banded neutrophils could also be identified in pleural fluid. NSCLC low-density blood neutrophils were then further characterised, into two distinct subpopulations by flow cytometry phenotyping:

1) **CD66b^{high}**CD11b^{+}CD15^{+}CD14^{-}CD49d^{-}CD10^{-}CD62L^{-}LOX-1^{+} immature cells
2) **CD66b^{+}**CD11b^{high}CD15^{+}CD14^{-}CD49d^{-}CD10^{+}CD62L^{+}LOX-1^{-} mature cells

Concurrent **CD66b^{high}** neutrophils were found in NSCLC pleural fluid, but were not present in the NSCLC normal-density blood neutrophil population nor in the blood of healthy donors. Marini et al. have previously demonstrated CD10^{-} low-density blood neutrophils to have banded nuclei.[62] This would therefore imply that the **CD66b^{high}**CD10^{-} NSCLC low-density blood neutrophils identified here by flow cytometry, are indeed the banded nuclei neutrophils seen by cellular morphology, in both the NSCLC low-density blood and NSCLC pleural fluid populations. Nonetheless, it would be useful to carry out a fluorescence-activated cell sorting experiment to confirm this.

LOX-1 was first described as a G-MDSC marker by Condamine et al., who found OLR1 to be upregulated in low-density blood neutrophils and surface expression of LOX-1 to match this, in a cancer patient population including patients with NSCLC.[65] These LOX-1^{+} neutrophils supressed T cells and were also identified in NSCLC primary tumours. This would suggest that the **CD66b^{high}**CD10^{-} LOX-1^{+} NSCLC low-density blood neutrophils identified in this chapter are G-MDSC, although T cell proliferation studies need to be carried out to prove this.

Finally, the flow cytometry phenotyping data in this chapter builds upon previous work that identified two low-density blood neutrophil subpopulations by nuclear morphology in lung cancer patients. The study noted low-density blood neutrophils to have higher CD66b than normal-density blood neutrophils from the same patients, but did not define flow cytometry features by which to separate the low-density blood neutrophil subpopulations.[58]

4.3.3 Neutrophil populations in advanced NSCLC are phenotypically and functionally different to pneumonia

Aside from cancer, low-density blood neutrophils have also been studied in several non-cancer conditions including systemic lupus erythematosus,[158 159] rheumatoid arthritis,[160] asthma,[161] psoriasis,[162] HIV,[163] severe infection,[164 165] and tuberculosis.[166] However, the precise role low-density neutrophils play at target organs following migration is ongoing. It is also apparent that the pathophysiological function of low-density neutrophils will vary between diseases. In this body of work, there was the wish to investigate how neutrophil populations in the blood and the end-target site (pleural space) may vary between NSCLC and pneumonia. Parapneumonic effusions represent an acute inflammatory response to infection, that usually spontaneously resolve. In contrast, NSCLC pleural effusions represent part of the chronic inflammatory response to metastatic malignancy, that is ineffective, with patients succumbing to metastatic disease burden. Differences in neutrophil populations may contribute to these divergent outcomes.

The data in this chapter demonstrates that pneumonia neutrophil populations differ from NSCLC, with proportionally fewer low-density blood neutrophils and evidence that they either do not migrate into the pleural fluid in pneumonia, or that their phenotype alters during migration to that of a mature neutrophil. There were increased numbers of pleural fluid neutrophils in pneumonia compared with NSCLC, likely reflecting the acute inflammatory nature of pneumonia. It was also interesting to note that blood neutrophils in advanced NSCLC were pro-survival, whereas those in pneumonia were not. These key differences in low-density neutrophil populations and in neutrophil survival, could be of pathophysiological importance, which will need to be clarified in future work.

A final and key consideration is that whilst immature low-density neutrophils appear to migrate into the pleural fluid of NSCLC (and do not do this in pneumonia), they still form a minority population when compared with normal-density neutrophils in this metastatic tumour microenvironment. Furthermore, in advanced NSCLC, pleural metastatic burden progresses over time. This raises the question of whether normal-density neutrophils in this setting are simply ineffective, or whether the minority low-density neutrophil population is having a significant detrimental effect upon whole neutrophil population responses at this metastatic site. This requires further investigation.

4.3.4 Evidence that neutrophil populations in advanced NSCLC are phenotypically and functionally different to early stage NSCLC neutrophil populations, and that the tumour microenvironments have opposing effects on neutrophil function

It is helpful to make a point of comparing and contrasting the data shown in this chapter with that of the Eruslanov group.[46 47 57] This group have extensively studied neutrophils in early human lung cancer (stage I-II NSCLC). Whilst there are some similarities in the data, there are some stark differences that will be of key importance in disease outcome. In short, whilst Eruslanov et al. show evidence that neutrophils are helpful at the primary site in early stage lung cancer, evidence in this chapter suggests the opposite is true at the metastatic site in advanced disease.

Eruslanov et al. have shown that tumour-associated neutrophils from primary NSCLC tumours are NOT pro-survival in *ex-vivo* culture (80% 20-hour apoptosis) unless tumour-culture media at a concentration of 50% is added (40% 20-hour apoptosis). Furthermore, tumour-associated neutrophils had preserved phagocytosis, expressed low levels of PD-L1 and stimulated T cell proliferation.[47] The same group then went on to show that there is a tumour-associated neutrophil subpopulation with immature nuclei, originating from $CD10^-$ immature neutrophils, that stimulates and supports T cell responses. In addition, if they took mature human blood neutrophils and cultured them with tumour-culture media they died, but if they took immature human bone marrow neutrophils and conditioned them with tumour culture media, they lived longer and became like the tumour-associated neutrophil subpopulation i.e. in their surface markers and they stimulated T cells.[46]

In contrast, the data in this chapter shows that neutrophils from the pleural metastatic site and populations from the blood in advanced NSCLC, were pro-survival in *ex-vivo* culture, with increased expression of pro-survival TNFα receptor CD120b. The addition of autologous pleural fluid supernatant, akin to 'tumour-culture media', had no added effect upon the survival of NSCLC whole blood neutrophils, counter to the findings in early NSCLC. Advanced NSCLC blood neutrophils had preserved phagocytosis, in a similar manner to tumour-associated neutrophils in early stage lung cancer. However, opposed to the findings in early stage NSCLC, neutrophil populations in advanced NSCLC all expressed high levels of PD-L1, suggesting an immunosuppressive role. The pleural fluid supernatant

studies found in the pleural environment chapter of this thesis also had contrary findings compared with the Eruslanov group studies in early NSCLC. Pleural fluid supernatant conditioned healthy donor blood neutrophils to live longer, express PD-L1, and suppress T cells.

4.3.5 Mechanisms underlying the neutrophil apoptosis phenotype in advanced NSCLC

It is interesting to note in this chapter, that blood neutrophils in advanced NSCLC were pro-survival before they had even migrated to the pleural space. More than that, culturing blood neutrophils from NSCLC patients with autologous pleural supernatant had no additional survival benefit at 20 hours. This raises the question as to what the mechanism behind this was.

Based on the pleural environment chapter of this thesis, it could be thought that the blood neutrophils in NSCLC are pro-survival due to TNFα signalling in the blood. However it has previously been shown that TNFα levels in NSCLC blood are not elevated.[167] The same group, also showed that in stage III-IV NSCLC, normal-density neutrophils expressed increased levels of CD47 and that this was associated with decreased levels of apoptosis.[142] Of note, the intrinsic properties chapter of this thesis attempts to further address possible intrinsic mechanisms that may be behind this pro-survival NSCLC blood neutrophil phenotype. Indeed, it may be that in NSCLC there is functional imprinting of neutrophil bone marrow precursors, before they are even recruited to the blood.

Another consideration, is that whilst autologous pleural fluid supernatant does not appear to have an additional survival benefit effect on NSCLC blood neutrophils at 20 hours, it could act to sustain neutrophils at a later time-point. This could be investigated in future work. The Eruslanov group for instance, carried out neutrophil apoptosis studies following 7 days of culture with tumour-culture media.[46]

TNFα signalling may also still be of importance to the survival of neutrophils in the pleural space. Not only does the data in the pleural environment chapter of this thesis and this chapter support this, but work from Aleman et al. does also.[93] They showed that neutrophils from tuberculosis pleural effusions had a higher rate of apoptosis (although this was an immediate measure following fresh extraction,

rather than following 20 hours of culture) than neutrophils from malignant pleural effusions. Furthermore, the tuberculosis pleural effusion neutrophils had upregulation of CD120a (pro-apoptosis TNFα receptor) and phosphorylated p38 kinase (pro-apoptosis). It would therefore be of interest in future work to measure 20-hour apoptosis of parapneumonic effusion neutrophils and their CD120a/ CD120b/ phosphorylated p38 kinase expression.

4.3.6 Summary

The data from this chapter provides evidence for an expanded population of low-density blood neutrophils in advanced NSCLC, that are not present in health, and that a proportion of which are immature with banded nuclei. A subpopulation of advanced NSCLC low-density neutrophils is $CD66^{high}$, immature ($CD10^{-}$), activated ($CD62L^{-}$) and positive for a G-MDSC marker ($LOX\text{-}1^{+}$). There is further evidence that these cells are also present in NSCLC pleural fluid, but in contrast these cells are not present in pneumonia pleural fluid. NSCLC pleural fluid neutrophils express PD-L1 and are long-lived with increased CD120b expression. Together this is suggestive that advanced (stage IV) NSCLC pleural fluid neutrophils may contribute to an environment of sustained inflammation that is ineffective in its response to increasing metastatic tumour burden. The advanced NSCLC neutrophil population features are summarised in Table 4.2. The findings of this chapter are the opposite of what has been described previously with regard to the role of neutrophils in primary tumours of early stage (I-II) NSCLC.[46 47 57]

	Normal-density blood neutrophils	Low-density blood neutrophils	Pleural fluid neutrophils
Morphology	Mature	Mature and immature	Mature and immature
$CD66^{high}CD10^{-}$ $CD62L^{-}LOX\text{-}1^{+}$ population	No	Yes	Yes
Pro-survival at 20 hours	Yes	Yes	Yes
Increased CD120b expression	No	Yes	Yes
PD-L1 positive	Yes	Yes	Yes

Table 4.2: Summary of advanced NSCLC neutrophil population features.

Chapter 5 Intrinsic properties of neutrophil populations in advanced NSCLC define their function

5.1 Introduction

In this chapter, transcriptomics and proteomics are used in order to gain functional and mechanistic insight into advanced NSCLC neutrophil populations. Using these methods in tandem gives a large quantity of unbiased discovery-based data. Several studies have investigated the transcriptome of neutrophils in cancer, but none have done so with the purpose of correlating neutrophil populations in metastatic cancer across different cellular compartments in the same human donor, attempting to identify intrinsic mechanisms that may explain their function. To date, there have not been any publications regarding the proteome of human cancer neutrophil-specific populations.

5.1.1 Mouse neutrophil transcriptomics in cancer

Fridlender et al. carried out some of the earliest neutrophil transcriptomic work in cancer. They compared bone marrow neutrophils from mice without cancer, to immature spleen neutrophils from mice with flank tumours (lung cancer cell lines), and tumour neutrophils from mice with cancer. They found genes related to the respiratory burst were downregulated in the tumour neutrophils. Immature spleen neutrophils and tumour neutrophils upregulated antigen presenting genes and the genes for tumour necrosis factor and Interleukin-1. There was no significant difference in the apoptosis-related genes and pathways between the three populations. However, the anti-apoptotic members of the NF-κB family were upregulated in tumour neutrophils, and BH3 pro-apoptotic genes were upregulated in immature spleen neutrophils.[168] Of note, a key limitation of this study was cell purity; above 85% neutrophil purity was the cut off (flow sorted cells from spleen and tumour samples). This may have led to transcriptomic data that over-represents antigen presenting capacity. They did not look at bone marrow neutrophils from mice with cancer.

The Fridlender group has been instrumental in showing that the cytokine TGFβ can polarise mouse neutrophils to a pro-tumour phenotype.[25] Shaul et al. from the same research group, used the identical mouse flank tumour model discussed above. The transcriptome of neutrophils isolated from the tumours of mice treated with a TGFβ inhibitor (deemed anti-tumour neutrophils, N1) were compared with those from tumours of mice without inhibitor (deemed pro-tumour neutrophils, N2), and bone marrow neutrophils from non-tumour bearing mice. Antigen presentation genes were upregulated in N1 neutrophils. TNFα message expression and TNFR1 (pro-apoptosis TNFα receptor) were upregulated in N1 compared with N2 neutrophils. Again, a key limitation of this study was cell purity; above 85% neutrophil purity was the cut off (flow sorted cells from tumour samples).[169]

Finally, Zilionis et al. used single-cell RNA sequencing to demonstrate that tumour neutrophils exhibit phenotypes that are conserved between mouse and man in NSCLC. They analysed the transcriptome of early-stage human NSCLC blood and primary tumour immune cells, and compared them with tumour immune cells in NSCLC mouse models and immune cells in healthy mouse lung.[170]

5.1.2 Human neutrophil transcriptomics in cancer

Condamine et al. investigated the transcriptome of human cancer low-density blood neutrophils (referred to as granulocytic myeloid-derived suppressor cells in this study), from patients with NSCLC and head and neck cancer. These were compared with normal-density blood neutrophils from the same patients and healthy donor blood normal-density neutrophils. The primary aim of this study was to identify specific markers by which cancer low-density blood neutrophils could be distinguished from normal-density neutrophils.

LOX-1 was identified as a cancer low-density blood neutrophil marker (transcription of its gene OLR1 was upregulated), and in subsequent assays 1/3rd of cancer low-density blood neutrophils expressed LOX-1 on their cell surface. Flow sorting was used to isolate LOX-1^{+} and LOX-1^{-} cells separately. LOX-1^{+} neutrophils had immature banded nuclei and suppressed T cells in culture. LOX-1^{-} neutrophils had mature nuclei and did not suppress T cells in culture.

Normal-density blood neutrophils from healthy donors and cancer patients had similar transcriptomes. Cancer low-density blood neutrophils had upregulation of transcription of genes involved in translational initiation, the MAPK pathway and the NF-κB pathway.[65]

5.1.3 Proteogenomic studies of neutrophil differentiation

It is apparent that immature neutrophil populations are of key importance in cancer pathophysiology.[63] Therefore it is pertinent to consider proteogenomic studies of neutrophil differentiation that have previously been carried out, in order to identify which bone marrow populations immature cancer neutrophils align to. The transcriptome of human bone marrow populations was described in detail by Theilgaard-Monch et al. demonstrating an elegant stepwise process of differentiation. As neutrophils differentiate they develop granules, loose proliferative capacity and become less pro-survival, and this is reflected in their gene transcription.[171] Adding to this data, Rorvig et al. studied how the transcriptome and proteome of neutrophil granule proteins matches up during differentiation.[172] Complementary developmental analysis of murine bone marrow neutrophils has also been carried out.[173]

5.1.4 Neutrophil granule development

Transcriptomic and proteomic studies of neutrophils at various stages of development, have shown that neutrophil granules are produced at an immature stage of development in a controlled order.[171 172] Primary granules are formed during the myeloblast to promyelocyte stage, secondary during myelocyte to metamyelocyte stage and tertiary from the band cell to segmented cell.[17] The dogma is that mature neutrophils do not form new granules. Neutrophil granules, their proteins and associated genes are summarised in Table 5.1.

Primary (Azurophilic)	Secondary (Specific)	Tertiary
MPO (myeloperoxidase)	LTF (lactotransferrin)	MMP9 (gelatinase)
ELANE (neutrophil elastase)	PTX3 (pentraxin-3)	LYZ (lysozyme C)
CTSG (cathepsin G)	CAMP (cathelicidin)	PFC (properdin)
AZU1 (azurocidin)	MMP8 (neutrophil collagenase)	SCAMP2 (secretory carrier-associated membrane protein 2)
PRTN3 (myeloblastin)	LCN2 (neutrophil gelatinase)	
DEFA (defensin)	STOM (stomatin)	
ARG1 (arginase-1)	CYBB (cytochrome b)	

Table 5.1: Neutrophil granules, their proteins and associated genes.

5.1.5 Summary

Using transcriptomics and proteomics in tandem, gives a large quantity of unbiased discovery-based data, regarding the intrinsic workings of a cell. This can be used in order to gain functional and mechanistic insights into advanced NSCLC neutrophil populations. Mouse studies have shown interesting changes in the transcriptome of primary tumour neutrophils and immature neutrophils in cancer. Human studies have demonstrated important differences in the transcriptome of cancer low-density blood neutrophils. However, there is a lack of proteomic data for human cancer neutrophils. Furthermore, the transcriptome of neutrophils from a metastatic site has never been compared to neutrophils from the blood in the same donor.

5.1.6 Hypotheses

NSCLC neutrophil populations would have distinct transcriptional and proteomic signatures. Intrinsic features and mechanisms would explain some of the functional phenotypes observed previously in this thesis e.g. apoptosis. The large quantity of unbiased discovery-based data would enable the identification of novel areas of interest for future work, with regard to the influence of neutrophils in metastatic NSCLC progression.

5.1.7 Aims

To carry out transcriptomics and proteomics with NSCLC neutrophil populations and compare these with healthy control blood neutrophils. Identify novel mechanisms and key processes that may determine neutrophil behaviour and tumour responses at the metastatic site.

5.2 Results

5.2.1 Terminology used for neutrophil populations

In this chapter, several neutrophil populations are described. The methods chapter of this thesis describes in full detail how each was harvested from samples. However, to aid interpretation of the results that follow, a brief overview is given below:

Normal-density neutrophils (NDN) are blood neutrophils, defined by the layer in which they resided following a discontinuous Percoll™ density gradient separation.

Low-density neutrophils (LDN) are blood neutrophils, defined by the layer in which they resided following a discontinuous Percoll™ density gradient separation.

Pleural fluid neutrophils (PFN) are neutrophils that were extracted from pleural fluid by fluorescence-activated cell sorting.

Healthy donor control neutrophils (CTL) refers to blood neutrophils from healthy donors.

5.2.2 NSCLC neutrophil populations are transcriptionally distinct

Through NanoString™ technology, the transcriptional behaviour of healthy donor control blood neutrophils (CTL) was compared with three NSCLC neutrophil populations; normal-density blood neutrophils (NDN), low-density blood neutrophils (LDN) and pleural fluid neutrophils (PFN).

Principle component analysis (Figure 5.1), illustrated that although there was significant heterogeneity between samples, biological replicates from each population did cluster together. NDN clustered most closely to CTL and LDN clustered the furthest from CTL.

Volcano plots of each NSCLC population versus CTL (Figure 5.2A-C), further demonstrated that LDN had the most differences compared with CTL, followed by PFN, with NDN the most similar to CTL. Tables of the statistically significant differentially expressed transcripts (LOG2 fold change >1 or <-1 and $p<0.05$) can be found in Appendix 1.

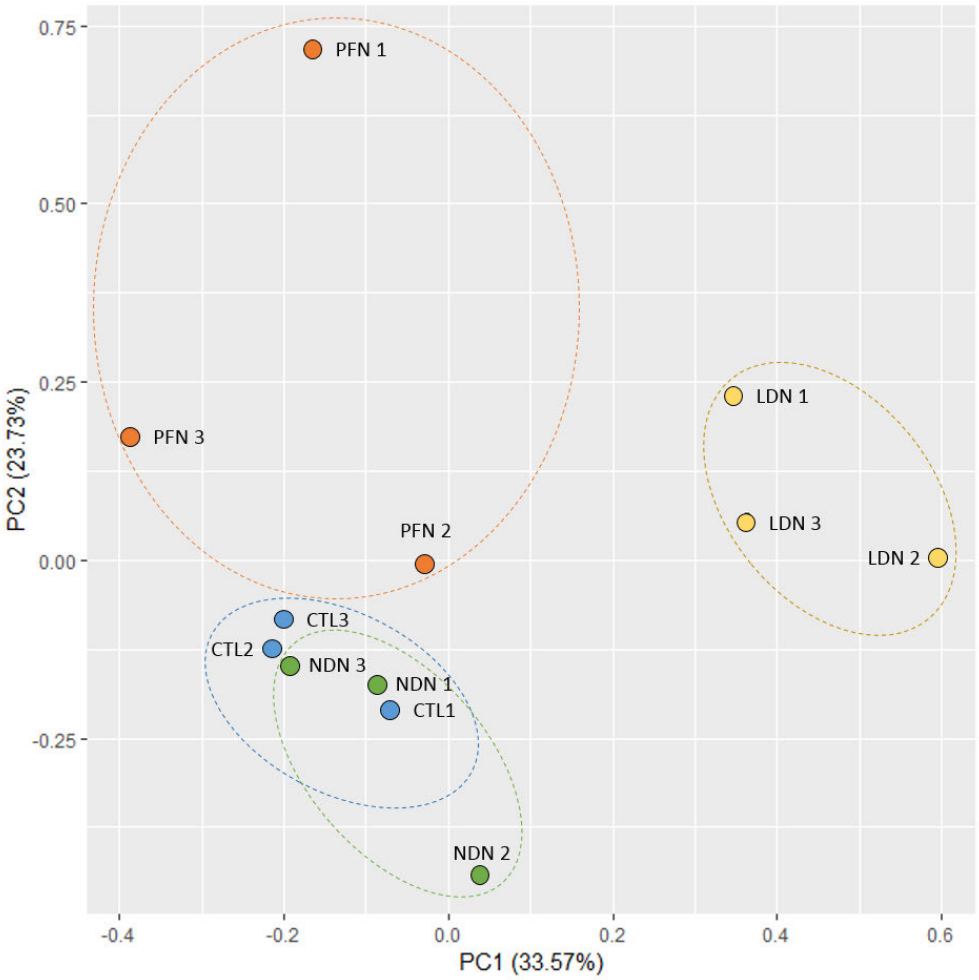

Figure 5.1: Principal component analysis of NanoString™ data.
NSCLC neutrophil populations were compared with healthy donor control blood neutrophils through NanoString™ technology, n=3 biological replicates each group. CTL, healthy donor control neutrophils; NDN, normal-density neutrophils; LDN, low-density neutrophils; PFN, pleural fluid neutrophils.

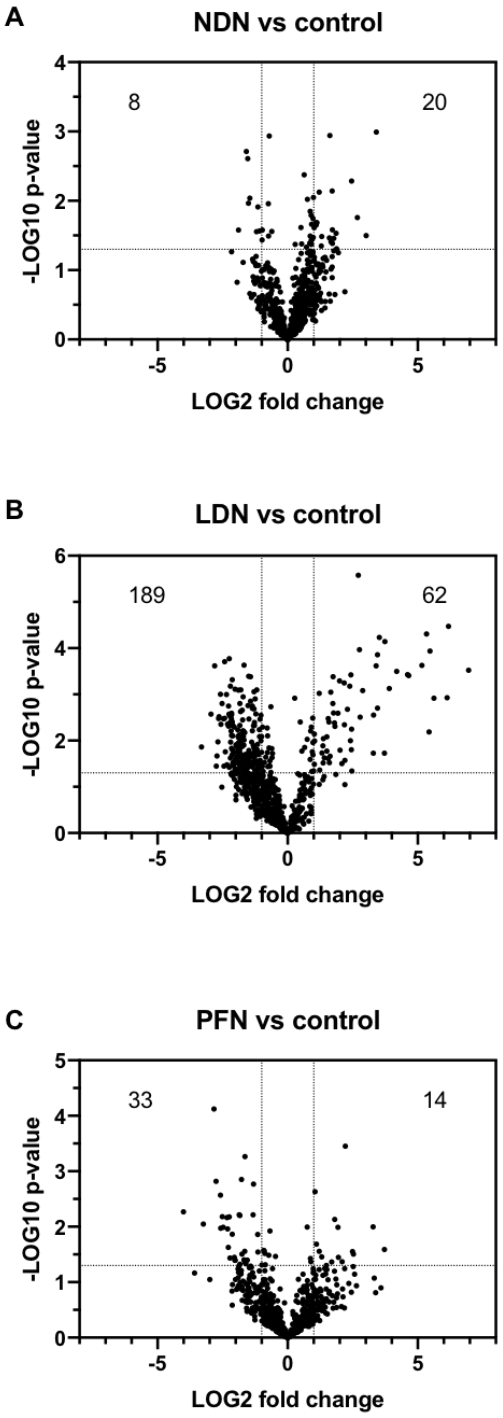

Figure 5.2: NSCLC neutrophil populations are transcriptionally distinct from healthy donor control blood neutrophils.
NSCLC neutrophil populations were compared with healthy donor control blood neutrophils through NanoString™ technology, n=3 biological replicates each group. (A-C) Volcano plots; significantly upregulated (right) and downregulated (left) transcripts in NSCLC populations (number indicated, tables of transcripts can be found in Appendix 1) when compared with control. Analysed by t-test. Lines indicate LOG2 fold change >1 or <-1 and p<0.05. Data points represent individual gene transcripts. CTL, healthy donor control neutrophils; NDN, normal-density neutrophils; LDN, low-density neutrophils; PFN, pleural fluid neutrophils.

5.2.3 NanoString™ data supports flow cytometry surface marker phenotyping of NSCLC neutrophil populations

It was sought to establish whether there was consistency between the flow cytometry surface marker phenotyping of NSCLC populations (found in the NSCLC neutrophil populations chapter of this thesis) and the transcription of genes coding for these markers. Transcription of genes coding for CD66b, CD62L and LOX-1 were compared in NSCLC neutrophil populations (NDN, LDN and PFN) versus CTL (Figure 5.3A-C).

In keeping with the flow cytometry surface marker phenotyping, LDN had significantly higher levels of transcription of the genes coding for CD66b (Figure 5.3A) and LOX-1 (Figure 5.3C), and lower levels of transcription of the gene coding for CD62L (Figure 5.3B), when compared with CTL. Similar patterns of transcription were also seen in PFN when compared with control, with lower levels of transcription of the gene coding for CD62L (Figure 5.3B) reaching statistical significance. NDN were indistinguishable from CTL.

Of note, the changes in the transcription of CD62L are modest, and must be interpreted with caution when correlated with CD62L surface marker expression measured by flow cytometry, as surface marker expression is likely to be influenced more by cell shedding of CD62L than by new CD62L protein production.

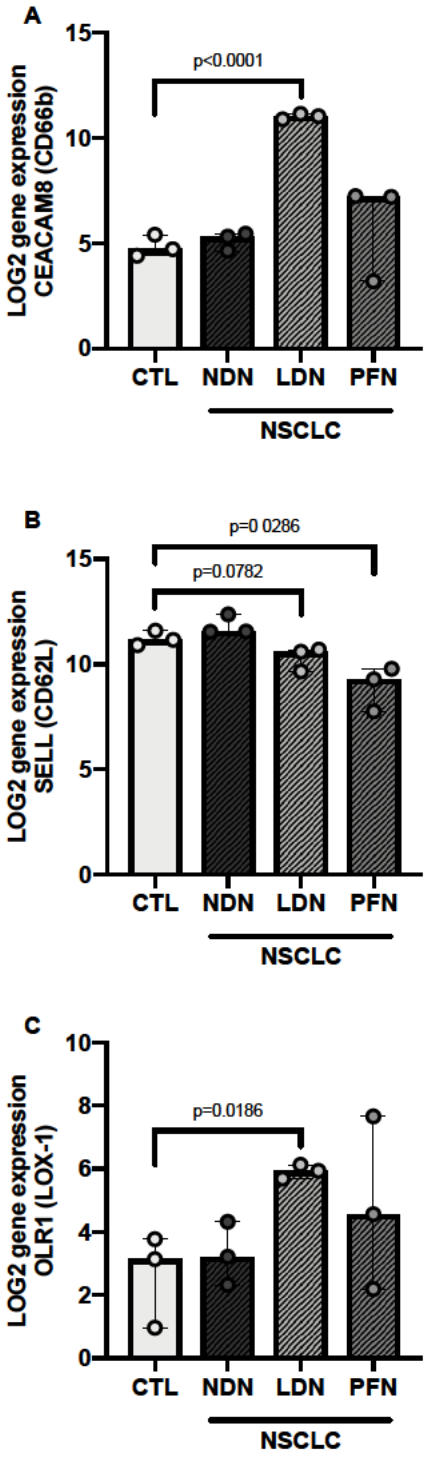

Figure 5.3: Changes in the transcription of genes coding for CD66b, CD62L and LOX-1 in NSCLC populations is in keeping with flow cytometry phenotyping data.
NSCLC neutrophil populations were compared with healthy donor control blood neutrophils (CTL) through NanoString™ technology, n=3 biological replicates each group. (A) CEACAM8 gene expression. (B) SELL gene expression. (C) OLR1 expression. Data analysed by unpaired t-test. Data represents individual values and mean ± SEM. CTL, healthy donor control neutrophils; NDN, normal-density neutrophils; LDN, low-density neutrophils; PFN, pleural fluid neutrophils.

5.2.4 NSCLC low-density blood neutrophils have altered transcription of genes associated with apoptosis pathways and neutrophil granule production

In order to interrogate how changes in the transcription of genes may impact upon neutrophil function in NSCLC, the DAVID 6.8 bioinformatics resource[97] was used to carry out biological process over-representation analyses.

Biological process over-representation analysis of NSCLC LDN downregulated gene transcripts versus CTL (LOG2 fold change<-1 and $p<0.05$), highlighted several key pathways relating to apoptosis (in bold, Table 5.2). Of particular interest was the TNF-mediated signalling pathway, due to evidence in the previous chapters of this thesis implicating its importance. A volcano plot highlighting significantly upregulated and downregulated TNF-mediated signalling pathway gene transcripts in NSCLC LDN versus CTL, revealed that pro-survival gene transcripts were upregulated, and pro-apoptosis gene transcripts were downregulated (Figure 5.4).

Biological process over-representation analysis of NSCLC LDN upregulated gene transcripts versus control (LOG2 fold change>1 and $p<0.05$), indicated the term innate immune response (in bold, Table 5.3). On closer inspection, the gene transcripts that contributed to this finding were for genes coding neutrophil granule proteins. A Volcano plot highlighting neutrophil granule protein gene transcripts in NSCLC LDN versus CTL, revealed them to all be upregulated (Figure 5.5).

DOWNREGULATED LDN vs control	p-value	Fold change
GO:0006955~immune response	8.57E-04	1.44
GO:0070098~chemokine-mediated signaling pathway	3.22E-03	1.77
GO:0007165~signal transduction	1.10E-02	1.33
GO:0033209~TNF-mediated signaling pathway	**1.61E-02**	**2.04**
GO:0006954~inflammatory response	1.68E-02	1.31
GO:0097191~extrinsic apoptotic signaling pathway	**2.02E-02**	**2.51**
GO:0007186~G-protein coupled receptor signaling pathway	4.29E-02	1.38
GO:0051770~positive regulation of nitric-oxide synthase biosynthetic process	4.31E-02	2.72
GO:0043122~regulation of I-kappaB kinase/NF-kappaB signaling	**4.68E-02**	**4.08**
GO:0032735~positive regulation of interleukin-12 production	4.75E-02	2.04

Table 5.2: Biological process over-representation analysis of NanoString™ NSCLC LDN downregulated transcripts.
770 genes in the NanoString™ human myeloid innate immunity panel were used as the background.

UPREGULATED LDN vs control	p-value	Fold change
GO:0051493~regulation of cytoskeleton organization	1.58E-02	13.11
GO:0045087~innate immune response	**2.12E-02**	**2.15**
GO:0045454~cell redox homeostasis	2.43E-02	5.82
GO:0030099~myeloid cell differentiation	4.77E-02	7.86

Table 5.3: Biological process over-representation analysis of NanoString™ NSCLC LDN upregulated gene transcripts.
770 genes in the NanoString™ human myeloid innate immunity panel were used as the background.

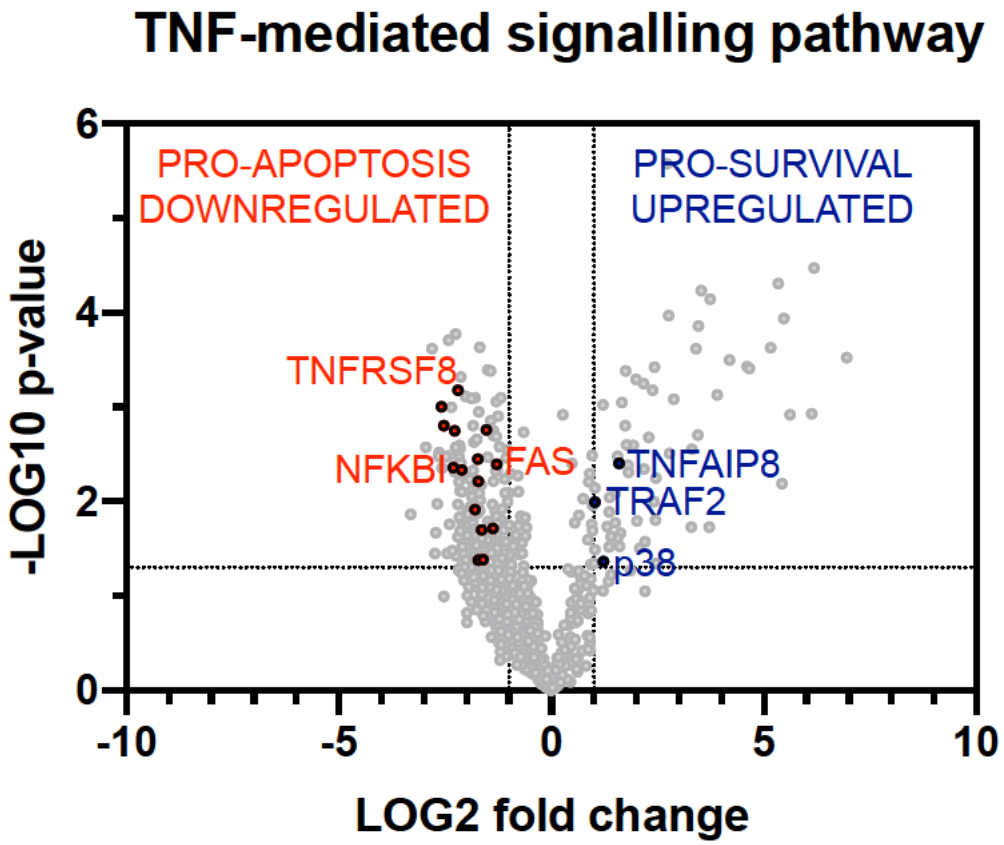

Figure 5.4: Changes in the transcription of genes from the TNF-mediated signalling pathway favour NSCLC low-density blood neutrophil survival.
Volcano plot highlighting significantly upregulated (blue) and downregulated (red) TNF-mediated signalling pathway gene transcripts in NSCLC low-density blood neutrophils versus healthy donor blood neutrophils. Analysed by t-test. Lines indicate LOG2 fold change >1 or <-1 and p<0.05. Data points represent individual gene transcripts.

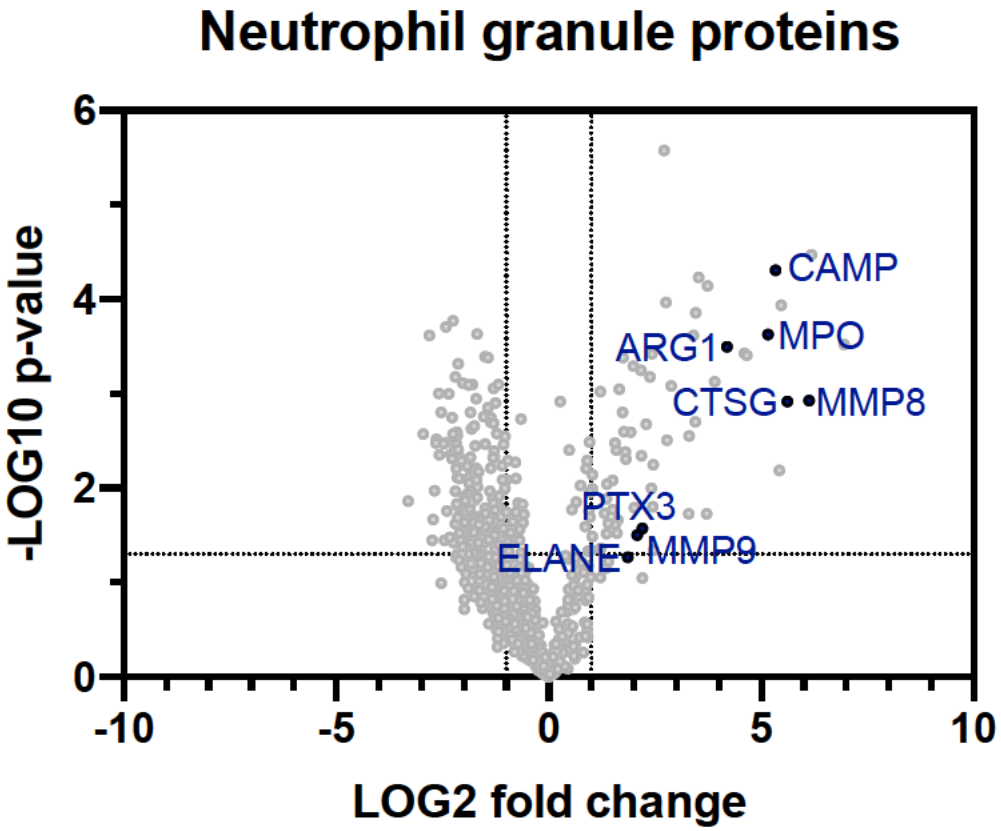

Figure 5.5: Transcription of neutrophil granule protein genes is upregulated in NSCLC low-density blood neutrophils.
Volcano plot highlighting neutrophil granule protein gene transcripts (blue) in NSCLC low-density blood neutrophils versus healthy donor blood neutrophils. Analysed by t-test. Lines indicate LOG2 fold change >1 or <-1 and p<0.05. Data points represent individual gene transcripts.

5.2.5 NSCLC pleural fluid neutrophils have altered transcription of genes associated with apoptosis pathways

Following the discovery of the pro-survival NSCLC LDN NanoString™ phenotype, the NSCLC PFN data was analysed to look for any common features. Biological process over-representation analysis of NSCLC PFN downregulated gene transcripts versus CTL (LOG2 fold change<-1 and p<0.05), highlighted the GOBP 6915 apoptotic process pathway (p=0.0445, fold change 2.51). On closer examination, in common with NSCLC LDN, the transcription of both pro-apoptotic genes FAS (Figure 5.6A) and NF-κBI (Figure 5.6B) was downregulated in NSCLC PFN compared with CTL.

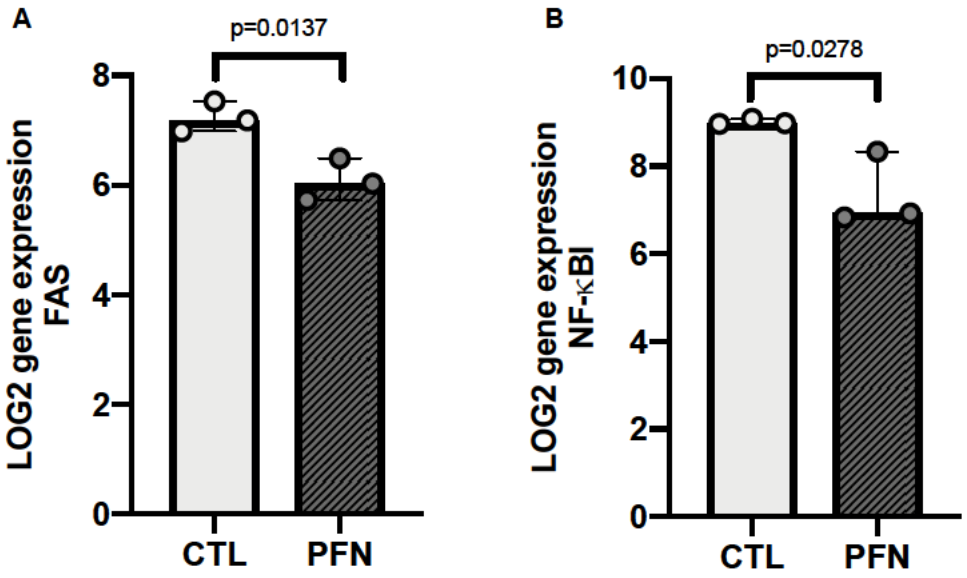

Figure 5.6: There is downregulation in the transcription of pro-apoptotic genes in NSCLC pleural fluid neutrophils versus healthy donor control blood neutrophils.
(A) FAS gene expression in NSCLC pleural fluid neutrophils versus healthy donor control blood neutrophils, n=3. (B) NF-κBI gene expression in NSCLC pleural fluid neutrophils versus healthy donor control blood neutrophils, n=3. Data analysed by unpaired t-test. Data represents individual values and mean ± SEM. CTL, healthy donor control neutrophils; PFN, pleural fluid neutrophils.

5.2.6 NSCLC low-density blood neutrophils have increased transcription of S100A8 and S100A9 genes

The S100 family of calcium binding proteins are released during the inflammatory response to malignancy, and S100A8/A9 (calprotectin) can act as a myeloid-derived suppressor cell chemoattractant.[66] When processing the NanoString™ data, it was noted that S100A8 and S100A9 were the most highly expressed genes in NSCLC LDN. Moreover, the expression of S100A8 (Figure 5.7A) and S100A9 (Figure 5.7B) was significantly higher in NSCLC LDN than CTL.

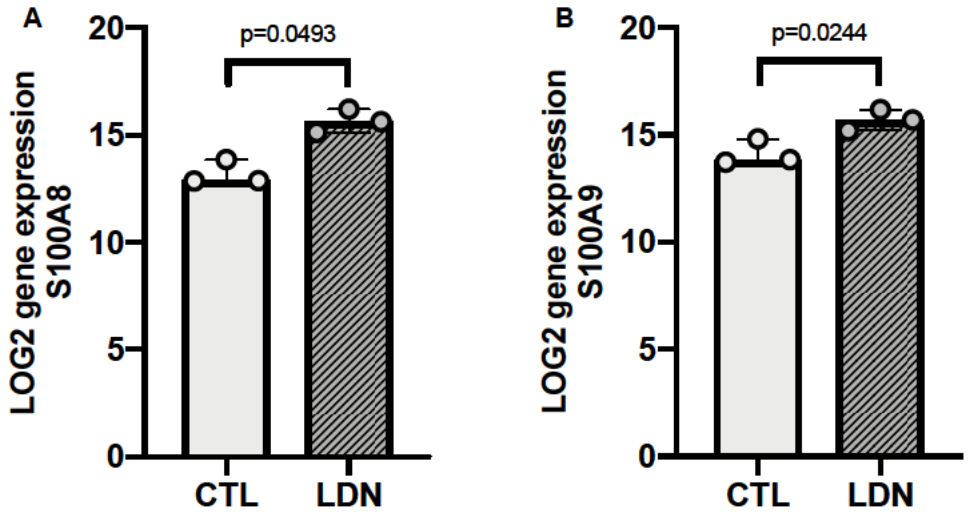

Figure 5.7: NSCLC low-density blood neutrophils have increased transcription of S100A8 and S100A9 genes versus healthy donor control blood neutrophils.
(A) S100A8 gene expression in NSCLC low-density blood neutrophils versus healthy donor control blood neutrophils, n=3. (B) S100A9 gene expression in NSCLC low-density blood neutrophils versus healthy donor control blood neutrophils, n=3. Data analysed by unpaired t-test. Data represents individual values and mean ± SEM. CTL, healthy donor control neutrophils; LDN, low-density neutrophils.

5.2.7 NSCLC neutrophil populations and healthy donor blood neutrophils have similar distributions of protein by abundance and mass

The proteome of healthy donor control blood neutrophils (CTL) was compared with three NSCLC neutrophil populations; normal-density blood neutrophils (NDN), low-density blood neutrophils (LDN) and pleural fluid neutrophils (PFN). Each sample was formed from $2.5x10^5$ neutrophils.

Before more detailed analysis of differential protein expression was undertaken, a global perspective of protein distribution within each neutrophil population was examined. Approximately 3500 proteins were identified in each population. All neutrophil populations had similar distributions of protein by abundance (Figure 5.8A-D). The top 25 proteins by abundance were also similar in all populations (Figure 5.8E)

Next, it was sought to establish if there was a difference between neutrophil populations in the distribution of proteins by mass (Figure 5.8F). The contribution of each protein to the total protein mass of each neutrophil population, was calculated using mean copy number and molecular mass for each of the identified proteins. The number of proteins contributing to each quartile of total protein mass of each neutrophil population was then calculated, along with the percentage they represented of total proteins identified in that same population. In all populations, around 5 proteins accounted for first 25% of total protein mass, and around 3400 proteins accounted for the last 25% of total protein mass.

Finally, to interrogate whether low-density neutrophils are such, as a result of differences in protein content, total protein mass was calculated using the proteomic ruler. LDN had a similar amount of total protein to CTL (Figure 5.8G).

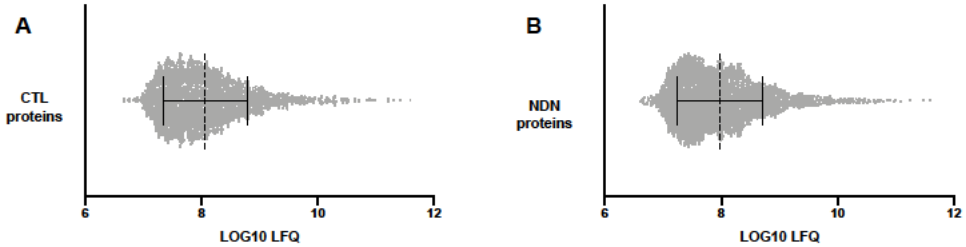

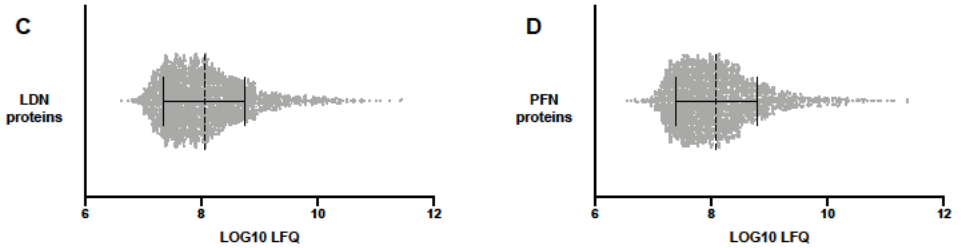

E

TOP 25 BY ABUNDANCE
Lactotransferrin
Actin cytoplasmic 1
Protein S100-A8
Histone H2B
Histone H4
Cathepsin G
Neutrophil elastase
Myosin-9
Myeloperoxidase
Histone H3 2
Histone H2A
Alpha-enolase
Pyruvate kinase PKM
Leukocyte elastase inhibitor
Glyceraldehyde-3-phosphate dehydrogenase
Annexin A3
Matrix metalloproteinase-9
Transketolase
Coronin-1A
Lysozyme C
Annexin A1
Gelsolin
Plastin-2
Protein S100-A9
Cofilin-1

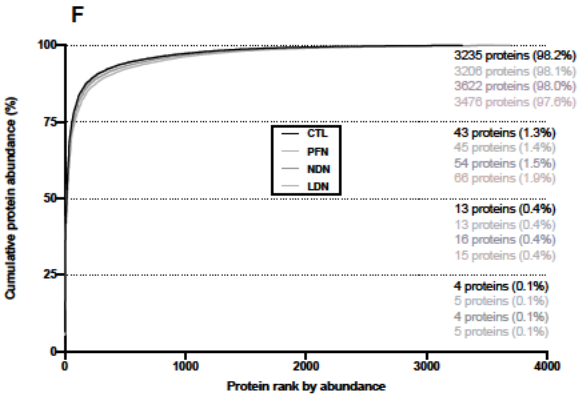

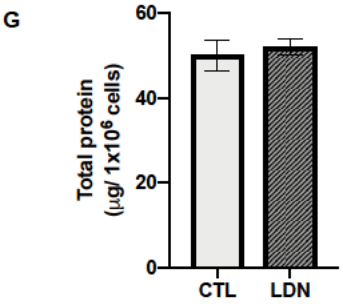

Figure 5.8: NSCLC neutrophil populations and healthy donor blood neutrophils have similar distributions of proteins by abundance and mass.

The proteomes of NSCLC neutrophil populations were compared with healthy donor control blood neutrophils. (A-D) Distribution of proteins within each neutrophil population by abundance. (E) Example of the top 25 proteins by abundance, NSCLC normal-density blood neutrophils shown. (F) The contribution of each protein to the total protein mass of each population. The number of proteins contributing to each quartile of total protein mass is shown, along with the percentage they represent of total proteins identified in that same population. (G) Total protein, NSCLC low-density blood neutrophils versus healthy donor control blood neutrophils. For all data n=5. Data represents individual proteins and mean ± standard deviation (A-D). Data represents mean ± SEM (G). CTL, healthy donor control neutrophils; NDN, normal-density neutrophils; LDN, low-density neutrophils; PFN, pleural fluid neutrophils.

5.2.8 NSCLC neutrophil populations have distinct proteomes with differential expression of proteins

The proteome of healthy donor control blood neutrophils (CTL) was compared with three NSCLC neutrophil populations; normal-density blood neutrophils (NDN), low-density blood neutrophils (LDN) and pleural fluid neutrophils (PFN).

A heat map of Pearson's correlations between samples, showed samples PFN4 and PFN5 to be outliers. After further investigation, one of these samples was found to have a very low amount of material and the other to be contaminated. Both were excluded from all subsequent analyses (Figure 5.9)

Volcano plots illustrating significantly upregulated and downregulated proteins in each NSCLC neutrophil population when compared with CTL (Figure 5.10A-C), revealed NSCLC LDN to have the most differences. Tables of the statistically significant differentially expressed proteins (LOG2 fold change >1 or <-1 and $p<0.05$) can be found in Appendix 2.

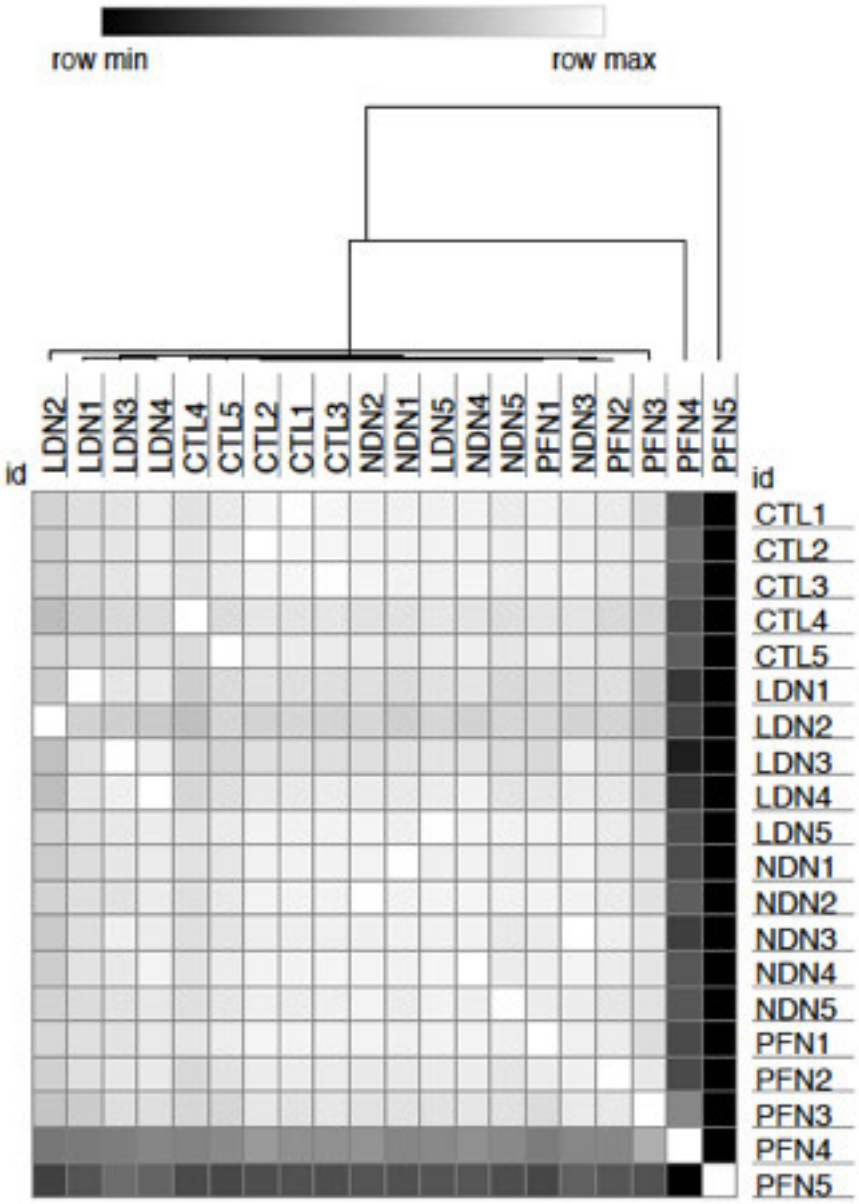

Figure 5.9: Heat map of Pearson's correlations between proteomic samples.
The proteomes of all neutrophil populations were compared, n=5. Stronger correlations have a lighter colour. CTL, healthy donor control neutrophils; NDN, normal-density neutrophils; LDN, low-density neutrophils; PFN, pleural fluid neutrophils.

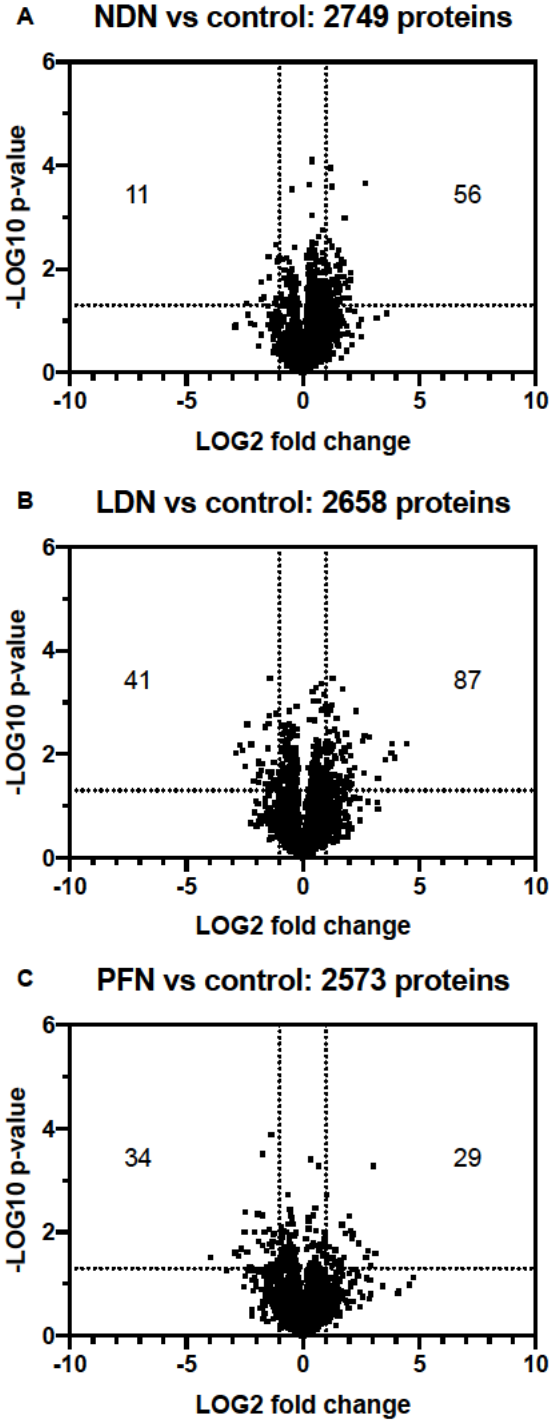

Figure 5.10: NSCLC neutrophil populations have distinct proteomes with differential expression of proteins when compared with healthy donor control blood neutrophils. *The proteomes of NSCLC neutrophil populations were compared with healthy donor control blood neutrophils, n=5. (A-C) Volcano plots illustrating significantly upregulated (right) and downregulated (left) proteins in NSCLC populations when compared with control (number indicated, tables of proteins can be found in Appendix 2). Analysed by t-test. Lines indicate LOG2 fold change >1 or <-1 and p<0.05. Data represents individual proteins. CTL, healthy donor control neutrophils; NDN, normal-density neutrophils; LDN, low-density neutrophils; PFN, pleural fluid neutrophils.*

5.2.9 NSCLC low-density blood neutrophils have reduced inflammatory response proteins and neutrophil granule proteins

In order to interrogate how differences in the proteome may impact upon neutrophil function in NSCLC, the DAVID 6.8 bioinformatics resource[97] was used to carry out biological process over-representation analyses. Biological process over-representation analysis of NSCLC LDN downregulated proteins versus CTL (LOG2 fold change<-1 and p<0.05), indicated the term inflammatory response (in bold, Table 5.4). A volcano plot highlighting significantly upregulated and downregulated inflammatory response proteins in NSCLC LDN versus CTL, revealed that most were downregulated (Figure 5.11A). Statistically significant downregulated NSCLC LDN inflammatory response proteins are shown in Figure 5.11B, and these proteins are further described in Table 5.5. To determine if the proteomic signature of NSCLC LDN matched up to their transcriptional profile, the differential expression of neutrophil granule proteins was examined in NSCLC LDN versus CTL. Most granule proteins were downregulated in NSCLC LDN with the exceptions of Azurocidin and Arginase (Figure 5.11C, gene symbols and associated neutrophil granules explained in Table 5.1). Indeed, neutrophil granule proteins as a proportion of total protein in each neutrophil sample, was significantly lower in NSCLC LDN (Figure 5.11D). However, of note, when human cytokine array data was re-visited to identify the relative expression of neutrophil granule proteins MMP-9 and Pentraxin-3 in the pleural fluid of patients with NSCLC versus pneumonia, they were not increased (Figure 5.12).

DOWNREGULATED LDN vs control	p-value	Fold change
GO:0006954~inflammatory response	**7.87E-04**	**5.95**
GO:0007186~G-protein coupled receptor signaling	1.04E-02	8.39
GO:2000427~positive regulation of apoptotic cell clearance	2.88E-02	67.13
GO:0007155~cell adhesion	2.94E-02	5.71
GO:0045766~positive regulation of angiogenesis	3.62E-02	9.59
GO:0006935~chemotaxis	4.98E-02	8.06

Table 5.4: Biological process over-representation analysis of NSCLC LDN downregulated proteins.
2658 detected proteins used as the background.

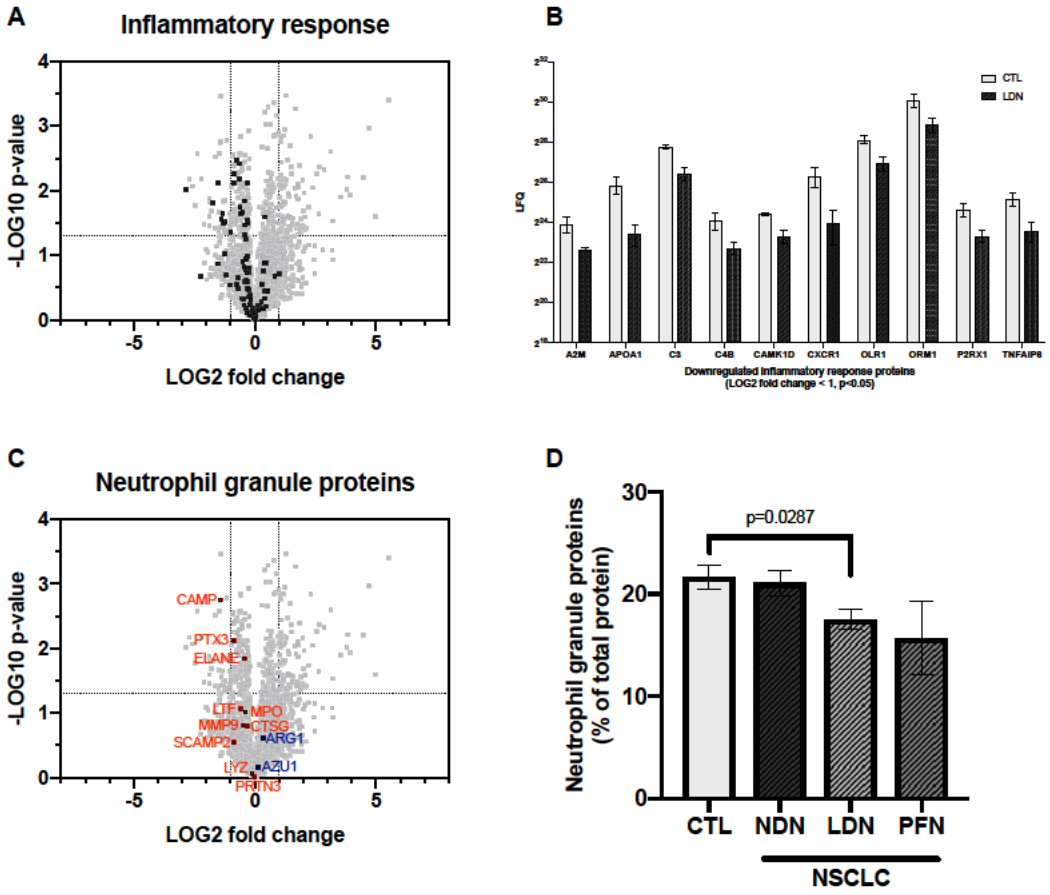

Figure 5.11: NSCLC low-density blood neutrophils have reduced inflammatory response proteins and neutrophil granule proteins.
(A) Volcano plot highlighting inflammatory response proteins in NSCLC low-density blood neutrophils versus healthy donor control blood neutrophils. (B) NSCLC low-density blood neutrophil population downregulated inflammatory response proteins. (C) Volcano plot highlighting upregulated (blue) and downregulated (red) neutrophil granule proteins in NSCLC low-density blood neutrophils versus healthy donor control blood neutrophils. (D) Neutrophil granule proteins as a proportion of total protein in each neutrophil sample, n=5 (PFN n=3). Analysed by t-test. Volcano plot lines indicate LOG2 fold change >1 or <-1 and p<0.05. Data points represent individual proteins. Other data represents mean ± SEM. CTL, healthy donor control neutrophils; NDN, normal-density neutrophils; LDN, low-density neutrophils; PFN, pleural fluid neutrophils.

Gene symbol	Protein	Role
A2M	Alpha-2-macroglobulin	Protease inhibitor/ inflammatory cytokine inhibitor
APOA1	Apolipoprotein A1	Promotes cholesterol efflux
C3	Complement C3	Central role in activation of complement system
C4B	Complement C4B	Classical complement pathway
CAMK1D	Calcium dependent protein kinase 1D	Required for activation of respiratory burst
CXCR1	C-X-C motif chemokine receptor 1	Receptor for IL8
OLR1	Oxidised low-density lipoprotein receptor 1 (LOX-1)	Uptake of oxidised low-density lipoprotein
ORM1	Orosomucoid 1	Modulates acute-phase response
P2RX1	Purinergic receptor P2X 1	ATP-gated ion channel (linked to apoptosis)
TNFAIP6	TNF alpha induced protein 6	Cell-cell interactions

Table 5.5: NSCLC low-density blood neutrophil population downregulated inflammatory response proteins.
(compared with healthy donor neutrophils).

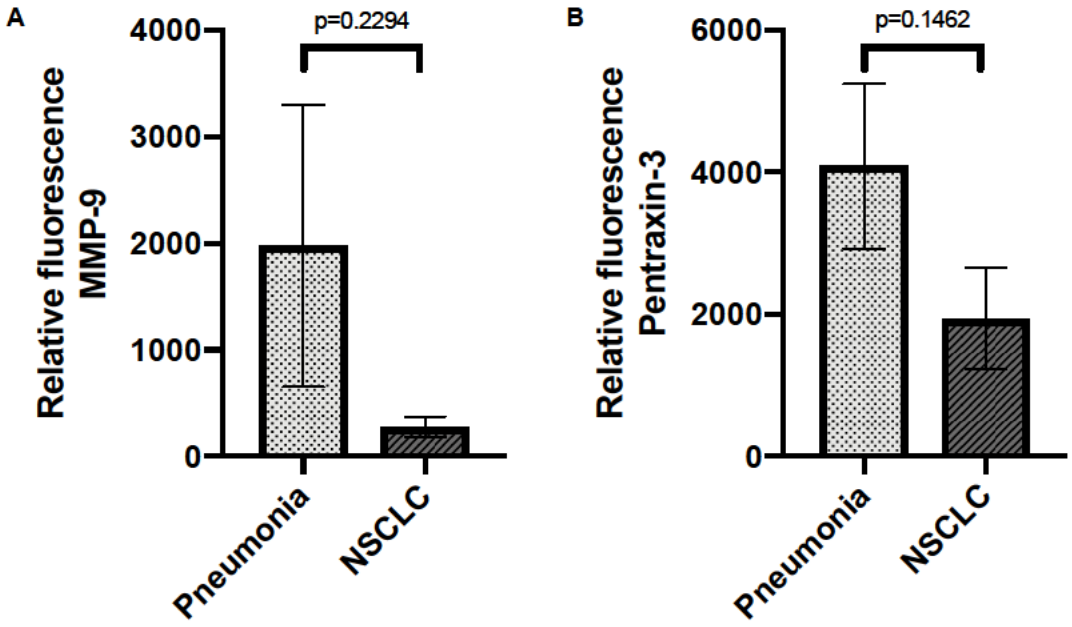

Figure 5.12: Human cytokine array of pleural fluid supernatant suggests that there is not increased neutrophil degranulation in the pleural space of NSCLC compared with pneumonia.

The relative expression of neutrophil granule proteins MMP-9 (A) and Pentraxin-3 (B) were measured in pleural fluid supernatant of patients with pneumonia (indicated by dotted shading) and NSCLC (indicated by striped shading) by human cytokine array (n=6). Analysed by unpaired t-test. Data represents mean ± SEM.

5.2.10 NSCLC low-density blood neutrophils have increased translational initiation proteins/ ribosomal proteins

Biological process over-representation analysis of NSCLC LDN upregulated proteins versus CTL (LOG2 fold change>1 and p<0.05), indicated the term translational initiation (in bold, Table 5.6). A volcano plot highlighting significantly upregulated and downregulated translational initiation proteins in NSCLC LDN versus CTL, revealed that most were upregulated (Figure 5.13A).

Indeed, many eukaryotic translation initiation factor (EIF) proteins were upregulated in NSCLC LDN when compared with CTL (Figure 5.13B). There was statistically significant upregulation of subunits of EIF3 (subunits C, E, I and L) and EIF4 (subunit E). During the initiation of transcription, EIF3 controls the assembly of the 40S ribosomal subunit on mRNA, and EIF4 interacts with EIF3 and binds the 5' cap structure of mRNA.

Furthermore, when ribosomal proteins (identified by KEGG) were quantified as a proportion of neutrophil total protein, this was found to be upregulated in NSCLC LDN (Figure 5.14A). In fact, a wide range of both 40S ribosomal proteins (Figure 5.14B) and 60S ribosomal proteins (Figure 5.14C) were upregulated in NSCLC LDN.

UPREGULATED LDN vs control	p-value	Fold change
GO:0006364~rRNA processing	1.22E-16	8.71
GO:0006614~SRP-dependent co-translational protein targeting to membrane	1.42E-16	9.29
GO:0000184~nuclear-transcribed mRNA catabolic process, nonsense-mediated decay	1.10E-15	8.56
GO:0006412~translation	3.06E-14	7.41
GO:0006413~translational initiation	**1.69E-13**	**6.87**
GO:0006270~DNA replication initiation	8.68E-07	24.57
GO:0006260~DNA replication	**8.97E-07**	**8.69**
GO:0002181~cytoplasmic translation	2.85E-05	14.33
GO:0006268~DNA unwinding involved in DNA replication	4.28E-05	20.47
GO:0000082~G1/S transition of mitotic cell cycle	1.16E-04	8.36
GO:0042254~ribosome biogenesis	3.77E-04	22.93
GO:0000028~ribosomal small subunit assembly	7.36E-04	19.11
GO:0051291~protein hetero-oligomerization	1.44E-02	5.12
GO:0042274~ribosomal small subunit biogenesis	1.61E-02	14.33

Table 5.6: Biological process over-representation analysis of NSCLC LDN upregulated proteins.
2658 detected proteins used as the background.

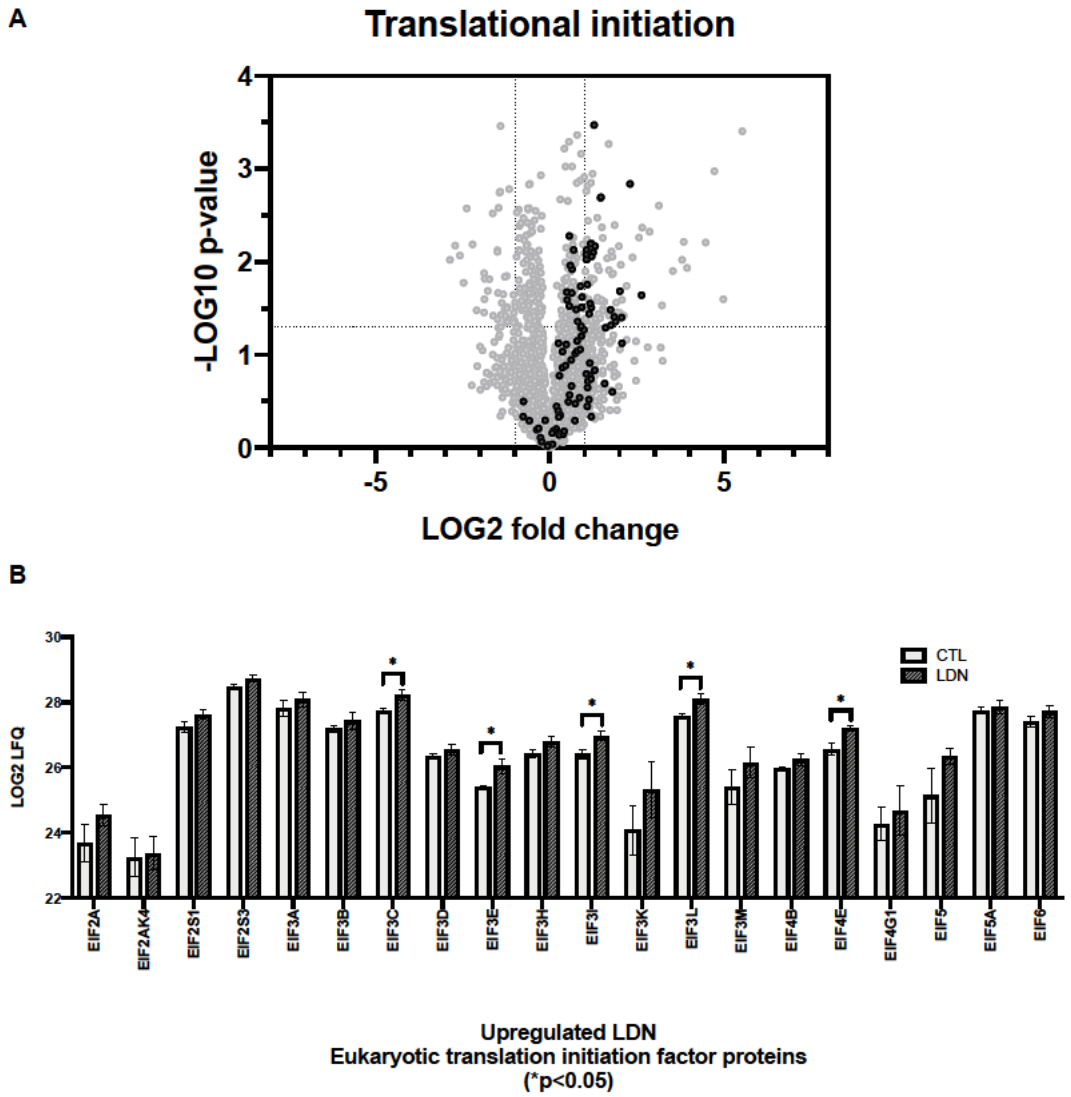

Figure 5.13: NSCLC low-density blood neutrophils have increased translational initiation proteins.
(A) Volcano plot highlighting significantly upregulated and downregulated translational initiation proteins in NSCLC low-density blood neutrophils versus healthy donor control blood neutrophils, n=5. (B) Eukaryotic translation initiation factor (EIF) proteins that were upregulated in NSCLC low-density blood neutrophils. Analysed by t-test. Volcano plot lines indicate LOG2 fold change >1 or <-1 and p<0.05. Data represents individual proteins and mean ± SEM. CTL, healthy donor control neutrophils; LDN, low-density neutrophils.

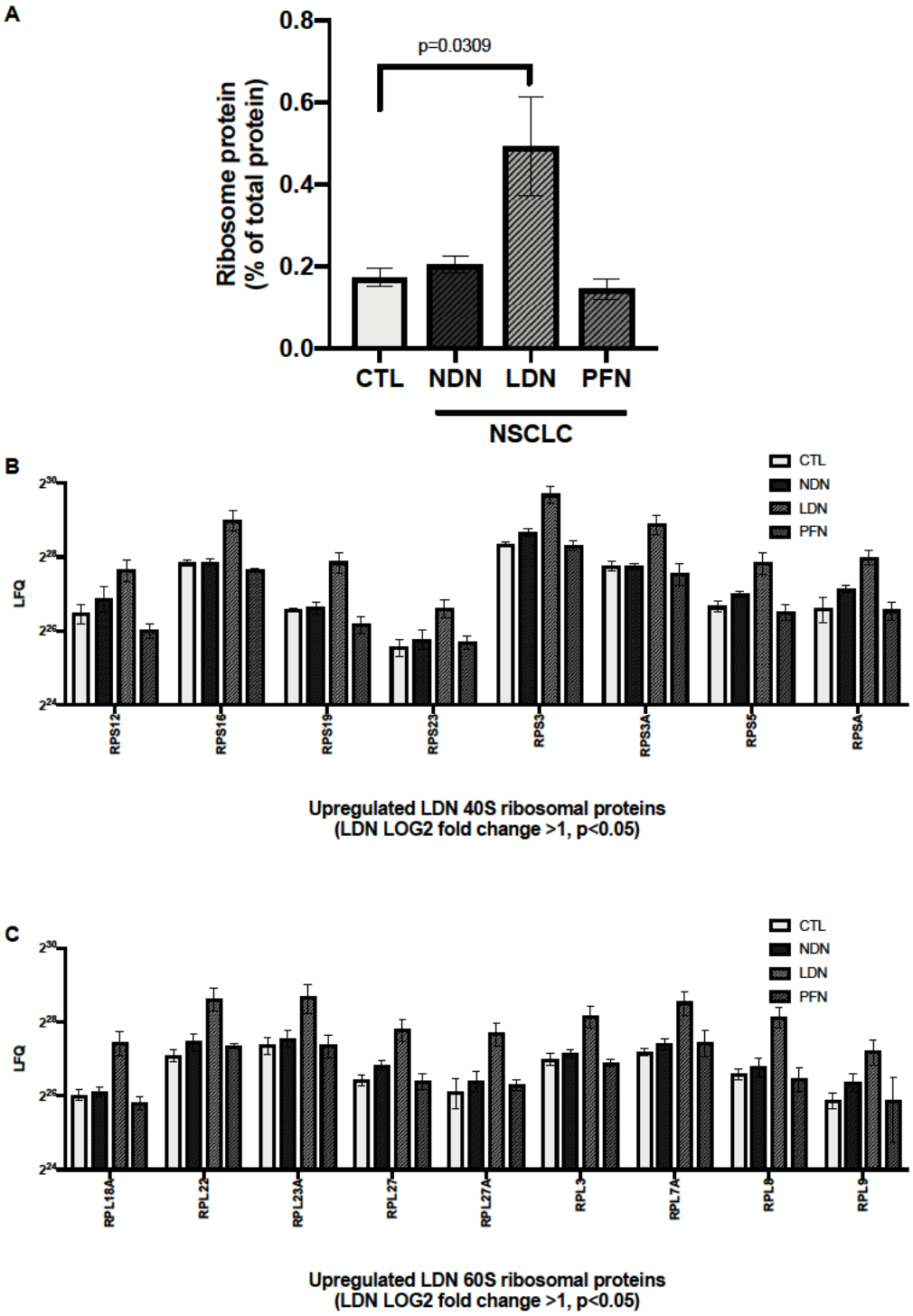

Figure 5.14: Ribosomal proteins are upregulated in NSCLC low-density blood neutrophils.

(A) Ribosomal protein (KEGG) as a proportion of neutrophil total protein, n=5 (pleural fluid neutrophils n=3). (B) NSCLC low-density blood neutrophil upregulated 40S ribosomal proteins, n=5 (pleural fluid neutrophils n=3). (C) NSCLC low-density blood neutrophil upregulated 60S ribosomal proteins, n=5 (pleural fluid neutrophils n=3). Analysed by t-test. Data represents mean ± SEM. CTL, healthy donor control neutrophils; NDN, normal-density neutrophils; LDN, low-density neutrophils; PFN, pleural fluid neutrophils.

5.2.11 NSCLC low-density blood neutrophils have increased DNA replication proteins

Network analysis of NSCLC LDN upregulated proteins versus CTL (LOG2 fold change>1 and p<0.05), was carried out using GeneMania.[103] This demonstrated clustering of translational initiation proteins (orange) and also DNA replication proteins (green) (Figure 5.15). Indeed, biological process over-representation analysis had already indicated the term DNA replication (in bold, Table 5.6). DNA replication licensing factor proteins that were upregulated in NSCLC LDN (LOG2 fold change>1 and p<0.05) versus CTL are shown in Figure 5.16. Eukaryotic minichromosome maintenance protein complex consists of six gene products (MCM2-7), which form a heterohexamer that is central to DNA replication initiation and elongation. MCM2-7 were all upregulated in NSCLC LDN versus CTL.

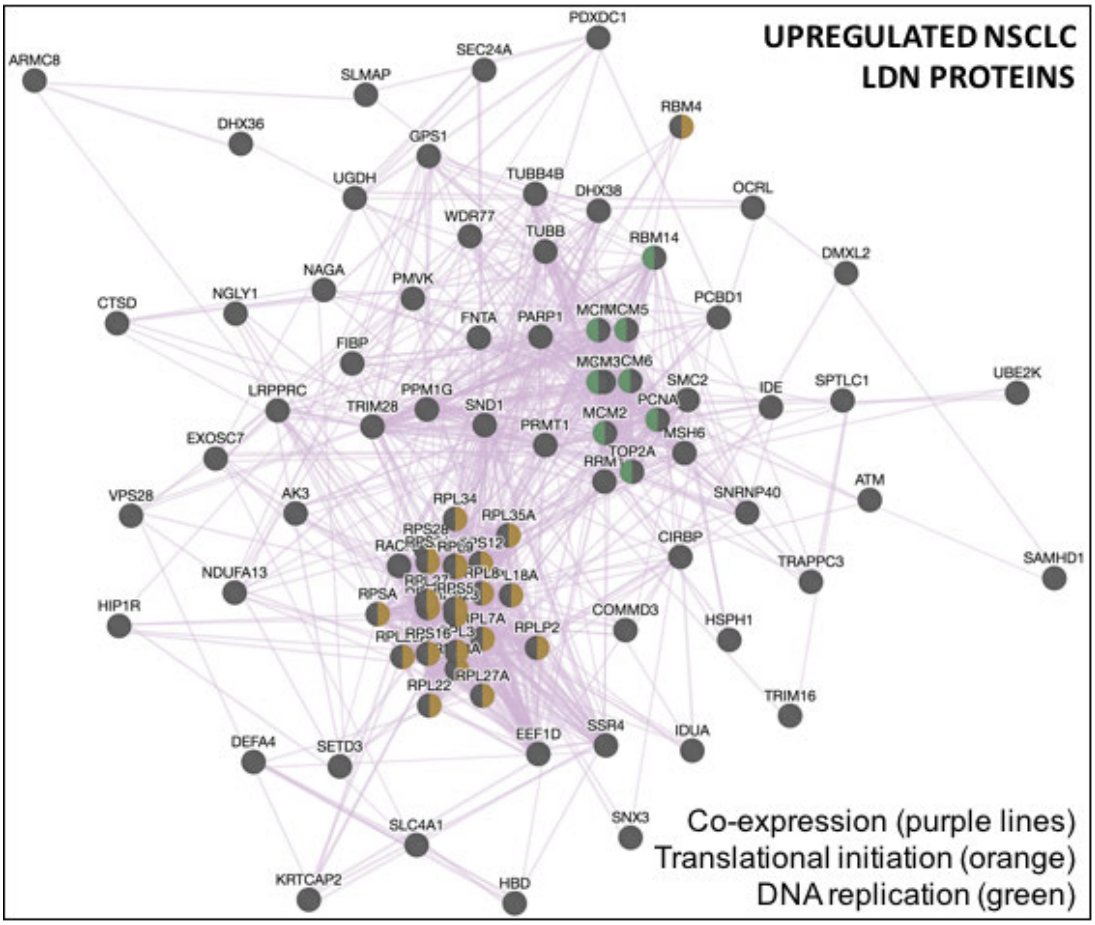

Figure 5.15: GeneMania[103] network analysis of NSCLC low-density blood neutrophil upregulated proteins.
Upregulated NSCLC low-density blood neutrophil (LDN) proteins (LOG2 fold change>1 and p<0.05) versus healthy donor control blood neutrophils. Translational initiation proteins highlighted in orange and DNA replication proteins in green.

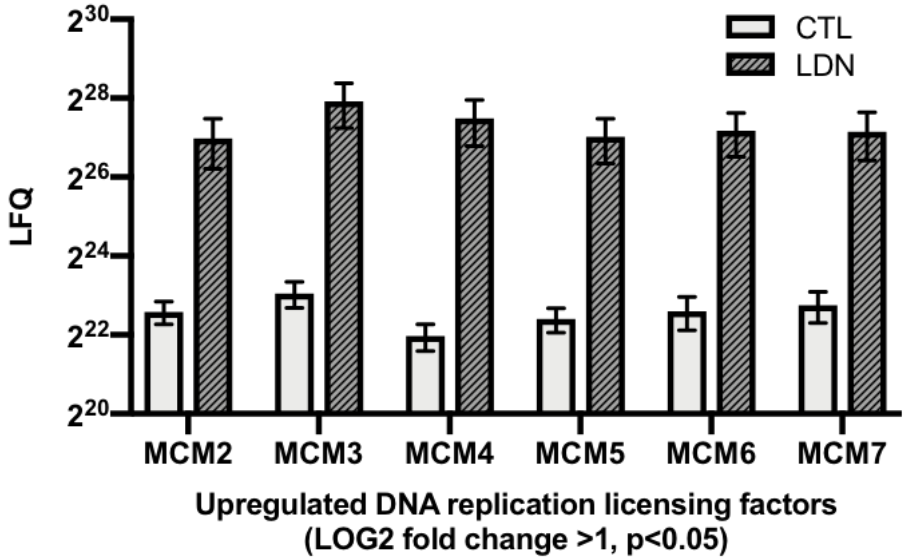

Figure 5.16: NSCLC low-density blood neutrophils have increased DNA replication proteins.

DNA replication licensing factor proteins upregulated in NSCLC low-density blood neutrophils (LOG2 fold change>1 and p<0.05) versus healthy donor control blood neutrophils, n=5. Analysed by t-test. Data represents mean ± SEM. CTL, healthy donor control neutrophils; LDN, low-density neutrophils.

5.2.12 NSCLC low-density blood neutrophils and pleural fluid neutrophils have pro-survival proteomic signatures

Finally, to establish whether NSCLC LDN and NSCLC PFN had pro-survival proteomic signatures in keeping with NanoString™ transcription data, volcano plots highlighting differentially expressed apoptosis pathway proteins (KEGG) when compared with CTL were plotted (Figure 5.17A and B). These indicated that several pro-survival apoptosis proteins were upregulated (blue) and several pro-apoptosis proteins were downregulated (red), in both NSCLC LDN and NSCLC PFN, in keeping with the established phenotypes.

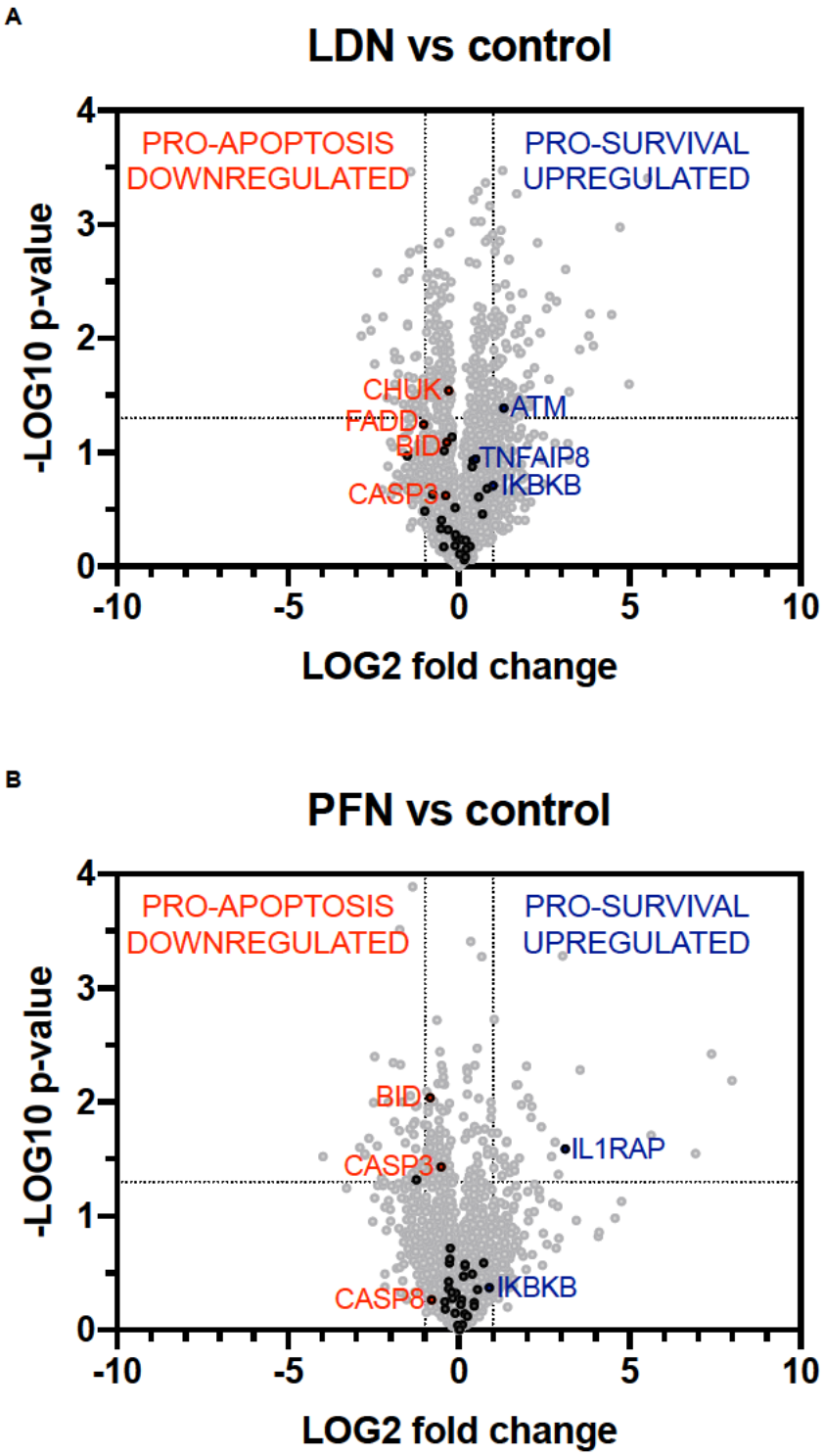

Figure 5.17: NSCLC low-density blood neutrophils and NSCLC pleural fluid neutrophils have pro-survival proteomic signatures.
Volcano plots highlighting differential expression of apoptosis pathway proteins (KEGG) (dark grey) in both NSCLC low-density blood neutrophils (A) and NSCLC pleural fluid neutrophils (B), when compared with healthy donor control blood neutrophils. Upregulated pro-survival apoptosis proteins are in blue and downregulated pro-apoptosis proteins are in red. Data represents individual proteins. Lines indicate LOG2 fold change >1 or <-1 and p<0.05. LDN, low-density neutrophils; PFN, pleural fluid neutrophils.

5.3 Discussion

The data in this chapter provide novel insights into the transcriptome and proteome of advanced NSCLC neutrophil populations, identifying features that distinguish each of them, and that may also contribute to disease outcome.

5.3.1 NSCLC low-density blood neutrophils are the most different

Both transcriptomic and proteomic studies in this chapter confirm that NSCLC low-density blood neutrophils are the most different from healthy donor blood neutrophils. This is followed by pleural fluid neutrophils (of which a subpopulation is likely to be migrated low-density neutrophils). NSCLC normal-density blood neutrophils are similar to healthy donor blood neutrophils. It was interesting to note that the protein distribution by abundance and mass was similar between all populations. NSCLC low-density blood neutrophils also had a similar amount of total protein to healthy donor blood neutrophils. Therefore, low-density neutrophils are not low-density due to total protein content.

5.3.2 CD66b, LOX-1 and CD62L as advanced NSCLC neutrophil population markers

Transcription of the genes coding for CD66b, LOX-1 and CD62L in NSCLC low-density blood neutrophils and pleural fluid neutrophils, matched the pattern that would be expected from the flow cytometry data in the neutrophil populations chapter of this thesis. As well as confirming the population phenotypes, this strengthens the argument that the low-density blood population likely migrates into the pleural space. It builds upon the work of Condamine et al.,[65] who identified LOX-1 to be transcriptionally upregulated in, and also expressed at higher levels on the surface of, G-MDSCs in several human cancers including NSCLC. It must however be noted, that in this chapter the low-density blood neutrophil transcriptional signature seen, is a composite of both $CD66^{+}CD10^{+}LOX\text{-}1^{-}$ and $CD66^{high}CD10^{-}LOX\text{-}1^{+}$ subpopulations together (low-density blood neutrophils were analysed as a whole population).

5.3.3 Altered neutrophil granule proteins in advanced NSCLC

The transcriptomic and proteomic data found in this chapter raises some interesting questions regarding neutrophil granule proteins. For a reminder of the different types of neutrophil granule and their proteins, refer back to Table 5.1. NSCLC low-density blood neutrophils were seen to have upregulated transcription of neutrophil granule proteins. This is in keeping with previous studies of low-density blood neutrophils in rheumatoid arthritis,[160] psoriasis,[162] and systemic lupus erythematosus.[158 159] In fact, Teague et al. went on to perform transmission electron microscopy of psoriasis low-density blood neutrophils, demonstrating they had more primary granules.[162] Yet in apparent opposition to this transcriptomic data, the proteomic analysis of NSCLC neutrophils in this chapter indicated an overall downregulation of granule proteins in low-density blood neutrophils, and the suggestion of a similar pattern in pleural fluid neutrophils. It must be noted that the most downregulated low-density blood neutrophil granule proteins were pentraxin-3 and cathelicidin, both found in secondary granules, and azurocidin and arginase-1 found in primary granule proteins, were not downregulated at all. However, this mismatch between transcripts and proteins raises a couple of possibilities; that the neutrophils are degranulating, or that they have not finished producing granules yet i.e. an indication of immature cell status. Some possible evidence against degranulation comes from the human cytokine array analysis of pleural fluid supernatant: pentraxin-3 (found in secondary granules) and MMP-9 (found in tertiary granules) are not increased in the pleural fluid supernatant of NSCLC, when compared with pneumonia pleural fluid supernatant. In future work, transmission electron microscopy to look at granules in NSCLC low-density blood neutrophils, may provide added information for this debate.

5.3.4 Intrinsic features of NSCLC neutrophils contributing to the pro-survival phenotype

The transcriptomic and proteomic signatures of NSCLC low-density blood neutrophils and pleural fluid neutrophils favour neutrophil survival, with downregulation of pro-apoptotic genes/ proteins, and upregulation of pro-survival genes/ proteins. Common features to both populations are downregulation in the transcription of the genes NF-κBI and FAS, and downregulation of the proteins BH3 interacting domain death agonist and caspase 3/ caspase 8. This is particularly interesting, as there are strong correlations with the work of Wright et al. investigating low-density blood neutrophils in patients with rheumatoid arthritis.[160] They found that rheumatoid arthritis low-density blood neutrophils were also pro-survival, with 20% apoptosis following 18 hours in culture. Furthermore, RNA-sequencing revealed downregulation in the transcription of several highly relevant genes: BID, CASP8, NF-κBI, RELA, TNFRSF1A (CD120a) and TNFRSF1B (CD120b). In addition, they confirmed downregulation of CASP8, NF-κBI, RELA, TNFRSF1A and TNFRSF1B by quantitative polymerase chain reaction. Finally, they showed that if healthy donor blood neutrophils were exposed to recombinant TNFα, this reduced 18-hour apoptosis, but if rheumatoid arthritis low-density blood neutrophils were exposed to recombinant TNFα, there was no added survival benefit. This has strong parallels to the autologous pleural fluid supernatant experiments found in the cancer-specific neutrophil populations chapter of this thesis, where autologous supernatant (containing significant TNFα) did not trigger any added survival benefit in NSCLC blood neutrophils, but did reduce healthy donor blood neutrophil 20-hour apoptosis. It is therefore clear that altered TNF-signalling is important to neutrophil survival, resulting in sustained inflammation in both rheumatoid arthritis and NSCLC. This has never been shown before in NSCLC. Future supportive work would include quantitative polymerase chain reaction of NF-κBI, FAS and CASP8 in NSCLC low-density blood neutrophils.

5.3.5 Increased translational initiation in NSCLC low-density blood neutrophils

Proteomic studies revealed NSCLC low-density blood neutrophils to have upregulation of translational initiation, with increased ribosomal proteins and eukaryotic translation initiation factors. This has previously been seen in human cancer low-density blood neutrophils (samples including NSCLC), where elevation of eukaryotic translation initiation factors 2 and 4 was observed.[65] Of interest, in systemic lupus erythematosus it was the $CD10^-$ subset of low-density blood neutrophils with immature banded nuclei, that were seen to be more transcriptionally active, with more peaks in the promoter regions found by assay for transposase-accessible chromatin (ATAC) sequencing.[158] It would be interesting to define said features of NSCLC low-density blood $CD66^+CD10^+LOX\text{-}1^-$ and $CD66^{high}CD10^-LOX\text{-}1^+$ neutrophil subpopulations in future work.

5.3.6 Upregulation of DNA replication proteins in NSCLC low-density blood neutrophils

It is reported in this chapter the NSCLC low-density blood neutrophils have upregulation of DNA replication proteins. This has not been previously published in human cancer research. It has been observed in rheumatoid arthritis, with increased cell-cycle gene transcripts and upregulation of CDK2, CDK4 and CDK6 by quantitative polymerase chain reaction in low-density blood neutrophils. Furthermore, 1% stained for the G2/S phase of the cell cycle.[160] In addition this was observed in systemic lupus erythematosus bioinformatics study,[159] but was a questionable finding due to contamination of the original datasets with other cells. However, it was confirmed in another systemic lupus erythematosus study, where upregulation of genes for cell cycle progression were found in the immature subset of low-density blood neutrophils.[158] Future work should include analysis of NSCLC low-density blood neutrophil cell cycle and proliferation by flow cytometry, for example by combining Ki67 and Hoechst 33342.[174]

5.3.7 Other low-density blood neutrophil transcriptomic and proteomic signatures of interest: type I interferons and S100A8/A9

In systemic lupus erythematosus, low-density blood neutrophils are thought to contribute to vascular disease through mechanisms including release of type I interferons that disrupt the function of vascular endothelial cells. Mistry et al. carried out transcriptomics of mature and immature low-density blood neutrophil subsets in systemic lupus erythematosus, noting that the mature subset of low-density blood neutrophils had upregulation of type I interferon signalling.[158] Increased type I interferon transcriptional signatures in low-density neutrophils have also been found to be associated with worse outcome in other diseases e.g. malaria.[175] In the transcriptomic and proteomic analysis of NSCLC low-density blood neutrophils carried out here, there were no significant changes in type I interferon signalling pathways. It must be noted, in contrast to the diseases described above, in cancer research, type I interferons have been associated with anti-tumour responses and lack of type I interferons associated with increased metastasis.[26 145]

Proteomics studies in systemic lupus erythematosus have identified S100A9 as a signature for low-density blood neutrophils.[176] Interestingly, in the transcriptomic analysis of NSCLC low-density blood neutrophils carried out in this chapter, S100A8 and S100A9 were both found to be upregulated. S100A8 and S100A9 were also ranked in the top 25 proteins by abundance in the proteomic studies of this chapter. In mouse models of malignancy, S100A8/A9 proteins have been shown to regulate the accumulation of MDSCs.[66] Indeed in models of colon cancer, MDSCs have been found to produce S100A8/A9, leading to an autocrine pathway for accumulation of MDSCs at metastatic sites, and furthermore, S100A8/A9 activated tumour cells promoting cancer progression.[67] Additionally, S100A8/A9 is also important in lung metastasis models, promoting the pre-metastatic niche through recruitment of myeloid cells.[54 177]

5.3.8 Wider interpretation of the data

The data in this chapter shows that NSCLC normal-density blood neutrophils are quite similar to healthy donor blood neutrophils in their transcriptomic and proteomic signatures. NSCLC low-density blood neutrophils have the most differences. NSCLC Pleural fluid neutrophils have some key differences, but likely reflect a combination of both blood populations that have migrated to the pleural space (which could explain why some of the low-density blood neutrophil signatures are lost in the pleural fluid neutrophil signatures). In addition, expression of neutrophil surface marker genes in this chapter match the phenotyping found in previous chapters of this thesis.

The key findings of this chapter (Figure 5.18) are that NSCLC low-density blood neutrophils have increased transcription of granule proteins, but reduced total granule protein, compared with healthy donor blood neutrophils. Of note, it is the primary granule proteins that are actually present in NSCLC low-density blood neutrophils. NSCLC low-density neutrophils have increased translational initiation and upregulation of DNA replication proteins versus healthy donor blood neutrophils. NSCLC low-density blood neutrophils do not upregulate type I interferons, but do upregulate S100A8/A9. Both NSCLC low-density blood neutrophils and pleural fluid neutrophils have pro-survival transcriptomic and proteomic signatures.

A key question this raises, is whether NSCLC low-density blood neutrophils are proliferating, and what impact this has upon the ability of these cells to carry out other functions e.g. pro- or anti-tumour activity.

It is widely known that acute inflammation/ infection, leads to a ‘left shift’ of the bone marrow with emergency granulopoeisis and release of immature neutrophils into the circulation. In this setting, the immature neutrophils are functional. However, in chronic inflammatory states, it would appear that this pressure on the bone marrow to release immature cells remains, but that the recruited immature cells are dysfunctional. The degree to which low-density blood neutrophils represent immature cells prematurely released from the marrow is debated.[178] Nonetheless, the data in this chapter supports the notion that, at least, the immature NSCLC low-density blood neutrophil subpopulation is indeed this. The mature NSCLC low-density blood neutrophil subpopulation may be something different, for example they may represent cells that have been modulated by their local tissue environment.

Yet, it must be noted that for the data in this chapter, all NSCLC low-density blood neutrophils were considered as a single population together. Reasoning for these theories will now be explained.

Transcriptomic and proteomic studies of neutrophils at various stages of development, have shown that neutrophil granules are produced at an immature stage of development in a controlled order.[171 172] Primary granules are formed during the myeloblast to promyelocyte stage, secondary during myelocyte to metamyelocyte stage and tertiary from the band cell to segmented cell.[17] The dogma is that mature neutrophils do not form new granules. The data from this chapter would fit with NSCLC low-density granulocytes being akin to myelocytes/ metamyelocytes i.e. formed primary granules and starting to produce their next granules. The nuclear morphology shown in previous chapters could also be in keeping with this. Of note, it has also been postulated in the literature that neutrophil nuclear morphology determines which parts of DNA are available to transcribe, resulting if a different balances of gene transcription, with the consequence of altered functional outcomes.[178] In conjunction with this, myelocytes/ metamyelocytes are known to have downregulation of pro-apoptotic transcripts for genes TNFRSF1A (CD120a), FADD, CASP8 and BID.[171] This pro-survival phenotype has uncanny similarities to that seen in this chapter in NSCLC low-density blood neutrophils and pleural fluid neutrophils. The upregulation of S100A8/A9 proteins in NSCLC low-density blood neutrophils and NSCLC neutrophil population apoptosis phenotypes, would support a model of persistent neutrophilic inflammation and recruitment.

It is interesting that NSCLC low-density blood neutrophils do not upregulate type I interferon signalling in contrast to those found in systemic lupus erythematosus. This highlights the fact that these diseases are quite different, and that parallels between studies of cancer neutrophil populations and autoimmune/ inflammatory disease neutrophil populations can only be taken so far. Indeed, in the literature low-density neutrophils in autoimmune diseases are considered to be of a predominant ‘pro-inflammatory’ phenotype, whereas those in cancer are seen to have a predominantly ‘immunosuppressive’ phenotype.[179]

The limitations of the data in the chapter are that it provides avenues that will be important to explore going forward, but more functional studies of each NSCLC neutrophil population are needed. For example, cell cycle studies of low-density

neutrophils are needed. T cell proliferation studies would confirm which populations/ subpopulations are immunosuppressive (although this has been done previously to an extent by Condamine et al.[65] see 5.1.2). It would also be very informative to study the NSCLC immature and mature low-density blood neutrophil populations separately, to tease apart which are responsible for the features observed in this chapter. Other limitations include the fact that there is no direct evidence of the effect these populations have upon tumour cells themselves. In addition, the proteomic data was limited by the relatively small number of neutrophils used, leading to loss of detection of low-abundance proteins. Changes in these low-abundance proteins could be of functional importance. Finally, whether there is any degree of plasticity in the function of neutrophils that have migrated to pleural space, needs to be investigated.

5.3.9 Summary

This chapter provides evidence that implies NSCLC low-density blood neutrophils represent immature cells that have been recruited from the bone marrow. In addition, it suggests that they retain proliferative capacity, have reduced neutrophil granules, and are pro-survival. These features are likely to impact upon their function at the pleural metastatic site; they favour sustained and ineffective inflammation, but further functional studies are needed to clarify this.

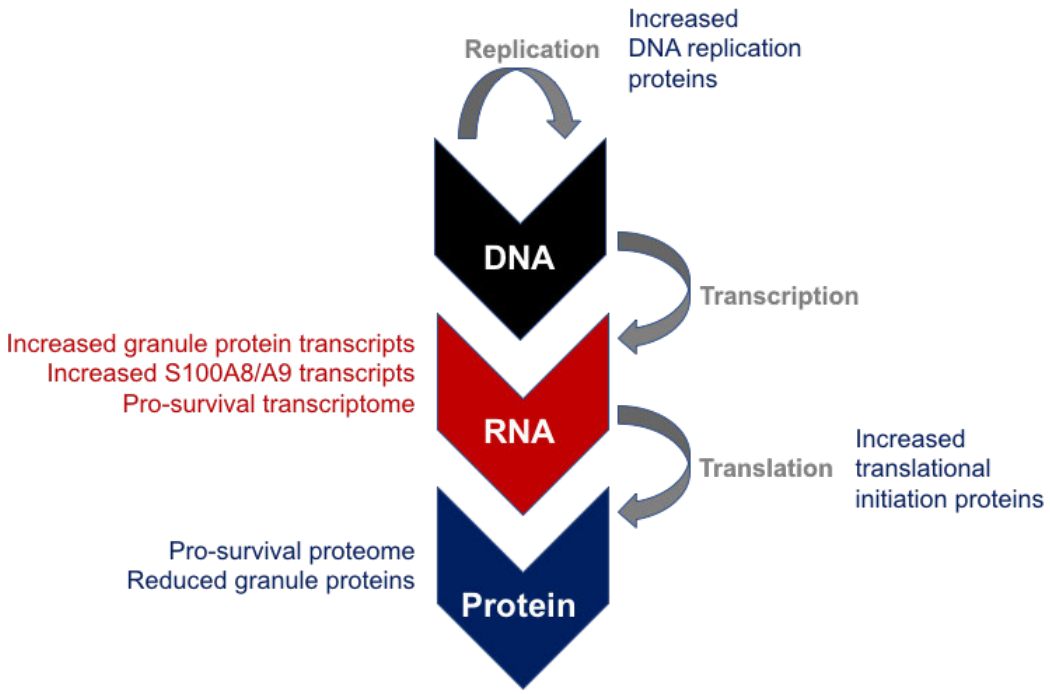

Figure 5.18: The transcriptome and proteome of NSCLC low-density blood neutrophils compared with healthy donor blood neutrophils.

Chapter 6 General discussion and future directions

6.1 Summary of key findings

Neutrophils are considered to be active players in the metastatic environment, forming an important part of the tumour niche. Neutrophil populations have been described in early stage human lung cancer, and animal models have demonstrated their importance in both pre-metastatic and established metastatic sites. However, to date there is limited data regarding human neutrophil populations in advanced lung cancer and their role. Furthermore, the underlying drivers of neutrophil behaviour at metastatic sites needs to be delineated, and could identify new therapeutic targets for immunomodulation in advanced malignancy.

The aims of this project were to investigate how neutrophil function is influenced by extrinsic signals in the NSCLC pleural metastatic microenvironment, define the neutrophil populations present in advanced NSCLC, and explore whether intrinsic properties of neutrophil populations in advanced NSCLC may define their role.

In this study, neutrophils were extracted from the pleural fluid (from the pleural metastatic site) and blood of patients with advanced NSCLC, so that their features and function could be determined. Blood and pleural fluid neutrophils were compared with those from patients with pneumonia (where neutrophil responses are generally appropriate and effective) and with blood neutrophils from healthy donors. This enabled the identification of cancer-specific signatures.

6.1.1 The NSCLC pleural environment influences neutrophil function

It is well known that malignant pleural metastatic site is hypoxic.[113-116] This study confirmed that it is also cytokine-rich, and has variable levels of glucose. Human cytokine array and ELISA studies, demonstrated that the cytokine profile of NSCLC pleural fluid is different to that seen in acute infection, favouring a phenotype of sustained and immunosuppressive inflammation.

The NSCLC pleural environment was modelled *in vitro* by culturing healthy donor neutrophils in conditions emulating the pleural space and observing the impact of these manipulations (i.e. oxygen/ glucose availability and cell conditioning with pleural fluid supernatant). This provided evidence that the NSCLC pleural environment conditions neutrophils into a state of persistent counterproductive inflammation. TNFα and hypoxia acted as pro-survival signals leading to neutrophil persistence. NSCLC pleural fluid conditioned neutrophils to suppress $CD8^+$ T cells through mechanisms that included PD-L1 expression.

The data described above is novel, as human tissue from the NSCLC pleural metastatic site has not been used in this way before. However, there were several limitations. Firstly, freshly extracted blood neutrophils were used for *in vitro* culture, rather than recruited neutrophils from a target site. It may be that changes neutrophils undergo during the process of recruitment from the blood, are relevant to their response at the target pleural site. Secondly, when PD-L1 inhibitors were used, they only partially reversed the suppression of $CD8^+$ T cells by NSCLC pleural fluid-conditioned neutrophils. There were therefore other mechanisms of suppression that have not been identified. The mechanism by which NSCLC pleural fluid conditions neutrophils to express PD-L1 has not been found either. Finally, suppression of the adaptive immune response is an indirect measure of neutrophil pro- or anti-tumour activity, and direct assays e.g. using cancer cell lines, were not utilised.

6.1.2 There are cancer-specific neutrophil populations in advanced NSCLC

To establish the phenotype of neutrophil populations in advanced NSCLC, cellular morphology, surface marker expression and functional assays were utilised. In order to find correlations across the different cell compartments, neutrophils from the blood where compared with neutrophils from the pleural space.

There was an expanded population of low-density blood neutrophils in advanced NSCLC, that were not present in health, and a proportion of which were immature with banded nuclei. A subpopulation of advanced NSCLC low-density neutrophils was $CD66^{high}$, immature ($CD10^-$), activated ($CD62L^-$) and positive for a G-MDSC marker ($LOX\text{-}1^+$). There was further evidence that these cells were also present in NSCLC pleural fluid, but in contrast these cells were not present in pneumonia

pleural fluid. NSCLC pleural fluid neutrophils expressed PD-L1 and were long-lived with increased CD120b expression (pro-survival TNFα receptor). Together this was suggestive that advanced NSCLC pleural fluid neutrophils may contribute to an environment of sustained inflammation that is immunosuppressive.

This data was particularly interesting, as the advanced NSCLC neutrophil population phenotypes identified were the exact opposite of those attributed to neutrophils in early stage NSCLC, where neutrophils are believed to be helpful at the primary tumour site.[46 47 57]

A key limitation of the above data, is that T cell co-culture assays were not carried out using patient-derived neutrophils. The data also raised further questions that have not been answered. Autologous pleural fluid supernatant did not act as a survival signal to NSCLC neutrophils at 20 hours. It may be that this was because cell-intrinsic changes in apoptosis pathways, or other environmental signals e.g. hypoxia, were more powerful drivers of survival.

6.1.3 Intrinsic properties of neutrophil populations in advanced NSCLC define their function

In order to explore whether intrinsic properties of neutrophil populations in advanced NSCLC dictate their role, NSCLC low-density blood neutrophils, NSCLC normal-density neutrophils and NSCLC pleural fluid neutrophils, were defined by their transcriptomic and proteomic signatures.

This provided evidence that implied NSCLC low-density blood neutrophils represent immature cells that have been recruited from the bone marrow. NSCLC low-density blood neutrophils appear to retain proliferative capacity (upregulation of DNA replication proteins), are translationally active (upregulation of translational initiation proteins), have reduced neutrophil granule proteins (in the context of upregulated neutrophil granule gene transcripts), and are pro-survival (both in apoptosis proteins expressed and gene transcripts). These features are likely to impact upon their function once recruited to the pleural metastatic site; favouring sustained and ineffective inflammation.

Whilst there is transcriptomic data for human cancer neutrophil populations, to date, there have not been any publications regarding the proteome of human cancer neutrophil populations. A strength of this study is that the transcriptomic data could be directly compared with the proteomic data to look for connections and also to highlight discordance. A further strength of the proteomic data is that this unbiased approach leads to the identification of novel changes. A weakness of the data, was that by using a targeted transcriptomic assay, some gene transcripts of interest were not measured. Another weakness is that being limited to small numbers of neutrophils for proteomics, meant that detection of some low abundance proteins, which may be important, will have been lost. Finally, it must be remembered that whilst this –omics data raises some very interesting findings and theories, these need to be confirmed or refuted through functional studies.

A final consideration is what this thesis says in terms of how the neutrophil populations described correlate to neutrophil populations described elsewhere in cancer research, and whether some of the terminology used in the literature can be harmonised. The data presented here, would point toward G-MDSC and immature low-density neutrophils being one and the same population, reflecting a dysregulation of bone marrow neutrophil release, resulting in an expanded dysfunctional immature circulating neutrophil population, with detrimental actions when recruited to the target site. The data also highlights the importance of both the local tissue environment and intrinsic programming, in determining neutrophil function.

6.2 Future directions

6.2.1 Pleural environment

It is interesting that NSCLC pleural fluid glucose is not low. This could be because it is being replenished, but another explanation may be that immune cells are not utilising it. It would therefore be of intrigue to explore what form of metabolism NSCLC neutrophil populations carry out.

In terms of NSCLC pleural fluid supernatant conditioning of healthy donor neutrophils, transcriptomics, proteomics or cytokine profiling of the conditioned cells, could give more information regarding how pleural fluid supernatant does this. Indeed, it would be informative to investigate whether NSCLC pleural fluid supernatant can condition bone marrow neutrophils of healthy donors i.e. immature cells, or pleural fluid neutrophils from pneumonia patients into a 'pro-tumour' state.

With regard to T cell co-culture studies, these could be repeated with pneumonia pleural fluid supernatant to see if the phenotype is different. Furthermore, to thoroughly interrogate the mechanism of T cell suppression by NSCLC pleural fluid-conditioned neutrophils, mechanisms other than PD-L1 e.g. arginase or reactive oxygen species, should be sought. In addition, separate experiments using cancer cell lines could be used to look directly at pro- or anti-tumour activity of pleural fluid-conditioned neutrophils.

6.2.2 NSCLC neutrophil populations

Whilst it seems likely that the $CD66b^{high}CD11b^{+}CD15^{+}CD14^{-}CD49d^{-}CD10^{-}CD62L^{-}LOX\text{-}1^{+}$ NSCLC low-density neutrophil population identified represents the neutrophils with banded nuclei seen by cellular morphology, this needs to be proven. One approach would be to use fluorescence-activated cell sorting to isolate the cells and then make cytospins to observe their morphology.

The data would also suggest that autologous pleural fluid supernatant (and therefore possibly TNFα) does not act as a survival signal for NSCLC neutrophils (at 20 hours). Future work could use longer time points or recombinant TNFα to test this further.

To test whether NSCLC neutrophil populations are pro- or anti- tumour with a functional assay, T cell co-culture (or tumour cell line co-culture) needs to be carried out with NSCLC neutrophil populations (although this has been done previously to an extent with NSCLC blood neutrophil populations by Condamine et al.[65]).

Lastly, it would helpful to test whether NSCLC neutrophil populations display plasticity, for example by investigating whether they can by polarised to an anti-tumour phenotype through exposure to IFNβ.

6.2.3 Avenues highlighted by –omics studies

In order to prove that NSCLC low-density blood neutrophils are proliferative, analysis of cell cycle and proliferation is needed e.g. by flow cytometry combining Ki67 and Hoechst 33342. In addition, it would be highly informative to carry out transcriptomic and proteomic studies with pneumonia neutrophil populations to see how they differ from cancer. Finally, in future work it may be pertinent to study the immature and mature low-density neutrophil populations separately, as they may have important differences.

6.3 Conclusions

To summarise, this study defines the neutrophil populations present in advanced NSCLC and the influence of the NSCLC pleural metastatic environment upon their function, as well as their intrinsic features. The data favours a phenotype of sustained neutrophilic inflammation that is immunosuppressive at the metastatic site, with a subpopulation of immature cells. A more complete understanding of the mechanisms, and proof of neutrophil functional impact upon tumour outcome, may help to identify new therapeutic targets for immunomodulation in advanced cancer.

References

1. Curnutte, J. T., Kipnes, R. S. & Babior, B. M. Defect in pyridine nucleotide dependent superoxide production by a particulate fraction from the cranulocytes of patients with chronic granulomatous disease. *N. Engl. J. Med.* **293,** 628–632 (1975).
2. Hidalgo, A., Chilvers, E. R., Summers, C. & Koenderman, L. The Neutrophil Life Cycle. *Trends Immunol.* **40,** 584–597 (2019).
3. Cartwright, G. E., Athens, J. W. & Wintrobe, M. M. The kinetics of granulopoiesis in normal man. *Blood* **24,** 780–803 (1964).
4. Wochenschrift, J. A. D.-D. M. Die neutrophilen Leukozyten bei Infektionskrankheiten. *thieme-connect.com* (1904). doi:10.1055/s-0029-1187277
5. Amulic, B., Cazalet, C., Hayes, G. L., Metzler, K. D. & Zychlinsky, A. Neutrophil function: from mechanisms to disease. *Annu. Rev. Immunol.* **30,** 459–489 (2012).
6. Lee, W. L., Harrison, R. E. & Grinstein, S. Phagocytosis by neutrophils. *Microbes Infect.* **5,** 1299–1306 (2003).
7. Winterbourn, C. C., Kettle, A. J. & Hampton, M. B. Reactive Oxygen Species and Neutrophil Function. *Annu. Rev. Biochem.* **85,** 765–792 (2016).
8. Brinkmann, V. *et al.* Neutrophil extracellular traps kill bacteria. *Science* **303,** 1532–1535 (2004).
9. Savill, J. S. *et al.* Macrophage phagocytosis of aging neutrophils in inflammation. Programmed cell death in the neutrophil leads to its recognition by macrophages. *Journal of Clinical Investigation* **83,** 865–875 (1989).
10. Whyte, M., Renshaw, S., Lawson, R. & Bingle, C. Apoptosis and the regulation of neutrophil lifespan. *Biochem. Soc. Trans.* **27,** 802–807 (1999).
11. Pillay, J. *et al.* In vivo labeling with 2H2O reveals a human neutrophil lifespan of 5.4 days. *Blood* **116,** 625–627 (2010).
12. Ichim, G. & Tait, S. W. G. A fate worse than death: apoptosis as an oncogenic process. *Nature Reviews Cancer* **16,** 539–548 (2016).
13. Colotta, F., Re, F., Polentarutti, N., Sozzani, S. & Mantovani, A. Modulation of granulocyte survival and programmed cell death by cytokines and bacterial products. *Blood* **80,** 2012–2020 (1992).
14. Hannah, S. *et al.* Hypoxia prolongs neutrophil survival in vitro. *FEBS Lett.* **372,** 233–237 (1995).
15. Fuchs, T. A. *et al.* Novel cell death program leads to neutrophil extracellular traps. *J. Cell Biol.* **176,** 231–241 (2007).
16. Joyce, J. A. & Pollard, J. W. Microenvironmental regulation of metastasis. *Nature Reviews Cancer* **9,** 239–252 (2009).
17. Coffelt, S. B., Wellenstein, M. D. & de Visser, K. E. Neutrophils in cancer: neutral no more. *Nature Reviews Cancer* **16,** 431–446 (2016).
18. Jablonska, J., Lang, S., Sionov, R. V. & Granot, Z. The regulation of pre-metastatic niche formation by neutrophils. *Oncotarget* **8,** 112132–112144 (2017).
19. Kim, H. K., La Luz Sierra, De, M., Williams, C. K., Gulino, A. V. & Tosato, G. G-CSF down-regulation of CXCR4 expression identified as a mechanism for mobilization of myeloid cells. *Blood* **108,** 812–820 (2006).

20. Templeton, A. J. *et al.* Prognostic role of neutrophil-to-lymphocyte ratio in solid tumors: a systematic review and meta-analysis. *J. Natl. Cancer Inst.* **106,** dju124 (2014).
21. Shen, M. *et al.* Tumor-associated neutrophils as a new prognostic factor in cancer: a systematic review and meta-analysis. *PLoS ONE* **9,** e98259 (2014).
22. Gentles, A. J. *et al.* The prognostic landscape of genes and infiltrating immune cells across human cancers. *Nat. Med.* **21,** 938–945 (2015).
23. Shitara, K. *et al.* Meta-analysis of neutropenia or leukopenia as a prognostic factor in patients with malignant disease undergoing chemotherapy. *Cancer Chemother. Pharmacol.* **68,** 301–307 (2011).
24. Mouchemore, K. A., Anderson, R. L. & Hamilton, J. A. Neutrophils, G-CSF and their contribution to breast cancer metastasis. *FEBS J.* **285,** 665–679 (2018).
25. Fridlender, Z. G. *et al.* Polarization of tumor-associated neutrophil phenotype by TGF-beta: "N1" versus 'N2' TAN. *Cancer Cell* **16,** 183–194 (2009).
26. Andzinski, L. *et al.* Type I IFNs induce anti-tumor polarization of tumor associated neutrophils in mice and human. *Int. J. Cancer* **138,** 1982–1993 (2016).
27. Qian, B.-Z. & Pollard, J. W. Macrophage Diversity Enhances Tumor Progression and Metastasis. *Cell* **141,** 39–51 (2010).
28. Houghton, A. M. *et al.* Neutrophil elastase-mediated degradation of IRS-1 accelerates lung tumor growth. *Nat. Med.* **16,** 219–223 (2010).
29. Dallegri, F. *et al.* Tumor cell lysis by activated human neutrophils: analysis of neutrophil-delivered oxidative attack and role of leukocyte function-associated antigen 1. *Inflammation* **15,** 15–30 (1991).
30. Finisguerra, V. *et al.* MET is required for the recruitment of anti-tumoural neutrophils. *Nature* **522,** 349–353 (2015).
31. Tecchio, C. *et al.* IFNalpha-stimulated neutrophils and monocytes release a soluble form of TNF-related apoptosis-inducing ligand (TRAIL/Apo-2 ligand) displaying apoptotic activity on leukemic cells. *Blood* **103,** 3837–3844 (2004).
32. de Looff, M., de Jong, S. & Kruyt, F. A. E. Multiple Interactions Between Cancer Cells and the Tumor Microenvironment Modulate TRAIL Signaling: Implications for TRAIL Receptor Targeted Therapy. *Front Immunol* **10,** 1530 (2019).
33. Bergers, G. & Benjamin, L. E. Tumorigenesis and the angiogenic switch. *Nature Reviews Cancer* **3,** 401–410 (2003).
34. Shojaei, F. *et al.* Bv8 regulates myeloid-cell-dependent tumour angiogenesis. *Nature* **450,** 825–831 (2007).
35. Deryugina, E. I. *et al.* Tissue-infiltrating neutrophils constitute the major in vivo source of angiogenesis-inducing MMP-9 in the tumor microenvironment. *Neoplasia* **16,** 771–788 (2014).
36. Nozawa, H., Chiu, C. & Hanahan, D. Infiltrating neutrophils mediate the initial angiogenic switch in a mouse model of multistage carcinogenesis. *Proc. Natl. Acad. Sci. U.S.A.* **103,** 12493–12498 (2006).
37. Aldabbous, L. *et al.* Neutrophil Extracellular Traps Promote Angiogenesis: Evidence From Vascular Pathology in Pulmonary Hypertension. *Arteriosclerosis, Thrombosis, and Vascular Biology* **36,** ATVBAHA.116.307634–2087 (2016).

38. Loffredo, S. *et al.* Group V Secreted Phospholipase A2Induces the Release of Proangiogenic and Antiangiogenic Factors by Human Neutrophils. *Front Immunol* **8,** 443 (2017).
39. Rodriguez, P. C. *et al.* Arginase I production in the tumor microenvironment by mature myeloid cells inhibits T-cell receptor expression and antigen-specific T-cell responses. *Cancer Res.* **64,** 5839–5849 (2004).
40. Coffelt, S. B. *et al.* IL-17-producing γδ T cells and neutrophils conspire to promote breast cancer metastasis. *Nature* **522,** 345–348 (2015).
41. Negorev, D. *et al.* Human neutrophils can mimic myeloid-derived suppressor cells (PMN-MDSC) and suppress microbead or lectin-induced T cell proliferation through artefactual mechanisms. *Sci Rep* **8,** 3135 (2018).
42. Michaeli, J. *et al.* Tumor-associated neutrophils induce apoptosis of non-activated CD8 T-cells in a TNFα and NO-dependent mechanism, promoting a tumor-supportive environment. *Oncoimmunology* **6,** e1356965 (2017).
43. Wang, T.-T. *et al.* Tumour-activated neutrophils in gastric cancer foster immune suppression and disease progression through GM-CSF-PD-L1 pathway. *Gut* **66,** 1900–1911 (2017).
44. Faget, J. *et al.* Neutrophils and Snail Orchestrate the Establishment of a Pro-tumor Microenvironment in Lung Cancer. *Cell Rep* **21,** 3190–3204 (2017).
45. Mishalian, I. *et al.* Neutrophils recruit regulatory T-cells into tumors via secretion of CCL17--a new mechanism of impaired antitumor immunity. *Int. J. Cancer* **135,** 1178–1186 (2014).
46. Singhal, S. *et al.* Origin and Role of a Subset of Tumor-Associated Neutrophils with Antigen-Presenting Cell Features in Early-Stage Human Lung Cancer. *Cancer Cell* **30,** 120–135 (2016).
47. Eruslanov, E. B. *et al.* Tumor-associated neutrophils stimulate T cell responses in early-stage human lung cancer. *J. Clin. Invest.* **124,** 5466–5480 (2014).
48. Mensurado, S. *et al.* Tumor-associated neutrophils suppress pro-tumoral IL-17+ γδ T cells through induction of oxidative stress. *PLoS Biol.* **16,** e2004990 (2018).
49. Cools-Lartigue, J. *et al.* Neutrophil extracellular traps sequester circulating tumor cells and promote metastasis. *J. Clin. Invest.* **123,** 3446–3458 (2013).
50. Kanamaru, R. *et al.* Low density neutrophils (LDN) in postoperative abdominal cavity assist the peritoneal recurrence through the production of neutrophil extracellular traps (NETs). *Sci Rep* **8,** 632–10 (2018).
51. Decker, A. S. *et al.* Prognostic Role of Blood NETosis in the Progression of Head and Neck Cancer. *Cells* **8,** 946 (2019).
52. Szczerba, B. M. *et al.* Neutrophils escort circulating tumour cells to enable cell cycle progression. *Nature* **13,** 273 (2019).
53. Huh, S. J., Liang, S., Sharma, A., Dong, C. & Robertson, G. P. Transiently entrapped circulating tumor cells interact with neutrophils to facilitate lung metastasis development. *Cancer Res.* **70,** 6071–6082 (2010).
54. Kowanetz, M. *et al.* Granulocyte-colony stimulating factor promotes lung metastasis through mobilization of Ly6G+Ly6C+ granulocytes. *Proc. Natl. Acad. Sci. U.S.A.* **107,** 21248–21255 (2010).

55. Granot, Z. *et al.* Tumor entrained neutrophils inhibit seeding in the premetastatic lung. *Cancer Cell* **20,** 300–314 (2011).
56. Gershkovitz, M. *et al.* TRPM2 mediates neutrophil killing of disseminated tumor cells. *Cancer Res.* canres.3614.2017 (2018). doi:10.1158/0008-5472.CAN-17-3614
57. Eruslanov, E. B. Phenotype and function of tumor-associated neutrophils and their subsets in early-stage human lung cancer. *Cancer Immunol. Immunother.* **23,** 139–10 (2017).
58. Sagiv, J. Y. *et al.* Phenotypic diversity and plasticity in circulating neutrophil subpopulations in cancer. *Cell Rep* **10,** 562–573 (2015).
59. Mishalian, I., Granot, Z. & Fridlender, Z. G. The diversity of circulating neutrophils in cancer. *Immunobiology* **222,** 82–88 (2016).
60. Galdiero, M. R., Varricchi, G., Loffredo, S., Mantovani, A. & Marone, G. Roles of neutrophils in cancer growth and progression. *J. Leukoc. Biol.* **103,** 457–464 (2018).
61. Eruslanov, E. B., Singhal, S. & Albelda, S. M. Mouse versus Human Neutrophils in Cancer: A Major Knowledge Gap. *Trends in Cancer* **3,** 149–160 (2017).
62. Marini, O. *et al.* Mature CD10(+) and immature CD10(-) neutrophils present in G-CSF-treated donors display opposite effects on T cells. *Blood* **129,** 1343–1356 (2017).
63. Mackey, J. B. G., Coffelt, S. B. & Carlin, L. M. Neutrophil Maturity in Cancer. *Front Immunol* **10,** 1912 (2019).
64. Veglia, F., Perego, M. & Gabrilovich, D. Myeloid-derived suppressor cells coming of age. *Nat. Immunol.* **19,** 108–119 (2018).
65. Condamine, T. *et al.* Lectin-type oxidized LDL receptor-1 distinguishes population of human polymorphonuclear myeloid-derived suppressor cells in cancer patients. *Sci Immunol* **1,** aaf8943–aaf8943 (2016).
66. Sinha, P. *et al.* Proinflammatory S100 proteins regulate the accumulation of myeloid-derived suppressor cells. *J. Immunol.* **181,** 4666–4675 (2008).
67. Ichikawa, M., Williams, R., Wang, L., Vogl, T. & Srikrishna, G. S100A8/A9 activate key genes and pathways in colon tumor progression. *Mol. Cancer Res.* **9,** 133–148 (2011).
68. Brandau, S., Moses, K. & Lang, S. The kinship of neutrophils and granulocytic myeloid-derived suppressor cells in cancer: cousins, siblings or twins? *Semin. Cancer Biol.* **23,** 171–182 (2013).
69. Moses, K. & Brandau, S. Human neutrophils: Their role in cancer and relation to myeloid-derived suppressor cells. *Semin. Immunol.* **28,** 187–196 (2016).
70. Shaul, M. E. & Fridlender, Z. G. Tumour-associated neutrophils in patients with cancer. *Nat Rev Clin Oncol* **14,** 1014 (2019).
71. Walmsley, S. R. *et al.* Hypoxia-induced neutrophil survival is mediated by HIF-1α–dependent NF-κB activity. *Journal of Experimental Medicine* **201,** 105–115 (2005).
72. Sadiku, P. *et al.* Prolyl hydroxylase 2 inactivation enhances glycogen storage and promotes excessive neutrophilic responses. *J. Clin. Invest.* **127,** 3407–3420 (2017).
73. Kumar, S. & Dikshit, M. Metabolic Insight of Neutrophils in Health and Disease. *Front Immunol* **10,** 2099 (2019).
74. Rice, C. M. *et al.* Tumour-elicited neutrophils engage mitochondrial metabolism to circumvent nutrient limitations and maintain immune inhibition. *The Journal of Immunology* **200,** 108.19–108.19 (2018).

75. Veglia, F. *et al.* Fatty acid transport protein 2 reprograms neutrophils in cancer. *Nature* **569,** 73–78 (2019).
76. Wellenstein, M. D. & de Visser, K. E. Fatty Acids Corrupt Neutrophils in Cancer. *Cancer Cell* **35,** 827–829 (2019).
77. Hsu, B. E., Tabariès, S., Johnson, R. M., reports, S. A. C.2019. Immature Low-Density Neutrophils Exhibit Metabolic Flexibility that Facilitates Breast Cancer Liver Metastasis. *cell.com*
78. Hossain, F. *et al.* Inhibition of Fatty Acid Oxidation Modulates Immunosuppressive Functions of Myeloid-Derived Suppressor Cells and Enhances Cancer Therapies. *Cancer Immunol Res* **3,** 1236–1247 (2015).
79. van Egmond, M. & Bakema, J. E. Neutrophils as effector cells for antibody-based immunotherapy of cancer. *Semin. Cancer Biol.* **23,** 190–199 (2013).
80. Kousis, P. C., Henderson, B. W., Maier, P. G. & Gollnick, S. O. Photodynamic therapy enhancement of antitumor immunity is regulated by neutrophils. *Cancer Res.* **67,** 10501–10510 (2007).
81. Suttmann, H. *et al.* Neutrophil granulocytes are required for effective Bacillus Calmette-Guérin immunotherapy of bladder cancer and orchestrate local immune responses. *Cancer Res.* **66,** 8250–8257 (2006).
82. Steele, C. W. *et al.* CXCR2 Inhibition Profoundly Suppresses Metastases and Augments Immunotherapy in Pancreatic Ductal Adenocarcinoma. *Cancer Cell* **29,** 832–845 (2016).
83. Colak, S. & Dijke, Ten, P. Targeting TGF-β Signaling in Cancer. *Trends in Cancer* **3,** 56–71 (2017).
84. Ho, A.-S. *et al.* Neutrophil elastase as a diagnostic marker and therapeutic target in colorectal cancers. *Oncotarget* **5,** 473–480 (2014).
85. Glodde, N. *et al.* Reactive Neutrophil Responses Dependent on the Receptor Tyrosine Kinase c-MET Limit Cancer Immunotherapy. *Immunity* **47,** 789–802.e9 (2017).
86. Cancer Research UK. Lung Cancer. *Lung Cancer (CRUK)* Available at: https://www.cancerresearchuk.org/about-cancer/lung-cancer. (Accessed: 10 January 2020)
87. Herbst, R. S., Morgensztern, D. & Boshoff, C. The biology and management of non-small cell lung cancer. *Nature* **553,** 446–454 (2018).
88. Sharpe, A. H. & Pauken, K. E. The diverse functions of the PD1 inhibitory pathway. *Nat. Rev. Immunol.* **18,** 153–167 (2018).
89. Leach, D. R., Krummel, M. F. & Allison, J. P. Enhancement of antitumor immunity by CTLA-4 blockade. *Science* **271,** 1734–1736 (1996).
90. Dong, H. *et al.* Tumor-associated B7-H1 promotes T-cell apoptosis: a potential mechanism of immune evasion. *Nat. Med.* **8,** 793–800 (2002).
91. Haslett, C., Guthrie, L. A., Kopaniak, M. M., Johnston, R. B. & Henson, P. M. Modulation of multiple neutrophil functions by preparative methods or trace concentrations of bacterial lipopolysaccharide. *Am. J. Pathol.* **119,** 101–110 (1985).
92. Hamburger, A. W., Dunn, F. E. & White, C. P. Percoll density gradient separation of cells from human malignant effusions. *Br. J. Cancer* **51,** 253–258 (1985).
93. Aleman, M. *et al.* In tuberculous pleural effusions, activated neutrophils undergo apoptosis and acquire a dendritic cell-like phenotype. *J. Infect. Dis.* **192,** 399–409 (2005).

94. Dorward, D. A. *et al.* Technical Advance: Autofluorescence-based sorting: rapid and nonperturbing isolation of ultrapure neutrophils to determine cytokine production. *J. Leukoc. Biol.* **94,** 193–202 (2013).
95. Murray, J. *et al.* Regulation of neutrophil apoptosis by tumor necrosis factor-alpha: requirement for TNFR55 and TNFR75 for induction of apoptosis in vitro. *Blood* **90,** 2772–2783 (1997).
96. Cowburn, A. S., Deighton, J., Walmsley, S. R. & Chilvers, E. R. The survival effect of TNF-alpha in human neutrophils is mediated via NF-kappa B-dependent IL-8 release. *Eur. J. Immunol.* **34,** 1733–1743 (2004).
97. Huang, D. W., Sherman, B. T. & Lempicki, R. A. Systematic and integrative analysis of large gene lists using DAVID bioinformatics resources. *Nat Protoc* **4,** 44–57 (2009).
98. Howden, A. J. M. *et al.* Quantitative analysis of T cell proteomes and environmental sensors during T cell differentiation. *Nat. Immunol.* **20,** 1542–1554 (2019).
99. Hughes, C. S. *et al.* Ultrasensitive proteome analysis using paramagnetic bead technology. *Mol. Syst. Biol.* **10,** 757 (2014).
100. Cox, J. & Mann, M. MaxQuant enables high peptide identification rates, individualized p.p.b.-range mass accuracies and proteome-wide protein quantification. *Nat. Biotechnol.* **26,** 1367–1372 (2008).
101. Tyanova, S., Temu, T. & Cox, J. The MaxQuant computational platform for mass spectrometry-based shotgun proteomics. *Nat Protoc* **11,** 2301–2319 (2016).
102. Tyanova, S. *et al.* The Perseus computational platform for comprehensive analysis of (prote)omics data. *Nat. Methods* **13,** 731–740 (2016).
103. Warde-Farley, D. *et al.* The GeneMANIA prediction server: biological network integration for gene prioritization and predicting gene function. *Nucleic Acids Res.* **38,** W214–20 (2010).
104. Walmsley, S. R. *et al.* Prolyl hydroxylase 3 (PHD3) is essential for hypoxic regulation of neutrophilic inflammation in humans and mice. *J. Clin. Invest.* **121,** 1053–1063 (2011).
105. Thompson, A. A. R. *et al.* Hypoxia-inducible factor 2α regulates key neutrophil functions in humans, mice, and zebrafish. *Blood* **123,** 366–376 (2014).
106. Watts, E. R. & Walmsley, S. R. Inflammation and Hypoxia: HIF and PHD Isoform Selectivity. *Trends in Molecular Medicine* **25,** 33–46 (2019).
107. Hiramatsu, S. *et al.* Gastric cancer cells alter the immunosuppressive function of neutrophils. *Oncol. Rep.* (2019). doi:10.3892/or.2019.7410
108. Singel, K. L. *et al.* Mature neutrophils suppress T cell immunity in ovarian cancer microenvironment. *JCI Insight* **4,** 11310 (2019).
109. Sahn, S. A. Pleural diseases related to metastatic malignancies. *Eur. Respir. J.* **10,** 1907–1913 (1997).
110. Light, R. W., MacGregor, M. I., Luchsinger, P. C. & Ball, W. C. Pleural effusions: the diagnostic separation of transudates and exudates. *Ann. Intern. Med.* **77,** 507–513 (1972).
111. Clive, A. O. *et al.* Predicting survival in malignant pleural effusion: development and validation of the LENT prognostic score. *Thorax* **69,** 1098–1104 (2014).

112. Psallidas, I. *et al.* Development and validation of response markers to predict survival and pleurodesis success in patients with malignant pleural effusion (PROMISE): a multicohort analysis. *Lancet Oncol.* **19,** 930–939 (2018).
113. Funahashi, A., Sarkar, T. K., Kory, R. C. PO 2 , PCO 2 , and pH in pleural effusion. *J Lab Clin Med* ***78,*** *1006* (1971).
114. Houston, M. C. Pleural effusion: diagnostic value of measurements of PO2, PCO2, and pH. *South. Med. J.* **74,** 585–589 (1981).
115. Ayoub, A. K. & Kerkeni, A. H. [The pH, PCO2 and PO2 of pleural fluid. Variations and diagnostic value]. *Rev Pneumol Clin* **40,** 243–250 (1984).
116. Limthongkul, S., Charoenlap, P., Nuchprayoon, C. & Songkhla, Y. N. Relationships between pleural fluid pH, PCO2 to pleural fluid PO2, amylase, protein, glucose and white cells in tuberculous and malignant effusions. *J Med Assoc Thai* **73,** 429–432 (1990).
117. Light, R. W., MacGregor, M. I., Ball, W. C., Jr. & Luchsinger, P. C. Diagnostic Significance of Pleural Fluid pH and PCO2. *Chest* **64,** 591–596 (1973).
118. Thomas, R., Cheah, H. M., Creaney, J., Turlach, B. A. & Lee, Y. C. G. Longitudinal Measurement of Pleural Fluid Biochemistry and Cytokines in Malignant Pleural Effusions. *Chest* **149,** 1494–1500 (2016).
119. Donnenberg, A. D., Luketich, J. D., Dhupar, R. & Donnenberg, V. S. Treatment of malignant pleural effusions: the case for localized immunotherapy. *J Immunother Cancer* **7,** 110–5 (2019).
120. Sterman, D. H. *et al.* A phase I clinical trial of single-dose intrapleural IFN-beta gene transfer for malignant pleural mesothelioma and metastatic pleural effusions: high rate of antitumor immune responses. *Clin. Cancer Res.* **13,** 4456–4466 (2007).
121. Dallegri, F. & Ottonello, L. Neutrophil--mediated cytotoxicity against tumour cells: state of art. *Arch. Immunol. Ther. Exp. (Warsz.)* **40,** 39–42 (1992).
122. Gon, S., Gatanaga, T. & Sendo, F. Involvement of two types of TNF receptor in TNF-alpha induced neutrophil apoptosis. *Microbiol. Immunol.* **40,** 463–465 (1996).
123. Ward, C. *et al.* NF-κB Activation Is a Critical Regulator of Human Granulocyte Apoptosis in Vitro. *Journal of Biological Chemistry* **274,** 4309–4318 (1999).
124. Millares, L. *et al.* Tumor-associated metabolic and inflammatory responses in early stage non-small cell lung cancer: Local patterns and prognostic significance. *Lung Cancer* **122,** 124–130 (2018).
125. Charles, K. A. *et al.* The tumor-promoting actions of TNF-alpha involve TNFR1 and IL-17 in ovarian cancer in mice and humans. *J. Clin. Invest.* **119,** 3011–3023 (2009).
126. Pelletier, M., Micheletti, A. & Cassatella, M. A. Modulation of human neutrophil survival and antigen expression by activated CD4+ and CD8+ T cells. *J. Leukoc. Biol.* **88,** 1163–1170 (2010).
127. Dumitru, C. A., Fechner, M. K., Hoffmann, T. K., Lang, S. & Brandau, S. A novel p38-MAPK signaling axis modulates neutrophil biology in head and neck cancer. *J. Leukoc. Biol.* **91,** 591–598 (2012).
128. He, G. *et al.* Peritumoural neutrophils negatively regulate adaptive immunity via the PD-L1/PD-1 signalling pathway in hepatocellular carcinoma. *J. Exp. Clin. Cancer Res.* **34,** 141–11 (2015).

129. Leliefeld, P. H. C., Koenderman, L. & Pillay, J. How Neutrophils Shape Adaptive Immune Responses. *Front Immunol* **6,** 471 (2015).
130. Hu, X. *et al.* Transmembrane TNF-α Promotes Suppressive Activities of Myeloid-Derived Suppressor Cells via TNFR2. *The Journal of Immunology* **192,** 1320–1331 (2014).
131. Comen, E. *et al.* TNF is a key cytokine mediating neutrophil cytotoxic activity in breast cancer patients. *NPJ Breast Cancer* **2,** 16009 (2016).
132. Li, Q. *et al.* Efficacy and safety of recombinant human tumor necrosis factor application for the treatment of malignant pleural effusion caused by lung cancer. *Thorac Cancer* **7,** 136–139 (2016).
133. Li, L. *et al.* Impaired T cell function in malignant pleural effusion is caused by TGF-β derived predominantly from macrophages. *Int. J. Cancer* **139,** 2261–2269 (2016).
134. Ceyhan, B. B., Ozgün, S., Celikel, T., Yalçin, M. & Koç, M. IL-8 in pleural effusion. *Respir Med* **90,** 215–221 (1996).
135. Iglesias, D. *et al.* Metalloproteinases and tissue inhibitors of metalloproteinases in exudative pleural effusions. *Eur. Respir. J.* **25,** 104–109 (2005).
136. Zhou, J., Zhao, Q. & Yao, H. [The significance of detecting tumor necrosis factor-alpha and its receptors in serum and pleural effusion in differentiating tuberculosis and malignant pleural effusions]. *Zhonghua Jie He He Hu Xi Za Zhi* **23,** 158–160 (2000).
137. Li, M. *et al.* Diagnostic accuracy of tumor necrosis factor-alpha, interferon-gamma, interleukin-10 and adenosine deaminase 2 in differential diagnosis between tuberculous pleural effusion and malignant pleural effusion. *J Cardiothorac Surg* **9,** 118 (2014).
138. Qian, Q. *et al.* Role of monocyte chemoattractant protein-1, tumor necrosis factor-alpha and interleukin-6 in the control of malignant pleural effusion and survival in patients with primary lung adenocarcinoma. *Int. J. Biol. Markers* **27,** e118–24 (2012).
139. Atef, H. M., Okab, A. A., mehy, Al, G. F. & Beheisy, El, M. M. The role of tumor necrosis factor alpha in differentiation between malignant and non malignant pleural effusion. *Egyptian Journal of Chest Diseases and Tuberculosis* **65,** 605–612 (2016).
140. Shiraz, Iran & Attar, A. Changes in the Cell Surface Markers During Normal Hematopoiesis: A Guide to Cell Isolation. *Global Journal of Hematology and Blood Transfusion* **1,** 20–28 (2014).
141. Steinbach, K. H. *et al.* Estimation of kinetic parameters of neutrophilic, eosinophilic, and basophilic granulocytes in human blood. *Blut* **39,** 27–38 (1979).
142. Barrera, L. *et al.* CD47 overexpression is associated with decreased neutrophil apoptosis/phagocytosis and poor prognosis in non-small-cell lung cancer patients. *Br. J. Cancer* **117,** 385–397 (2017).
143. Park, J. *et al.* Cancer cells induce metastasis-supporting neutrophil extracellular DNA traps. *Sci Transl Med* **8,** 361ra138–361ra138 (2016).
144. Yan, H. H. *et al.* Gr-1+CD11b+ myeloid cells tip the balance of immune protection to tumor promotion in the premetastatic lung. *Cancer Res.* **70,** 6139–6149 (2010).
145. Wu, C.-F. *et al.* The lack of type I interferon induces neutrophil-mediated pre-metastatic niche formation in the mouse lung. *Int. J. Cancer* **137,** 837–847 (2015).
146. Coffelt, S. B. *et al.* IL-17-producing γδ T cells and neutrophils conspire to promote breast cancer metastasis. *Nature* **522,** 345–348 (2015).

147. Wang, D., Sun, H., Wei, J., Cen, B. & DuBois, R. N. CXCL1 Is Critical for Premetastatic Niche Formation and Metastasis in Colorectal Cancer. *Cancer Res.* **77,** 3655–3665 (2017).
148. Light, R. W., Erozan, Y. S. & Ball, W. C. Cells in Pleural Fluid: Their Value in Differential Diagnosis. *Arch Intern Med* **132,** 854–860 (1973).
149. Basak, S. K. *et al.* The malignant pleural effusion as a model to investigate intratumoral heterogeneity in lung cancer. *PLoS ONE* **4,** e5884 (2009).
150. Light, R. W. Pleural Effusion. *NEJM* **346,** 1971–1977 (2009).
151. Gustafson, M. P. *et al.* A method for identification and analysis of non-overlapping myeloid immunophenotypes in humans. *PLoS ONE* **10,** e0121546 (2015).
152. Teixeira, L. R. *et al.* Profile of Metalloproteinases and Their Association with Inflammatory Markers in Pleural Effusions. *Lung* **194,** 1021–1027 (2016).
153. Lee, Y. S. *et al.* Prognostic impact of a new score using neutrophil-to-lymphocyte ratios in the serum and malignant pleural effusion in lung cancer patients. *BMC Cancer* **17,** 557–8 (2017).
154. Nieto, J. C. *et al.* Migrated T lymphocytes into malignant pleural effusions: an indicator of good prognosis in lung adenocarcinoma patients. *Sci Rep* **9,** 2996 (2019).
155. Lee, J. *et al.* Laboratory Discrimination Between Neutrophilic Malignant and Parapneumonic Pleural Effusions. *Am. J. Med. Sci.* **358,** 115–120 (2019).
156. Liu, Y. *et al.* Phenotypic and clinical characterization of low density neutrophils in patients with advanced lung adenocarcinoma. *Oncotarget* **8,** 90969–90978 (2017).
157. Barrera, L. *et al.* Levels of peripheral blood polymorphonuclear myeloid-derived suppressor cells and selected cytokines are potentially prognostic of disease progression for patients with non-small cell lung cancer. *Cancer Immunol. Immunother.* **67,** 1393–1406 (2018).
158. Mistry, P. *et al.* Transcriptomic, epigenetic, and functional analyses implicate neutrophil diversity in the pathogenesis of systemic lupus erythematosus. *PNAS* **3,** 201908576 (2019).
159. Kegerreis, B. J. *et al.* Genomic Identification of Low-Density Granulocytes and Analysis of Their Role in the Pathogenesis of Systemic Lupus Erythematosus. *J. Immunol.* **202,** 3309–3317 (2019).
160. Wright, H. L., Makki, F. A., Moots, R. J. & Edwards, S. W. Low-density granulocytes: functionally distinct, immature neutrophils in rheumatoid arthritis with altered properties and defective TNF signalling. *J. Leukoc. Biol.* (2016). doi:10.1189/jlb.5A0116-022R
161. Herteman, N., Vargas, A. & Lavoie, J.-P. Characterization of Circulating Low-Density Neutrophils Intrinsic Properties in Healthy and Asthmatic Horses. *Sci Rep* **7,** 7743 (2017).
162. Teague, H. L. *et al.* Neutrophil Subsets, Platelets, and Vascular Disease in Psoriasis. *JACC Basic Transl Sci* **4,** 1–14 (2019).
163. Cloke, T., Munder, M., Taylor, G., Müller, I. & Kropf, P. Characterization of a novel population of low-density granulocytes associated with disease severity in HIV-1 infection. *PLoS ONE* **7,** e48939 (2012).
164. Drifte, G., Dunn-Siegrist, I., Tissières, P. & Pugin, J. Innate immune functions of immature neutrophils in patients with sepsis and severe systemic inflammatory response syndrome. *Crit. Care Med.* **41,** 820–832 (2013).

165. Cohen, T. S. *et al.* Staphylococcus aureus drives expansion of low-density neutrophils in diabetic mice. *Journal of Clinical Investigation* **129,** 2133–2144 (2019).
166. Deng, Y. *et al.* Low-Density Granulocytes Are Elevated in Mycobacterial Infection and Associated with the Severity of Tuberculosis. *PLoS ONE* **11,** e0153567 (2016).
167. Barrera, L. *et al.* Cytokine profile determined by data-mining analysis set into clusters of non-small-cell lung cancer patients according to prognosis. *Ann. Oncol.* **26,** 428–435 (2015).
168. Fridlender, Z. G. *et al.* Transcriptomic analysis comparing tumor-associated neutrophils with granulocytic myeloid-derived suppressor cells and normal neutrophils. *PLoS ONE* **7,** e31524 (2012).
169. Shaul, M. E. *et al.* Tumor-associated neutrophils display a distinct N1 profile following TGFβ modulation: A transcriptomics analysis of pro- vs. antitumor TANs. *Oncoimmunology* **5,** e1232221 (2016).
170. Zilionis, R. *et al.* Single-Cell Transcriptomics of Human and Mouse Lung Cancers Reveals Conserved Myeloid Populations across Individuals and Species. *Immunity* **50,** 1317–1334.e10 (2019).
171. Theilgaard-Mönch, K. *et al.* The transcriptional program of terminal granulocytic differentiation. *Blood* **105,** 1785–1796 (2005).
172. Rørvig, S., Østergaard, O., Heegaard, N. H. H. & Borregaard, N. Proteome profiling of human neutrophil granule subsets, secretory vesicles, and cell membrane: correlation with transcriptome profiling of neutrophil precursors. *J. Leukoc. Biol.* **94,** 711–721 (2013).
173. Evrard, M. *et al.* Developmental Analysis of Bone Marrow Neutrophils Reveals Populations Specialized in Expansion, Trafficking, and Effector Functions. *Immunity* **48,** 364–379.e8 (2018).
174. Tan, T. C. J. *et al.* Suboptimal T-cell receptor signaling compromises protein translation, ribosome biogenesis, and proliferation of mouse CD8 T cells. *PNAS* **114,** E6117–E6126 (2017).
175. Rocha, B. C. *et al.* Type I Interferon Transcriptional Signature in Neutrophils and Low-Density Granulocytes Are Associated with Tissue Damage in Malaria. *Cell Rep* **13,** 2829–2841 (2015).
176. Pavón, E. J. *et al.* Increased expression and phosphorylation of the two S100A9 isoforms in mononuclear cells from patients with systemic lupus erythematosus: a proteomic signature for circulating low-density granulocytes. *J Proteomics* **75,** 1778–1791 (2012).
177. Hiratsuka, S., Watanabe, A., Aburatani, H. & Maru, Y. Tumour-mediated upregulation of chemoattractants and recruitment of myeloid cells predetermines lung metastasis. *Nat. Cell Biol.* **8,** 1369–1375 (2006).
178. Ng, L. G., Ostuni, R. & Hidalgo, A. Heterogeneity of neutrophils. *Nat. Rev. Immunol.* **70,** 3813 (2019).
179. Silvestre-Roig, C., Fridlender, Z. G., Glogauer, M. & Scapini, P. Neutrophil Diversity in Health and Disease. *Trends Immunol.* **40,** 565–583 (2019).

Appendix

Appendix 1: List of statistically significant differentially expressed transcripts

NSCLC Normal Density Neutrophils versus Healthy Donor Controls

Probe Name	Log2 Fold Change	p-value
ARG1	3.41	0.0010
IL18R1	3.02	0.0317
ANXA1	2.68	0.0174
IL1R2	2.46	0.0052
S100A8	1.88	0.0493
CEBPA	1.86	0.0294
TXN	1.77	0.0348
SCIN	1.72	0.0262
CD40	1.72	0.0413
CD244	1.71	0.0072
TGFA	1.67	0.0389
PTGER2	1.62	0.0011
ITGAM	1.60	0.0343
CD84	1.31	0.0327
ALOX5	1.30	0.0447
NOL7	1.21	0.0075
PELI1	1.12	0.0207
TUBA4A	1.10	0.0223
SKI	1.09	0.0207
CPA3	1.02	0.0245
ABCF1	1.08	0.0272
ADAMTS14	1.14	0.0123
PSME2	1.19	0.0278
DDR2	1.45	0.0092
LAMB3	1.51	0.0108
ADAMTS9	1.54	0.0025
TNF	1.59	0.0019
RAD51	1.89	0.0264

NSCLC Low Density Neutrophils versus Healthy Donor Controls

Probe Name	Log2 Fold Change	p value
NKG7	6 95	0 0003
CEACAM8	6 18	0 0000
MMP8	6 13	0 0012
CTSG	5 62	0 0012
RNASE2	5 47	0 0001
RNASE3	5 43	0 0065
CAMP	5 34	0 0000
MPO	5 16	0 0002
CYBB	4 66	0 0004
ANXA1	4 61	0 0004
ARG1	4 19	0 0003
PGLYRP1	3 91	0 0007
LGALS3	3 74	0 0001
TMEM173	3 72	0 0187
COL17A1	3 53	0 0001
H ST1H1C	3 46	0 0001
ANXA4	3 45	0 0020
PTGER2	3 40	0 0002
TOP2A	3 30	0 0028
OLR1	3 30	0 0186
CLEC5A	2 88	0 0008
FCN1	2 78	0 0031
LTA4H	2 76	0 0001
CASP10	2 71	0 0000
CLC	2 47	0 0457
S100A8	2 46	0 0057
CEACAM1	2 45	0 0158
FUT4	2 43	0 0004
CEBPA	2 41	0 0100
TM7SF3	2 39	0 0007
TUBB	2 30	0 0021
PTX3	2 20	0 0268
ERG	2 18	0 0045
SPTBN1	2 17	0 0006
MMP9	2 08	0 0313
L18	2 01	0 0162
FAF1	1 99	0 0005
CALR	1 93	0 0026
SERP NB6	1 82	0 0049
GSN	1 80	0 0041
CD47	1 77	0 0025
HPRT1	1 75	0 0004
NOL7	1 74	0 0016
TGB1	1 66	0 0009
TGAM	1 63	0 0217
L18R1	1 60	0 0299
TNFA P8	1 59	0 0040
PFDN6	1 56	0 0033
S100A9	1 56	0 0244
GUSB	1 51	0 0082
GRN	1 50	0 0169
TXN	1 41	0 0235
PRDX3	1 37	0 0091
C3AR1	1 36	0 0305
ETS1	1 36	0 0130
HMGB1	1 32	0 0185
MAPK14	1 23	0 0435
H ST2H2AA3	1 21	0 0009
TRAF2	1 03	0 0102
B RC5	1 03	0 0326
KZF1	1 02	0 0072

Probe Name	Log2 Fold Change	p value
DNAJC14	1 02	0 0100
MAP2K4	1 03	0 0028
CTSS	1 04	0 0324
H VEP1	1 06	0 0295
MAPK13	1 06	0 0268
PSME2	1 06	0 0035
TLR6	1 08	0 0082
C4A	1 08	0 0395
NR2F6	1 09	0 0058
MMP1	1 11	0 0202
CYT P	1 12	0 0351
B D	1 15	0 0190
CXCL13	1 16	0 0121
TUBA1A	1 16	0 0401
L1RL1	1 17	0 0462
FPR3	1 18	0 0160
SK L	1 18	0 0008
CXCL3	1 18	0 0156
ER3	1 20	0 0278
CCL23	1 22	0 0184
NS G1	1 22	0 0027
COSLG	1 24	0 0314
SMAD1	1 25	0 0012
PLAU	1 26	0 0288
TGAX	1 26	0 0445
PRRX1	1 26	0 0172
NAMPT	1 27	0 0284
STAT6	1 27	0 0315
MAFB	1 27	0 0223
CXCR4	1 28	0 0047
FAS	1 28	0 0040
L27RA	1 29	0 0009
YES1	1 29	0 0020
GF1	1 30	0 0144
VAMP2	1 31	0 0047
CD36	1 32	0 0128
ADORA3	1 32	0 0291
ADAMTS17	1 32	0 0233
HOXD4	1 35	0 0374
CD1C	1 36	0 0018
DDR2	1 36	0 0061
TLR10	1 36	0 0020
PSMB9	1 37	0 0193
BMP8A	1 38	0 0108
RGS6	1 39	0 0317
P M2	1 40	0 0221
TLR3	1 40	0 0352
TNFSF9	1 41	0 0354
L9	1 42	0 0348
SERP NB7	1 42	0 0014
SQSTM1	1 43	0 0004
TAPBP	1 48	0 0185
MX2	1 49	0 0034
MAPK11	1 49	0 0164
SELE	1 50	0 0255
K TLG	1 50	0 0004
KCNAB1	1 50	0 0286
L5RA	1 51	0 0377
STAT1	1 53	0 0017
COL1A2	1 53	0 0270
TAP1	1 55	0 0194
GATA2	1 55	0 0212
CXCL5	1 55	0 0315

Probe Name	Log2 Fold Change	p value
CCL20	1 58	0 0383
CCL11	1 58	0 0389
CLEC1B	1 58	0 0276
CDKN1A	1 59	0 0243
ANOS1	1 60	0 0442
TNFSF4	1 61	0 0413
CD34	1 62	0 0461
CD70	1 64	0 0201
CXCL9	1 64	0 0379
TNFA P6	1 64	0 0243
TLR9	1 65	0 0067
XCR1	1 65	0 0376
CETP	1 68	0 0098
DO1	1 68	0 0486
TREX1	1 68	0 0002
GPR65	1 69	0 0126
CCL22	1 69	0 0386
GEM	1 70	0 0062
RF1	1 70	0 0082
C1QB	1 71	0 0011
TNFRSF12A	1 72	0 0419
NFKB E	1 72	0 0061
CD40LG	1 73	0 0036
ENPEP	1 74	0 0266
LAMB2	1 74	0 0313
CXCL16	1 74	0 0135
CXCL11	1 75	0 0022
CD80	1 75	0 0370
L3	1 75	0 0071
ROS1	1 76	0 0292
SERP NB9	1 76	0 0230
ABCC8	1 76	0 0471
FNG	1 77	0 0489
LPL	1 77	0 0228
RGS16	1 78	0 0217
B RC3	1 79	0 0122
CCL14	1 80	0 0119
MSC	1 80	0 0008
ACOT1	1 80	0 0225
CCL26	1 81	0 0100
MMP19	1 81	0 0296
CX3CR1	1 81	0 0023
NOD2	1 81	0 0196
FSCN1	1 82	0 0139
CTLA4	1 83	0 0367
ANGPT1	1 84	0 0047
CXCL2	1 84	0 0016
DPP4	1 84	0 0383
NR1H3	1 85	0 0211
CAM1	1 85	0 0170
CCR5	1 86	0 0158
ADAMTS9	1 86	0 0131
L27	1 86	0 0075
MPEG1	1 87	0 0089
RGL1	1 89	0 0008
ACOD1	1 89	0 0315
PROS1	1 90	0 0115
CD276	1 91	0 0082
CRABP2	1 91	0 0176
CLEC7A	1 92	0 0140
OSM	1 92	0 0058
L12A	1 92	0 0298
RAPGEF4	1 92	0 0237

Probe Name	Log2 Fold Change	p value
FZD4	1 94	0 0421
CXCR5	1 96	0 0177
SPHK1	1 96	0 0135
L33	1 97	0 0488
VTCN1	1 97	0 0232
RND3	1 98	0 0124
CCR7	1 99	0 0433
L15	1 99	0 0256
COL12A1	2 00	0 0288
GATA3	2 00	0 0253
PLAUR	2 02	0 0008
NR4A1	2 02	0 0421
RASAL1	2 04	0 0496
CD1E	2 05	0 0051
COL11A1	2 08	0 0306
CSF1R	2 08	0 0354
CCL16	2 09	0 0191
L1RN	2 10	0 0300
HES4	2 11	0 0079
MAP3K14	2 11	0 0047
ADAMTS3	2 12	0 0159
CCL2	2 12	0 0333
ADAMTS14	2 13	0 0005
PF4	2 13	0 0039
L23A	2 14	0 0205
MRC1	2 14	0 0498
EN1	2 15	0 0041
HNF1B	2 15	0 0028
CCL25	2 15	0 0077
DO2	2 16	0 0146
TAP2	2 16	0 0026
SG15	2 17	0 0034
CDH2	2 17	0 0062
SOCS1	2 19	0 0107
TNFRSF8	2 20	0 0007
CXCL8	2 20	0 0240
MAFF	2 20	0 0046
CD247	2 22	0 0041
MARCKSL1	2 23	0 0029
L1A	2 24	0 0378
GADD45B	2 25	0 0002
TREM2	2 25	0 0027
TNFRSF1B	2 27	0 0049
TNFRSF14	2 27	0 0018
NFKB A	2 31	0 0044
KRBA1	2 33	0 0332
ZKSCAN5	2 35	0 0010
CREM	2 40	0 0175
BMP6	2 42	0 0002
CYP3A4	2 42	0 0033
COL3A1	2 45	0 0359
LAMB3	2 47	0 0034
TNF	2 52	0 0016
SERP NE3	2 57	0 0045
TNFA P3	2 58	0 0010
DUSP2	2 64	0 0030
FGF10	2 65	0 0033
CD14	2 68	0 0107
F T1	2 72	0 0215
CCL3	2 74	0 0357
HLA DOB	2 81	0 0002
CD83	2 95	0 0027
L1B	3 31	0 0137

NSCLC Pleural Fluid Neutrophils versus Healthy Donor Controls

Probe Name	Log2 Fold Change	p-value
LGALS3	3.72	0.0258
HLA-DRB3	3.28	0.0100
RHOC	2.53	0.0310
HLA-DQB1	2.50	0.0281
HLA-DRA	2.22	0.0004
CTSL	2.10	0.0428
PFDN6	1.95	0.0357
TOP2A	1.94	0.0102
BATF	1.81	0.0074
CLIC4	1.70	0.0432
COG7	1.31	0.0351
KITLG	1.21	0.0278
TM7SF3	1.11	0.0206
NOL7	1.05	0.0023
BCL10	-1.14	0.0287
FAS	-1.15	0.0137
ARHGEF6	-1.31	0.0017
VAMP2	-1.33	0.0061
FPR1	-1.55	0.0401
STAT6	-1.60	0.0465
DUSP1	-1.64	0.0438
MAP2K4	-1.64	0.0005
NFKBIZ	-1.65	0.0278
GNAI3	-1.67	0.0399
EPHB6	-1.67	0.0395
NFIL3	-1.75	0.0311
DNAJB6	-1.78	0.0014
PIM2	-1.83	0.0063
MTMR14	-1.84	0.0474
PELI1	-1.86	0.0061
S100A4	-2.02	0.0406
ITGAL	-2.03	0.0399
CLEC7A	-2.05	0.0355
CDH2	-2.13	0.0136
MPEG1	-2.22	0.0367
NAMPT	-2.24	0.0067
SELL	-2.28	0.0236
PTPRC	-2.30	0.0109
CTSS	-2.34	0.0069
GPR65	-2.47	0.0102
CYTIP	-2.51	0.0066
PLAUR	-2.57	0.0106
AOAH	-2.58	0.0027
NR4A2	-2.75	0.0015
G6PD	-2.83	0.0001
C5AR1	-3.24	0.0089
PTGS2	-4.00	0.0054

Appendix 2: List of statistically significant differentially expressed proteins

NSCLC Normal Density Neutrophils versus Healthy Donor Controls

Protein names	Log2 fold change	Log10 p value
60S r bosoma prote n L34	2 68	3 66
Vacuo ar prote n sort ng assoc ated prote n 25	2 05	1 94
F am n nteract ng prote n FAM101B	2 04	1 79
Armad o repeat conta n ng prote n 8	1 98	1 44
Neutroph defens n 4	1 97	1 77
nos to monophosphatase 2	1 95	1 64
SCY1 ke prote n 2	1 84	1 72
COMM doma n conta n ng prote n 3	1 80	2 99
Park nson d sease 7 doma n conta n ng prote n 1	1 78	2 12
R bonuc eos de d phosphate reductase arge subun t	1 76	1 85
Programmed ce death prote n 4	1 74	1 85
COP9 s gna osome comp ex subun t 3	1 73	1 43
40S r bosoma prote n S28	1 64	2 19
M tochondr a d carboxy ate carr er	1 61	1 36
B funct ona 3 phosphoadenos ne 5 phosphosu fate synthase 1	1 59	1 36
M crotubu e act n cross nk ng factor 1, soforms 1/2/3/5	1 58	1 99
N F3 ke prote n 1	1 58	1 59
Pyr doxa dependent decarboxy ase doma n conta n ng prote n 1	1 57	1 67
Lon protease homo og, m tochondr a	1 56	1 54
DNA rep cat on cens ng factor MCM7	1 55	1 73
sopenteny d phosphate De ta somerase 1	1 54	2 09
COMM doma n conta n ng prote n 1	1 52	2 37
COP9 s gna osome comp ex subun t 1	1 51	1 65
ntraf age ar transport prote n 25 homo og	1 50	1 42
Gamma tubu n comp ex component 2	1 50	1 37
CWF19 ke prote n 1	1 47	1 84
Caspase 10;Caspase 10 subun t p23/17;Caspase 10 subun t p12	1 47	2 26
DDB1 and CUL4 assoc ated factor 7	1 47	1 79
Vacuo ar prote n sort ng assoc ated prote n 13C	1 46	1 31
Nuc ear pore comp ex prote n Nup133	1 46	2 05
Leuc ne r ch PPR mot f conta n ng prote n, m tochondr a	1 44	1 36
Ub qu t n con ugat ng enzyme E2 K	1 43	1 65
Putat ve N acety g ucosam ne 6 phosphate deacety ase	1 40	1 54
Ser ne/threon ne prote n k nase 17B	1 38	1 75
Ub qu t n con ugat ng enzyme E2 var ant 3	1 38	1 30
UDP g ucose 6 dehydrogenase	1 37	1 70
Ethy ma ony CoA decarboxy ase	1 34	1 39
SH3 doma n b nd ng g utam c ac d r ch ke prote n	1 31	1 53
C term na b nd ng prote n 2	1 27	1 79
WD repeat conta n ng prote n 82	1 24	3 59
Tubu n spec f c chaperone D	1 24	2 43
Euka yot c trans at on e ongat on factor 1 eps on 1	1 23	1 35
Catecho O methy transferase	1 22	1 34
60S r bosoma prote n L35a	1 21	1 44
NAD dependent prote n deacy ase s tu n 5, m tochondr a	1 21	3 96
Acy oxyacy hydro ase	1 18	1 35
GH3 doma n conta n ng prote n	1 17	1 74
GTPase NRas	1 15	2 54
Co d nduc b e RNA b nd ng prote n	1 14	1 49
Phosphomeva onate k nase	1 14	1 97
Prote n argonaute 4	1 13	1 31
Deoxycyt d ne k nase	1 12	1 65
mpo t n 11	1 09	1 41
TNF receptor assoc ated factor 2	1 07	2 09
Capr n 1	1 06	1 53
Catheps n D;Catheps n D ght cha n;Catheps n D heavy cha n	1 00	1 59

Protein names	Log2 fold change	-Log10 p-value
Serine/threonine protein kinase WNK1	1.01	2.22
High mobility group protein B1	1.08	2.15
FAS associated death domain protein	1.16	1.43
Histone H1x	1.16	2.47
Voltage gated hydrogen channel 1	1.18	1.34
Complement C4 B	1.43	1.84
Histone H1.0;Histone H1.0, N terminally processed	1.46	2.23
High affinity copper uptake protein 1	1.67	1.45
Histone H2B type 1 O;Histone H2B type 1 B	1.78	1.42
Protein quaking	1.78	1.75
WAS/WASL interacting protein family member 1	2.40	1.34

NSCLC Low Density Neutrophils versus Healthy Donor Controls

Protein names	Log2 fold change	-Log10 p-value
DNA rep cat on cens ng factor MCM4	4.47	2.21
DNA rep cat on cens ng factor MCM3	3.94	1.93
DNA rep cat on cens ng factor MCM5	3.84	2.21
DNA rep cat on cens ng factor MCM6	3.80	2.02
DNA rep cat on cens ng factor MCM7	3.53	1.90
DNA rep cat on cens ng factor MCM2	3.22	1.53
Leuc ne-r ch PPR mot f-conta n ng prote n, m tochondr a	2.86	2.33
DNA m smatch repa r prote n Msh6	2.66	2.37
60S r bosoma prote n L35a	2.63	1.64
R bonuc eos de-d phosphate reductase arge subun t	2.57	2.26
40S r bosoma prote n S21	2.31	2.84
Neutroph defens n 4	2.21	1.74
Structura ma ntenance of chromosomes prote n 2	2.13	1.42
Insu n-degrad ng enzyme	2.08	1.59
Pter n-4-a pha-carb no am ne dehydratase	2.07	1.41
60S r bosoma prote n L34	2.07	1.40
UDP-g ucose 6-dehydrogenase	2.04	1.97
40S r bosoma prote n S28	2.01	1.68
Ub qu t n-conjugat ng enzyme E2 K	2.01	1.45
Deoxynuc eos de tr phosphate tr phosphohydro ase SAMHD1	2.01	1.42
A pha-L- duron dase	1.98	2.17
Pyr doxa -dependent decarboxy ase doma n-conta n ng prote n 1	1.94	1.46
NADH dehydrogenase [ub qu none] 1 a pha subcomp ex subun t 13	1.91	1.56
60S ac d c r bosoma prote n P2	1.89	1.36
Kerat nocyte-assoc ated prote n 2	1.86	2.40
60S r bosoma prote n L27a	1.85	1.41
GTP:AMP phosphotransferase AK3, m tochondr a	1.82	1.88
Ac d c f brob ast growth factor ntrace u ar-b nd ng prote n	1.80	2.05
Methy osome prote n 50	1.79	1.86
Pro ferat ng ce nuc ear ant gen	1.77	2.11
40S r bosoma prote n SA	1.76	1.32
RNA-b nd ng prote n 4	1.75	1.49
Armad o repeat-conta n ng prote n 8	1.70	1.91
Traff ck ng prote n part c e comp ex subun t 3	1.70	1.42
H stone- ys ne N-methy transferase setd3	1.69	3.27
COMM doma n-conta n ng prote n 3	1.65	2.04
A pha-N-acety ga actosam n dase	1.57	1.57
Tr part te mot f-conta n ng prote n 16	1.53	1.50
Exosome comp ex component RRP42	1.53	1.47
Pept de-N(4)-(N-acety -beta-g ucosam ny)asparag ne am dase	1.52	2.26
Sept n-11	1.50	2.37
Prote n farnesy transferase/gerany gerany transferase type-1 subun t a pha	1.49	1.59
60S r bosoma prote n L8	1.47	2.69
Po y [ADP-r bose] po ymerase 1	1.47	1.58

Protein names	Log2 fold change	-Log10 p-value
60S r bosoma prote n L22	1.46	2.69
Vacuo ar prote n sort ng-assoc ated prote n 28 homo og	1.45	1.39
Catheps n D;Catheps n D ght cha n;Catheps n D heavy cha n	1.42	1.91
Transcr pt on ntermed ary factor 1-beta	1.40	1.44
COP9 s gna osome comp ex subun t 1	1.37	1.61
Prote n arg n ne N-methy transferase 1	1.37	1.96
ATP-dependent RNA he case DHX36	1.36	2.48
Hunt ngt n- nteract ng prote n 1-re ated prote n	1.35	1.58
DNA topo somerase 2-a pha	1.34	1.36
Ser ne-prote n k nase ATM	1.32	1.39
RNA-b nd ng prote n 14	1.31	1.39
60S r bosoma prote n L18a	1.30	2.17
Prote n transport prote n Sec24A	1.30	1.34
40S r bosoma prote n S3	1.28	3.47
Phosphomeva onate k nase	1.27	1.81
60S r bosoma prote n L27	1.25	2.10
Sort ng nex n-3	1.24	1.32
Guan ne nuc eot de-b nd ng prote n subun t beta-2- ke 1	1.23	2.95
60S r bosoma prote n L7a	1.20	2.06
60S ac d c r bosoma prote n P0;60S ac d c r bosoma prote n P0- ke	1.20	2.20
60S r bosoma prote n L9	1.20	1.51
Pre-mRNA-sp c ng factor ATP-dependent RNA he case PRP16	1.19	2.85
Inos to po yphosphate 5-phosphatase OCRL-1	1.19	1.83
40S r bosoma prote n S19	1.18	2.19
Sarco emma membrane-assoc ated prote n	1.17	1.78
60S r bosoma prote n L23a	1.16	1.55
40S r bosoma prote n S12	1.13	1.44
Trans ocon-assoc ated prote n subun t de ta	1.12	1.60
Prote n phosphatase 1G	1.10	2.44
Tubu n beta-4B cha n	1.09	2.82
40S r bosoma prote n S5;40S r bosoma prote n S5, N-term na y processed	1.08	1.75
60S r bosoma prote n L3	1.07	2.03
E ongat on factor 1-de ta	1.07	2.24
40S r bosoma prote n S16	1.06	2.13
Heat shock prote n 105 kDa	1.06	1.36
DmX- ke prote n 2	1.06	2.76
40S r bosoma prote n S23	1.06	2.08
40S r bosoma prote n S3a	1.05	2.02
Ser ne pa m toy transferase 1	1.03	1.78
Tubu n beta cha n	1.03	1.90
U5 sma nuc ear r bonuc eoprote n 40 kDa prote n	1.02	1.39
Staphy ococca nuc ease doma n-conta n ng prote n 1	1.01	1.62
Co d- nduc b e RNA-b nd ng prote n	1.00	1.38

Protein names	Log2 fold change	-Log10 p-value
Leukocyte immunoglobulin-like receptor subfamily A member 3	-1.03	1.45
Alpha-2-macroglobulin	-1.03	1.38
Rho-related GTP-binding protein RhoB	-1.03	1.35
Serine/threonine-protein kinase B-raf	-1.04	1.65
Urokinase plasminogen activator surface receptor	-1.16	2.78
2-5A-dependent ribonuclease	-1.18	1.39
WD repeat domain phosphoinositide-interacting protein 2	-1.21	1.36
Alpha-1-acid glycoprotein 1	-1.22	1.51
RalA-binding protein 1	-1.23	1.50
Low affinity immunoglobulin gamma Fc region receptor III-B	-1.23	1.85
Probable phospholipid-transporting ATPase IM	-1.26	1.34
Transmembrane protein 192	-1.27	1.42
Complement C4-B;Complement C4 beta chain	-1.28	1.50
P2X purinoceptor 1	-1.28	1.84
Calcium/calmodulin-dependent protein kinase type 1D	-1.33	1.65
Oxidized low-density lipoprotein receptor 1	-1.38	1.56
Mitogen-activated protein kinase kinase kinase kinase 4	-1.39	1.43
Voltage-gated hydrogen channel 1	-1.40	1.30
Vascular non-inflammatory molecule 2	-1.41	3.46
Cathelicidin antimicrobial peptide	-1.42	2.75
Protein S100-A4	-1.44	2.75
Ankyrin repeat domain-containing protein 13D	-1.46	2.58
GMP reductase 2	-1.48	1.66
Tropomyosin alpha-1 chain	-1.49	1.38
Solute carrier family 12 member 6	-1.50	2.11
Complement C3	-1.50	2.13
Aldose 1-epimerase	-1.62	1.42
Oxoeicosanoid receptor 1	-1.63	2.52
Tumor necrosis factor-inducible gene 6 protein	-1.73	1.82
Serotransferrin	-1.77	1.69
Neprilysin	-1.86	1.82
NHL repeat-containing protein 3	-1.87	1.60
Pituitary tumor-transforming gene 1 protein-interacting protein	-1.88	1.46
Interferon-induced protein with tetratricopeptide repeats 2	-1.88	1.88
CMRF35-like molecule 8	-2.09	1.48
Serglycin	-2.21	2.19
Solute carrier family 2, facilitated glucose transporter member 5	-2.38	2.58
Apolipoprotein A-I;Proapolipoprotein A-I;Truncated apolipoprotein A-I	-2.46	1.77
P2Y purinoceptor 13	-2.57	2.07
Retinoid-binding protein 7	-2.71	2.17
C-X-C chemokine receptor type 1	-2.85	2.02

NSCLC Pleural Fluid Neutrophils versus Healthy Donor Controls

Protein names	Log2 fold change	-Log10 p-value
Inter euk n-1 receptor accessory prote n	3.12	1.59
EGF- ke modu e-conta n ng muc n- ke hormone receptor- ke 2	3.04	3.28
Gamma-eno ase	2.92	1.37
Pro y 4-hydroxy ase subun t a pha-1	2.82	1.65
Interferon gamma receptor 1	2.71	1.52
A ka ne phosphatase, t ssue-nonspec f c sozyme	2.42	1.78
M crotubu e-act n cross- nk ng factor 1, soforms 1/2/3/5	2.14	1.96
Import n subun t a pha-4	2.12	1.87
G utam ne synthetase	2.04	2.04
Sarco emma membrane-assoc ated prote n	1.98	2.31
Interce u ar adhes on mo ecu e 1	1.83	1.97
Ga ect n-8	1.78	1.51
GTP:AMP phosphotransferase AK3, m tochondr a	1.73	2.15
A pha-1-ant chymotryps n;A pha-1-ant chymotryps n H s-Pro- ess	1.69	2.15
Methy osome prote n 50	1.64	1.40
Surfe t ocus prote n 4	1.62	1.45
Catecho O-methy transferase	1.49	1.38
Cu n-2	1.40	1.66
UDP-g ucose 6-dehydrogenase	1.39	1.64
Tr carboxy ate transport prote n, m tochondr a	1.36	1.44
Anc ent ub qu tous prote n 1	1.33	1.51
E3 ub qu t n-prote n gase TRIM33	1.28	1.36
Pept dy -pro y c s-trans somerase FKBP5	1.26	1.35
Interferon- nduced GTP-b nd ng prote n Mx2	1.23	1.50
NAD-dependent prote n deacy ase s rtu n-5, m tochondr a	1.13	1.73
N cot nam de phosphor bosy transferase	1.04	2.72
6-phosphofructo-2-k nase/fructose-2,6-b sphosphatase 2	1.03	1.42
Noda modu ator 2;Noda modu ator 3	1.02	1.55
Ethano am ne-phosphate cyt dy y transferase	1.01	1.57

Protein names	Log2 fold change	-Log10 p-value
Pept dy -pro y c s-trans somerase FKBP3	-1.01	1.80
NHL repeat-conta n ng prote n 3	-1.04	1.43
Prote n S100-A12;Ca c term n	-1.09	1.44
Lysosoma a pha-mannos dase	-1.10	1.46
Prote n FAM91A1	-1.22	1.97
Phosphat dy nos to 4,5-b sphosphate 3-k nase cata yt c subun t gamma soform	-1.24	1.32
Tyros ne-prote n k nase JAK1	-1.26	1.39
Cyste ne-r ch secretory prote n LCCL doma n-conta n ng 2	-1.26	1.96
PDZ and LIM doma n prote n 5	-1.26	1.59
Transcr pt ona repressor CTCF	-1.29	1.83
Cyste ne-r ch secretory prote n 3	-1.32	1.72
Oxoe cosano d receptor 1	-1.33	1.81
MAGUK p55 subfam y member 7	-1.35	3.89
Prote n b cauda D homo og 2	-1.36	1.37
Membrane cofactor prote n	-1.42	2.06
Transmembrane channe - ke prote n 8	-1.42	1.77
Lymphocyte ant gen 75	-1.54	1.32
Meva onate k nase	-1.56	1.64
Ga ect n-3-b nd ng prote n	-1.64	2.00
Nespr n-3	-1.70	2.33
Guan ne nuc eot de exchange factor VAV3	-1.72	3.51
Transcr pt on factor BTF3 homo og 4	-1.74	1.75
Ox d zed ow-dens ty poprote n receptor 1	-1.89	1.83
40S r bosoma prote n S9	-1.91	2.35
DENN doma n-conta n ng prote n 2D	-2.06	2.00
CSC1- ke prote n 1	-2.26	1.33
60S r bosoma prote n L13	-2.38	1.61
Op o d growth factor receptor	-2.46	2.40
Cytoso c carboxypept dase 1	-2.50	2.00
F-box on y prote n 50	-2.63	1.68
Apo poprote n A-I;Proapo poprote n A-I;Truncated apo poprote n A-I	-2.74	1.53
Immunog obu n superfam y member 2	-2.75	1.54
Prote n PBDC1	-2.90	1.60
COMM doma n-conta n ng prote n 2	-3.97	1.52